

UNCLASSIFIED

AD NUMBER

AD882855

LIMITATION CHANGES

TO:

Approved for public release; distribution is unlimited.

FROM:

Distribution authorized to U.S. Gov't. agencies and their contractors; Critical Technology; FEB 1971. Other requests shall be referred to Air Force Flight Dynamics Lab., Attn: FEM, Wright-Patterson AFB, OH 45433. This document contains export-controlled technical data.

AUTHORITY

AFWAL ltr dtd 20 Dec 1985

THIS PAGE IS UNCLASSIFIED

AD 882 855

AUTHORITY:

AFM L 14 20 Dec 85



①

**AIRCRAFT ANTISKID PERFORMANCE
AND SYSTEM COMPATIBILITY
ANALYSIS**

BYRON H. ANDERSON
WAYNE C. KREGER
GENERAL DYNAMICS
CONVAIR AEROSPACE DIVISION
FORT WORTH OPERATION

TECHNICAL REPORT AFFDL-TR-70-128

FEBRUARY 1971

Approved for public release; distribution unlimited

This document is subject to special export controls and each transmittal to foreign governments or foreign nationals may be made only with prior approval of the Air Force Flight Dynamics Laboratory (FEM), Wright-Patterson Air Force Base, Ohio 45433.

AIR FORCE FLIGHT DYNAMICS LABORATORY
AIR FORCE SYSTEMS COMMAND
WRIGHT-PATTERSON AIR FORCE BASE, OHIO

DTIC
ELECTE
JAN 02 1986
S
E
D

85 12 31 006

ASD 85 2475

AD-882855

NOTICE

When Government drawings, specifications, or other data are used for any purpose other than in connection with a definitely related Government procurement operation, the United States Government thereby incurs no responsibility nor any obligation whatsoever; and the fact that the government may have formulated, furnished, or in any way supplied the said drawings, specifications, or other data, is not to be regarded by implication or otherwise as in any manner licensing the holder or any other person or corporation, or conveying any rights or permission to manufacture, use, or sell any patented invention that may in any way be related thereto.

Copies of this report should not be returned unless return is required by security considerations, contractual obligations, or notice on a specific document.

AIRCRAFT ANTISKID PERFORMANCE AND SYSTEM COMPATIBILITY ANALYSIS

BYRON H. ANDERSON

WAYNE C. KREGER

~~Approved for public release; distribution unlimited~~

This document is subject to special export controls and each transmittal to foreign governments or foreign nationals may be made only with prior approval of the Air Force Flight Dynamics Laboratory (FEM), Wright-Patterson Air Force Base, Ohio 45433.

The distribution of this report is limited because release of information would significantly diminish the technological lead time of the United States and friendly foreign nations by revealing formulas, processes, or techniques having a potential strategic or economic value not generally known throughout the world.

DTIC
JAN 0 1971

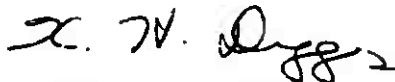
FOREWORD

The study of aircraft antiskid performance and system compatibility reported herein was performed by the Fort Worth Division of General Dynamics Corporation under U. S. Air Force Contract No. F33615-70-C-1004. The contract was initiated under Project No. 1369 "Mechanical Subsystems for Advanced Military Flight Vehicles" and Task No. 136910 "Steering and Deceleration Subsystems for Advanced Military Flight Vehicles." This study was administered under the direction of the Air Force Flight Dynamics Laboratory, Mr. Paul M. Wagner (FEM), Project Engineer.

This report describes work conducted during the period from August 1969 to August 1970. The study was performed under the project leadership of Mr. R. C. Churchill. The General Dynamics Report Number is FZM-5560. The authors wish to acknowledge the assistance of Mr. R. C. Barron, Mr. C. W. Austin and Mrs. L. J. Schnacke for their efforts in analog and digital computer programming.

The authors wish to thank Mr. Wagner for his guidance and assistance throughout the program. The cooperation of the Antiskid Engineering Department of the Goodyear Aerospace Corporation is also acknowledged. This report was submitted by the authors in September 1970.

Publication of this technical report does not constitute Air Force approval of the report's findings or conclusions. It is published only for the exchange and stimulation of ideas.



KENNERLY H. DIGGES
Chief, Mechanical Branch
Vehicle Equipment Division
Air Force Flight Dynamics Laboratory

ABSTRACT

The operation of an aircraft antiskid wheel brake control system has the potential for producing adverse aircraft dynamic behavior and structural damage. Antiskid operation is also a major influence upon stopping performance. Unless the characteristics and effects of antiskid operation can be defined, an aircraft's capability for safe, reliable and economical accomplishment of its intended usage cannot be assured. This report presents an analysis procedure for predicting antiskid operational characteristics and the inter-related effects upon the aircraft and its performance. The analytical procedure is the development of mathematical equations for a comprehensive description of the antiskid system components, the significantly influencing aircraft systems and the characteristics of the surface upon which the aircraft is operating. The mathematical description includes such considerations as landing gear dynamics, tire elasticity, brake torque response characteristics, antiskid electronic circuitry, brake hydraulic control system dynamics, runway surface profile and tire-to-runway friction characteristics. Both on-off and "modulated" antiskid systems are analyzed. Procedures for quantitative evaluation of the influencing parameters and examples of their usage are also presented. The implementation of the analytical prediction procedure by simultaneous solution of all the mathematical equations on an electronic computer is described.

Accession For	
NTIS GRA&I	<input checked="" type="checkbox"/>
DTIC	<input type="checkbox"/>
Unannounced	<input type="checkbox"/>
Distribution	
Available	
Dist	Sp
A-1	

UNANNOUNCED

CONTENTS

Section	Page
I INTRODUCTION	1
II ANALYTICAL APPROACH.	4
1. Problem Definition	4
2. Background	7
3. Analytical Procedure and Rationale	8
4. Parameter Investigations	10
III DEVELOPMENT OF MATHEMATICAL MODELS	17
1. Brake System	21
2. Hydraulic System	31
3a. Airplane System (Flywheel)	51
3b. Airplane System (3 Degree)	62
3c. Airplane System (6 Degree)	81
4a. Wheel and Tire System (Flywheel)	108
4b. Wheel and Tire System (3 Degree)	126
4c. Wheel and Tire System (6 Degree)	136
5. Wheel Speed Sensor	146
6a. Modulated-Antiskid Control Circuit	154
6b. On-Off Antiskid Control Circuit.	173
7. Antiskid Control Valve	191
8. Horizontal Tail Control.	201
9a. Runway System (3 Degree)	208
9b. Runway System (6 Degree)	210
IV TOTAL SYSTEM ANALYSIS	219
V SAMPLE CASE ANALYSIS	224
REFERENCES	227
APPENDIX I	229

ILLUSTRATIONS

No.	Title	Page
1	Aircraft Antiskid Arrangement Block Diagram. .	5
2	Friction Coefficient Versus Wheel Slip Ratio .	14
3	Forces Acting on the Brake Discs	22
4	Keyway Friction Characteristic	23
5	Brake System Equation Flow Diagram	25
6	Brake Pressure Volume Characteristic	26
7	Hydraulic System Components.	32
8	Hydraulic System Schematic	32
9	Hydraulic System Equation Flow Diagram	36
10	Hydraulic Fluid Damping Characteristic	41
11	Flywheel System Model.	52
12	Airplane System (Flywheel) Equation Flow Diagram.	54
13	Main Gear Damping Curve.	55
14	Main Gear Air Load Curve	55
15	Airplane Coordinates	62
16	Airplane Geometry.	63
17	Airplane Dynamics.	65
18	Main Strut Model	66
19	Airplane System (3 Degree) Equation Flow Diagram	68
20	Nose Gear Damping Curve.	69
21	Nose Gear Air Load Curve	70
22	Main Gear Strut and Wheel Model.	71
23	Airplane Initial Equilibrium Forces.	73
24	Airplane Coordinates	81
25	Airplane Geometry.	82
26	Airplane Dynamics (Pitch).	84
27	Airplane Dynamics (Yaw).	85
28	Airplane Dynamics (Roll)	86
29	Nose Tire Cornering Force.	87
30	Side View of Main Gear Strut	89
31	Main Gear Model	90
32	Airplane System (6 Degree) Equation Flow Diagram	94
33	Components of the Wheel and Tire System. . . .	108
34	Tire Horizontal Model.	109
35	Tire Rotational Model.	110
36	Wheel and Tire System (Flywheel) Equation Flow Diagram	112
37	Tire Tread Model	114
38	Tire Damping Models.	116

ILLUSTRATIONS (Concluded)

No.	Title	Page
39	Model Loss Factors.	118
40	Tire Sliding Friction Coefficient	120
41	Components of the Wheel and Tire System	126
42	Tire Horizontal Model	127
43	Tire Rotational Model	128
44	Wheel and Tire System (3 Degree) Equation Flow Diagram.	130
45	Footprint Friction Components	137
46	Wheel and Tire System (6 Degree) Equation Flow Diagram.	138
47	Wheel Speed Signal System	147
48	Wheel Speed Sensor Equation Flow Diagram (Option 1)	148
49	Modulated Antiskid Control Functional Block Diagram	155
50	Modulated Antiskid Control Circuit Schematic. .	157
51	Modulated Antiskid Circuit Equation Flow Diagram	166
52	On-Off Antiskid Control Functional Block Diagram	174
53	Electrical On-Off Antiskid Control Circuit. . .	175
54	Electrical On-Off Circuit Equation Flow Diagram	181
55	Mechanical On-Off Antiskid Device	184
56	Mechanical On-Off Device Equation Flow Diagram.	190
57	First Stage Spring Mass System.	191
58	First Stage Control Pressure - Mass Position Relationship	192
59	Antiskid Valve Second Stage	193
60	Second Stage Spool Forces	194
61	Antiskid Control Valve Equation Flow Diagram. .	196
62	Stability Augmentation System	201
63	Horizontal Tail Control Equation Flow Diagram .	204
64	Flywheel System	221
65	Three Degree System	222
66	Six Degree System	223
67	Analog Computer On-Off Antiskid Operation . . .	225
68	Modulated Antiskid Schematic with Mathematical Identification and Incorporating Equivalent Circuits for Transistors and Diodes	230

TABLES

No.	Title	Page
1	Explanation of Mathematical Conventions	19
2	Brake System Parameters	29
3	Control Line Restrictions	39
4	Hydraulic System Parameters	46
5	Airplane System (Flywheel) Parameters	59
6	Airplane System (3 Degree) Parameters	76
7	Airplane System (6 Degree) Parameters	99
8	Runway Friction Characteristics	119
9	Wheel and Tire System (Flywheel) Parameters	122
10	Wheel and Tire System (3 Degree) Parameters	132
11	Wheel and Tire System (6 Degree) Parameters	141
12	Wheel Speed Sensor Parameters	152
13	Modulated Antiskid Circuit Equation Summary	160
14	Pressure Bias Signal Condition Test Equations	162
15	Summary of Equations for Computing Current AD5.	162
16	Capacitor C4 Current Mode Test Equations	163
17	Valve Amplifier Operating Mode Test Equations	164
18	Modulated Antiskid Circuit Conditions	165
19	Modulated Control System Parameters	167
20	On-Off Control System Parameters	182
21	Antiskid Control Valve Parameters	199
22	Horizontal Tail Control Parameters.	205
23	Runway System Parameters (Flywheel & 3 Degree).	209
24	Three Track Elevation Profiles	212
25	Runway System Parameters (6 Degree)	213

SECTION I

INTRODUCTION

An antiskid system is provided as a part of the landing gear wheel brake control system of most large aircraft, particularly those having full power brake actuation. Aircraft operational experience has shown that an anti-skid system is required because there are many occasions where the maximum available friction force between the tires and runway surface is insufficient to react the applied brake torque. For cases where excessive brake torque is applied the antiskid system functions to control tire motion so that skids are prevented and so that the associated problems and hazardous circumstances which are detrimental to safe, predictable and economical aircraft operation are avoided. The antiskid function is accomplished by a group of ancillary components which provide an automatic means for detecting and alleviating an incipient tire skid condition by controlling brake torque. An incipient skid is alleviated by temporarily reducing brake torque to a value less than the torque being produced by the friction force at the tire-runway interface. Brake torque reduction is sustained for a time interval of sufficient duration to allow the wheel to regain speed. After the wheel has regained speed, brake torque is reapplied.

The reduction and subsequent reapplication of brake torque results in an oscillatory braking force being applied to the airplane. This oscillatory force has the potential for causing adverse dynamic loading of the airplane structure, for causing directional control difficulty and for degrading the aircraft's stopping performance. Therefore, the antiskid system must control tire motion in a way such that objectionable or unsafe conditions other than those related to tire skidding are not incurred. The need for evaluating the potentially deleterious effects of an oscillatory braking force is now recognized because there have been a number of instances where failure to do so has resulted in severe operational difficulty and in some cases catastrophic landing gear failure.

The objective of this study is to develop analytical procedures and techniques for predicting aircraft antiskid operational behavior and its effects. These analysis

techniques are intended to help overcome some of the previously experienced problems or uncertainties and to provide a foundation for a comprehensive evaluation of aircraft antiskid performance and total system compatibility. It is also intended that these procedures be capable of application during the conceptual design phase of new airplanes. In the initial design of a new airplane the capabilities of various candidate equipment which might be used for stopping during the landing sequence or rejected takeoff should be evaluated with respect to the airplane's mission requirements. Factors such as stopping performance, weight, cost and reliability should be considered when the influence of the braking equipment is being examined to establish the overall effect upon the aircraft's configuration. In such an evaluation, the performance of the wheel braking system, including any applicable antiskid equipment, is a major consideration. Use of an analysis procedure whereby the effects of antiskid operation can be accurately predicted provides the means for minimizing the technical and financial risks of both the aircraft manufacturer and the aircraft user. Inaccurately predicting the wheel braking system's performance can result in an airplane design unsuited for its intended usage, a costly redesign program, or both.

This study mathematically describes the physical operation of antiskid equipment in conjunction with the airplane and its other applicable components. The basis of the mathematical relationships is the description of actual (or conceivable) hardware behavior rather than a compilation of equations relating various parameters in a desirable or compatible manner without regard to detail design features. This approach is taken to assure all influencing parameters are accounted for and to provide criteria for equipment detail design and test. Also, by examining the individual component behavior, the evaluation can include such considerations as cost and weight along with performance characteristics.

The essence of antiskid operation is the cumulative effect of a number of successive events, where the intervening occurrences and outcome of each is influenced by and dependent upon the conditions resulting from preceding events. Since these events occur quite rapidly and involve

the behavior of the aircraft and many of its components, the instantaneous condition of a very large number of variables must be continually maintained with high accuracy so that they are available when needed. Consequently, one of the major problems associated with analyzing antiskid operation is the magnitude of the computation task. It will be noted that the study has analytical components encompassing several engineering and scientific disciplines such as electronics, aerodynamics, mechanics and hydraulics. Each of the individual analytical components is often deserving of considerable more elaborate and complete treatment. However, to provide an economically feasible and comprehensible composite solution, the scope of the individual analytical components has been limited to account for only those effects or influencing factors which are of traditional interest and which are required to achieve reasonable agreement between observed operational behavior and analytical results.

SECTION II

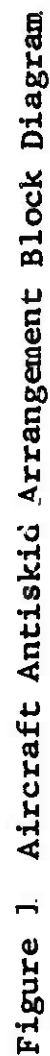
ANALYTICAL APPROACH

The analytical approach of this study is directed toward predicting the existence of adverse circumstances which have caused various problems in the past and toward providing information which is typically needed to establish detail design criteria and to define aircraft operating procedures. Specific consideration is given to providing the means for:

- (a) Establishing the magnitude and frequency of dynamic loading applied to the landing gear.
- (b) Establishing the value of the braking force which can be predictably and dependably achieved for various runway surface and aircraft operating conditions.
- (c) Determining individual component and system operational characteristics which are required so that overall aircraft performance objectives are achieved.
- (d) Establishing the effects of varying performance characteristics of individual components within the brake control system to assure no incompatibilities exist.

1. PROBLEM DEFINITION

Figure 1 is a block diagram showing the typical arrangement of an antiskid system and its relationship within the total aircraft system. This arrangement is representative of most antiskid systems in current use and the various types of airplanes on which they are installed. The major components, the significant forces and their controlling elements are shown for a single wheel main gear configuration of a nose wheel type airplane which is the usual case for fighter type aircraft. For airplanes having multiple wheeled landing gears and/or multiple landing gears the same basic relationships prevail with the addition of similar type components as appropriate.



Antiskid systems usually operate by measuring a wheel's motion, comparing the measurement to an index of acceptability and causing brake torque to be decreased or increased in accordance with some function of the difference between the measured motion and comparison index. A detailed description of the operational behavior and influence of the individual elements is presented in Section III.

Since antiskid operation is basically the control of tire motion and since the motion of a tire is determined by the forces imposed (the same as for any other object) the study of antiskid operation resolves itself into (1) defining the forces on the tire and wheel and (2) establishing the resultant effects of these forces. It is easily observed that the forces acting upon an airplane tire and wheel are the forces between the tire tread and runway surface and the forces from the airplane's landing gear and brake. The values of these forces are established by the wheel's relative position and relative motion with respect to the runway surface and to the airplane. The wheel's relative motion and position is determined by considering simultaneous and interrelated actions of the aircraft and a number of its systems. The effects of the following parameters are considered in this study.

- (a) Tire circumferential deformation and its rate
- (b) Tire radial deformation and its rate
- (c) Brake torque as a function of velocity, the brake's inertia, and actuation pressure
- (d) Brake actuation pressure as a function of the actuation media's compressibility and inertia, line restrictions and elasticity, variable flow areas within valves and the actuation media's containment vessels' (lines, brake housing, valve bodies) volume
- (e) Elastic and inertia properties of the landing gear
- (f) Aerodynamic forces upon the airplane
- (g) Runway surface profile
- (h) Tire-to-runway friction coefficient as a function of relative velocity and runway surface condition including hydroplaning effects
- (i) The aircraft's inertia and control surface position including stability augmentation system effects.

2. BACKGROUND

During the initial design and system development phase for most new aircraft, it has become a customary practice to analyze antiskid operation to define its effects and thereby assure compliance with the airplane's stopping performance objectives and assure adverse dynamic loading conditions or directional control problems will not be encountered. These analyses have usually been accomplished by utilizing a set-up composed of hardware representative of aircraft components interfaced with an electronic computer (most often an analog computer). The computer is used to solve mathematical equations describing the motion of the aircraft and the landing gear, forces on the aircraft, tire and wheel motion and tire-to-runway friction, etc. The actual behavior of a laboratory set-up including such components as the antiskid control circuit, hydraulic brake valves and interconnecting lines is measured by suitable instrumentation and fed into the computer to obtain a composite solution. This analysis procedure is used because a complete mathematical computer setup requires greater computer capacity than is usually available and because an accurate mathematical description for some components such as the electronic antiskid control circuit is often unavailable.

Some antiskid analyses have been performed using an "all mathematical" approach; however, these have usually been associated with academic endeavors or a comparative evaluation of a specific device and did not account for all of the known significant influencing parameters and constraints for an actual aircraft antiskid system installation. While the hybrid hardware-computer analyses have often satisfied their objectives, several factors have led to a number of uncertainties for which the bounds are not adequately established, either because of great difficulty and expense or because of inadequate knowledge. These uncertainties tend to obscure the analysis results and generally detract from their credibility. The most significant factor causing uncertainty is that the usual definition for the friction force between the tire and runway surface does not account for all the observed variations. A second factor is the analytical limitations

associated with the use of actual hardware. The use of actual hardware dictates that the analysis be performed "real time" and complicates or prevents examination of some parameter variations. Since some parameters have a very high rate of variation with respect to time, the outputs from a "real time" solution can be extremely difficult to observe and interpret. Also, the instrumentation used to interface the hardware with the computer introduces additional variables to an otherwise very complex system. This study is intended to provide the means for overcoming these problems and for minimizing uncertainty.

3. ANALYTICAL PROCEDURE AND RATIONALE

The evaluation of antiskid operation is conducted using a modular analysis technique whereby the problem is divided into a number of modules or component parts, each having defined inputs and outputs such that the outputs from one or more components are provided as inputs to other components. By combining all the analytical components, a composite simultaneous solution is obtained. The analytical modules are formulated so as to correspond to various aircraft components or systems. The modules can be arranged in a number of combinations representative of a variety of aircraft configurations. In addition, the modular approach allows maximum computation flexibility in that changes can be made within individual modules without affecting the overall analysis program. The predominate influencing factors governing the choice of each analytical component's content and treatment are experience and judgment as to the degree of detail which is required to accurately establish the timing or relative sequence of significant events. Each analytical module is formulated so that particular effects or circumstances can be examined and so that its outputs will supply the information needed as inputs to other modules. It will be noted that some relatively insignificant parameters must be considered to achieve mathematical continuity. To exemplify the analysis procedure antiskid operation for a fighter type aircraft having a single wheel main landing gear arrangement is evaluated. All of the analytical components, except for the antiskid control circuit, are expressed in general terms and could be applied to almost any airplane. The antiskid control circuits considered are those specifically utilized on the F104 and the F-111.

For the case of the F-104 on-off antiskid control circuit, the wheel speed input signal is arbitrarily adjusted to account for the difference between the F-104 and F-111 tire sizes. All parameter values used to prove the validity of the analysis procedures are those associated with the F-111 airplane so that the analytical results can be compared to available records of actual aircraft operation. To analyze other control circuits will require that their mathematical models be formulated and incorporated in the compcsite solution. The detail assumptions and procedures for establishing parameter values are presented in Section III within the description of each analytical module.

4. PARAMETER INVESTIGATIONS

The basic intent of this study is to account for the influence of parameters and effects which have been identified as responsible for previously experienced operational difficulties or which are otherwise known to significantly affect antiskid performance. Such items as tire radial and circumferential spring rate, the characteristics of brake torque variations with velocity and actuation pressure, brake chatter and squeal, hydraulic system response as affected by line-sizes, component flow restrictions and metering valve characteristics, the airplane's response to aerodynamic forces and runway roughness, landing gear elastic characteristics and the characteristic of the tire-to-runway friction force variations are given particular attention. The treatment of most parameters is that which experience has proven gives satisfactory results. However, to overcome some previous antiskid evaluation analytical difficulties associated with tire-to-runway friction and hydraulic system operation and to examine the effects of brake chatter and squeal, some preliminary investigations were conducted.

A. Brake Investigation

Since an antiskid system controls brake torque implicitly by controlling brake application pressure, the hysteresis in the brake's torque response to pressure changes must be accounted for. This hysteresis results from inertia of the brake moving parts, friction forces on the actuating pistons due to hydraulic seals and piston side loading, and from friction in the splined connections between the brake discs and the wheel and between the discs and the torque tube. To evaluate a typical brake's torque response to rapidly changing actuation pressure and to briefly investigate brake chatter and squeal effects, a relatively complex six-degree of freedom brake mathematical model was initially formulated. In this model six discs were treated as separate masses with individual axial position, velocity and acceleration computation, non-linear keyway and piston friction as a function of axial velocity, non-linear brake lining friction as a function of rotational velocity, and variable

elasticity to simulate the effects of disc warpage. The model was set up on an analog computer and subjected to step input pressures and to sinusoidal pressure oscillations of various amplitudes and mean values at frequencies from 10 cps to 1000 cps. The computer setup also included rotational and longitudinal elastic deformations within the tire and brake supporting structure. The set up was operated at 1/100 real time and at a number of aircraft velocities. By suitable choice of elastic, damping and friction characteristics, both chatter and squeal were produced at low aircraft speed. Using a keyway friction coefficient varying from 0.15 at zero velocity to 0.10 at high velocity, it was found that the brake torque oscillated in response to oscillating pressure at all frequencies up to 1000 cps. At low brake rotational velocities (20-40 rad/sec) with low frequency pressure oscillation where the minimum pressure was the value for full brake release, the brake torque oscillation had considerable deviation from a sinusoidal variation. The phase lag between instants of maximum torque and maximum pressure varied from 15-20 degrees at 10 cps to 40-50 degrees at 100 cps to 110-150 degrees at 1000 cps. The oscillatory component of the brake torque exhibited appreciable attenuation at high frequency such that the amplitude at 1000 cps was about 20 percent of the 10 cps amplitude with constant pressure amplitude. Even though there was noticeable phase lag in the pressure-torque characteristic, it was found that throughout the 10-1000 cps frequency range there was no appreciable phase difference between the displacement, velocity or acceleration of the individual discs. Therefore, a simplified model was formulated where all the discs were treated as a single mass. The simple model was set up and tested on the analog computer where its torque response to varying pressure was confirmed to be identical to the more complex model. The more simple brake mathematical model is used in this study and is described in Section III. A significant and somewhat unexpected finding of this investigation is that a typical airplane brake can be expected to have appreciable torque response when subjected to pressure oscillations in the 100-200 cps frequency range as might be associated with a hydraulic line resonance.

B. Tire-to-Runway Friction Investigation

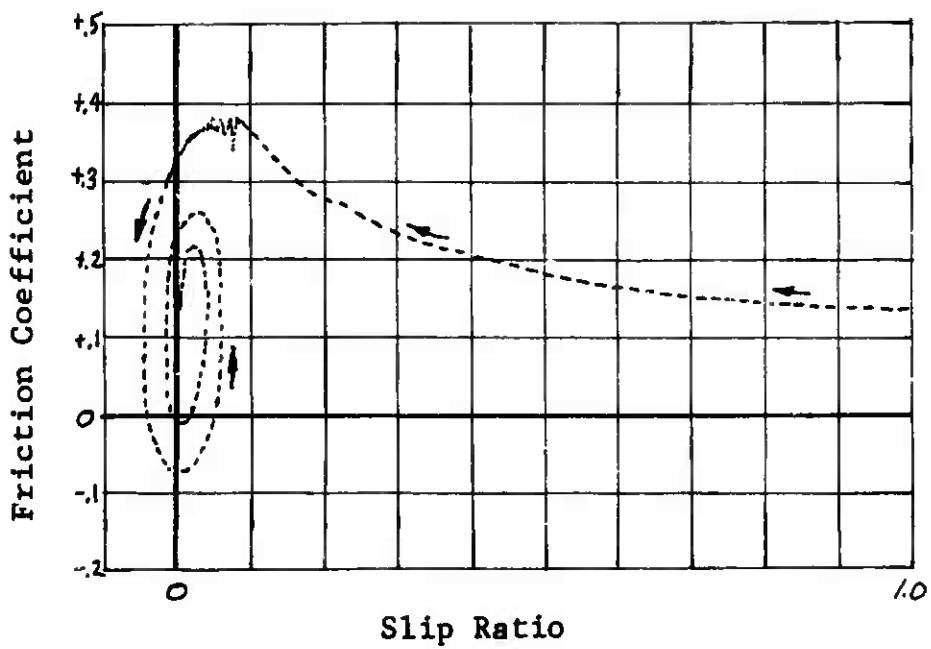
The usual and relatively arbitrary function relating coefficient of friction to tire or wheel slip ratio has been used in most prior antiskid analyses to establish the tire-to-runway friction force. While there are many circumstances where the slip ratio approach is adequate for examining most of the aspects of antiskid operation, a number of difficulties and undesirable effects are associated with its use. A major analytical problem is that examination of antiskid operation at low aircraft speed is prohibited because the slip ratio computation would require division by zero. In addition, the large differences in the friction coefficient-slip ratio characteristic variation which have been observed for changes such as aircraft speed, runway surface condition and tire properties lead to a number of uncertainties, particularly with respect to stopping performance predictions.

To satisfy the objectives of this study, it was considered necessary that a mathematical description of the tire-to-runway friction coefficient be used which would not have the above undesirable qualities. To develop such a description, several hypotheses were formulated considering the tire's elastic deformation and its response to ground friction forces. Effects such as tread stretch, tread circumferential displacement and variation of relative velocity between tire tread particles and the runway surface throughout the footprint were examined mathematically. Because of the extremely complex nature of a tire's elastic behavior, these examinations quickly lead to an analytical task at least equal to the scope of the entire antiskid study. Even though this subject deserves further investigation, a more simple hypothesis accounting for most known variations and effects was adopted to comply with this program's objectives. For the purpose of this analysis, it is assumed that: (1) the tire tread is a perfectly flexible inelastic belt with radial and torsional elastic attachment to the wheel. (2) All tread particles within the footprint have the same relative velocity with respect to the runway surface and the coefficient of friction between the tire tread and runway surface is a function of relative

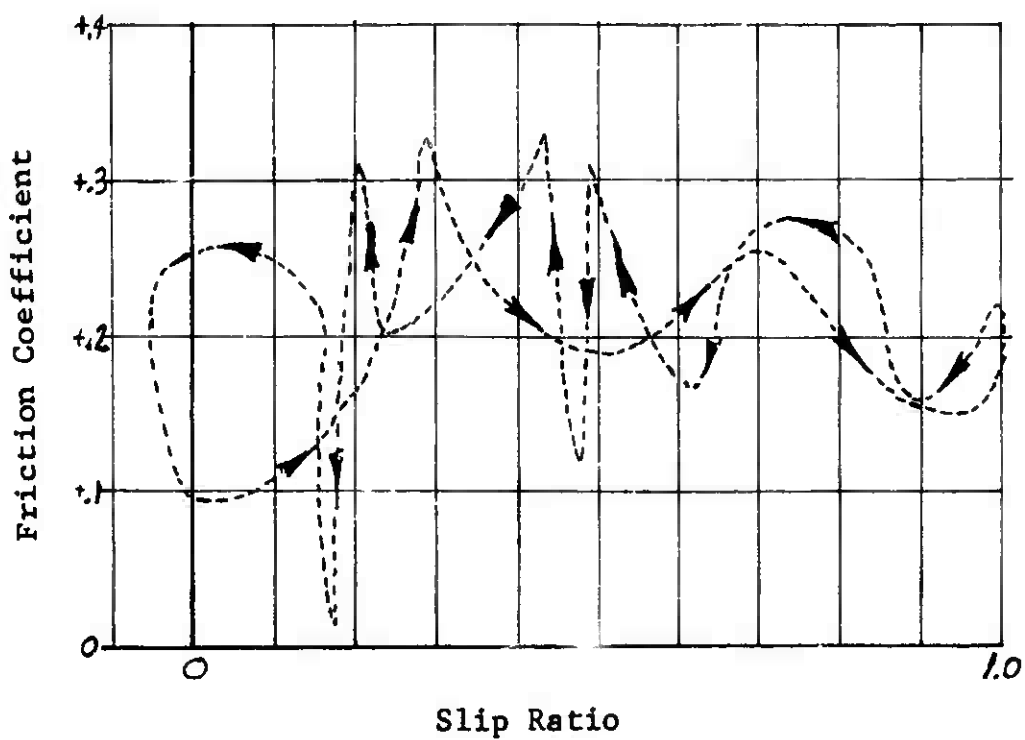
velocity. (3) The function defining the friction coefficient variation with relative velocity is that established by testing a tire in a full skid.

A description of the tire and wheel mathematical model utilizing these assumptions is contained in Section III. The equations listed show that the relative velocity between the tire footprint and runway surface is determined by computing the tread belt's C. G. (center of gravity) translational velocity component parallel to the runway surface and the angular velocity of a point on the tread belt about the C. G. The footprint horizontal velocity component relative to the C. G. is computed from the angular velocity and an apparent rolling radius. The apparent rolling radius is the unbraked rolling radius plus a fraction of the tread belt's C. G. horizontal displacement with respect to the wheel's rotational axis. The net footprint velocity relative to the runway surface is then the sum of the tread belt C. G. translational velocity and the velocity of the footprint relative to the tread belt C. G. The mathematical expression for friction coefficient as a function of relative velocity is of exponential form with coefficients chosen to fit test data.

This model was set up on an analog computer and examined statically and dynamically. Statically, the friction coefficient versus slip ratio (with respect to the wheel) characteristic varies with axle velocity in accordance with observations. This observed variation is that the slip ratio value associated with maximum friction coefficient is greater at low axle velocity than at high axle velocity, and the value of friction coefficient at maximum slip ratio decreases as axle velocity increases. Figure 2A shows friction coefficient versus slip ratio (with respect to the wheel) recorded dynamically during an analog computer run with an ON-OFF antiskid system. Figure 2B is a similar curve recorded dynamically during wheel spinup from a full skid. For both cases shown on Figure 2 axle velocity is constant.



(B) Recorded During Wheel Spin Up



(A) Recorded During On-Off Antiskid Operation

Figure 2 Friction Coefficient Versus Wheel Slip Ratio

C. Hydraulic System Investigation

From experience gained in conjunction with practically all antiskid development programs, it is generally accepted that one of the more predominate influences upon antiskid operation and aircraft stopping performance is the time lag between the antiskid control device's command for a brake torque change and the actual brake torque response. Hydraulic flow restrictions and the response characteristics of the antiskid control valve and other hydraulic system elements are responsible for most of this time lag. In an attempt to minimize the effects of the time lag many antiskid control devices actually issue commands in anticipation of a predicted circumstance. Confident prediction of antiskid overall operational effects including the resultant airplane stopping performance requires that the hydraulic time lag be accurately accounted for. Therefore, to comply with the objectives of this study, a preliminary exploration was conducted to establish a suitable mathematical model permitting evaluation of antiskid control valve and pilot's metering valve response characteristics and such effects as hydraulic line resonant oscillation. During these explorations the operation of the pilot's metering valve, antiskid control valve and the hydraulic line connecting the control valve to the brake were examined. In each case several different mathematical descriptions were formulated and investigated on an analog computer.

For both the pilot's metering valve and antiskid control valve mathematical descriptions accounting for all component characteristics of an actual physical device and simpler descriptions eliminating spool mass considerations were examined. While by suitable choice of parameter values either mathematical model can produce an accurate description, the second order equations resulting from consideration of spool mass cause analytical difficulty because the inertia is very small in comparison with hydraulic pressure and spring forces. These very high gain second order systems necessitate very rapid integration; therefore, using the "massless" first order equations is highly desirable to achieve

computation economy. In Section III the pilot's metering valve description (a part of the hydraulic system) is the simpler first order system while the control valve equations account for spool mass. This approach is taken to permit easy recognition of the relationship between the control valve's physical construction and its performance characteristics. While having the same facility for the metering valve is desirable, it was considered analytically too extravagant. A metering valve having satisfactory performance, by whatever physical means it is achieved, will exhibit behavior in accordance with the "massless" equation.

To explore hydraulic line resonant oscillation and "water hammer" effects, a ten element hydraulic line model (ten degree of freedom) was initially formulated and examined on an analog computer with On-Off antiskid operation at one hundredth real time. This model produced very excellent results; however, the low intensity of the higher frequency harmonics (above 100 cps) showed that a more simplified model would probably be satisfactory. Accordingly, a single degree of freedom model was formulated and tested in the same manner as the ten element model. For the purpose of antiskid evaluation, the single degree of freedom model gave satisfactory results and is described in Section III.

SECTION III

DEVELOPMENT OF MATHEMATICAL MODELS

This section is devoted to the exposition of mathematical models for each of the following total system components:

1. Brake System
2. Hydraulic System
3. Airplane System
4. Wheel and Tire System
5. Wheel Speed Sensor
6. Antiskid Control Circuit
7. Antiskid Control Valve
8. Horizontal Tail Control
9. Runway System

For some of the system components alternate models are provided. These alternate models are listed alphabetically within each section. For example, 3a describes an airplane system modeled as a laboratory flywheel, 3b describes an airplane which has three degrees of freedom, and 3c describes an airplane with six degrees of freedom. Each component model is discussed as a self-contained unit without any particular reference to the total system and each model, in general, contains its complete mathematical description such that it is essentially immune to changes within other models of the total system.

Format and Convention Usage

The presentation of the various systems follows a common format. Each system discussion begins with an introductory explanation of its function or its characteristics relevant to antiskid operation. Following this introduction is the main body of the discussion under the heading, "A. Mathematical Description," containing the derivation of the equations that describe the system dynamically. This section is concluded with an equation flow diagram showing the relationship among the various system equations. A final discussion follows under the heading, "B. Parameter Evaluation," which sets forth methods of determining the values of the constants appearing in the system equations. The system presentation

closes with a "Table of Parameters" which lists all of the system variables and constants.

The flow diagram which appears at the end of Section A is provided principally as an aid in the preparation of the digital computer program which solves the system equations. This flow diagram could also be used for an analog solution although other flow diagram arrangements would be more efficient for that purpose. The following conventions apply as to the usage of the flow diagrams: The triangles outside the enclosing phantom line denote variables which are used as inputs and outputs to other systems. The numbered rectangles refer to equations within the system. As an example, in Figure 5 the rectangle numbered 9 indicates that $T_{\theta r}$ is a function of u_B and F_a and that the equation that gives the exact relationship is equation 1.9. No constants are shown in these diagrams. The triangles denoting integrators do not always contain an equation number. If the input to an integrator is \dot{x}_p and its output is x_p , then the equation is implied. Thus, as in Figure 63, if the input to an integrator is R_4 and the output is u_{R4} , then the equation $u_{R4} = \int R_4 dt$, or equivalently, $\dot{u}_{R4} = R_4$, is implied. Because of the size of the six degree airplane system, the flow diagram in Figure 32 is slightly different. Its use is strictly limited to the digital program generation. It says that all equations within one block must be written before proceeding to the next block. Thus, the first variables to be solved for are Z_{SN} , Z_{SN} , Y_{DLN} , ..., S_{ML} . After this F_{W} , F_{LN} , ..., Z_{GLR} are solved for. After this \dot{x}_{AAL} , \dot{x}_{AAL} , ..., F_{NN} etc.

The "Table of Parameters" is a listing of all variables and constants found in the equations of that system. Each variable is identified by its symbol, description, units, and "Type." The "Type" is listed as v, v(i), and v(o) depending on whether the variable is only used within the system, is received as an input from another system, or is an output to another system. Each constant is identified by its symbol, units, description, "type," and value. The "type" for each constant is always "c" and its value is that used with the F-111 antiskid system.

Table 1 lists the mathematical conventions utilized throughout this study.

Table 1 Explanation of Mathematical Convention

Convention	Description
\dot{x}	A dot over a variable denotes differentiation with respect to time.
Computer Notation	All variables are expressed in a form to harmonize with Fortran character utilization. Thus a variable w_{TK} would appear as WTE. Also, in general, the following practice is adhered to. If x_{TT} is a variable, then XTT is its Fortran form. The symbol for \dot{x}_{TT} is XTTD. The symbol for \ddot{x}_{TT} is XTDD. The initial condition is denoted by adding 0 (zero). Thus \dot{x}_{TT} at time = 0 is denoted by XTDO.
$Z_{GD} \langle \alpha \rangle$	The brackets " $\langle \rangle$ " are used exclusively to denote the position of a function argument. The script α is used to denote an arbitrary variable. The parentheses " $()$ " are normally used to denote multiplication.
Parameter Type	<p>Within each table of parameters is a column which lists the parameter "type."</p> <p>V a variable</p> <p>C a constant</p> <p>V(o) a variable used as output to another system.</p> <p>V(i) a variable received as an input from another system.</p>

Table 1 Explanation of Mathematical Convention

Convention	Description
$I, i, \Theta, O, 2, Z$	<p>For symbols appearing in equations the following conventions are used.</p> <p>I = Capital "i"</p> <p>i = One</p> <p>Θ = Capital "Oh"</p> <p>O = Zero</p> <p>Z = Capital "zee"</p> <p>2 = Two</p> <p>Θ = Greek letter "Theta" but is treated in Fortran as capital Θ.</p>
$ T_{ST} $	<p>Placing a parameter symbol between two vertical bars denotes the absolute value of the parameter. The absolute value of a signed number N is defined as N when N is positive and as $-N$ when N is negative. For example: $3 = 3$ and $-3 = 3$.</p>
$\text{MIN} \{ X_1, X_2, \dots, X_n, C_i \}$ OR $\text{MAX} \{ X_1, X_2, \dots, X_n, C_i \}$	<p>The braces preceded by "MIN" or "MAX" denote the value of the least (or largest) of the constant or the parameters enclosed within the braces.</p>

1. BRAKE SYSTEM

The conventional airplane brake consists of a series of discs which are alternately stators and rotors. The stators are restrained from rotating about the axle by splines or keyways. The rotors are similarly connected to the wheel and hence rotate with the wheel and tire. The brake torque is produced by axially compressing the disc stack; usually by hydraulically actuated pistons. Many brakes use return springs to release the brake stack against the return pressure of the hydraulic system.

A. Mathematical Description

In this analysis X_p will denote the brake piston linear displacement. The pistons, rotors, and stators are treated as a single mass system in the axial mode (X_p direction). The forces acting on the brake mass in the axial mode are:

- a. Brake actuation force: equals (brake pressure) x (piston area)
- b. Force due to axial restraint
- c. Keyway friction force
- d. Brake piston seal friction force
- e. Brake return spring force
- f. Brake piston bottoming force

Figure 3 shows the brake system and the forces acting in the axial mode. Each of the axial forces is established as follows:

a. Brake Actuation Force

The brake actuation pressure P_0 is received as an input from the hydraulic system. The brake actuation force is given by $P_0 A_{BP}$, where A_{BP} is the total brake piston area.

b. Force due to Axial Restraint

The axial restraining force reflects the elasticity in the brake discs, the back plate, and the piston housing and is a function of their cumulative displacements. A way to derive this characteristic is from a curve of brake volumetric displacement vs. brake pressure. This characteristic does not include friction or return spring effects.

Let F_p denote the force due to axial restraint. And be defined by

$$(1.1) F_B = F_{B1} + F_{B2}$$

$$(1.2) F_{B1} = \begin{cases} C_{B1}(X_p - S_{B1}) + D_{B1}\dot{X}_p & \text{if } X_p \geq S_{B1} \\ 0 & \text{if } X_p < S_{B1} \end{cases}$$

$$(1.3) F_{B2} = \begin{cases} C_{B2}(X_p - S_{B2}) + D_{B2}\dot{X}_p & \text{if } X_p \geq S_{B2} \\ 0 & \text{if } X_p < S_{B2} \end{cases}$$

c. Keyway Friction Force

Let the keyway friction characteristic be defined by a function, G_F , where:

$$(1.4) G_F = \begin{cases} 1.0 & \text{if } \dot{X}_p \geq V_{FS} \\ G_{FM} + (1 - G_{FM})\dot{X}_p/V_{FS} & \text{if } V_{FS} > \dot{X}_p > 0 \\ 0.0 & \text{if } \dot{X}_p = 0 \\ -G_{FM} + (1 - G_{FM})\dot{X}_p/V_{FS} & \text{if } 0 > \dot{X}_p > -V_{FS} \\ -1.0 & \text{if } -V_{FS} \geq \dot{X}_p \end{cases}$$

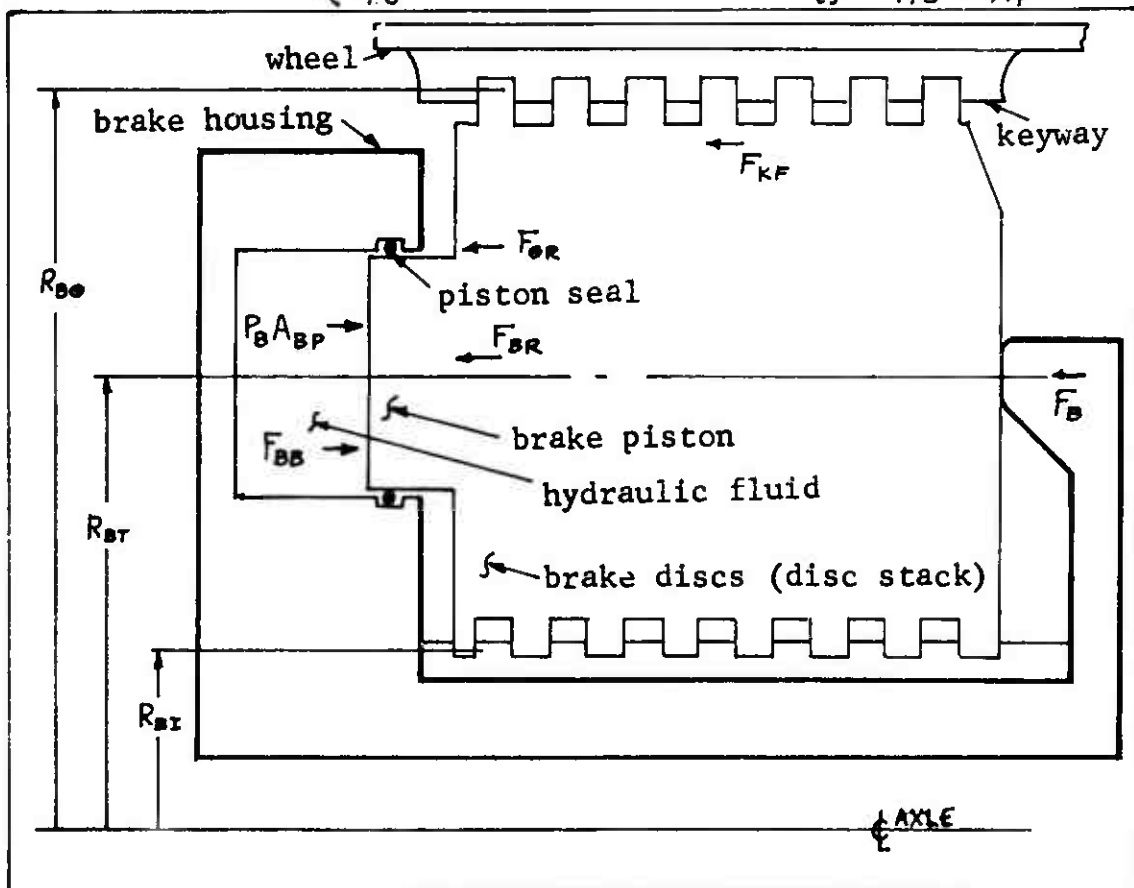


Figure 3 Forces Acting on the Brake Discs

Figure 4 shows G_F as a function of \dot{X}_P

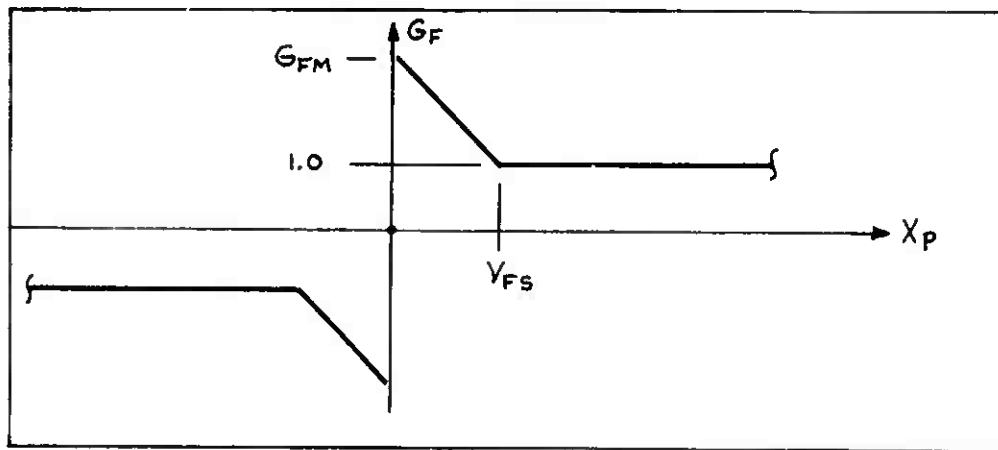


Figure 4 Keyway Friction Characteristic

The brake torque, T_{BT} , is transferred to the wheel and tire through the rotor keyways. Torque, T_{BT} , is also transmitted to the axle. The major portion is transmitted through the stator keyways. The remaining portion of the torque is transmitted as piston side loading which results from friction between the pistons and the pressure plate. Let $100 H_{B1}$ denote the percentage of brake torque transferred through the stator keyways and let $100 H_{B2}$ denote the percentage of torque transferred through the pistons. Naturally, $H_{B1} + H_{B2} = 1$. The normal force on the stator keys is thus $H_{B1}|T_{BT}|/R_{B1}$, while the normal force on the rotor keys is $|T_{BT}|/R_{B2}$. The total keyway friction force is then given by

$$(1.5) \quad F_{KF} = |T_{BT}| G_F \mu_K (H_{B1}/R_{B1} + 1/R_{B2})$$

d. Brake Piston Seal Force

Let F_{OR} denote the seal friction force. Then

$$(1.6) \quad F_{OR} = G_F (H_{OFC} + H_{OFP} P_B + |T_{BT}| \mu_{KP} H_{B2}/R_{BT})$$

e. Brake Return Spring Force

The piston return force F_{BR} is given by

$$(1.7) \quad F_{BR} = F_{BR0} + C_{BR} X_P$$

f. Brake Piston Bottoming Force

In the brake released condition, an axial force is developed between the pistons and housing to balance return spring preload. This piston bottoming force is defined as:

$$(1.8) \quad F_B = \begin{cases} -C_{BB}(X_P - S_{BB}) - D_{BB} \dot{X}_P & \text{FOR } X_P \leq S_{BB} \\ 0 & \text{FOR } X_P > S_{BB} \end{cases}$$

This concludes the discussion of the axial brake forces.

Let R_{NR} be the number of rotors. Let W_B be the relative angular velocity between the rotors and stators as received from the wheel and tire system. The brake torque T_{BT} is then given by

$$(1.9) \quad T_{BT} = 2 R_{NR} F_B R_{BT} \mu_B$$

Where μ_B is:

$$(1.10) \quad \mu_B = \begin{cases} \mu_{B1} + \mu_{B2} e^{-\alpha_B V_B} & \text{IF } V_B > 0 \\ 0 & \text{IF } V_B = 0 \\ -\mu_{B1} - \mu_{B2} e^{-\alpha_B V_B} & \text{IF } V_B < 0 \end{cases}$$

Where V_B is:

$$(1.11) \quad V_B = R_{BT} \dot{W}_B$$

Summing the forces in the axial direction yields:

$$(1.12) \quad W_{BE} \ddot{X}_P = P_B A_{BP} - F_B - F_{KF} - F_{BR} - F_{ER} + F_{BB}$$

In Equation (1.12) W_{BE} is the brake mass which experiences axial motion. Generally, W_{BE} is the brake heat sink mass. Figure 5 shows the relationship of the brake system equations. Table 2 lists the system parameters.

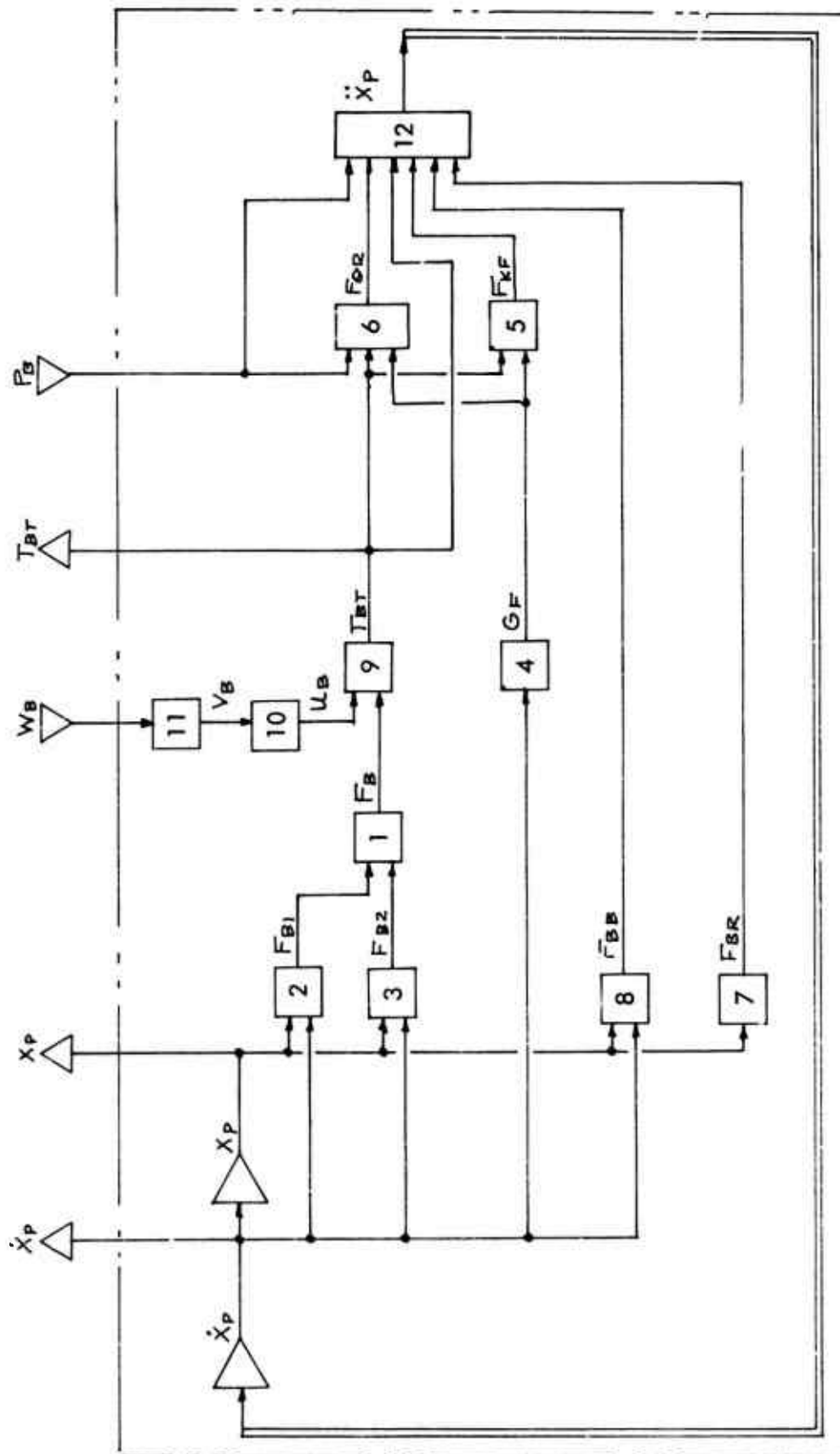


Figure 5 Brake System Equation Flow Diagram

B. Parameter Evaluation

Figure 6 shows a plot of brake piston displacement as a function of brake application pressure for a new brake.

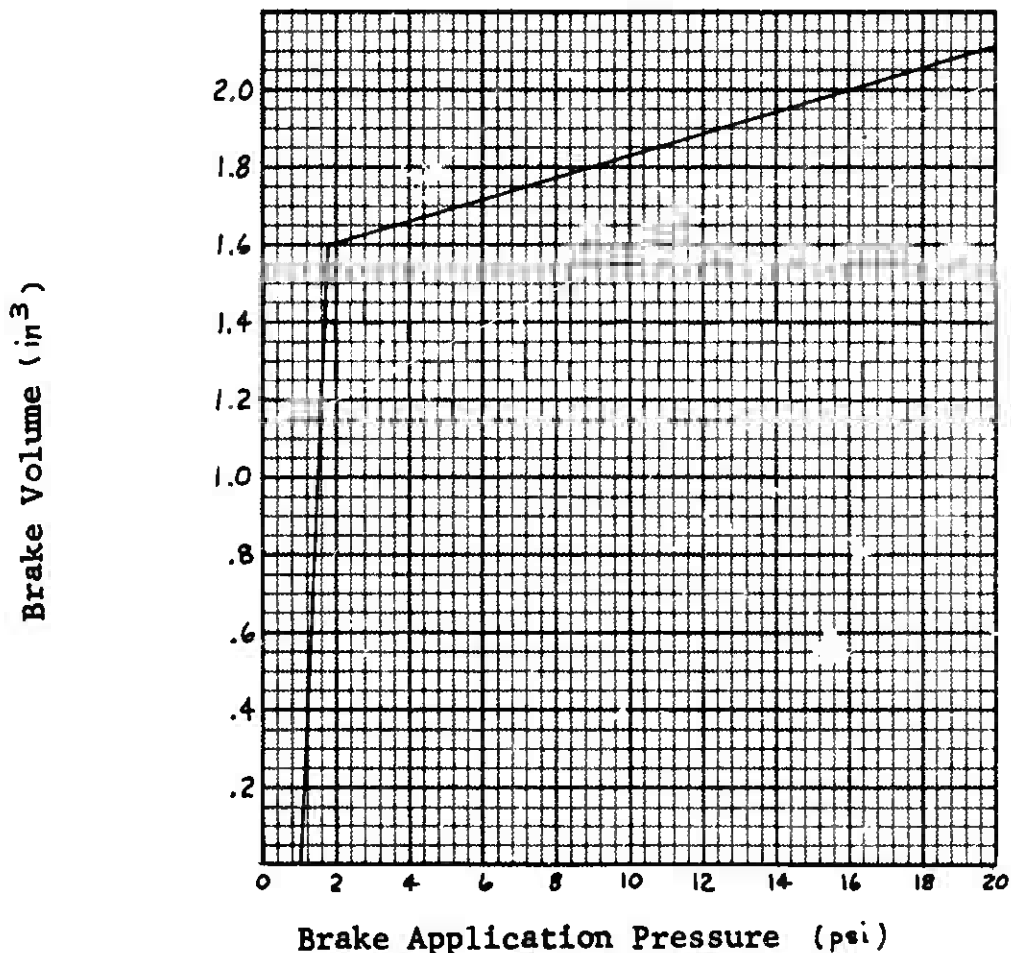


Figure 6 Brake Pressure Volume Characteristic

Assuming that no frictional effects are present, C_{BR} and C_{B1} can be derived as follows: Since the initial slope is due to spring return force only, then

$$(1.13) C_{BR} = \left(\frac{\Delta P}{\Delta V} \right) A_{BP}^2 = \left(\frac{80}{1.6} \right) (13.3)^2 = 8850 \text{ lb/in}$$

From the other slope on the curve,

$$(1.14) C_{B1} = \left(\frac{\Delta P}{\Delta V} \right) A_{BP}^2 = \left(\frac{1420}{.4} \right) (13.3)^2 - 8850 = 6.20 \times 10^5 \text{ lb/in}$$

For a new brake $C_{B2} = 0$.

Assuming that the discs all move together, since the heat sink weight is 138 LBM, then $W_{BE} = 138/386 = .358$ LBF SEC²/IN. The natural frequency is then $\omega_n = \sqrt{k/m}$
 OR $\omega_n = \sqrt{(6.2 \times 10^5)/(1.358)} = 1315$ RAD/SEC
 Assuming that $\eta = .01$ (see page 117),

$$(1.15) \quad D_{B1} = \frac{\eta C_{B1}}{\omega_n} = \frac{(.01)(6.2 \times 10^5)}{(1315)} = 4.71 \text{ lbf sec/in}$$

It is assumed that $X_p = 0$ when the brake pressure is 100 psi. Thus

$$(1.16) \quad F_{BPO} = A_{BP} P_B = (13.3)(100) = 1330 \text{ lbf}$$

Since the brake piston displacement is 1.55 IN³ before the brake discs come into contact, then $S_{B1} = 1.55/13.3 = .1165$ in.

Since the F-111 brake has 8 stators with 14 rubbing surfaces, H_{B1} cannot be greater than 1/14. A conservatively high value of $H_{B1} = .05$ has been assumed and it follows that $H_{B2} = .95$.

The brake piston seals are equivalent to MS28775-219. The seal friction force is established using the procedures described in Reference 4. The seal sliding friction force is a function of rubber compound hardness, amount of installed compression, length of rubbing surface, seal groove projected area and applied hydraulic pressure. For the MS28775-219 size seal having 10 percent installed compression and 70 degree Shore A hardness the sliding friction force is 2.88 lbf plus 0.02 lbf per psi applied pressure per seal. There are 10 pistons in the brake housing; therefore,

$$(1.17) \quad H_{OFC} = (10)(2.88) = 28.8 \text{ lbf}$$

$$(1.18) \quad H_{OFP} = (10)(0.02) = 0.20 \text{ lbf/psi}$$

Conservatively high values for the friction coefficients μ_K and μ_{KP} are estimated as $\mu_K = .15$ and $\mu_{KP} = .10$. G_{FM} is estimated to be 1.50.

Values for the following brake dimensional characteristics are then from the appropriate brake component drawings:
 $R_{BT} = 4.40$ IN, $R_{BT} = 6.25$ IN, and $R_{BD} = 8.25$ IN.

Observations of braking stops indicate that for an average F-111 brake lining,

$$u_{B1} = .15$$

$$u_{B2} = .10$$

$$\alpha_B = .03 \text{ SEC/IN}$$

Table 2 Brake System Parameters

SYMBOL	TYPE	VALUE	UNITS	DESCRIPTION
A_{BP}	C	13.3	IN	Piston area per brake
α_B	C	0.03	SEC/IN	Brake lining friction parameter
C_{B1}	C	6.2×10^5	LB/IN	} Brake Disc spring rate characteristic
C_{B2}	C	0.0	LB/IN	
C_{BB}	C	1.0×10^5	LB/IN	Bottoming spring rate
C_{BR}	C	8850.	LB/IN	Return spring rate
D_{B1}	C	4.71	LB SEC/IN	} Brake Disc damping coeff.
D_{B2}	C	0.0	LB SEC/IN	
D_{BB}	C	400.	LB SEC/IN	Bottoming damping coeff.
F_B	V		LB	Force between brake plates
F_{B1}	V		LB	} $F_B = F_{B1} + F_{B2}$
F_{B2}	V		LB	
F_{BB}	V		LB	Bottoming Force
F_{BR}	V		LB	Return Force
F_{BQ0}	C	1330.	LB	Return force when $X_p = 0$
F_{KF}	V		LB	Keyway friction force
F_{OR}	V		lb	"O-ring" friction force
G_F	V			Friction breakout function to
G_{FM}	C	1.50	Dimensionless	Ratio of breakout friction to running friction
H_{B1}	C	0.05	Dimensionless	Fraction of brake torque removed by stator keys
H_{B2}	C	0.95	Dimensionless	Fraction of brake torque removed thru pistons
H_{OFC}	C	28.8	LBF	} O-ring friction
H_{OFFP}	C	0.20	LBF/PSI	

Table 2 (Continued)

SYMBOL	TYPE	VALUE	UNITS	DESCRIPTION
P_b	v (i)		LB/IN	Brake pressure
R_{s1}	c	4.40	IN	Radius to center of press on stator key
R_{s2}	c	8.25	IN	Radius to center of press on rotor key
R_{s3}	c	6.25	IN	Radius to piston centers
R_{nr}	c	7	Dimensionless	Number of rotors
S_{b1}	c	.1165	IN	Displacement of piston to engage C_{b1}
S_{b2}	c	0.0	IN	Spring Rate Displacement of piston to engage C_{b2}
S_{b3}	c	0.0	IN	Spring Rate Value of X_p when bottoming occurs
T_{br}	v (o)		IN LB	Brake torque
U_b	v		Dimensionless	Brake lining friction coeff.
U_{b1}	c	0.15	Dimensionless	Brake lining friction characteristic
U_{b2}	c	0.10	Dimensionless	Friction coeff. of keyways (running)
U_k	c	0.15	Dimensionless	Friction coeff. between pistons and walls (running)
U_{kp}	c	0.10	Dimensionless	Friction coeff. between pistons and walls (running)
V_b	v		IN/SEC	Velocity of brake lining
V_{fs}	c	0.10	IN/SEC	Friction breakout parameter
W_b	v (i)		RAD/SEC	Rotational speed between stators and rotors
W_{b2}	c	0.358	LB SEC / IN	Brake mass
X_p	v (o)		IN	Brake piston displacement
X_{p0}	c	0.0	IN	Brake piston displacement when $t = 0$
\dot{X}_p	v (c)		IN/SEC	Brake Piston Velocity
\dot{X}_{p0}	c	0.0	IN/SEC	Brake piston velocity when $t = 0$
\ddot{X}_p	v		IN/SEC	Brake piston accel.

2. HYDRAULIC SYSTEM

The hydraulic system is the brake actuation power source and is made up of the four components as shown in Figure 7 : the pilot's metering valve, the antiskid control valve, the control line, and the brake piston housing. The pilot's metering valve is a pressure regulator, usually having a mechanical input, which has a steady state output pressure (P_{mv}) at a level commanded by the pilot (P_{com}). The antiskid valve is a pressure regulator which has a steady state output as dictated by the antiskid control device. For a modulated antiskid system, the control valve is a variable pressure servo type regulator and for an ON-OFF antiskid system the control valve is an ON-OFF valve. The control line is simply the fluid transmission line or containment vessel connecting the control valve to the brake housing. The brake housing is a collection of cylinders and pistons which act to compress the brake discs. From a hydraulic system aspect, the control valve is a variable area orifice, where the orifice area is a function of spool position. The control valve spool position is received as an input from computations described in a section devoted to the operation of the control valve.

In the description of the brake actuation system, there are two principal effects which should be accounted for. The first is the time lag which exists between the control valve output pressure (P_{cv}) and the actual brake pressure (P_b). This lag is caused by the fluid's resistance to flow due to inertia and friction and by the brake pressure's dependence upon fluid volume within the pressure cavity. The second effect is the instantaneous brake pressure intensity as influenced by fluid inertia and the combined elasticity of the fluid and the pressure cavity. Rapid valve operation can cause pressure overshoot and oscillation due to "water hammer" effects. This overshoot can cause excessive brake torque and may interfere with proper control valve operation. The pilot's metering valve pressure drop and response characteristics are included in the actuating system description so that these effects upon antiskid operation can be examined. To allow for a variety of brake actuation systems which might be encountered, provision is made to accommodate both hydraulic and pneumatic actuation media. The line connecting the control valve and the brake can be treated as a separate fluid cavity or the effects of its volume may be lumped with the brake as would be appropriate for a short line.

A. Mathematical Description

Figure 8 is a schematic of the brake hydraulic system. The analytical procedures of References 5 and 6 are utilized to mathematically describe the system.

Let P_{COM} denote the brake pressure which is commanded by the pilot and define P_{COM} such that it increases from a minimum value, P_R , (reservoir pressure) to the desired steady state value P_{CP} , as a linear function of time over an interval, T_{CP} , as follows:

$$(2.1) \quad P_{COM} = \begin{cases} T(P_{CP} - P_R)/T_{CP} + P_R & \text{IF } 0 \leq T \leq T_{CP} \\ P_{CP} & \text{IF } T_{CP} < T \end{cases}$$

The metering valve attempts to maintain P_{MV} at the level of P_{COM} . The metering valve spool displacement X_{MV} is defined by equations (2.2) and (2.3).

$$(2.2) \quad V_{MV} = G_{mv} (P_{COM} - P_{MV})$$

$$(2.3) \quad \dot{X}_{MV} = \begin{cases} \min \{ 0, V_{MV} \} & \text{IF } S_{MVU} \leq X_{MV} \\ V_{MV} & \text{IF } S_{MVL} < X_{MV} < S_{MVU} \\ \max \{ 0, V_{MV} \} & \text{IF } X_{MV} \leq S_{MVL} \end{cases}$$

Let $\phi\langle X, Y \rangle$ be a function defined as follows:

(a) For hydraulic fluid

$$(2.4) \quad \phi\langle X, Y \rangle = \text{SIGN}(X - Y) \sqrt{|X - Y|}$$

(b) For compressible pneumatic fluids

$$(2.5) \quad \text{IF } X > Y \text{ and } X \geq Y/R_{CRIT} \quad \text{WHERE } R_{CRIT} = \left[2/(\gamma_a + 1) \right]^{1/(\gamma_a - 1)}$$

$$\phi\langle X, Y \rangle = X \left[1 - (R_{CRIT})^{\frac{\gamma_a - 1}{\gamma_a}} \right]^{1/2} / \left[(R_{CRIT})^{\gamma_a} \right]$$

$$\text{IF } X \geq Y \text{ and } X \leq Y/R_{CRIT}$$

$$\phi\langle X, Y \rangle = X \left[1 - \left(1/X \right)^{\frac{\gamma_a - 1}{\gamma_a}} \right]^{1/2} / \left(1/X \right)^{\gamma_a}$$

$$\text{IF } Y \geq X \text{ and } Y \leq X/R_{CRIT}$$

$$\phi\langle X, Y \rangle = -\phi\langle Y, X \rangle$$

$$\text{IF } Y > X \text{ and } Y \geq X/R_{CRIT}$$

$$\phi\langle X, Y \rangle = -\phi\langle Y, X \rangle$$

Let $A_{MV}(x)$ be defined by:

$$(2.6) \cdot A_{MV}(x) = \begin{cases} A_{MVO} & \text{if } x \geq S_{MVO} \\ \max\{A_{MVL}, x A_{MVO}/S_{MVO}\} & \text{if } x < S_{MVO} \end{cases}$$

Let A_{MVS} and A_{MVR} be defined by:

$$(2.7) A_{MVS} = A_{MV}(X_{MV})$$

$$(2.8) A_{MVR} = A_{MV}(-X_{MV})$$

Then

$$(2.9) Q_S = A_{MVS} \phi(P_S, P_{MV})$$

$$(2.10) Q_R = A_{MVR} \phi(P_{MV}, P_R)$$

Let V_{MNV} be the fluid volume from the output of the metering valve up to the input of the control valve.

Then

$$(2.11) \dot{P}_{MV} = (B_{MV}/V_{MNV})(Q_S - Q_R - Q_{MV} + Q_{CV1})$$

Let $A_{CV}(x)$ be defined by:

$$(2.12) A_{CV}(x) = \begin{cases} A_{CVO} & \text{if } x \geq S_{CVO} \\ \max\{A_{CVL}, x A_{CVO}/S_{CVO}\} & \text{if } x < S_{CVO} \end{cases}$$

Let A_{CVS} and A_{CVR} be defined by

$$(2.13) A_{CVS} = A_{CV}(X_{CV} - S_{CL})$$

$$(2.14) A_{CVR} = A_{CV}(-S_{CL} - X_{CV})$$

Then

$$(2.15) Q_{MV} = A_{CVS} \phi(P_{MV}, P_{CV})$$

$$(2.16) Q_{CVR} = A_{CVR} \phi(P_{CV}, P_{CVR})$$

$$(2.17) \dot{P}_{CVR} = (B_{CVR}/V_{CVR})(Q_{CVR} - Q_{RC} + Q_{CV3})$$

$$(2.18) Q_{RC} = A_{RC} \phi(P_{CVR}, P_R)$$

The volume of the cavity occupied by the brake actuation media is established by equation (2.19) as follows:

$$(2.19) \quad V_B = V_{B0} + A_{BPS} \dot{X}_P$$

Three options for the control line mathematical description are provided to cover a variety of circumstances which may be encountered. The third option is representative of a typical aircraft installation and is used in analyzing the F-111 system.

The first option is for a control line with hydraulic fluid considering volume effects only. This option will not predict 'water hammer' but is satisfactory for many cases, particularly for the case of a short control line 50 inches or less in length. The following equations describe the first option:

$$(2.20a) \quad Q_{CV} = Q_{MV} - Q_{CVR} + Q_{CVZ}$$

$$(2.21a) \quad \dot{P}_{CV} = (B_B/V_B) (Q_{CV} - A_{BPS} \dot{X}_P)$$

$$(2.22a) \quad P_{BI} = P_{CV}$$

$$(2.23a) \quad P_B = P_{BI}$$

$$(2.24a) \quad Q_B = Q_{CV}$$

The following equations are applicable to the second option for the control line using compressible pneumatic fluid.

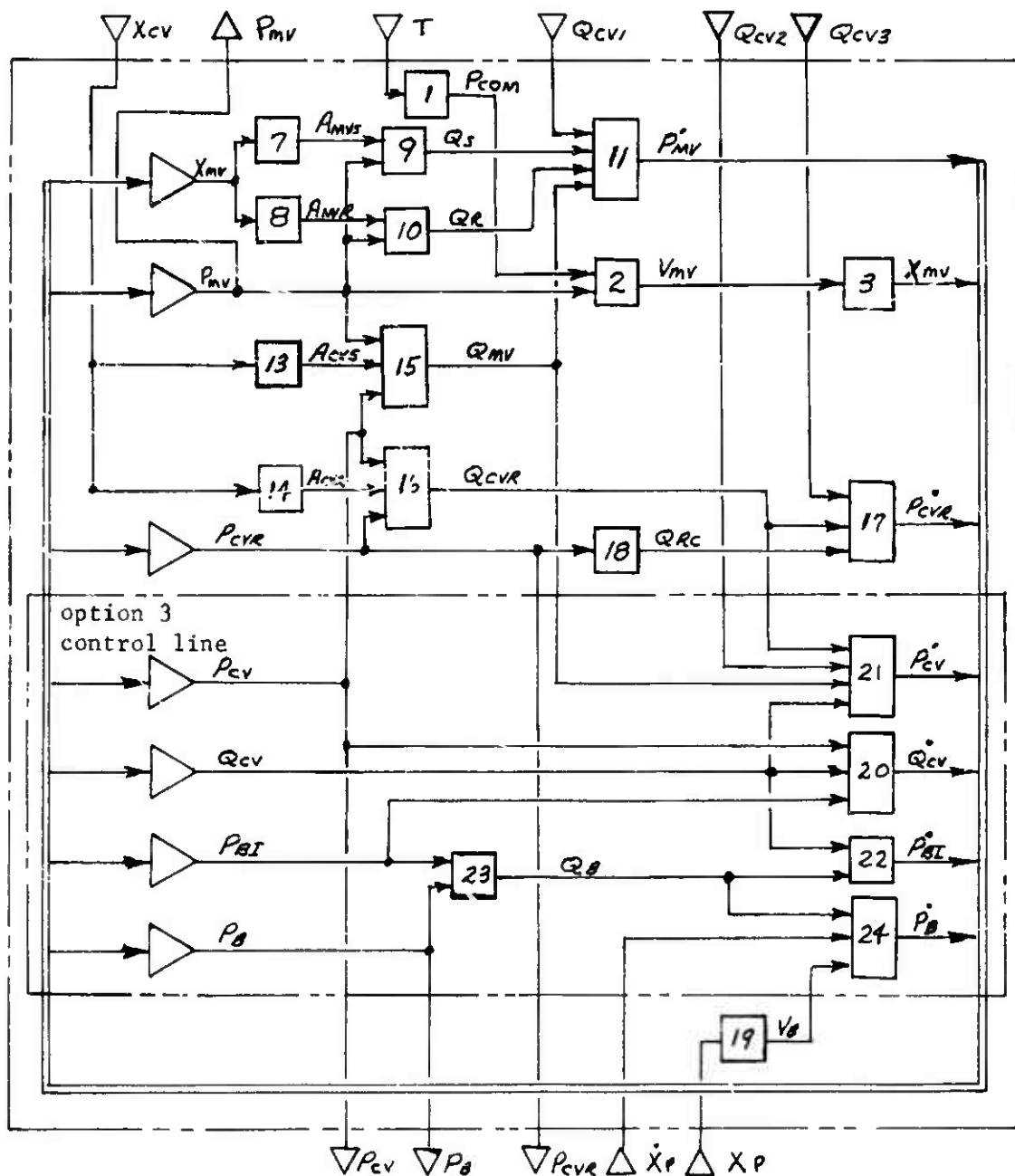
$$(2.20b) \quad Q_{CV} = Q_{MV} - Q_{CVR} + Q_{CVZ}$$

$$(2.21b) \quad \dot{P}_{CV} = (B_B/V_B) (Q_{CV} - P_{CV} A_{BPS} \dot{X}_P / B_B)$$

$$(2.22b) \quad P_{BI} = P_{CV}$$

$$(2.23b) \quad P_B = P_{BI}$$

$$(2.24b) \quad Q_B = Q_{CV}$$



Note: Substitute partial equation flow diagram below for control line options 1 and 2.

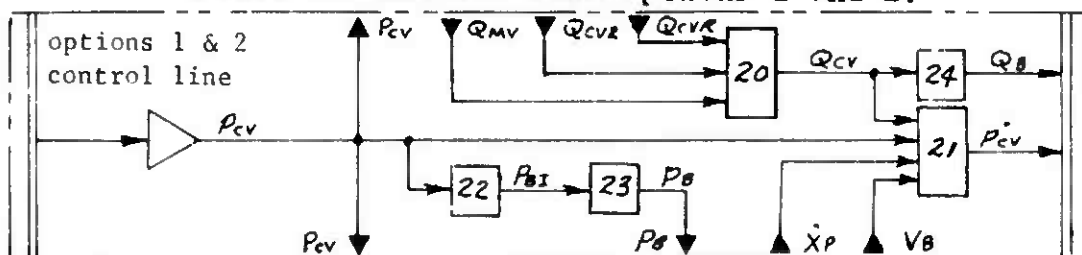


Figure 9 Hydraulic System Equation Flow Diagram

The third option is for a control line with hydraulic fluid where both volume and inertial effects are considered and is described by the following equations:

$$(2.20c) \quad \dot{Q}_{CV} = (A_{BL}/R_{HO} S_{BL}) (P_{CV} - P_{BI} - D_{RBL} Q_{CV} - D_{TBL} Q_{CV} / Q_{CV})$$

$$(2.21c) \quad \dot{P}_{CV} = (B_{BL}/V_{BL}) (Q_{MV} - Q_{CVR} - Q_{CV} + Q_{CV2})$$

$$(2.22c) \quad \dot{P}_{BI} = (B_{BL}/V_{BL}) (Q_{CV} - Q_B)$$

$$(2.23c) \quad Q_B = A_{BO} \phi (P_{BI}, P_B)$$

$$(2.24c) \quad \dot{P}_B = (B_B/V_B) (Q_B - A_{BPS} \dot{X}_P)$$

In this study the brake system hydraulic supply pressure, P_S , is treated as a constant. If P_S varies significantly due to operation of other aircraft hydraulic system equipment, this variable pressure defined as a function of time may be used.

B. Parameter Evaluation

For this study the third optional control line description as applied to the F-111 is of primary interest. For this case MIL-H-5606 hydraulic fluid is used. The hydraulic fluid properties for a mean temperature of 100°F and 1500 psi are:

(1) Adiabatic bulk modulus: $\beta = 248,000$ psi

(2) Density: $R_{HO} = .781 \times 10^{-4}$ LBF SEC²/IN⁴

(3) Kinematic viscosity: $\nu = .0267$ IN²/SEC

The system supply pressure is 3000 psi and the return pressure is 100 psi. Initially, all flows are zero and all pressures except the supply pressure are at 100 psi. The pilot's input command pressure P_{COM} is also 100 psi. The pilot's input P_{COM} will go from 100 to 1500 psi in 0.2 seconds. Thus $T_{CP} = 0.2$ sec and $P_{CP} = 1500$ psi.

Metering Valve

When the metering valve spool is centered, the flow area is essentially zero for both the return and supply lines. In this spool position $X_{MV} = 0.0$. From equation (2.3) the spool is constrained to stay between S_{MVL} and S_{MVU} .

For the metering valve, $S_{mvl} = -.06$ in and $S_{mvo} = .06$ in. However, when X_{mv} is at $+.05$, the valve area has reached its maximum for the flow Q_s . When $X_{mv} = -.05$, the area is maximum for the return flow Q_R . Thus $S_{mvo} = .05$. By actual measurement, with the valve full open (area = A_{mvo}) at 100° F, the flow is $9.23 \text{ in}^3/\text{sec}$. at $200 \text{ psi } \Delta P$. Thus from (2.9) or (2.10),

$$(2.25) \quad A_{mvo} = Q/\sqrt{\Delta P} = 9.23/\sqrt{200} = .653 \text{ in}^4/(\text{sec})(\text{lbf})^{1/2}$$

In the F-111 system, the metering valve is situated next to the control valve so that the volume V_{mv} is quite small. V_{mv} was calculated from the valve drawing as being about 1.0 in^3 . Also, the valve body is considered to be much stiffer than the hydraulic fluid so that the effective bulk modulus is the fluid modulus. Thus, $B_m = 248,000 \text{ psi}$. G_{mv} was estimated from analog studies to be about .05.

Control Valve

For the control valve, $X_{cv} = 0.0$ when the spool is centered. At this point the flow area is zero so that $A_{cvl} = 0.0$. The flow area remains zero for $-.005 \leq X_{cv} \leq .005$. Thus the valve has an overlap of .005 in. and $S_{cvl} = .005$. An additional movement of .030 in. produces full area so $S_{cvo} = .030$. By actual measurement at this position at 100° F, the flow is $7.7 \text{ in}^3/\text{sec}$. at $50 \text{ psi } \Delta P$. Thus

$$(2.26) \quad A_{cvo} = Q/\sqrt{\Delta P} = 7.7/\sqrt{50} = 1.090 \text{ in}^4/(\text{sec})(\text{lbf})^{1/2}$$

The following values are estimates of the return characteristics of the control valve: $V_{cvr} = 2.0 \text{ in}^3$, $B_{cvr} = 248,000 \text{ psi}$, $A_{rc} = 1.0 \text{ in}^4/(\text{sec})(\text{lbf})^{1/2}$.

Control Line

The control line is $1/4$ inch outside diameter steel tubing having 0.14 inch wall thickness and internal cross sectional area, A_{bl} , equal to $.0386 \text{ in}^2$. Because of the thin wall, the tube elasticity greatly reduces the bulk modulus. The equivalent bulk modulus, B_e , may be calculated from

$$(2.27) \quad B_e = B \left(\frac{1}{\left(\frac{B}{E} \right) \left(\frac{D}{t} \right) + 1} \right)$$

Where B = Fluid bulk modulus

E = Young's modulus of tube material

D = Mean tube diameter

t = Tube wall thickness

Thus

$$(2.28) B_{BL} = \frac{248000}{\frac{(.248 \times 10^6)(.236)}{(30 \times 10^6)(.014)} + 1} = 217,700 \text{ PSI}$$

The control/line length, S_{BL} , is 191 inches with various types of flow restrictors according to the following table.

Table 3 Control Line Restrictions

Description	"K" Value*	Number n	nk
An815-4J Union	.54	1	.54
AN832-4J Union	.54	1	.54
AN821-4J Elbow (90°)	1.23	4	4.92
AN837-4J Elbow (45°)	.89	1	.89
90° Tube Bend	.01	12	.12
90° Hose Fitting	1.25	1	<u>1.25</u>
Total			8.26

* $= KV^2/2g$ Where V is the velocity in the line.

The "K" values in Table 3 were derived from information contained in Reference "

Equation (2.20c) is the result of summing forces on the mass of fluid in the control line. The friction losses are depicted by a turbulent flow loss $D_{TBL} Q_{cv}^2$ and a laminar flow loss $D_{LBL} Q_{cv}$. It is assumed that all the turbulent flow losses come from elbows, etc., which are listed in Table 3. The loss due to the line itself is considered to be always laminar. This assumption of laminar flow for

the line is justified for two reasons: (1) the loss in the line is small compared to other losses in the system; (2) the flow is normally laminar anyway (Reynolds Number is less than 6000 for the F-111 system).

For the turbulent losses

$$\begin{aligned}(2.29) \Delta P &= \rho g \Delta h \\ &= K \rho v^2 / 2 \\ &= (K \rho / 2 A^2) Q^2\end{aligned}$$

Thus

$$\begin{aligned}(2.30) D_{TBL} &= \frac{K \rho}{2 (A_{BL})^2} \\ &= \frac{(8.26)(.781 \times 10^{-4})}{2 (.0386)^2} \\ &= .216 \text{ lbf sec}^2 / \text{IN}^3\end{aligned}$$

For laminar losses, at temperatures normally encountered, the "oscillatory" friction is higher than the steady state friction. See Reference 9. The pressure loss can be written as

$$(2.31) \Delta P = R_L (L/A^2) Q$$

For the steady state case as shown in Reference 6,

$$(2.32) R_L = 8 \pi \rho \nu$$

In Figure 10 values for this theoretical steady state R_L are compared over a range of temperatures to values from Reference 9 which were experimentally established for oscillatory flow. Since the hydraulic flow in the brake control line associated with antiskid operation is transitory, the laminar flow resistance base on experimental measurements for oscillatory flow is used.

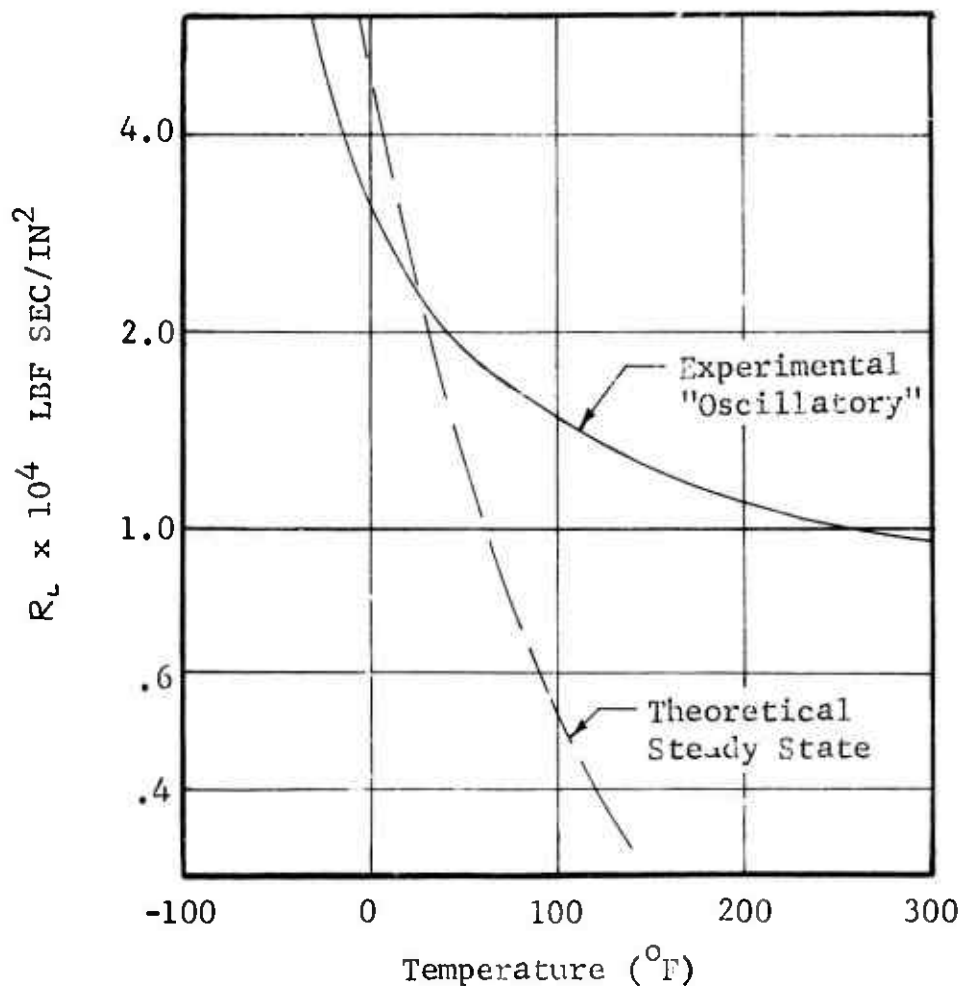


Figure 10 Hydraulic Fluid Damping Characteristic

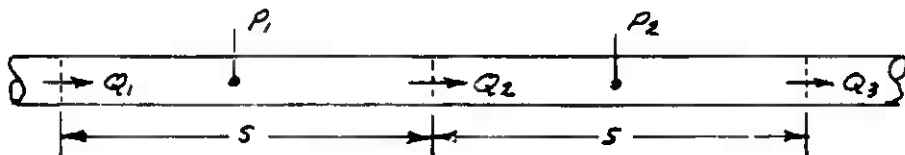
From Figure 10 at 100°F R_L for the experimental oscillatory case is 1.5×10^{-4} LBF SEC/IN²

Therefore:

$$\begin{aligned}
 (2.33) \quad D_{RBL} &= \frac{(R_L)(S_{BL})}{(A_{BL})^2} = \frac{(1.5 \times 10^{-4})(191)}{(.0386)^2} \\
 &= 19.22 \text{ lbf sec/in}^5
 \end{aligned}$$

When a "lumped parameter" type analysis as described by equations (2.20c), (2.21c) and (2.22c) is used for the control line the resulting natural frequency is somewhat lower than the actual line, if the actual line volume, V_{BL} , is used. The value of V_{BL} is adjusted as follows to achieve the correct natural frequency for the "lumped parameter" description.

Consider hydraulic fluid flowing through a line with cross sectional area, A , and divided into segments having equal length, S , as shown below.



If each segment is treated as a separate pressure vessel having volume, V , with a flow in and a flow out, and if equations of the form of (2.20c) (2.21c) and (2.22c) are written for these pressure vessels, neglecting friction, the following expressions are obtained:

$$(2.34) \quad \dot{Q}_2 = (A/\rho S)(P_1 - P_2)$$

$$(2.35) \quad \dot{P}_1 = (B/V)(Q_1 - Q_2)$$

$$(2.36) \quad \dot{P}_2 = (B/V)(Q_2 - Q_3)$$

By substituting equations (2.35) and (2.36) into equation (2.34) differentiated once with respect to time the following differential equation is formed:

$$(2.37) \quad \ddot{Q}_2 = (A/\rho S)(B/V) [(Q_1 - Q_2) - (Q_2 - Q_3)]$$

or

$$(2.38) \quad \ddot{Q}_2 + 2(AB/\rho SV) Q_2 = (AB/\rho SV)(Q_1 + Q_3)$$

Equation (2.38) establishes that the natural frequency of each line segment is:

$$(2.39) \quad f_n = \frac{1}{2\pi} \sqrt{\frac{2AB}{\rho SV}} \quad \text{cps}$$

However, vibration theory considering distributed mass and elasticity establishes the speed of sound, C , in the line as:

$$(2.40) \quad C = \sqrt{B/\rho} \quad \text{in/sec}$$

For fundamental mode oscillation in a closed end tube having length, S , the natural period, T_c , is:

$$(2.41) \quad T_c = 2S/c \quad \text{SEC}$$

Therefore, the natural frequency, g_n , of an actual tube segment is:

$$(2.42) \quad g_n = 1/T_c = (1/2S) \sqrt{B/\rho} \quad \text{CPS}$$

By equating the two expressions for natural frequency, equations (2.39) and (2.42), the volume of the line segment which will have the same natural frequency as the actual is established as:

$$(2.43) \quad V = 2AS/\pi^2$$

Thus,

$$(2.44) \quad V_{BL} = \frac{2}{\pi^2} A_{BL} S_{BL} = \frac{(2)(.0386)(191)}{\pi^2} = 1.495 \text{ in}^3$$

Brake Housing

The brake housing has ten pistons of 1.33 in^2 area each. Since the number of pistons serviced by one control line is five, then $A_{3ps} = 5(1.33) = 6.65 \text{ in}^2$.

The fluid volume in the brake housing with the pistons bottomed ($X_p = 0$) is 8.00 in^3 . Thus $V_{B0} = 4.00 \text{ in}^3$ or one-half the total volume. The orifice coefficient A_{B0} was estimated to be about $2.0 \text{ in}^4/\text{sec lbf}^{1/2}$.

Operational Systems

The option 1 system neglects the line inertial effects. The parameters have the same value as the corresponding parameters for the option 3 system, except that V_{B0} should include any line volume. Thus, for the F-111 system, with the option 1 system, $V_{B0} = 4.00 + .0386(191) = 11.36 \text{ in}^3$.

The option 2 description is used for systems with compressible pneumatic fluid. The appropriate parameters will be evaluated for nitrogen at 100°F as the fluid media and isothermal processes are assumed except for orifice flow calculations. While the heat transfer characteristics of the brake system components have not been rigorously evaluated, the usual component installation is such that assuming isothermal processes is valid. The mathematical description of the brake actuation control system using compressible pneumatic fluid is written using equations of the same general form as for those describing the hydraulic system, thereby minimizing the

the number of equations and enhancing computation flexibility. Utilizing the hydraulic equations when pneumatic fluid is used requires that the appropriate parameters be expressed in suitable mathematically equivalent terms. Consider the characteristic equation of state for a perfect gas:

$$(2.45) \quad P = \frac{MRT}{V}$$

And the definition:

$$(2.46) \quad \frac{dP}{dt} = \frac{\partial P}{\partial m} \frac{dm}{dt} + \frac{\partial P}{\partial V} \frac{dV}{dt} + \frac{\partial P}{\partial T} \frac{dT}{dt}$$

For the assumed isothermal process, substitution of equation (2.45) into equation (2.46) gives:

$$(2.47) \quad \dot{P} = \left(\frac{RT}{V}\right) \dot{m} - \left(\frac{RT}{V}\right) \frac{m}{V} \dot{V}$$

For those cases, such as for the metering valve and control valve pressure cavities, where the volume is not changing, \dot{V} is zero and equation (2.47) reduces to:

$$(2.48) \quad \dot{P} = \left(\frac{RT}{V}\right) \dot{m}$$

For hydraulic fluid, \dot{P} is described by equations having the form of equation (2.49) below. (See equation (2.11) for instance.)

$$(2.49) \quad \dot{P} = \left(\frac{\beta}{V}\right) Q$$

Noting the similarity between equation (2.48) and equation (2.49) it is obvious that if RT is used in place of β and if \dot{m} is used in place of Q , the "Hydraulic" equations can be used for computing performance of a system using pneumatic fluid. Thus, $\beta_B = \beta_{cVR} = \beta_{mV} = RT$.

For nitrogen $R = 662.4 \text{ in lbf/lbm}^\circ\text{F}$ and at 100°F
 $RT = (662.4) (460 + 100) = 371 \times 10^6 \text{ in lbf/lbm.}$

Since $P/RT = M/V$, equation (2.47) can be written as

$$(2.50) \quad \dot{P} = \left(\frac{RT}{V}\right) \left[\dot{m} - \left(\frac{P}{RT}\right) \dot{V} \right]$$

Equation (2.21b) is obtained by substituting β_B for RT , $A_{BPS} \dot{X}_P$ for \dot{V} , and Q for \dot{m} in equation (2.50), thereby accounting for the change in brake volume caused by piston movement.

Equation (2.51) below, from Reference 6, describes the mass flow rate of a gas from a container having high pressure, P_H , through an orifice of area, A_o , to a container having

low pressure, P_L .

$$(2.51) \quad \dot{m} = \left(\frac{C_o A_o}{R} \sqrt{\frac{2GC_p}{T}} \right) P_H \left(\frac{P_H}{P_L} \right)^{1/2} \sqrt{1 - \left(\frac{P_H}{P_L} \right)^{\frac{\gamma-1}{\gamma}}}$$

Equation (2.52) below, from Reference 6, describes the volumetric flow rate of hydraulic fluid through an orifice under similar circumstances.

$$(2.52) \quad Q = C_o A_o \left(\sqrt{2/\rho} \right) \sqrt{P_H - P_L}$$

Both equations (2.51) and (2.52) can be written in the form $Q = A_F \phi(P_H, P_L)$ where $\phi(P_H, P_L)$ is a flow function as defined by equations (2.4) and (2.5) for the appropriate circumstances and where A_F is a flow coefficient accounting for orifice and fluid properties. For the case of hydraulic fluids a value of $C_o \sqrt{2/\rho} = 103.5 \text{ in}^2/\text{lb}^{1/2}\text{sec}$ has been established by experience as being representative of an average orifice (i.e., $C_o \approx 0.65$). The metering valve flow coefficient, A_{mvo} , previously computed is $0.653 \text{ in}^4/\text{sec} \text{ lb}^{1/2}$; therefore, the apparent actual orifice area, A_o , for the metering valve is $A_o = 0.653/103.5 = .631 \times 10^{-2} \text{ in}^2$.

For the case of the pneumatic system with nitrogen at 100°F as the working fluid and using $C_p = 2300 \text{ in} \text{ lb}^{1/2}/\text{lbm}^\circ\text{F}$, and $R = 662.4 \text{ in} \text{ lb}^{1/2}/\text{lbm}^\circ\text{F}$:

$$\begin{aligned} (2.53) \quad A_{mvo} &= \frac{C_o A_o}{R} \sqrt{\frac{2GC_p}{T}} \\ &= \frac{(.8)(.631 \times 10^{-2})}{662.4} \sqrt{\frac{(1.2)(386)(2300)}{560}} \\ &= 0.43 \times 10^{-3} \text{ lbm in}^2/\text{lb}^{1/2}\text{sec} \end{aligned}$$

Using the same procedure establishes that:

$$A_{cvo} = 0.716 \times 10^{-3} \text{ lbm in}^2/\text{lb}^{1/2}\text{sec}$$

$$A_{RC} = 0.658 \times 10^{-3} \text{ lbm in}^2/\text{lb}^{1/2}\text{sec}$$

Table 4 Hydraulic System Parameters

SYMBOL	TYPE	VALUE	UNITS	OP*			DESCRIPTION
				1	2	3	
A_{BL}	c	.0386	IN^2			X	Cross sectional area of brake control line
A_{BS}	c	2.00	$IN^4/SEC \ LBF^{\frac{1}{2}}$			X	Brake housing orifice coefficient
A_{SPS}	c	6.65	IN^2	X	X	X	Brake piston area (per brake line)
$A_{CV}(\alpha)$	f			X	X	X	Control valve flow area function
A_{CVL}	c	0.00	$IN^4/SEC \ LBF^{\frac{1}{2}}$	X	X	X	Control valve leakage flow coeff.
A_{CVO}	c	0.00	$LBM \ IN^2/LBF \ SEC$				
		1.09	$IN^4/SEC \ LBF^{\frac{1}{2}}$	X	X	X	Control valve full open flow coeff.
		$.715 \times 10^{-3}$	$LBM \ IN^2/LBF \ SEC$				
A_{CVR}	v		$IN^4/SEC \ LBF^{\frac{1}{2}}$	X	X	X	Control valve return flow coeff.
A_{CVS}	v		$IN^4/SEC \ LBF^{\frac{1}{2}}$	X	X	X	Control valve supply coeff.
$A_{MV}(\alpha)$	f			X	X	X	
A_{MVL}	c	0.00	$IN^4/SEC \ LBF^{\frac{1}{2}}$	X	X	X	Metering valve flow area function.
		0.00	$LBM \ IN^2/SEC \ LBF$	X	X	X	Metering valve leakage coeff.
A_{MVO}	c	.653	$IN^4/SEC \ LBF^{\frac{1}{2}}$	X	X	X	Metering valve full open flow coeff.
		$.429 \times 10^{-3}$	$LBM \ IN^2/SEC \ LBF$				
A_{MVR}	v		$IN^4/SEC \ LBF^{\frac{1}{2}}$	X	X	X	Metering valve return flow coeff.
A_{MVS}	v		$IN^4/SEC \ LBF^{\frac{1}{2}}$	X	X	X	Metering valve supply flow coeff.
A_{RC}	c	1.00	$IN^4/SEC \ LBF^{\frac{1}{2}}$	X	X	X	Control valve return line restriction.
		$.658 \times 10^{-3}$	$LBM \ IN^2/SEC \ LBF$	X	X	X	
		$.248 \times 10^{-6}$	$LBM \ IN^2/LBF \ SEC$	X	X	X	Bulk modulus within the brake housing.
B_B	c	.371	$IN \ LBF/LBM$	X	X	X	Temp X gas constant.

*See page 37

Table 4 (Contd)

SYMBOL	TYPE	VALUE	UNITS	OP*			DESCRIPTION
				1	2	3	
B_{BL}	c	$.218 \times 10^6$	LBF/IN^2			X	fluid bulk modulus in control line.
B_{CVR}	c	$.248 \times 10^6$	LBF/IN^2	X		X	Fluid bulk modulus in return of control V.
B_{MV}	c	$.371 \times 10^6$	$IN \ LBF/LBM$		X		Temp. X gas constant
D_{BL}	c	$.248 \times 10^6$	LBF/IN^2	X		X	Bulk modulus at metering valve outlet.
D_{TBL}	c	$.371 \times 10^6$	$IN \ LBF/LBM$		X		Temp X gas constant
G_{MV}	c	19.22	$LBF \ SEC/IN^5$			X	Laminar line loss coeff
γ_a	c	.216	$LBF \ SEC^2/IN^8$			X	Turbulent line loss coeff.
P_B	c	.05	$IN^3/SEC \ LBF$	X		X	Metering valve gain
P_{BO}	c	.05	$IN^3/SEC \ LBF$		X		
\dot{P}_B	v(o)	1.40	Dimensionless		X		Ratio of specific heats $\gamma_a = (c_p/c_v)$
P_{BIO}	c	100	LBF/IN^2	X	X	X	Brake Pressure
\dot{P}_B	v		LBF/IN^2	X		X	Brake pressure at time = 0.
P_{BI}	v		LBF/IN^2		X		
P_{BIO}	v	100	$LBF/IN^2 \ SEC$		X	X	Time derivative of brake press.
\dot{P}_{BI}	v		LBF/IN^2	X	X	X	Press. at brake inlet.
P_{CEM}	c	1500	LBF/IN^2	X		X	Brake inlet press at time = 0
P_{CP}	c		LBF/IN^2		X		
P_{CV}	v(o)	100	LBF/IN^2	X	X	X	Time derivative of brake inlet press.
P_{CVO}	c	14.7	$LBF/IN^2 \ SEC$		X	X	Pilot's command press.
\dot{P}_{CV}	v		LBF/IN^2	X	X	X	Steady state command press.
				X	X	X	Control valve output press.
				X	X	X	Control valve press at time = 0.
				X	X	X	Derivative of control valve press.

Table 4 (Contd)

SYMBOL	TYPE	VALUE	UNITS	OP			DESCRIPTION
				1	2	3	
P_{cvr}	v(o)	100	LBF/IN ²	X	X	X	Return press in cont. valve.
P_{cvro}	c	14.7	LBF/IN ²	X	X	X	Return control valve press at time = 0
\dot{P}_{cvr}	c		LBF/IN ²	X	X	X	Return control valve press. time derivative
$\phi(x, y)$	v		LBF/IN ² SEC	X	X	X	Flow function
P_{mv}	f		LBF/IN ²	X	X	X	Metering valve output press.
P_{mvo}	v(o)	100	LBF/IN ²	X	X	X	Metering valve press at time = 0.
\dot{P}_{mv}	c	14.7	LBF/IN ²	X	X	X	Time derivative of metering valve press.
P_r	v	100	LBF/IN ² SEC	X	X	X	Return pressure
P_s	c	14.7	LBF/IN ²	X	X	X	System supply pressure.
Q_B	c	3000	LBF/IN ²	X	X	X	Flow into brake (per line)
Q_{cv}	v		IN ³ /SEC	X	X	X	Flow out of control valve
Q_{cvo}	v	0.0	LBM/SEC	X	X	X	Control valve flow at time = 0
\dot{Q}_{cv}	c		IN ³ /SEC	X	X	X	Time derivative of control valve flow.
Q_{cvi}	v		LBM/SEC	X	X	X	Feedback flows from control valve.
Q_{ci}	v(i)		IN ³ /SEC	X	X	X	
Q_{ci}	v(i)		LBM/SEC	X	X	X	
Q_{cv3}	v(i)		IN ³ /SEC	X	X	X	

Table 4 (Contd)

SYMBOL	TYPE	VALUE	UNITS	OP			DESCRIPTION
				1	2	3	
Q_{CVR}	V		IN ³ /SEC	X		X	Return flow in control valve
Q_{MV}	V		LBM/SEC	X	X	X	Metering valve flow
Q_R	V		IN ³ /SEC	X	X	X	Return flow from metering valve
Q_{RC}	V		LBM/SEC	X	X	X	Return flow from control valve
Q_S	V		IN ³ /SEC	X	X	X	Flow into system
R_{CRIT}	C		LBM/SEC				Critical pressure ratio
R_{HS}	C	#	Dimensionless		X	X	Fluid density
S_{BL}	C	.781X10 ⁻⁴	LBF SEC ² /IN ⁴	X		X	Control line length
S_{CL}	C	.91.0	IN	X	X	X	Control valve overlap
S_{CVO}	C	.005	IN	X	X	X	Spool distance from full closed to full open (C.V)
S_{MVL}	C	.030	IN	X	X	X	Min. Neg. spool travel (met. valve)
S_{MVO}	C	-.060	IN	X	X	X	Spool travel from full closed to full open (met. valve)
S_{MVU}	C	.050	IN	X	X	X	Max. Pos. Spool travel (met. valve)
T	C	.060	IN	X	X	X	Time
T_{CP}	V(i)	.200	SEC	X	X	X	Time for $P_{com} = P_{cp}$
V_B	C	.200	SEC	X	X	X	Brake fluid volume (per line)
V_{BO}	V	4.00	IN ³	X	X	X	Brake fluid volume when $X_p = 0$
V_{BL}	C	1.495	IN ³	X	X	X	Corrected line volume

Calculate from γ_a , see Equation (2.5)

Table 4 (Contd)

SYMBOL	TYPE	VALUE	UNITS	OP*			DESCRIPTION
				1	2	3	
V_{CVR}	C	2.00	IN ³	X	X	X	Control valve return volume.
V_{MV}	V		IN/SEC	X	X	X	Metering valve control variable.
V_{MUV}	C	1.00	IN ³	X	X	X	Volume between metering & control valve.
X_{CV}	V(i)		IN	X	X	X	Control valve spool position.
X_{MV}	V		IN	X	X	X	Metering valve spool position.
X_{MVO}	C	0.0	IN	X	X	X	Metering valve spool position at time=0
\dot{X}_{MV}	V		IN/SEC	X	X	X	Metering valve spool velocity.
X_P	V(i)		IN	X	X	X	Brake piston displacement
\dot{X}_P	V(i)		IN/SEC	X	X	X	Brake piston velocity

*An x denotes application in option 1, 2, or 3 as explained on page 35-37.

Option 1 Brake actuation system using hydraulic fluid where the control line description considers volume effects only.

Option 2 Brake actuation system using compressible pneumatic fluid.

Option 3 Brake actuation system using hydraulic fluid where the control line description considers both volume and inertia effects.

3a AIRPLANE SYSTEM (FLYWHEEL)

Figure 11 shows the model for the airplane system as it might be simulated with a dynamometer flywheel set-up. The mass W_A is supported by the tire and is determined by the percentage of the airplane weight carried on one main gear. The mass W_{AR} represents some part of the airplane structure which could vibrate in sympathy with certain ground discontinuities such as wing mounted fuel tanks or armament. The forces F_{LD} and F_{AL} act on W_A because of gravity and aerodynamic lift, respectively.

A. Mathematical Description

The shock strut stroke is denoted by Z_{SM} . This stroke is determined by Z and Z_{WM} .

$$(3a.1) \quad Z_{SM} = Z_{WM} - Z$$

$$(3a.2) \quad \dot{Z}_{SM} = \dot{Z}_{WM} - \dot{Z}$$

The shock strut force F_{VM} is given by equation (3a.3)

$$(3a.3) \quad F_{VM} = F_{VMS} \langle Z_{SM} \rangle + D_{VM} \dot{Z}_{SM} + A_{VM} \langle \dot{Z}_{SM} \rangle \dot{Z}_{SM} | \dot{Z}_{SM} |$$

Let Z_{GO} and Z_{GDP} denote the height and slope of the ground (or flywheel surface). Let S_M denote the tire deflection. Then S_M and \dot{S}_M are determined by

$$(3a.4) \quad S_M = \max \{ 0.0, Z_{GO} \langle X_F \rangle - Z_{WM} \}$$

$$(3a.5) \quad \dot{S}_M = Z_{GDP} \langle X_F \rangle V_F - \dot{Z}_{WM}$$

The force F_{NM} acting vertically upward on the tire is then given by

$$(3a.6) \quad F_{NM} = S_M (C_{MT} + D_{MT} \dot{S}_M)$$

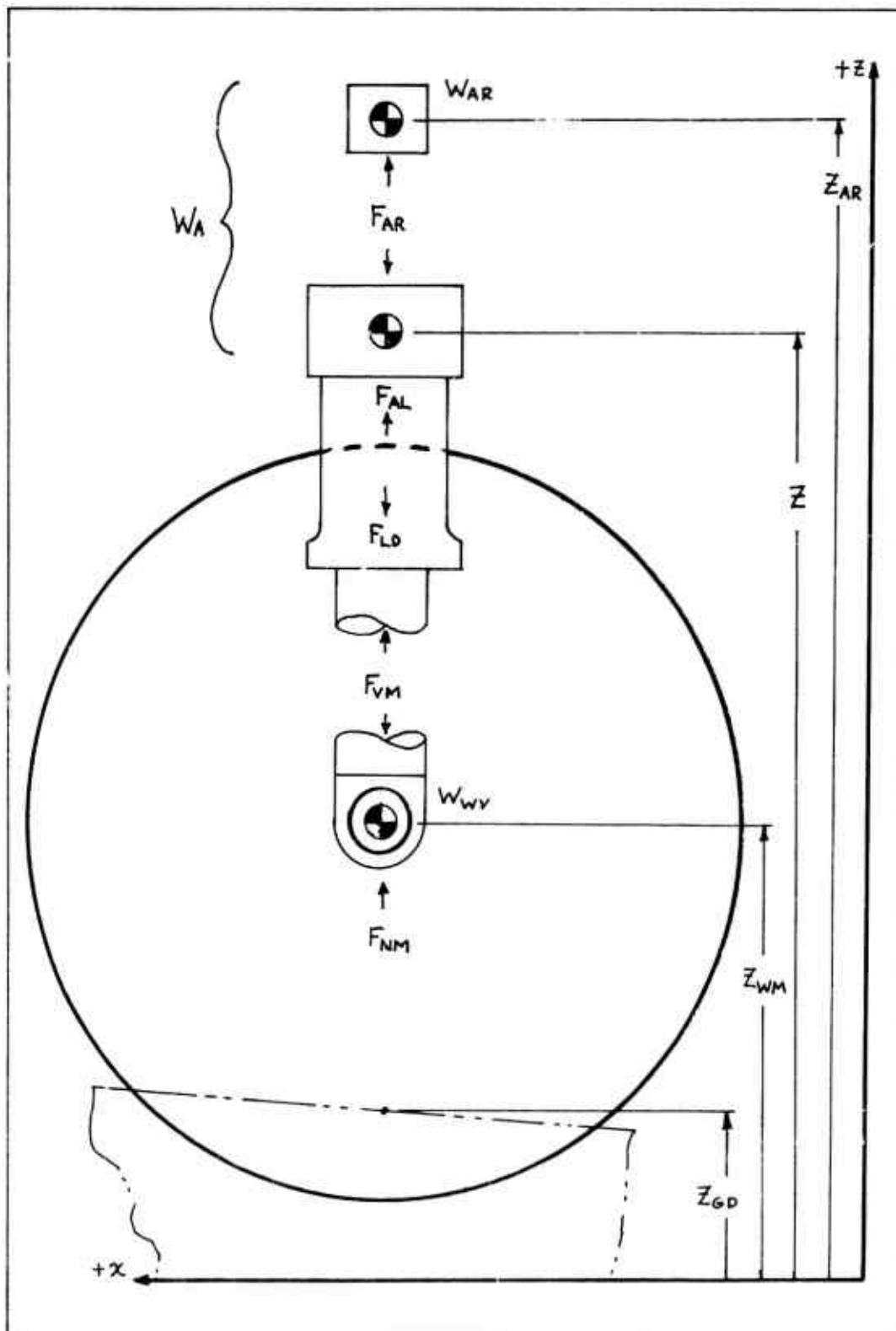


Figure 11 Flywheel System Model

Summing forces in the vertical direction on the unsprung mass W_{WV} , there follows:

$$(3a.7) \quad W_{WV} \ddot{Z}_{WM} = F_{NM} - F_{VM} + F_{ORV}$$

Where F_{ORV} is the tire unbalance force.

For the mass W_{AR} , summing forces vertically gives:

$$(3a.8) \quad W_{AR} \ddot{Z}_{AR} = F_{AR}$$

$$(3a.9) \quad F_{AR} = C_{AR} (Z - Z_{AR}) + D_{AR} (\dot{Z} - \dot{Z}_{AR})$$

The aerodynamic lift and drag forces F_{AL} and F_{AD} are defined as follows:

$$(3a.10) \quad F_{AL} = C_{AL} V_F^2$$

$$(3a.11) \quad F_{AD} = C_{AD} V_F^2$$

The equation which determines Z is given as

$$(3a.12) \quad (W_A - W_{AR}) \ddot{Z} = F_{VM} + F_{AL} - F_{LD} - F_{AR}$$

The equation for the flywheel velocity is given by

$$(3a.13) \quad W_{AT} \dot{V}_F = F_{TH} - F_{AD} - 2 F_{BT}$$

Where F_{TH} is a force equivalent to engine thrust and W_{AT} is the airplane mass. The aircraft's longitudinal displacement is established by

$$(3a.14) \quad X_F = \int V_F dt + X_{F0}$$

The equation flow diagram for the airplane system (flywheel) is shown on Figure 12.

B. Parameter Evaluation

Shock Strut Characteristics

Figures 13 and 14 show the main gear load and damping characteristics for one gear.

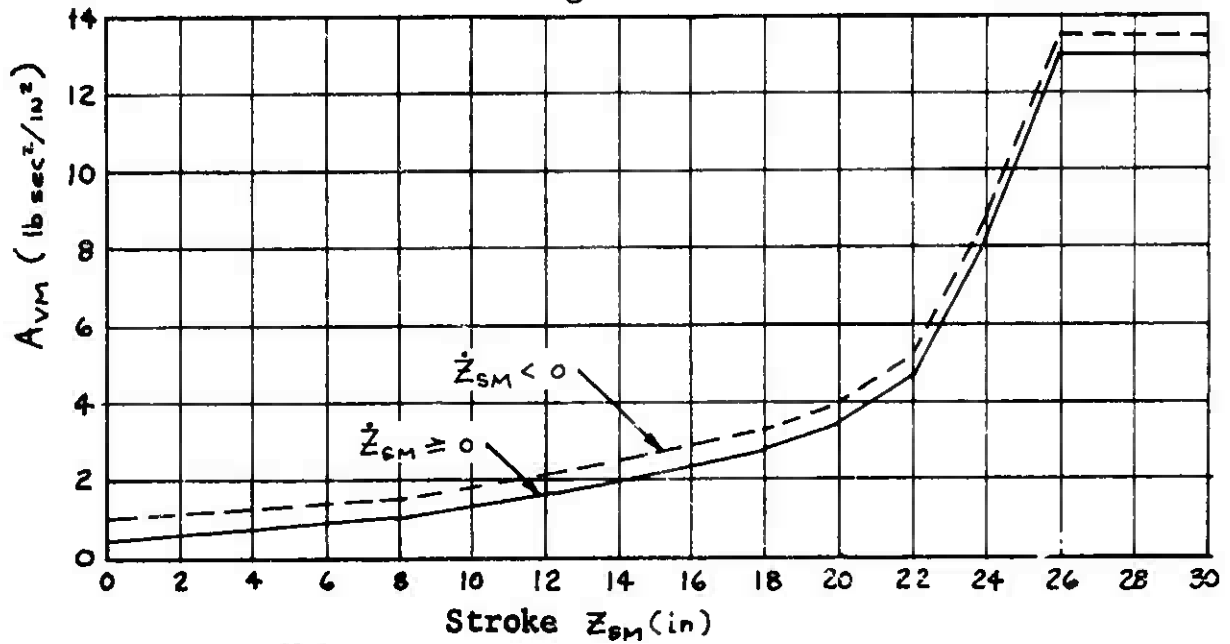


Figure 13 Main Gear Damping Curve

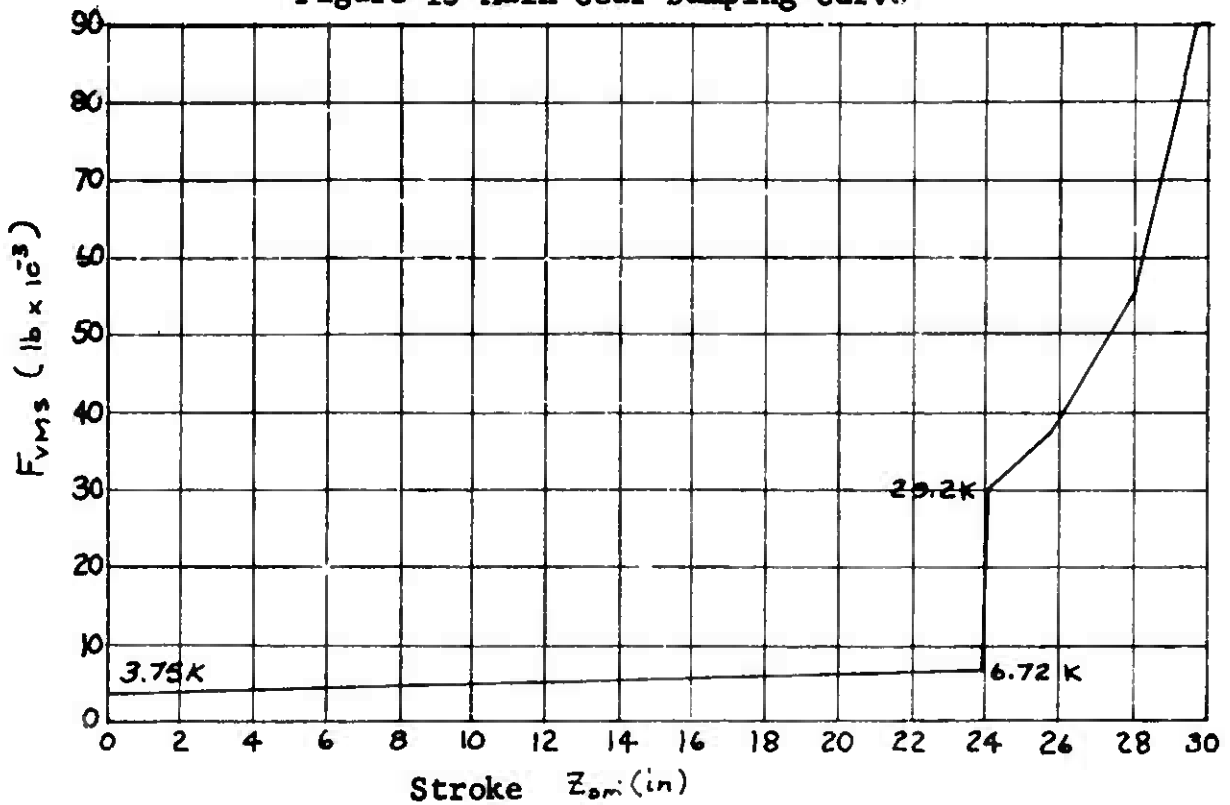


Figure 14 Main Gear Air Load Curve

Vertical Tire Characteristics

In equation (3a.6) it has been assumed that the tire loading characteristic is given by an equation of the form

$$(3a.15) \quad F = S(C + D\dot{S})$$

Let the following terms be defined for a tire:

F_R = Rated load

P_R = Rated pressure

S_R = Rated deflection

If P is the actual pressure, then obviously the tire spring rate, C , is

$$(3a.16) \quad C = \left(\frac{P}{P_R} \right) \left(\frac{F_R}{S_R} \right)$$

From reference 1 (Equation 132) the damping force, F_D , is established as:

$$(3a.17) \quad F_D = \left(\frac{\eta C}{\omega} \right) \dot{S}$$

It is assumed that the damping force is related to the undamped natural frequency at rated conditions. The undamped natural frequency, ω , is established as:

$$(3a.18) \quad \omega = \sqrt{\frac{K}{M}} = \sqrt{\frac{F_R G}{S_R F_R}} = \sqrt{\frac{G}{S_R}}$$

Where $G = 386 \text{ IN/SEC}^2$. Also from Equations 137 and 138 of Reference 1:

$$(3a.19) \quad \eta = 2 \eta_R / [1 + (P/P_R)]$$

Where $\eta_R = 0.1$.

The main landing gear shock strut linear damping coefficient, D_{VM} , is set equal to zero for the example problem.

The unsprung mass, W_{wv} , experiencing vertical motion is 6.44 lbm. Thus, $W_{wv} = (644)/386 = 1.667 \text{ lbf sec}^2/\text{in}$.

As previously assumed in Equation (3a.15), $\dot{F}_0 = S D \dot{S}$
Equating the two expressions for \dot{F}_0 at rated deflection

$$(3a.20) \quad \frac{\eta C}{\omega} = S_R D$$

Or

$$(3a.21) \quad D = \frac{\eta C}{\omega S_R} = \frac{\eta F_R}{(S_R)^2} \left(\frac{P}{P_R} \right) \sqrt{\frac{S_R}{G}}$$

For the 47 x 18 - 18 26 ply rating F-111 main tire,
 $P = P_R = 150$ psi

$F_R = 38,100$ lb. and $S_R = 4.00$ IN.

Thus

$$(3a.22) \quad C_{MT} = \left(\frac{P}{P_R} \right) \left(\frac{F_R}{S_R} \right) = \frac{(150)(38100)}{(150)(4.00)} = 9530 \text{ lbf/IN}$$

$$(3a.23) \quad D_{MT} = \left(\frac{P}{P_R} \right) \left(\frac{\eta F_R}{S_R^2} \right) \sqrt{\frac{S_R}{G}}$$

$$= \frac{(150)}{(150)} \frac{(.1)(38100)}{(4.00)^2} \sqrt{\frac{4.0}{386}} = 24.24 \text{ lbf sec/IN}^2$$

Aircraft Characteristics

For the example problem, an airplane weight of 57,000 lb. is used. The static vertical load on one main gear is 25,200 lbs. so that

$$(3a.24) \quad W_A = 25,200/G = 65.0 \text{ lbf sec}^2/\text{IN.}$$

For a velocity of $V_F = 2400$ IN/SEC and a representative tire-to-runway braking coefficient of .45 at the main wheel, the tire load is 21,400 lbs. Thus $F_{LD} = 21,400$ lb.

The total aircraft mass is $W_{AT} = 57000/G = 147.8 \text{ lbf sec}^2/\text{IN.}$

The mass W_{AR} is used to simulate some airplane resonant effect. For illustrative purposes, it is assumed that $W_{AR} = 1000 \text{ LBM} = 2.59 \text{ LBF SEC}^2/\text{IN}$ and has a natural frequency of 12 cps. Therefore, since $\omega = 2\pi(12) = 75.4 \text{ rad/sec}$ and $k = m\omega^2$,

$$(3a.25) \ C_{AR} = \omega^2 W_{AR} = (75.4)^2 (2.59) = 14,720 \text{ lb/in}$$

Using 3 percent critical damping gives

$$(3a.26) \ D_{AR} = (.03) 2 \sqrt{C_{AR} W_{AR}} = \\ = (.03) 2 \sqrt{(14,720)(2.59)} = 11.72 \text{ lb sec/in}$$

The initial conditions are calculated for equilibrium. At time = 0, let $X_F = 0$ so that $Z_{GD} \langle X_F \rangle = 0$ since $Z_{GD} \langle 0 \rangle$ is always 0. Let $V_{FO} = 1200 \text{ IN/SEC}$ and assume that $C_{AL} = C_{AD} = 0$

From equation (3a.6),

$$(3a.27) \ S_m = F_{NM} / C_{MT} = 21,400 / 9530 = 2.245 \text{ in}$$

From equation (3a.4),

$$(3a.28) \ Z_{WMO} = -2.245 \text{ in.}$$

From figure 14, when $F_{VMS} = 21,400 \text{ lb.}$,

$Z_{SM} = 23.98 \text{ in}$ and from equation (3a.1),

$$(3a.29) \ Z_O = Z_{WMO} - Z_{SM} = -2.245 - 23.980 = -26.225 \text{ IN.}$$

Also $Z_{ARO} = Z_O = -26.225 \text{ in.}$

For the example problem the effects of aerodynamic forces are not included in the flywheel simulation; therefore, $C_{AD} = 0.0$ and $C_{AL} = 0.0$.

The unsprung mass moving vertically, W_{WV} , is the same as W_{GW} described in the Section 4a Wheel and Tire System (Flywheel) for horizontal motion. Therefore, $W_{WV} = 1.60 \text{ lbf sec}^2/\text{in.}$

The average engine idle thrust is 1000 lbf. Therefore, $F_{TH} = 1000 \text{ lbf.}$

Table 5 Airplane System (Flywheel) Parameters

SYMBOL	TYPE	VALUE	UNITS	DESCRIPTION
A_{VM}	v^*		$lb\ sec^2/in^2$	Shock strut damping characteristic.
C_{AD}	c	0.0	$lb\ sec^2/in^2$	Aerodynamic drag coefficient.
C_{AL}	c	0.0	$lb\ sec^2/in^2$	Aerodynamic lift coefficient.
C_{AR}	c	14,720	lb/in	Spring rate associated with mass W_{AR}
C_{MT}	c	9530	lb/in	Tire vertical spring rate
D_{AR}	c	11.72	$lb\ sec/in$	Damping coeff. associated with mass W_{AR}
D_{MT}	c	38.8	$lb\ sec/in^2$	Tire damping coefficient
D_{VM}	c	0.0	$lb\ sec/in$	Shock strut linear damping coeff.
F_{AD}	v		lb	Aerodynamic drag force on airplane.
F_{AL}	v		lb	Aerodynamic lift force on airplane
F_{AR}	v		lb	Force associated with mass W_{AR}
F_{BT}	$v(i)$		lb	Braking force
F_{LD}	c	21,400	lb	Static force on tire
$F_{\phi v}$	$v(i)$		lb	Tire unbalance force (vertical)
F_{NM}	$v(o)$		lb	Tire normal force
F_{TH}	c	1000	lb	Engine thrust
F_{VM}	v		lb	Shock strut force
F_{VMS}	v^{**}		lb	Shock strut force with $\dot{Z}_{SM} = 0$
S_M	$v(o)$		in	Tire deflection
\dot{S}_M	v		in/sec	Rate of tire deflection
V_F	v		in/sec	Flywheel velocity
V_{FO}	c	2400	in/sec	Flywheel velocity at time = 0

*Point plot input see Figure 13

**Point plot input see Figure 14

Table 5 (Contd)

SYMBOL	TYPE	VALUE	UNITS	DESCRIPTION
W_A	C	65.0	lb sec ² /in	Airplane mass carried on main gear.
W_{AR}	C	2.59	lb sec ² /in	Mass of airplane substructure.
W_{AT}	C	147.8	lb sec ² /in	Total airplane mass
W_{WV}	C	1.667	lb sec ² /in	Unsprung mass
X_F	V(0)		in	Flywheel surface distance traveled.
X_{FO}	C	0.0	in	Flywheel distance at time = 0.
Z	V		in	Vertical location of equivalent apl. mass C.G.
Z_0	C	-26.225	in	Vertical location of equivalent mass at time = 0
\dot{Z}	V		in/sec	Velocity of apl. mass
\dot{Z}_0	C	0.0	in/sec	Velocity of apl mass at time = 0
\ddot{Z}	V		in/sec ²	Acceleration of apl mass
Z_{AR}	V		in	Auxiliary mass location
Z_{AR0}	C	-26.225	in	Auxiliary mass location at time = 0
\dot{Z}_{AR}	V		in/sec	Auxiliary mass velocity
\dot{Z}_{AR0}	C	0.0	in/sec	Auxiliary mass velocity at time = 0
\ddot{Z}_{AR}	V		in/sec ²	Auxiliary mass acceleration
Z_{GD}	V(i)		in.	Ground height
\dot{Z}_{GD}	V(i)		in/in	Ground slope
Z_{SDP}	V		in	Shock Strut Stroke
\dot{Z}_{SM}	V		in/sec	Shock strut stroke velocity

Table 5 (Contd)

SYMBOL	TYPE	VALUE	UNITS	DESCRIPTION
Z_{WM}	V		in	Axle location (vertical)
\dot{Z}_{WMO}	C	-2.245	in	Axle location at time = 0
\ddot{Z}_{WM}	V		in/sec	Axle velocity (vertical)
\ddot{Z}_{WMO}	C	0.0	in/sec	Axle location at time = 0
$\ddot{\ddot{Z}}_{WM}$	V		in/sec ²	Axle acceleration

3b. AIRPLANE SYSTEM (3 DEGREE)

The three degree airplane system is built around a rigid body airplane which is allowed to move vertically, horizontally (parallel to the runway centerline), and rotationally in the pitch mode. This model provides for the interaction of the anti-skid system with those effects which are related to airplane pitch. This includes such pitch effects as change in the aerodynamic lift, drag, and moment due to change in wing angle of attack, change in the aerodynamic lift, drag, and moment due to changes in elevator deflection as dictated by the stability augmentation system (pitch mode), change in tire loading due to braking pitch moment, and the effect of ground slope and roughness as reacted through both the main and nose gears.

A. Mathematical Description

Figure 15 shows the three coordinates which describe the airplane position relative to reference points on the earth's surface.

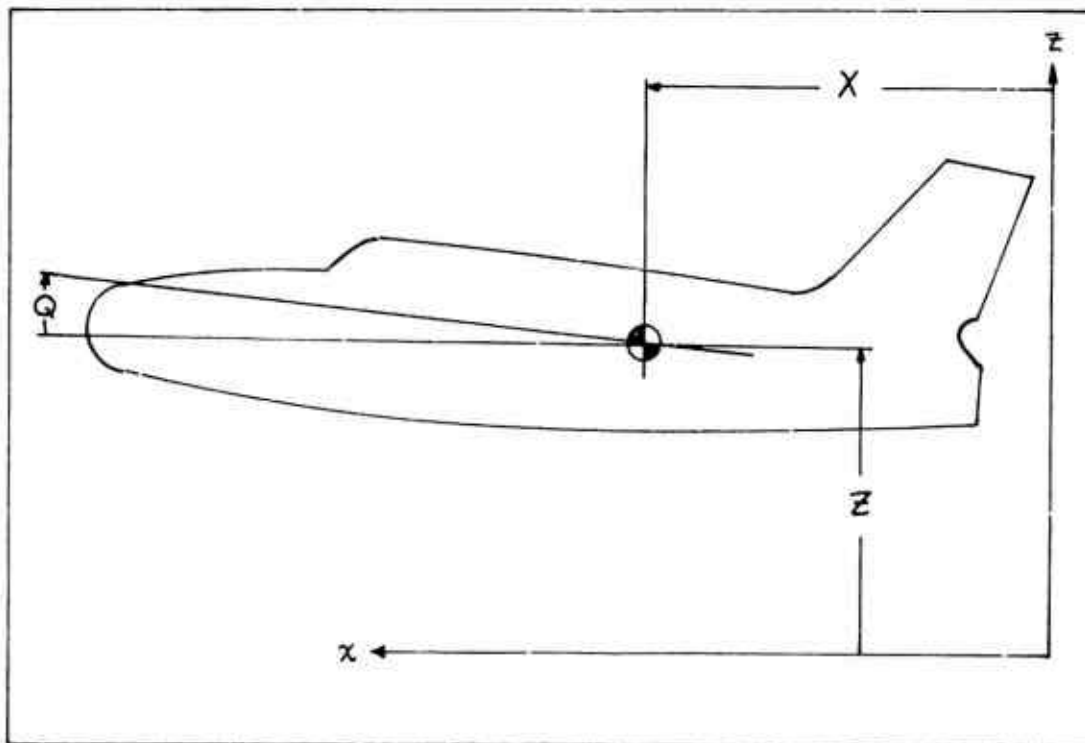


Figure 15 Airplane Coordinates

Figure 16 shows the gear extended dimensions as measured in the airplane's water line-fuselage station reference system.

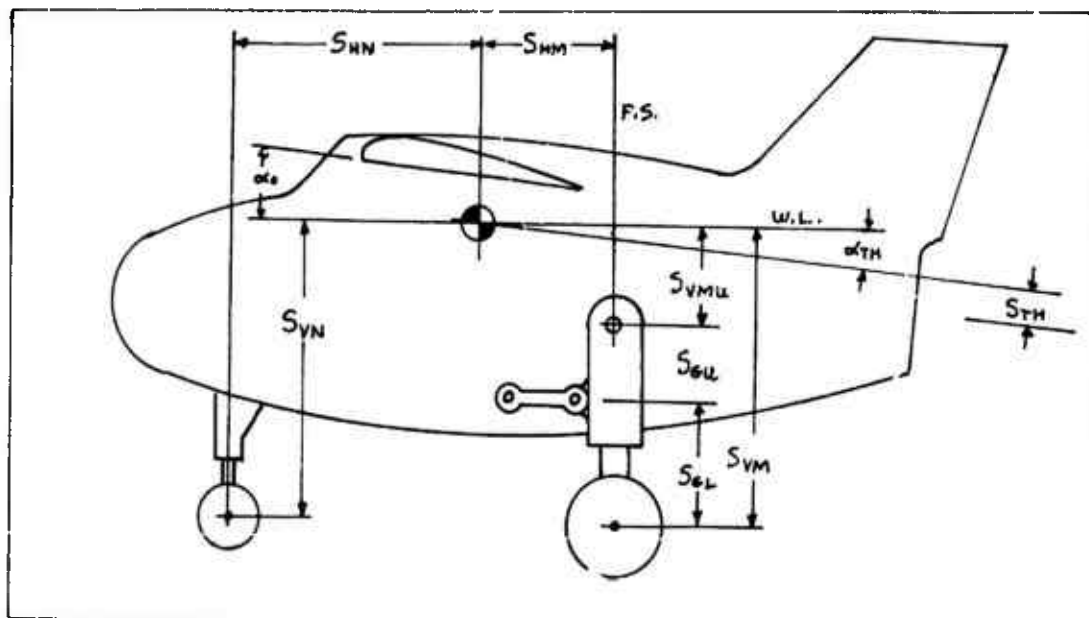


Figure 16 Airplane Geometry

Let $Z_{GD}(x)$ denote the runway profile height and let $Z_{GDP}(x)$ denote the runway profile slope.

Nose Gear

Let Z_{SN} and \dot{Z}_{SN} denote the nose strut stroke and stroke velocity. From Figure 17, Z_{SN} and \dot{Z}_{SN} are given by

$$(3b.1) \quad Z_{SN} = Z_{WN} + S_{VN} - Z - S_{HN}Q$$

$$(3b.2) \quad \dot{Z}_{SN} = \dot{Z}_{WN} - \dot{Z} - S_{HN} \dot{Q}$$

The nose gear shock strut force is then given by

$$(3b.3) \quad F_{VN} = F_{VNS}(Z_{SN}) + D_{NN} \dot{Z}_{SN} + A_{VN}(Z_{SN}) \dot{Z}_{SN} |\dot{Z}_{SN}|$$

F_{NN} , the normal ground force at the nose gear is given by

$$(3b.4) \quad F_{NN} = S_N (C_{NT} + D_{NT} \dot{S}_N)$$

where S_N is the nose tire deflection. S_N and \dot{S}_N are given by:

$$(3b.5) S_N = \max \{0.0, Z_{GD} \langle X_{WN} \rangle + R_{OTN} - Z_{WN}\}$$

$$(3b.6) \dot{S}_N = Z_{GDP} \langle X_{WN} \rangle \dot{X}_{WN} - \dot{Z}_{WN}$$

Summing vertical forces on the nose wheel,

$$(3b.7) W_{WN} \ddot{Z}_{WN} = F_{NN} - F_{VN}$$

$$(3b.8) F_{DN} = U_{RRN} F_{NN}$$

Main Gear

Let Z_{SM} and \dot{Z}_{SM} denote the main gear stroke and stroke velocity:

$$(3b.9) Z_{SM} = Z_{WM} - Z + S_{VM} + S_{HM} Q$$

$$(3b.10) \dot{Z}_{SM} = \dot{Z}_{WM} - \dot{Z} + S_{HM} \dot{Q}$$

The main gear shock strut force is given by:

$$(3b.11) F_{VM} = F_{VMS} \langle Z_{SM} \rangle + D_{VM} \dot{Z}_{SM} + A_{VM} \langle Z_{SM} \rangle \dot{Z}_{SM} |\dot{Z}_{SM}|$$

Let S_M denote the main gear tire deflection. Then the tire normal force is given by:

$$(3b.12) F_{NM} = S_M (C_{MT} + D_{MT} \dot{S}_M)$$

$$(3b.13) S_M = \max \{0.0, Z_{GD} \langle X_{WM} \rangle + R_{OTM} - Z_{WM}\}$$

$$(3b.14) \dot{S}_M = Z_{GDP} \langle X_{WM} \rangle \dot{X}_{WM} - \dot{Z}_{WM}$$

Summing vertical forces on the main wheel,

$$(3b.15) W_{WM} \ddot{Z}_{WM} = F_{NM} - F_{VM} + F_{ORV}$$

Figure 18 shows the model of the main gear. With the assumption that the gear weight is much less than the airplane weight (that is, $W_u \ll W_A$), it follows that:

$$(3b.16) W_u S_{Gu}^2 \ddot{\Theta}_G = F_u S_{Gu} - F_G (S_{Gu} + Z_{GL}) - T_S$$

Figure 17 Airplane Dynamics

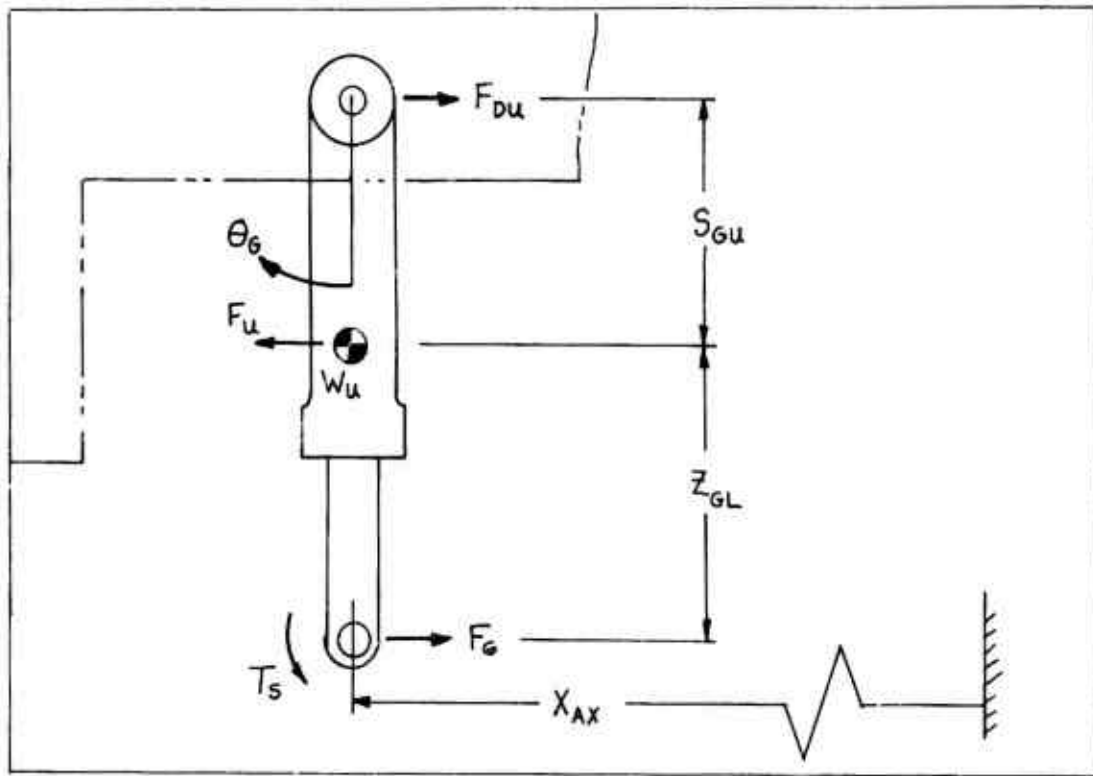


Figure 18 Main Strut Model

where Z_{GL} is determined by:

$$(3b.17) \quad Z_{GL} = S_{GL} - Z_{SM}$$

F_{Du} can then be computed from

$$(3b.18) \quad F_{Du} = (F_G Z_{GL} + T_s) / S_{Gu}$$

where

$$(3b.19) \quad F_u = S_{Gu} (C_u (Q - \theta_G) + D_u (\dot{Q} - \dot{\theta}_G))$$

T_s and F_G are outputs from the tire and wheel system. The horizontal axle reference location is denoted by X_{AX} . X_{AX} is given by:

$$(3b.20) \quad X_{AX} = X - S_{HM} + (S_{Gu} + Z_{GL}) \theta_G$$

$$(3b.21) \quad \dot{X}_{AX} = \dot{X} + (S_{Gu} + Z_{GL}) \dot{\theta}_G$$

Thrust

Referring to Figures 16 and 17, if \bar{F}_{TH} is the thrust, then

$$(3b.22) \quad F_{THV} = F_{TH} (\alpha_{TH} + Q)$$

$$(3b.23) \quad T_{TH} = S_{TH} F_{TH}$$

Aerodynamics

The dynamic Air Force Q_A is given by:

$$(3b.24) \quad Q_A = \dot{X}^2 A_{REF} R_{HA} / 288.0$$

The aerodynamic lift, drag, and moment are then given by:

$$(3b.25) \quad F_{AL} = C_{AL} Q_A$$

$$(3b.26) \quad F_{AD} = C_{AD} Q_A$$

$$(3b.27) \quad T_{AM} = C_{AM} Q_A$$

If α_w denotes the wing angle of attack relative to the air, then:

$$(3b.28) \quad \alpha_w = \alpha_o + (180/\pi)(Q - \dot{Z}/\dot{X})$$

Let S_{HT} denote the horizontal tail deflection. Then the aerodynamic coefficients are given by:

$$(3b.29) \quad C_{AL} = G_{AL} + B_{AL} \alpha_w + E_{AL} S_{HT}$$

$$(3b.30) \quad C_{AD} = G_{AD} + B_{AD} \alpha_w + E_{AD} S_{HT}$$

$$(3b.31) \quad C_{AM} = G_{AM} + B_{AM} \alpha_w + E_{AM} S_{HT}$$

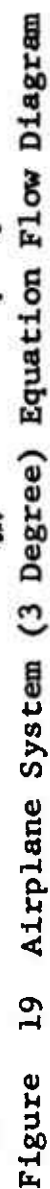
Dynamics

Referring to Figure 17,

$$(3b.32) \quad W_A \ddot{Z} = F_{AL} + F_{THV} - W_A G + 2F_{VM} + F_{VN}$$

$$(3b.33) \quad W_A \ddot{X} = F_{TH} - F_{AD} + 2F_{DU} - 2F_U - F_{DN}$$

$$(3b.34) \quad W_{IQ} \ddot{Q} = F_{VN} S_{HN} - 2F_{VM} S_{HM} + 2F_{DU} S_{VMU} + T_{TH} \\ + T_{AM} - 2F_U (S_{GU} + S_{VMU}) - F_{DN} (Z - Z_{GD} \langle X_{WN} \rangle)$$



where

$$(3b.35) \quad X_{WN} = X + S_{HN} + S_{VN} Q$$

$$(3b.36) \quad \dot{X}_{WN} = \dot{X} + S_{VN} \dot{Q}$$

Figure 19 shows the system flow diagram.

B. PARAMETER EVALUATION

Shock Strut Characteristics

Figures 20 and 21 show the nose gear load and damping characteristics.

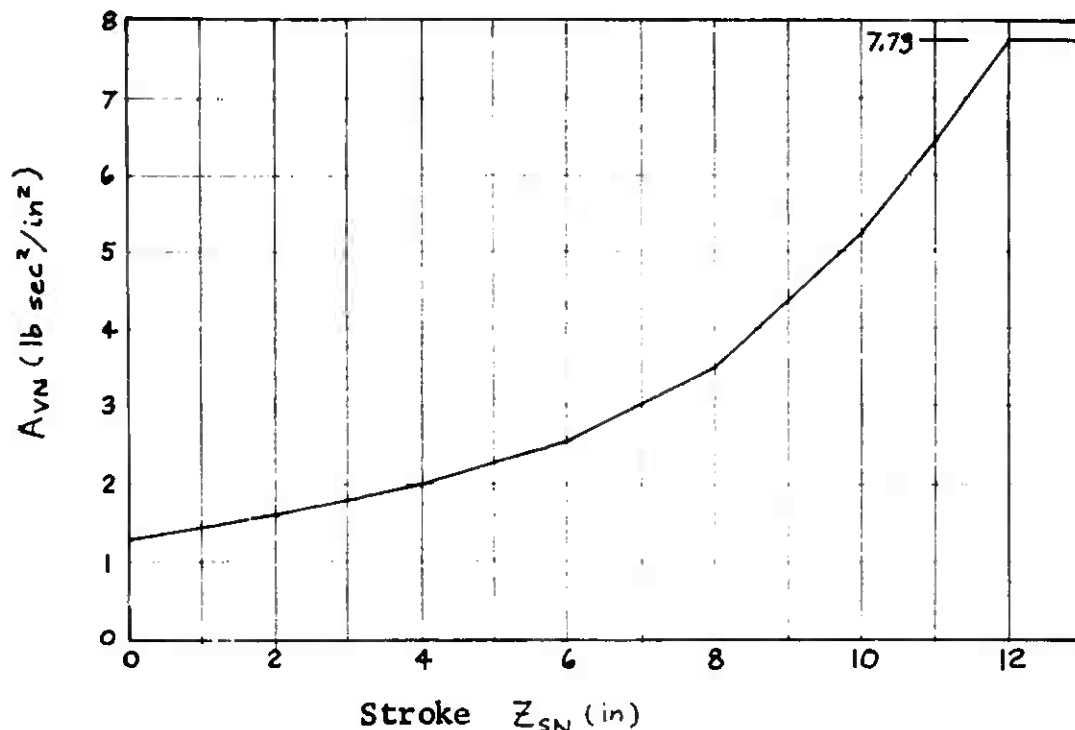


Figure 20 Nose Gear Damping Curve

Nose Tire Characteristics

See also page 57 of the flywheel system. The 22 x 6.6-10 16-ply rating nose tire has a rating of 9150 lbs. at 190 psi. The deflection is 1.50 inches. The operating pressure is 190 psi. Since these are two nose tires,

$$(3b.37) \quad C_{NT} = \left(\frac{P}{P_R} \right) \frac{F_R}{S_R} = \left(\frac{190}{190} \right) \frac{(2)(9150)}{(1.50)} = 12,200 \text{ lb/in}$$

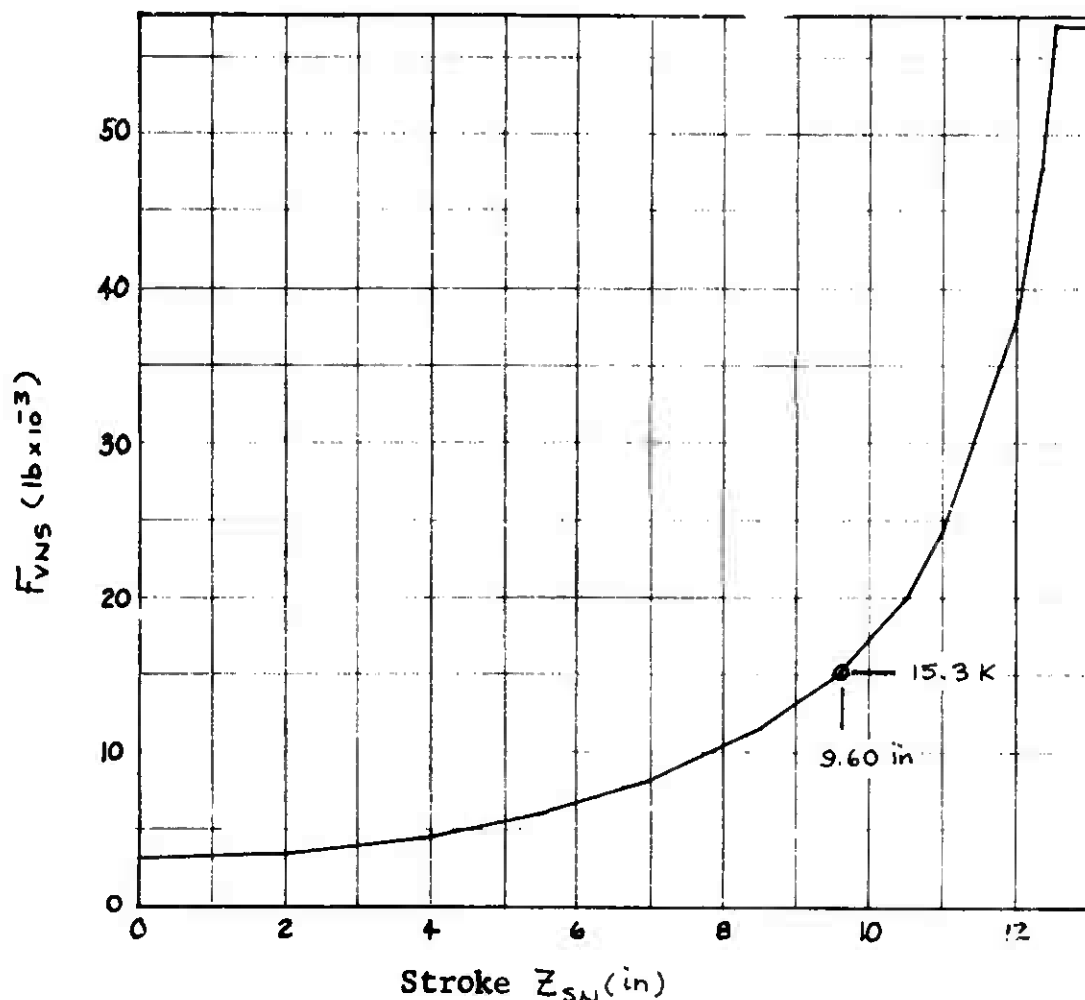


Figure 21 Nose Gear Air Load Curve

Since $\eta = 0.1$,

$$\begin{aligned}
 (3b.38) \ C_{NT} &= \frac{\eta F_R}{S_R^2} \left(\frac{P}{P_R} \right) \sqrt{\frac{S_R}{G}} \\
 &= \frac{(.1)(2)(9,150)}{(1,50)^2} \left(\frac{190}{190} \right) \sqrt{\frac{1,50}{386}} = 50.6 \frac{\text{lb sec}}{\text{in}^2}
 \end{aligned}$$

The nose tire rolling resistance coefficient is $U_{RRN} = .020$ and the unsprung nose tire mass (mass of tires, wheels, axle, and lower shock strut) is $W_{WN} = 175/386 = .453$ LBF SEC²/IN. The nose tire undeflected radius, R_{0TN} , is 10.8 in.

Main Tire Characteristics

The main tire undeflected radius, R_{0TM} , is 23.32 inches. The other main tire characteristics are computed as shown on page 56.

Main Gear Characteristics

The F-111 main gear spring rate parameters were computed from load-deflection data recorded during structural testing and correlated with data from jig drop tests and from flight tests.

Figure 22 shows the model which has the same form as that described in equations (3b.16) through (3b.21) and in the wheel and tire system. The rotational spring rate of one main gear about its pivot is 26×10^6 in lb/rad.

The remaining values are calculated (at static position) as:

$$(3b.39) \quad \begin{cases} S_{Gu} = 21.0 \text{ in} \\ W_u = 279 \text{ lbm} = .723 \text{ lb sec}^2/\text{in} \\ W_{GW} = W_{WM} = 644 \text{ lbm} = 1.667 \text{ lb sec}^2/\text{in} \\ C_G = 200,000 \text{ lb/in} \end{cases}$$

Thus from figure 22, C_u is given by

$$(3b.40) \quad C_u = C_{u(RET)} / S_{Gu}^2 = 26 \times 10^6 / 21^2 = 59,000 \text{ lb/in}$$

The first mode natural frequency of the model is 21.84 cps. Assuming that η is .054 (about 3% critical), then evaluating the damping at $\omega = (2\pi)(21.84) = 137.5 \text{ rad/sec}$ there follows:

$$(3b.41) \quad D_G = \frac{\eta C_G}{\omega} = \frac{(.054)(200,000)}{(137.5)} = 78.6 \frac{\text{lb sec}}{\text{in}}$$

$$(3b.42) \quad D_U = \frac{\eta C_U}{\omega} = \frac{(.054)(59,000)}{(137.5)} = 23.2 \frac{\text{lb sec}}{\text{in}}$$

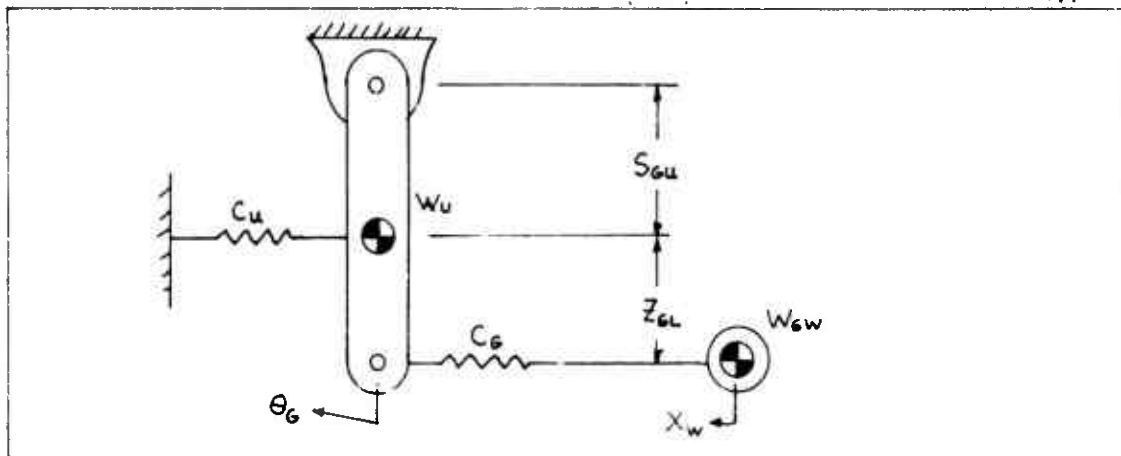


Figure 22 Main Gear Strut and Wheel Model

Aerodynamic Data

For finding the aerodynamic data, the F-111A is landing with flaps at 34° , wings swept to 26° , and spoilers applied. An equilibrium airplane condition of $\alpha_w = 2^\circ$ and $S_{HT} = -5^\circ$ is assumed. For these conditions,

$$(3b.43) \quad C_L = 0.13 \quad \frac{\partial C_L}{\partial \alpha_w} = .128 \text{ deg}^{-1} \quad \frac{\partial C_L}{\partial S_{HT}} = .022 \text{ deg}^{-1}$$

$$(3b.44) \quad C_D = .258 \quad \frac{\partial C_D}{\partial \alpha_w} = .000 \text{ deg}^{-1} \quad \frac{\partial C_D}{\partial S_{HT}} = -.0036 \text{ deg}^{-1}$$

$$(3b.45) \quad C_{MA} = 0.00 \quad \frac{\partial C_{MA}}{\partial \alpha_w} = -.025 \text{ deg}^{-1} \quad \frac{\partial C_{MA}}{\partial S_{HT}} = -.0352 \text{ deg}^{-1}$$

The aerodynamic reference point is F.S. 526.8, WL 197.2. Assuming the airplane C.G. at F.S. 519.0, WL 180.0, if Δx and Δy are given by:

$$(3b.46) \quad \Delta x = FSA - FSCG = 526.8 - 519.0 = 7.8 \text{ inches}$$

$$(3b.47) \quad \Delta y = WLA - WLCG = 197.2 - 180.0 = 17.2 \text{ inches}$$

Then if $\bar{C} = 108.5$ inches is the length of the M.A.C., then $C_m \bar{C}$ at the airplane C.G. is given by:

$$\begin{aligned} (3b.48) \quad C_m \bar{C} &= C_{MA} \bar{C} - C_L \Delta x + C_D \Delta y \\ &= (0.0)(108.5) - (0.13)(7.8) + (.258)(17.2) = 3.434 \text{ inches} \end{aligned}$$

Also,

$$\begin{aligned} (3b.49) \quad \frac{\partial C_m \bar{C}}{\partial \alpha_w} &= \frac{\partial C_{MA} \bar{C}}{\partial \alpha_w} - \frac{\partial C_L}{\partial \alpha_w} \Delta x + \frac{\partial C_D}{\partial \alpha_w} \Delta y \\ &= (-.025)(108.5) - (.128)(7.8) + (0.0)(17.2) = -.371 \end{aligned}$$

$$\begin{aligned} (3b.50) \quad \frac{\partial C_m \bar{C}}{\partial S_{HT}} &= \frac{\partial C_{MA} \bar{C}}{\partial S_{HT}} - \frac{\partial C_L}{\partial S_{HT}} \Delta x + \frac{\partial C_D}{\partial S_{HT}} \Delta y \\ &= (-.0352)(108.5) - (.022)(7.8) - (.0036)(17.2) = -.3759 \end{aligned}$$

Thus from equations (3b.29), (3b.30), and (3b.31),

$$(3b.51) \begin{cases} C_{AL} = C_L = 0.13 \\ B_{AL} = (\partial C_L / \partial \alpha_w) = .128 \text{ deg}^{-1} \\ E_{AL} = (\partial C_L / \partial S_{HT}) = .022 \text{ deg}^{-1} \end{cases}$$

$$(3b.52) \begin{cases} C_{AD} = C_D = .258 \\ B_{AD} = (\partial C_D / \partial \alpha_w) = 0.0 \text{ deg}^{-1} \\ E_{AD} = (\partial C_D / \partial S_{HT}) = -.0036 \text{ deg}^{-1} \end{cases}$$

$$(3b.53) \begin{cases} C_{AM} = C_{m\bar{c}} = 3.424 \text{ in} \\ B_{AM} = (\partial C_{m\bar{c}} / \partial \alpha_w) = -.371 \text{ in/deg} \\ E_{AM} = (\partial C_{m\bar{c}} / \partial S_{HT}) = -3.759 \text{ in/deg} \end{cases}$$

(3b.54)

$$(3b.55) \begin{aligned} G_{AL} &= C_{AL} - B_{AL} \alpha_w - E_{AL} S_{HT} \\ &= .013 - (.128)(2) - (.022)(-5.0) = -.016 \end{aligned}$$

$$(3b.56) \begin{aligned} G_{AD} &= C_{AD} - B_{AD} \alpha_w - E_{AD} S_{HT} \\ &= .258 - (0.0)(2) - (-.0036)(-5) = .240 \end{aligned}$$

$$(3b.56) \begin{aligned} G_{AM} &= C_{AM} - B_{AM} \alpha_w - E_{AM} S_{HT} \\ &= 3.424 - (-.371)(2) - (-3.759)(-5) = 2.286 \text{ IN} \end{aligned}$$

Initial Conditions

Assume that at time = 0.0 seconds the airplane velocity is 2400 in/sec = \dot{X}_0 . The airplane is shown in Figure 23 with brakes off.

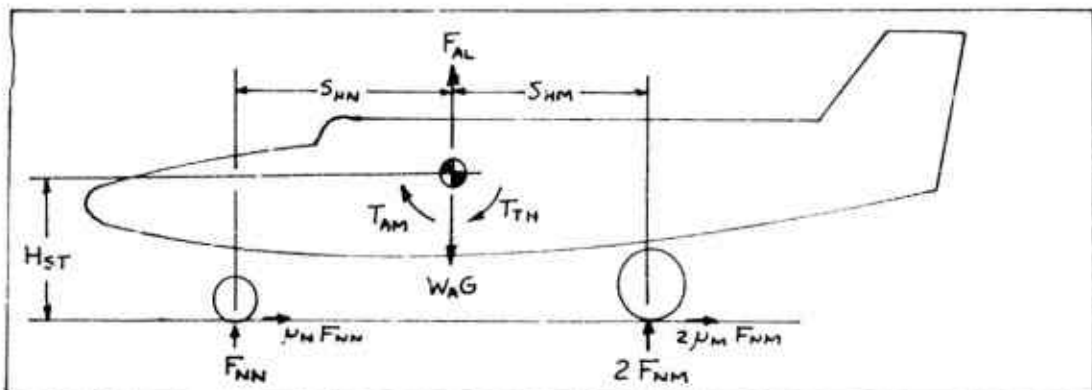


Figure 23 Airplane Initial Equilibrium Forces

Assume that $\alpha_w = 3^\circ$ and $S_{HT} = -5^\circ$, then from equations (3b.29) (3b.30) and (3b.31), there follows:

$$(3b.57) C_{AL} = (-.016) + (.128)(3) + (.022)(-5) = 0.222$$

$$(3b.58) C_{AM} = (2.286) + (-.371)(3) + (-3.759)(-5) = 19.973$$

Since $S_{HN} = 258.9$, $S_{HM} = 32.6$ inches, $T_{TH} = 20,000$ in/lb., and if the estimated value for H_{ST} is 97.2 inches, then

$$(3b.59) F_{NM} = \left(\frac{(T_{TH} + T_{AM}) + (S_{HN} - H_{ST}\mu_N)(WAG - F_{AL})}{(S_{HN} + S_{HM}) + H_{ST}(\mu_M - \mu_N)} \right) \frac{1}{2}$$

Now from equations (3b.24), (3b.25), and (3b.26),

$$(3b.60) Q_A = (2400)^2(525)(.00238)/288 = 25000 \text{ lb}$$

$$(3b.61) F_{AL} = (.222)(25000) = 5500 \text{ lb}$$

$$(3b.62) T_{AM} = (19.973)(25000) = 499,300 \text{ in/lb}$$

Thus,

$$(3b.63) F_{NM} = \frac{1}{2} \left(\frac{(499,300) + (257)(57000 - 5500)}{(258.9) + (97.2)(0)} \right)$$

So

$$(3b.64) F_{NM} = 22988 \text{ lb}$$

and

$$(3b.65) F_{NN} = WAG - F_{AL} - 2F_{NM} \\ = 57000 - 5500 - 2(22988) = 5524 \text{ lb}$$

Assume that when time = 0 that $X_{WM} = 0.0$ inches, then $Z_{GD}(X_{WM}) = 0.0$. Then $X_{WN} = 295.1$ inches so that $Z_{GD}(X_{WN}) = (9.676 - 9.703)12 = -.32$ inches. Refer to the runway system for values of Z_{GD} . From equation (3b.12):

$$(3b.66) S_M = (22988)/(9530) = 2.41 \text{ in}$$

Thus from equation (3b.13)

$$(3b.67) \quad Z_{WMO} = 23.32 - 2.41 = 20.91 \text{ in}$$

From Figure 14 in the flywheel system, if $F_{VMS} = 22,950$ lbs, then $Z_{SM} = 24.00$ inches. Now, from equation (3b.4)

$$(3b.68) \quad S_N = (5524) / (12,200) = .46 \text{ in}$$

From equation (3b.5), there follows:

$$(3b.69) \quad \bar{Z}_{WNO} = (-.32) + (10.80) - (.46) = 10.02 \text{ in}$$

Also, from Figure 21, if $F_{VNS} = 5,600$ lbs. then: $Z_{SN} = 5 \text{ in}$

Rearranging equations (3b.1) and (3b.9)

$$(3b.70) \quad Z_O + S_{HN} Q_O = S_{VN} + Z_{WNO} - Z_{SN}$$

$$(3b.71) \quad Z_O - S_{HM} Q_O = S_{VM} + Z_{WMO} - Z_{SM}$$

Solving these two equations,

$$(3b.72) \quad Q_O = .0329 \text{ RADIANS}$$

$$(3b.73) \quad Z_O = 82.36 \text{ in}$$

Finally,

$$(3b.74) \quad X_O = X_{WMO} + S_{HM} = 36.20 \text{ in}$$

$$(3b.75) \quad \Theta_{GO} = Q_O = .0329 \text{ RADIANS}$$

The values of the following parameters as listed in Table 6 are established by the airplane's dimensional and mass characteristics: $\alpha_O, \alpha_{TH}, AREF, S_{GL}, S_{HM}, S_{HN}, S_{VM}, S_{VN}, S_{TH}, W_A$ and W_{IQ} .

For the example problem the density of air at standard conditions, sea level and 59.6°F , is assumed. Thus,
 $R_{HA} = .00238 \text{ Slugs / Ft}^3$

The shock strut linear damping coefficients, D_{VN} for the nose gear and D_{VM} for the main gear, are set equal to zero for the example problem.

Table 6 Airplane System (3 Degree) Parameters

SYMBOL	TYPE	VALUE	UNITS	DESCRIPTION
α_0	C	1.00	deg	Wing Angle of Incidence
α_{TH}	C	-0.052	rad	Angle between Thrust \angle and W.L.
α_w	V		deg	Wing Angle of Attack
A_{REF}	C	525	ft ²	Wing Ref. Area
A_{VM}	V*		lb sec ² /in ²	M.G. Shock Strut Damping Characteristic
A_{VN}	V*		lb sec ² /in ²	N.G. Shock Strut Damping Characteristic
B_{AD}	C	0.0	deg ⁻¹	Aero Drag Parameter
B_{AL}	C	.128	deg ⁻¹	Aero Lift Parameter
B_{AM}	C	-.371	in/deg	Aero Moment Parameter
C_{AD}	V		-	Aero Drag Coefficient
C_{AL}	V		-	Aero Lift Coefficient
C_{AM}	V		in	Aero Moment Coefficient
C_{MT}	C	9530	lb/in	M.G. Tire Vertical Spring Rate
C_{NT}	C	12,200	lb/in	N.G. Tire(s) Vertical Spring Rate
C_u	C	59,000	lb/in	Drag Brace - Strut Spring Rate
D_{MT}	C	.382	lb sec/in ²	M.G. Tire Vertical Damping Coeff.
D_{NT}	C	50.6	lb sec/in ²	N.G. Tire Vertical Damping Coeff.
D_u	C	23.2	lb sec/in	Drag Brace - Strut Damping Coeff.
D_{VM}	C	0.0	lb sec/in	M.G. Strut Damping Coefficient
D_{VN}	C	0.0	lb sec/in	N.G. Strut Damping Coefficient
E_{AD}	C	-.0036	deg ⁻¹	Aero Drag Coefficient
E_{AL}	C	.022	deg ⁻¹	Aero Lift Coefficient
E_{AM}	C	-3.753	in/deg	Aero Moment Coefficient
F_{AD}	V		lb	Aero Drag
F_{AL}	V		lb	Aero Lift
F_{DM}	V		lb	Nose Tire Drag
F_{DN}	V		lb	Horizontal Load at M.G. Pivot

* Point Plot Input

Table 6 (Contd)

SYMBOL	TYPE	VALUE	UNITS	DESCRIPTION
F_G	V(I)		lb	Horizontal Load on M.G. Axle
F_{NM}	V(O)		lb	M.G. Tire Normal Load
F_{N2}	V		lb	N.G. Tire Normal Load
F_{TH}	C	1000	lb	Engine Thrust
F_{THV}	V		lb	Vertical Component of Engine Thrust
F_u	V		lb	Load in Fictitious Drag Brace
F_{VM}	V		lb	Shock Strut Load (M.G.)
F_{VMS}^*	V		lb	Shock Strut Air Load (M.G.)
F_{VN}	V		lb	Shock Strut Load (N.G.)
F_{VNS}^*	V		lb	Shock Strut Air Load (N.G.)
G	C	386	in/sec ²	Gravitational Constant
G_{AD}	C	.240	-	Aero Drag Parameter
G_{AL}	C	-.016	-	Aero Lift Parameter
G_{AM}	C	2.286	in	Aero Moment Parameter
\dot{G}_G	V(O)		rad	M.G. Rotation from Vertical
\dot{G}_{G0}	C	.0329	rad	\dot{G}_G at Time = 0 Sec.
\dot{G}_C	V(O)		rad/sec	Angular Velocity of Main Gear Strut
\dot{G}_{G0}	C	0.0	rad/sec	\dot{G}_G at Time = 0 Sec.
\dot{G}_C	V		rad/sec ²	Angular Acceleration of Main Gear Strut
$F_{\theta V}$	V(I)		lb	Tire Vertical Unbalance
Q	V		rad	Angle of APL W.L. to Horizontal (Pitch)
Q_0	C	.0329	rad	Q at Time = 0.0 Sec.
\dot{Q}	V(O)		rad/sec	APL Pitch Rate
\dot{Q}_0	C	0.0	rad/sec	APL Pitch Rate at Time = 0.0 Sec.

* Point Plot Input

Table 6 (Contd)

SYMBOL	TYPE	VALUE	UNITS	DESCRIPTION
$\dot{\theta}$	V		rad/sec ²	APL Pitch Acceleration
Q_A	V		lb	Aerodynamic Pressure x AREF
R_{HA}	C	.00238	slug/ft ³	Air Density
R_{ATM}	C	23.32	in	M.G. Tire Undelected Radius
R_{ETN}	C	10.80	in	N.G. Tire Undelected Radius
S_{GL}	C	26.50	in	*
S_{GU}	C	21.00	in	*
S_{HM}	C	36.20	in	*
S_{HN}	C	258.90	in	*
S_{HT}	V(I)		deg	Horizontal Tail Deflection
S_M	V(O)		in	M.G. Tire Deflection
\dot{S}_M	V		in/sec	M.G. Tire Deflection Rate
S_{VMA}	C	36.74	in	*
S_N	V		in	N.G. Tire Deflection
\dot{S}_N	V		in/sec	N.G. Tire Deflection Rate
S_{VM}	C	84.24	in	*
S_{VN}	C	85.86	in	*
S_{TH}	V	20.00	in	*
T_{AM}	V		in lb	Aero Moment
T_S	V(I)		in lb	Moment on M.G. Axle
T_{TH}	C	20,000	in lb	Moment at C.C. due to Thrust
U_{REN}	C	.020	-	N.G. Tire Rolling Resistance Coefficient
W_A	C	147.6	lb sec ² /in	APL Mass
W_{IQ}	C	366×10^6	lb sec ² /in	APL Pitch Moment of Inertia About C.G.
W_U	C	.723	lb sec ² /in	M.G. Upper Strut Mass
W_{WM}	C	1.667	lb sec ² /in	M.G. Unsprung Mass

* See Figure 16

Table 6 (Contd)

SYMBOL	TYPE	VALUE	UNITS	DESCRIPTION
\dot{W}_{WN}	C	.453	lb sec ² /in	N.G. Unsprung Mass
X	V		in	Horizontal C.G. Location of APL
\dot{X}_0	C	36.20	in	C.G. Location at Time = 0
\dot{X}	V		in/sec	APL Velocity
\dot{X}_0	C	2400	in/sec	APL Velocity at Time = 0
\ddot{X}	V		in/sec ²	APL Acceleration
\dot{X}_{AX}	V(O)		in	M.G. Axle (Undelected) Location
\dot{X}_{AX}	V(O)		in/sec	M.G. Axle Velocity (Undelected)
\dot{X}_{WN}	V(I)		in	M.G. Axle Location (Horizontal)
\dot{X}_{WM}	V(I)		in/sec	M.G. Axle Velocity
\dot{X}_{WN}	V		in	N.G. Axle Location (Horizontal)
\dot{X}_{WN}	V		in/sec	N.G. Axle Velocity
Z	V		in	Vertical Location of APL C.G.
\dot{Z}_0	C	82.36	in	Vertical Location of APL C.G. at Time = 0
\dot{Z}	V		in/sec	APL Vertical Velocity
\dot{Z}_0	C	0.0	in/sec	APL Vertical Velocity at Time = 0
\ddot{Z}	V		in/sec ²	APL Vertical Acceleration
\dot{Z}_{GD}	V(I)		in	Runway Contour Height
\dot{Z}_{GDP}	V(I)		in/in	Runway Contour Slope
\dot{Z}_{GL}	V		in	Distance from Mass W_u to Strut Axle
\dot{Z}_{SM}	V		in	M.G. Stroke
\dot{Z}_{SM}	V		in/sec	M.G. Stroke Velocity
\dot{Z}_{SN}	V		in	N.G. Stroke
\dot{Z}_{SN}	V		in/sec	N.G. Stroke Velocity
\dot{Z}_{WM}	V		in	M.G. Axle Height

Table 6 (Contd)

SYMBOL	TYPE	VALUE	UNITS	DESCRIPTION
Z_{WM0}	C	20.91	in	M.G. Axle Height at Time = 0 Sec.
\dot{Z}_{WM}	V		in/sec	M.G. Axle Vertical Velocity
\ddot{Z}_{WM0}	C	0.0	in/sec	M.G. Axle Vertical Velocity at Time = 0
\ddot{Z}_{WM}	V		in/sec ²	M.G. Axle Vertical Acceleration
Z_{WN}	V		in	N.G. Axle Height
\dot{Z}_{WN0}	C	10.02	in	N.G. Axle Height at Time = 0
\ddot{Z}_{WN}	V		in/sec	N.G. Axle Vertical Velocity
\ddot{Z}_{WN0}	C	0.0	in/sec	N.G. Axle Vertical Velocity at Time = 0
\ddot{Z}_{WN}	V		in/sec ²	N.G. Axle Vertical Acceleration

3c. AIRPLANE SYSTEM (6 DEGREE)

The six-degree airplane system is built around a rigid body airplane which is allowed to move vertically and horizontally (both parallel and perpendicular to the runway centerline). Also, the airplane's yaw, pitch, and roll effects are considered. This model considers all the effects found in the three-degree airplane system. The purpose of the six-degree airplane is primarily two-fold: the first is to evaluate the effects of the anti-skid system on the airplane's directional stability; the second is to evaluate any anti-skid system degradation caused by airplane yaw and side drift movement.

For the nose gear, the model considers the tire and strut characteristics in the vertical direction. Also, the nose tire's yawed rooling characteristics are included. The steering loop is closed by providing a "pilot" function which provides an input to the nose tire. The "pilot" function depends on the airplane's yaw angle. The two main gears are treated as two distinct systems except for any structural coupling which may exist between the two. Provisions are made for side wind perturbation and for aerodynamic effects caused by airplane yaw and roll.

A. Mathematical Description

Figure 24 shows the six coordinates which describe the airplane position relative to reference points on the earth's surface.

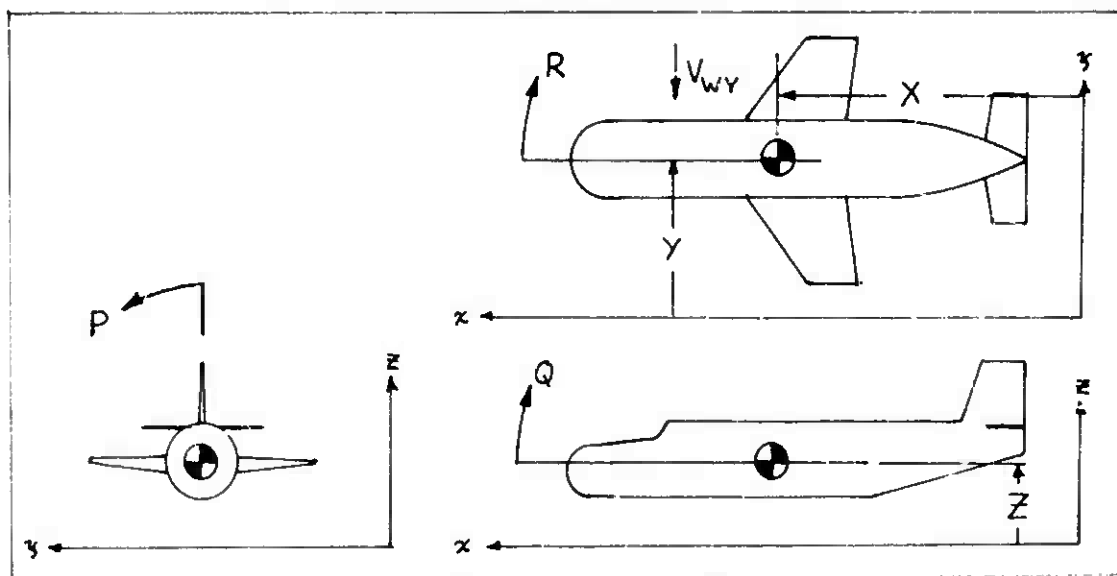


Figure 24 Airplane Coordinates

Figures 26 , 27 , and 28 show the forces acting on the airplane as seen in the different planes. Let F_{LN} denote the lateral force on the nose wheel at the axle. Then:

$$(3c.4) \quad W_{WN} \ddot{Y}_N = F_{SNS} - F_{LN}$$

Where F_{SNS} is the lateral component of the sliding or cornering force of the nose tire. The load F_{LN} is caused by the nose wheel trying to move laterally relative to the airplane. If this lateral displacement is denoted by Y_{DLN} , then:

$$(3c.5) \quad F_{LN} = C_{LN} Y_{DLN} + D_{LN} \dot{Y}_{DLN}$$

$$(3c.6) \quad Y_{DLN} = Y_N - Y + (Z + S_{HN}Q)P - S_{HN}R$$

$$(3c.7) \quad \dot{Y}_{DLN} = \dot{Y}_N - \dot{Y} + (Z + S_{HN}Q)\dot{P} + (\dot{Z} + S_{HN}\dot{Q})P - S_{HN}\dot{R}$$

Now F_{NN} is given by:

$$(3c.8) \quad F_{NN} = S_N (C_{NT} + D_{NT} \dot{S}_N)$$

where

$$(3c.9) \quad S_N = \max \{ 0.0, Z_{GD} \langle X_{WN}, Y_N \rangle + R_{\theta TN} - Z_{WN} \}$$

$$(3c.10) \quad \dot{S}_N = Z_{GDP} \langle X_{WN}, Y_N \rangle \dot{X}_{WN} - \dot{Z}_{WN}$$

Summing vertical forces on the nose gear unsprung weight:

$$(3c.11) \quad W_{WN} \ddot{Z}_{WN} = F_{NN} - F_{VN}$$

Assume that the pilot positions the nose wheel with a rate proportional to the airplane yaw angle. Thus:

$$(3c.12) \quad \dot{\theta}_N = \begin{cases} \min \{ 0, -G_{PIL} R \} & \text{if } \theta_N \geq \theta_{NMAX} \\ -G_{PIL} R & \text{if } |\theta_N| < |\theta_{NMAX}| \\ \max \{ 0, -G_{PIL} R \} & \text{if } \theta_N \leq -\theta_{NMAX} \end{cases}$$

θ_N gives the yaw angle of the nose wheel with respect to the airplane ϕ . The yaw angle of the tire with respect to its direction of motion is given by θ_{YAW} .

$$(3c.13) \quad \theta_{YAW} = \theta_N + R - (\dot{Y}_N / \dot{X}_{WN})$$

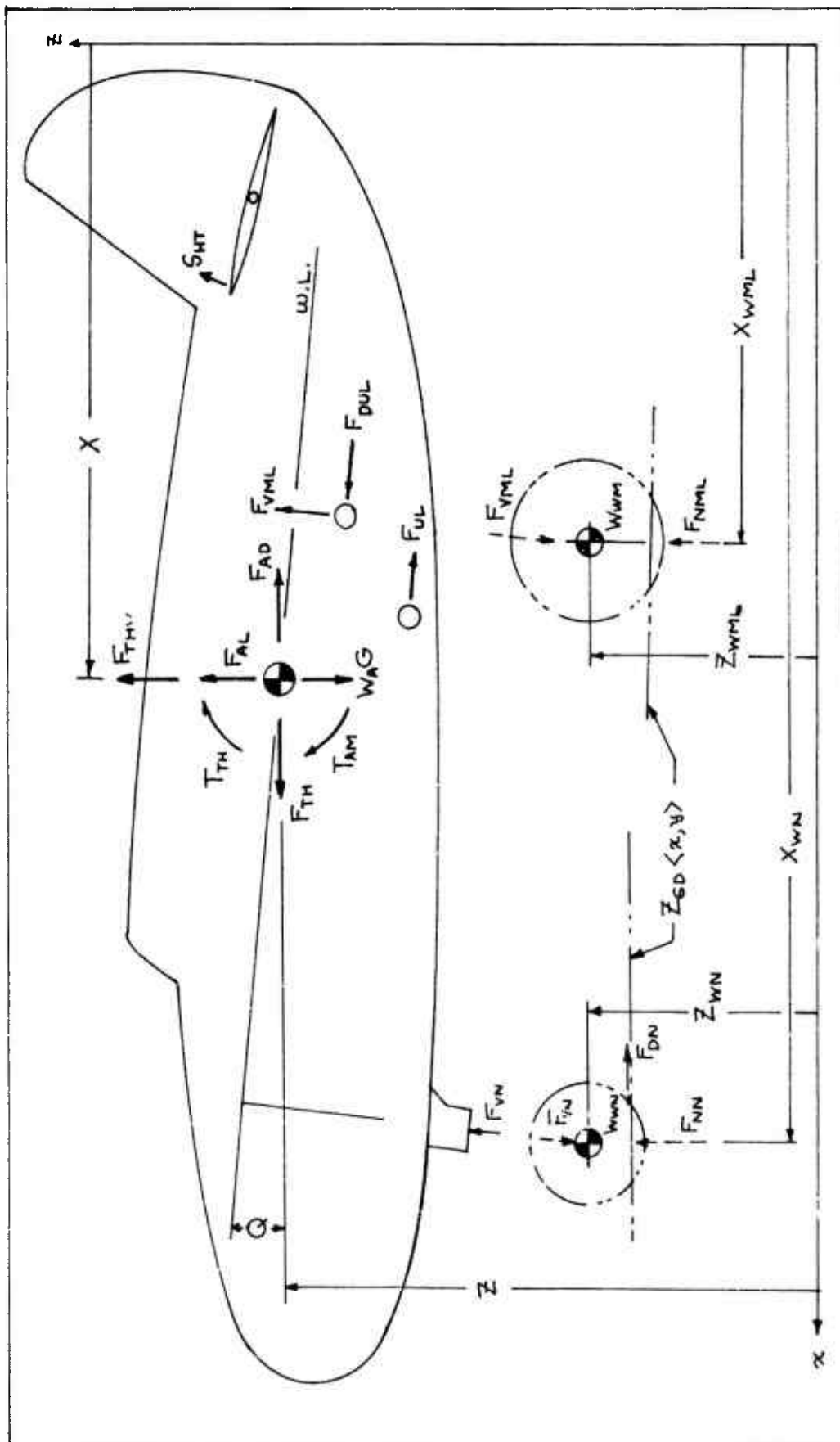


Figure 26 Airplane Dynamics (Pitch)

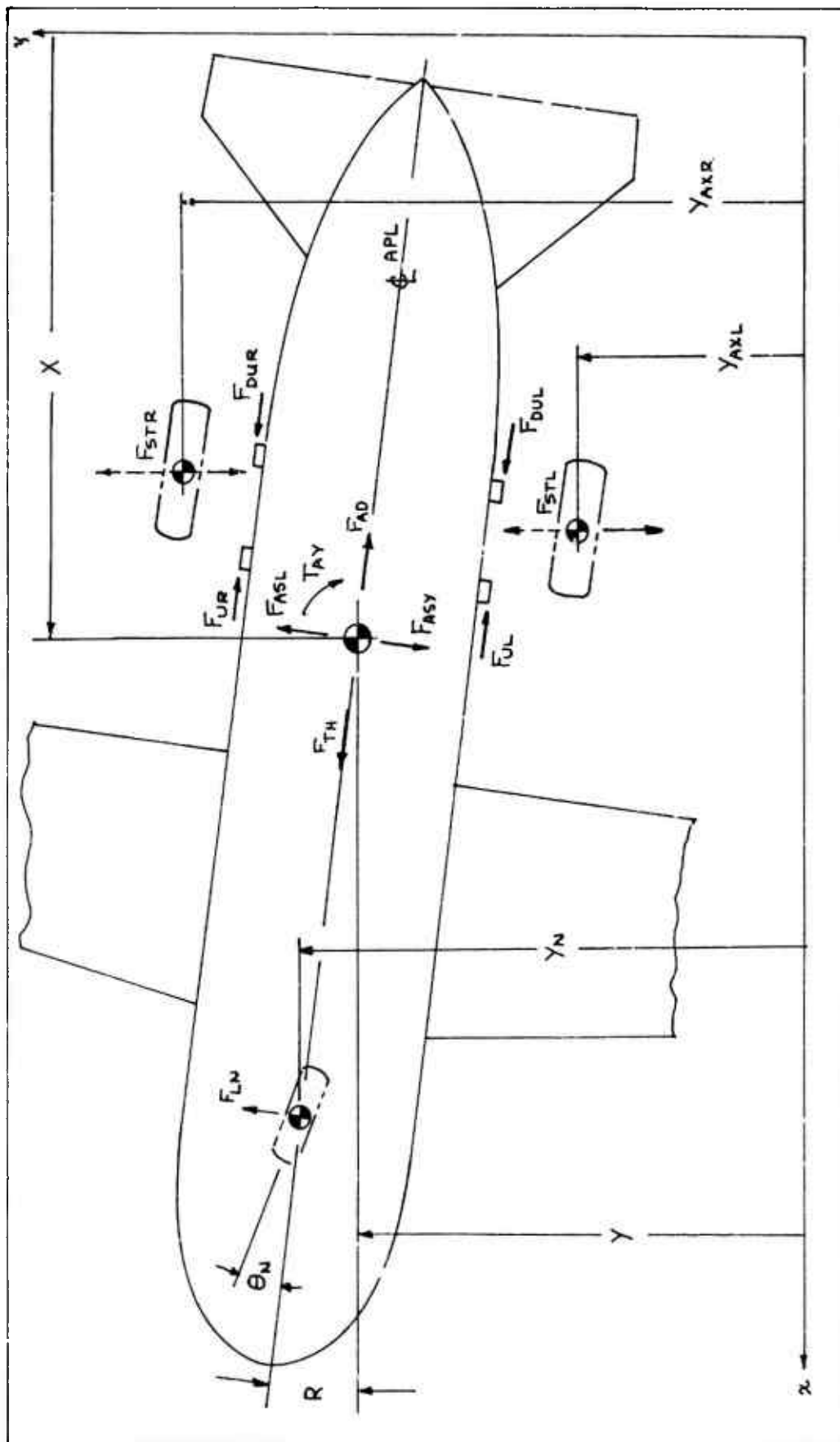


Figure 27 Airplane Dynamics (Yaw)

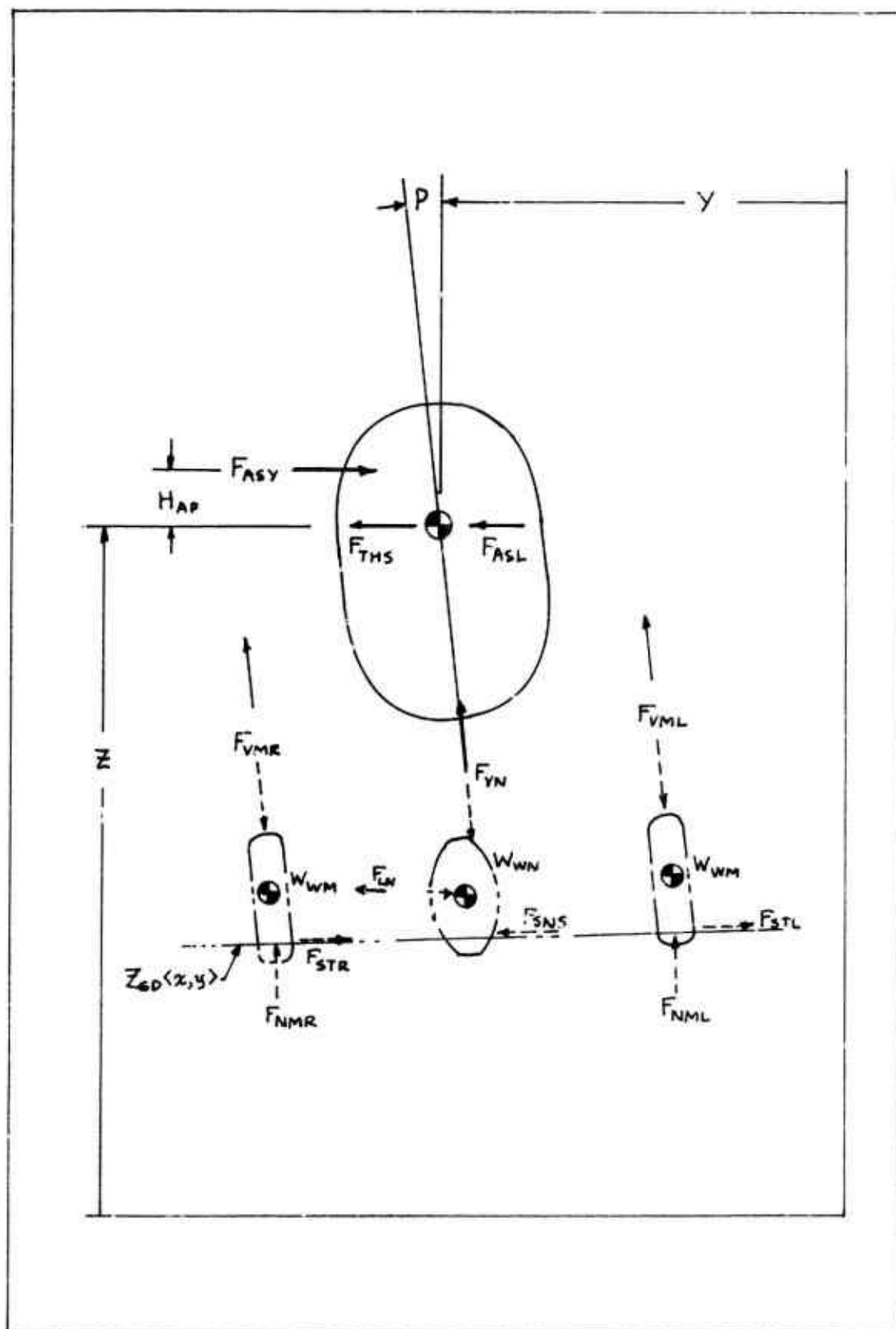


Figure 28 Airplane Dynamics (Roll)

The steering characteristic is developed from Reference 1 (p. 30). Let U_{NTF} be the coefficient of friction between the nose tire and the ground. Then the maximum force normal to the tire in the plane of the ground is F_{NTF} where:

$$(3c.14) F_{NTF} = U_{NTF} F_{NN}$$

Using equation (79) and 80) from Reference 1 :

$$(3c.15) U_{RT} = \begin{cases} P_{WC} \Theta_{YAW} / F_{NTF} & \text{if } F_{NTF} > 0 \\ 0 & \text{if } F_{NTF} \leq 0 \end{cases}$$

$$(3c.16) F_{NCFs} = \begin{cases} F_{NTF} & \text{if } U_{RT} \geq 1.5 \\ F_{NTF} (U_{RT} - 4 U_{RT}^3 / 27) & \text{if } |U_{RT}| < 1.5 \\ -F_{NTF} & \text{if } U_{RT} \leq -1.5 \end{cases}$$

Thus, F_{NCFs} corresponds to $F_{\Psi, r, e}$ in Reference 1 and P_{WC} is the cornering power given by:

$$(3c.17) P_{WC} = \begin{cases} C_{P1} S_N - C_{P2} S_N^2 & \text{if } S_N \leq S_{P1} \\ C_{P3} - C_{P4} S_N & \text{if } S_N > S_{P1} \end{cases}$$

The actual normal cornering force F_{NCF} is not F_{NCFs} , but lags F_{NCFs} because of the tire relaxation length. The expression for F_{NCF} is given by:

$$(3c.18) \dot{F}_{NCF} = (F_{NCFs} - F_{NCF})(\dot{X}_{WN} / S_{YRL})$$

Having obtained F_{NCF} , then from Figure 29 ,

$$(3c.19) F_{SNS} = F_{NCF} \cos(\Theta_N + R) - U_{RRN} F_{NN} \sin(\Theta_N + R)$$

$$(3c.20) F_{DN} = F_{NCF} \sin(\Theta_N + R) + U_{RRN} F_{NN} \cos(\Theta_N + R)$$

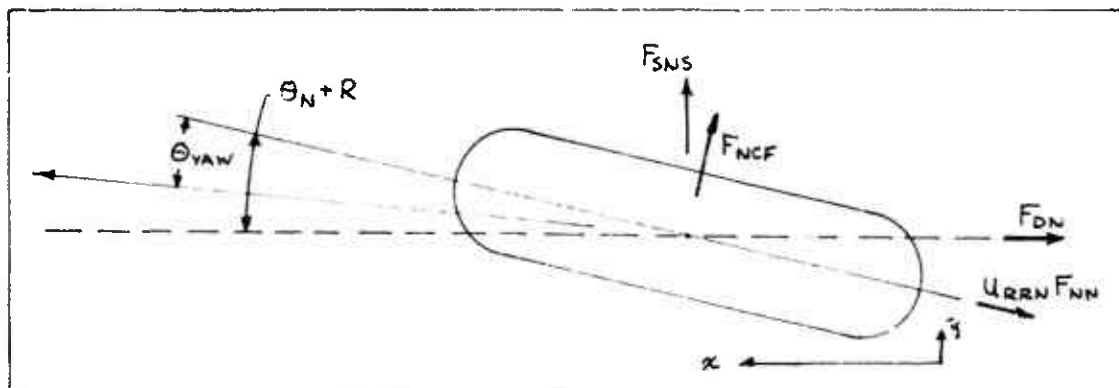


Figure 29 Nose Tire Cornering Force

Main Gear

Let Z_{SM} and \dot{Z}_{SM} denote the stroke and stroke velocity. The additional subscripts L and R refer to the left and right side of the airplane (looking forward).

$$(3c.21) \quad Z_{SMR} = Z_{WMR} - Z + S_{VM} + S_{HM}Q + S_{GW}P$$

$$(3c.22) \quad \dot{Z}_{SMR} = \dot{Z}_{WMR} - \dot{Z} + S_{HM}\dot{Q} + S_{GW}\dot{P}$$

$$(3c.23) \quad Z_{SML} = Z_{WML} - Z + S_{VM} + S_{HM}Q - S_{GW}P$$

$$(3c.24) \quad \dot{Z}_{SML} = \dot{Z}_{WML} - \dot{Z} + S_{HM}\dot{Q} - S_{GW}\dot{P}$$

The main gear shock strut forces are then given by:

$$(3c.25) \quad F_{VMR} = F_{VMS}\langle Z_{SMR} \rangle + D_{VM}\dot{Z}_{SMR} + A_{VM}\langle Z_{SMR} \rangle \dot{Z}_{SMR} |\dot{Z}_{SMR}|$$

$$(3c.26) \quad F_{VML} = F_{VMS}\langle Z_{SML} \rangle + D_{VM}\dot{Z}_{SML} + A_{VM}\langle Z_{SML} \rangle \dot{Z}_{SML} |\dot{Z}_{SML}|$$

Let S_M denote the main gear tire deflection and let F_{NM} be the associated load. Thus, in the vertical direction, the relation between the load and tire deflection is given as follows:

$$(3c.27) \quad F_{NMR} = S_{MR} (C_{MT} + D_{MT}\dot{S}_{MR})$$

$$(3c.28) \quad F_{NML} = S_{ML} (C_{MT} + D_{MT}\dot{S}_{ML})$$

$$(3c.29) \quad S_{MR} = \max\{0, Z_{GD}\langle X_{WMR}, Y_{MR} \rangle + R_{OTM} - Z_{WMR}\}$$

$$(3c.30) \quad \dot{S}_{MR} = Z_{GDP}\langle X_{WMR}, Y_{MR} \rangle \dot{X}_{WMR} - \dot{Z}_{WME}$$

$$(3c.31) \quad S_{ML} = \max\{0, Z_{GD}\langle X_{WML}, Y_{ML} \rangle + R_{OTM} - Z_{WML}\}$$

$$(3c.32) \quad \dot{S}_{ML} = Z_{GDP}\langle X_{WML}, Y_{ML} \rangle \dot{X}_{WML} - \dot{Z}_{WML}$$

Summing forces in the vertical direction on the main gear wheels,

$$(3c.33) \quad W_{WM} \ddot{Z}_{WMR} = F_{NMR} - F_{VMR} + F_{ORVR}$$

$$(3c.34) \quad W_{WM} \ddot{Z}_{WML} = F_{NML} - F_{VML} + F_{ORVL}$$

Figure 30 shows a side view of the left hand main gear. With the assumption that $W_u \ll W_A$, Θ_{GR} and Θ_{GL} are described by:

$$(3c.35) W_u S_{GU}^2 \ddot{\theta}_{GR} = S_{GU} F_{UR} + (S_{GU} + Z_{GLR})(F_{TL} - F_{TR} - F_{GR}) - T_{SR}$$

$$(3c.36) W_u S_{GU}^2 \ddot{\theta}_{GL} = S_{GU} F_{UL} + (S_{GU} + Z_{GLL})(F_{TR} - F_{TL} - F_{GL}) - T_{SL}$$

where

$$(3c.37) Z_{GLR} = S_{GL} - Z_{SMR}$$

$$(3c.38) Z_{GLL} = S_{GL} - Z_{SML}$$

The forces F_{TR} and F_{TL} are used to impart the correct moment into the gear.

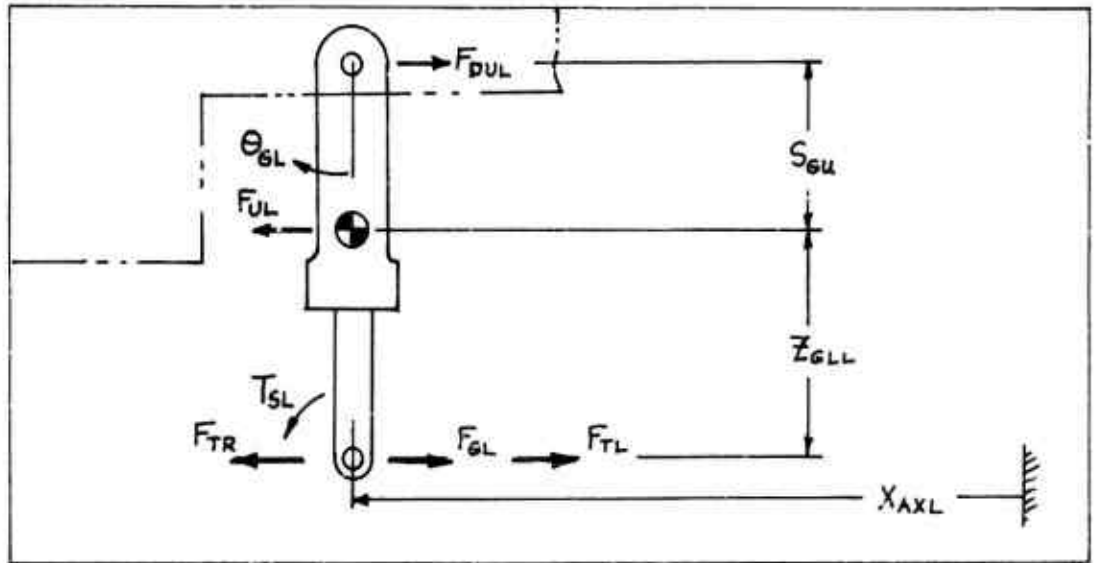


Figure 30 Side View of the Main Gear Strut

The overall gear system model is shown in Figure 31. In order to transmit torque properly, the forces $F_{TR\theta}$ and $F_{TL\theta}$ are applied equal and opposite on different sides of the gear. Thus,

$$(3c.39) F_{TR\theta} = F_{GR} (S_{GW} - S_{GS}) / 2 S_{GS}$$

$$(3c.40) F_{TL\theta} = F_{GL} (S_{GW} - S_{GS}) / 2 S_{GS}$$

If it is assumed that 100 H_A percent of this torque is taken directly into the airplane, then 100 $H_G = 100 - 100 H_A$ percent is transmitted through the gear. Thus,

$$(3c.41) F_{TR} = H_G F_{TR\theta}$$

$$(3c.42) F_{TL} = H_G F_{TL\theta}$$

All spring loads
positive in tension

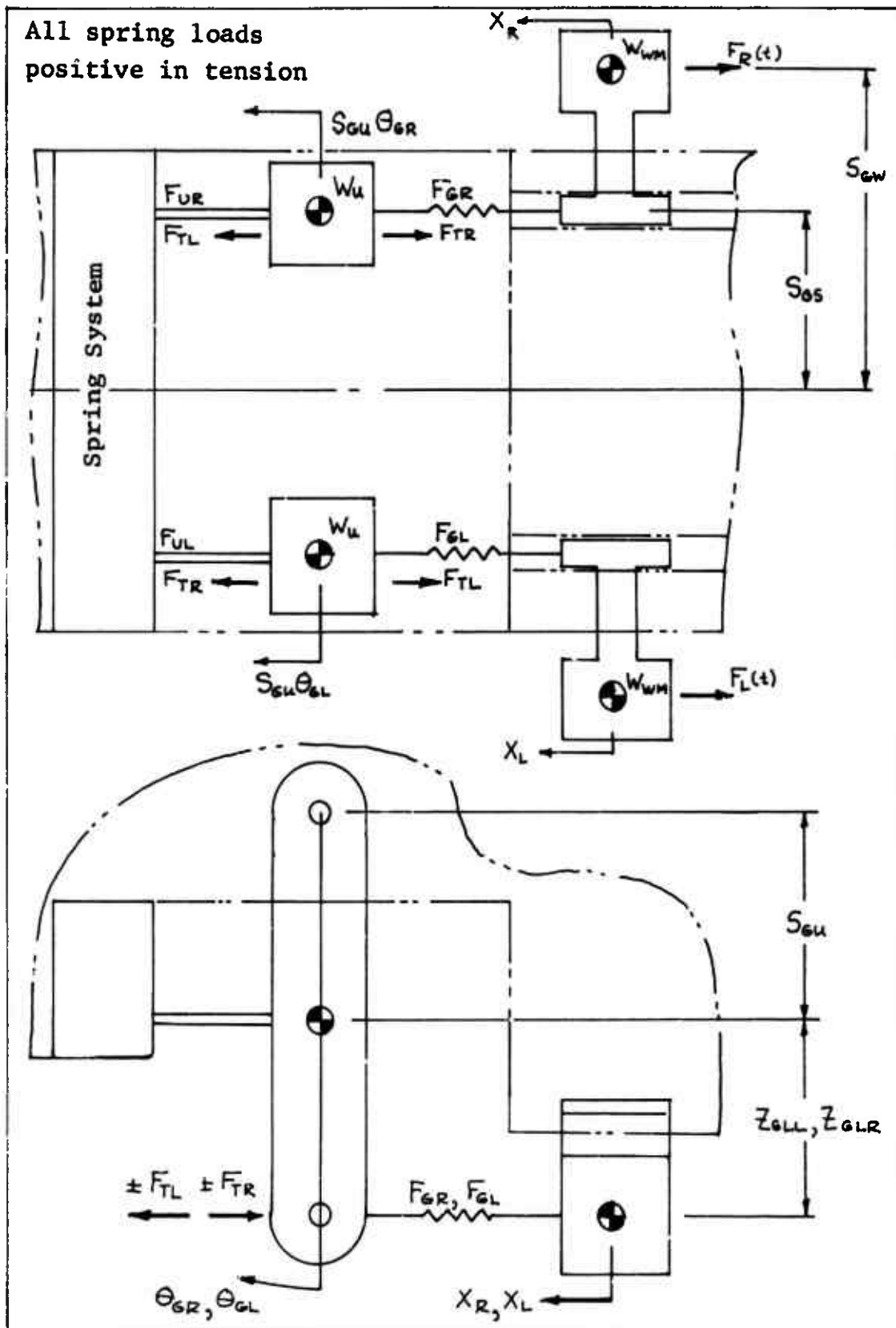


Figure 31 Main Gear Model

Let Q_R and Q_L be the difference between the gear rotation and the airplane rotation. That is,

$$(3c.43) \quad Q_R = Q - \theta_{GR}$$

$$(3c.44) \quad Q_L = Q - \theta_{GL}$$

$$(3c.45) \quad \dot{Q}_R = \dot{Q} - \dot{\theta}_{GR}$$

$$(3c.46) \quad \dot{Q}_L = \dot{Q} - \dot{\theta}_{GL}$$

Then we can find constants C_{u1} , C_{u2} , D_{u1} , and D_{u2} such that:

$$(3c.47) \quad F_{UR} = S_{GU}(C_{u1}Q_R - C_{u2}Q_L) + S_{GU}(D_{u1}\dot{Q}_R - D_{u2}\dot{Q}_L)$$

$$(3c.48) \quad F_{UL} = S_{GU}(C_{u1}Q_L - C_{u2}Q_R) + S_{GU}(D_{u1}\dot{Q}_L - D_{u2}\dot{Q}_R)$$

It then follows, assuming negligible strut moment of inertia that:

$$(3.49) \quad F_{DUR} = ((F_{GR} + F_{TR} - F_{TL})Z_{GLR} + T_{SE}) / S_{GU}$$

$$(3c.50) \quad F_{DUL} = ((F_{GL} + F_{TL} - F_{TR})Z_{GLL} + T_{SL}) / S_{GU}$$

As outputs to the tire and wheel systems we need to compute X_{AX} and Y_{AX} . X_{AX} is shown in Figure 30. Y_{AX} is assumed to be the undeflected tire footprint position in the y direction.

$$(3c.51) \quad X_{AXL} = X + S_{GW}R + S_{VMU}Q + (S_{GU} + Z_{GLL})\theta_{GL} - S_{HM}$$

$$(3c.52) \quad X_{AXR} = X - S_{GW}R + S_{VMU}Q + (S_{GU} + Z_{GLR})\theta_{GR} - S_{HM}$$

$$(3c.53) \quad \dot{X}_{AXL} = \dot{X} + S_{GW}\dot{R} + S_{VMU}\dot{Q} + (S_{GU} + Z_{GLL})\dot{\theta}_{GL}$$

$$(3c.54) \quad \dot{X}_{AXR} = \dot{X} - S_{GW}\dot{R} + S_{VMU}\dot{Q} + (S_{GU} + Z_{GLR})\dot{\theta}_{GR}$$

$$(3c.55) \quad Y_{AXL} = Y - S_{GW} - (S_{HM} - S_{VMU}Q - (S_{GU} + Z_{GLL})\theta_{GL})R - (S_{VMU} + S_{GU} + Z_{GLL})P$$

$$(3c.56) \quad Y_{AXR} = Y + S_{GW} - (S_{HM} - S_{VMU}Q - (S_{GU} + Z_{GLR})\theta_{GR})R - (S_{VMU} + S_{GU} + Z_{GLR})P$$

$$(3c.57) \quad \dot{Y}_{AXL} = \dot{Y} - (S_{HM} - S_{VMU}Q - (S_{GU} + Z_{GLL})\theta_{GL})\dot{R} + (S_{VMU}\dot{Q} + (S_{GU} + Z_{GLL})\dot{\theta}_{GL})R - (S_{VMU} + S_{GU} + Z_{GLL})\dot{P}$$

$$(3c.58) \dot{Y}_{AXR} = \dot{Y} - (S_{HM} - S_{VMU}Q - (S_{GU} + Z_{GLR})\dot{\Theta}_{GR})\dot{R} \\ + (S_{VMU}\dot{Q} + (S_{GU} + Z_{GLR})\dot{\Theta}_{GR})R \\ - (S_{VMU} + S_{GU} + Z_{GLR})\dot{P}$$

Engine Thrust

Referring to Figures 26 and 27, if F_{TH} is the engine thrust, then

$$(3c.59) F_{THV} = F_{TH} (\alpha_{TH} + Q)$$

$$(3c.60) T_{TH} = S_{TH} F_{TH}$$

$$(3c.61) F_{THS} = F_{TH} R$$

Aerodynamics

The following eight equations apply as in the three-degree model.

$$(3c.62) Q_A = \dot{X}^2 A_{REF} R_{HA} / Z_{BB}$$

$$(3c.63) F_{AL} = C_{AL} Q_A$$

$$(3c.64) F_{AD} = C_{AD} Q_A$$

$$(3c.65) T_{AM} = C_{AM} Q_A$$

$$(3c.66) \alpha_W = \alpha_0 + (180/\pi)(Q - \dot{Z}/\dot{X})$$

$$(3c.67) C_{AL} = G_{AL} + B_{AL}\alpha_W + E_{AL}S_{HT}$$

$$(3c.68) C_{AD} = G_{AD} + B_{AD}\alpha_W + E_{AD}S_{HT}$$

$$(3c.69) C_{AM} = G_{AM} + B_{AM}\alpha_W + E_{AM}S_{HT}$$

Let V_{wy} denote the wind gust velocity as shown in Figure 24. If Ψ and β are defined by:

$$(3c.70) \Psi = (V_{wy} + \dot{Y})/\dot{X}$$

$$(3c.71) \beta = (180/\pi)(\Psi - R)$$

Then β is the angle of sideslip.

Let Q_{AT} denote the dynamic air pressure (including side wind) multiplied by the reference area. Then:

$$(3c.72) \quad Q_{AT} = ((V_{wy} + \dot{Y})^2 + \dot{X}^2) A_{REF} R_{HA} / 288$$

Then the aerodynamic yaw moment is given by:

$$(3c.73) \quad T_{AY} = C_{AN} / \beta \quad Q_{AT}$$

and the aerodynamic side force is given by:

$$(3c.74) \quad F_{ASY} = C_{AY} / \beta \quad Q_{AT}$$

Finally, an aerodynamic force F_{ASL} due to a combination of lift and pitch is:

$$(3c.75) \quad F_{ASL} = F_{AL} P$$

Refer to Figure 27 as to the direction of these forces.

Dynamics

Referring to Figures 26 and 27, summing forces in the x, y, and z direction,

$$(3c.76) \quad W_A \ddot{Z} = F_{AL} + F_{THV} - W_A G + F_{VMR} + F_{VML} + F_{VN}$$

$$(3c.77) \quad W_A \ddot{X} = F_{TH} - F_{AD} + F_{DUR} + F_{DUL} - F_{UR} - F_{UL} - F_{DN}$$

$$(3c.78) \quad W_A \ddot{Y} = F_{THS} - F_{STR} - F_{STL} + F_{LN} + F_{ASL} - F_{ASY}$$

Summing moments about the C.G. we have:

$$(3c.79) \quad W_{IQ} \ddot{Q} = F_{VN} S_{HN} - F_{VMR} S_{HM} - F_{VML} S_{HM} + F_{DUR} S_{VMU} \\ + F_{DUL} S_{VMU} + T_{TH} + T_{AM} - F_{UR} (S_{GU} + S_{VMU}) \\ - F_{UL} (S_{GU} + S_{VMU}) - F_{DN} (Z - Z_{GD} \langle X_{WN} \rangle)$$

$$(3c.80) \quad W_{IR} \ddot{R} = F_{LN} S_{HN} + S_{GS} (F_{UR} - F_{UL} + F_{DUL} - F_{DUR}) + T_{AY} \\ + Z_{HA} (F_{TRO} - F_{TLO}) S_{GS}$$

$$(3c.81) \quad W_{IP} \ddot{P} = (F_{VML} - F_{VMR}) S_{GW} + F_{ASY} H_{AP} \\ - (Z - Z_{GD} \langle X, Y \rangle) (F_{STR} + F_{STL} + F_{LN})$$

$$(3c.82) \quad X_{WN} = X + S_{HN} + S_{VN} Q$$

$$(3c.83) \quad \dot{X}_{WN} = \dot{X} + S_{VN} \dot{Q}$$

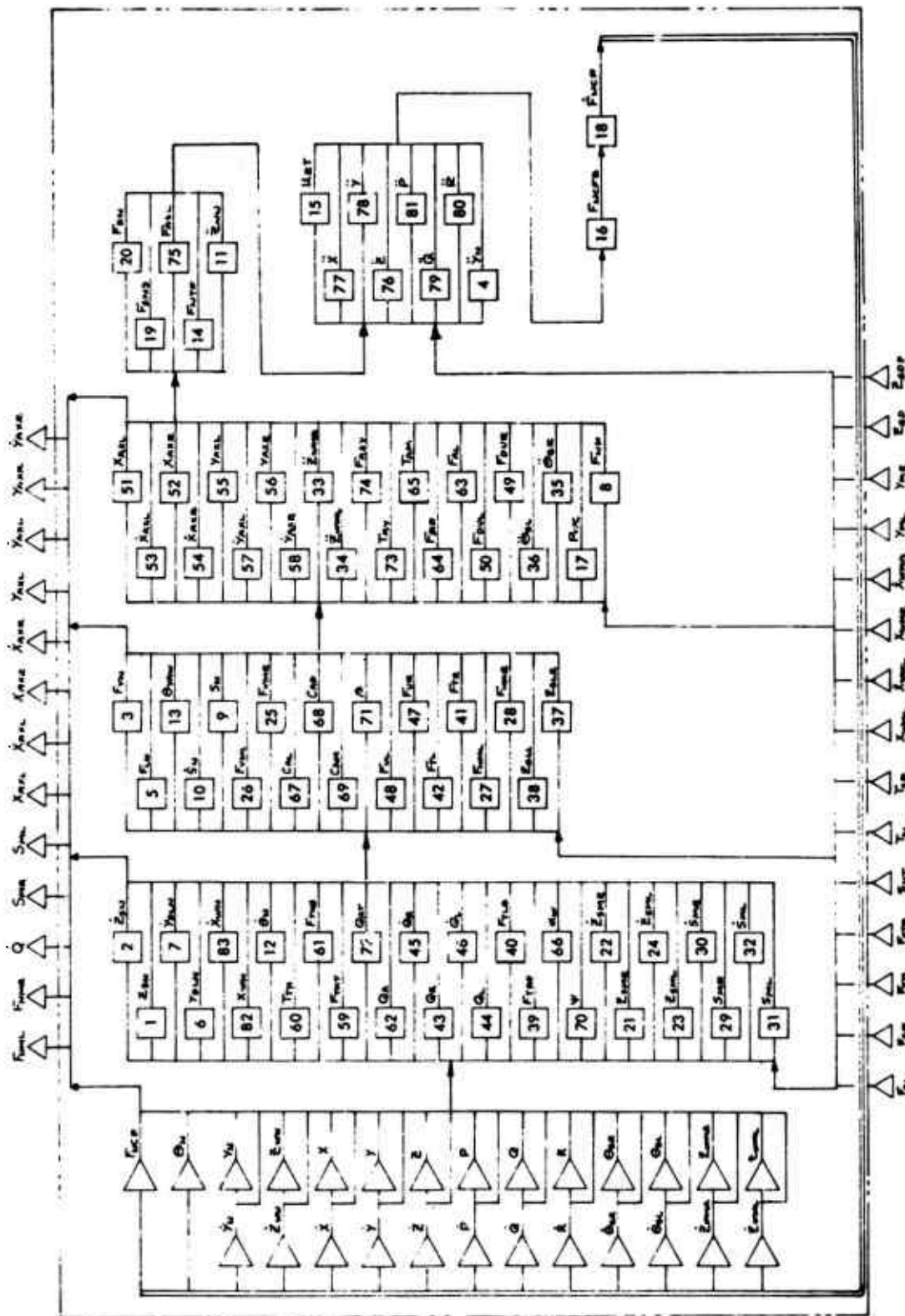


Figure 32 Airplane System (6 Degree) Equation Flow Diagram

B. Parameter Evaluation

Nose Gear Characteristics

Based on a nose gear lateral natural frequency of 12 cps, we have $\omega_n = 2\pi(12) = 75.5$ RAD/SEC. Since $W_{WN} = .435$, then:

$$(3c.84) C_{LN} = W_{WN} \omega_n^2 = .435 (75.5)^2 = 2480 \text{ lb/in}$$

Using $\eta = .054$ as in the calculation of D_G in the three-degree model.

$$(3c.85) D_{LN} = \eta C_{LN} / \omega_n = (.054)(2480) / 75.5 = 1.78 \text{ lb sec/in}$$

The steering or cornering characteristic parameters are obtained from Reference 1. Based on Figure 44(a) in Reference 1, the value for U_{NTF} is:

$$(3c.86) U_{NTF} = F_{\psi, r, e(\max)} / F_z = 25000 / 45200 = .553$$

Using equation 82 from Reference 1, if $K = (P + .44 P_R) w^2 = (1.44)(190)(6.6)^2 = 11,920$ lb. then:

$$(3c.87) C_{P1} = 1.2 C_c K / d = (1.2)(57)(11920) / 22 = 37060 \text{ lb/Rad in}$$

$$(3c.88) C_{P2} = 8.8 C_c K / d^2 = (8.8)(57)(11920) / (22)^2 = 12353 \text{ lb/Rad in}^2$$

$$(3c.89) C_{P3} = .0674 C_c K = (.0674)(57)(11920) = 45794 \text{ lb/Rad}$$

$$(3c.90) C_{P4} = .34 C_c K / d = (.34)(57)(11920) / 22 = 10500 \text{ lb/Rad in}$$

$$(3c.91) S_{P1} = .0875 d = (.0875)(22) = 1.925 \text{ in}$$

From Figure 43 in Reference 1 we see that the cornering force lags the yaw angle. Equation 63 in Reference 1 shows that the equation which describes the curves in Figure 43 is given by:

$$(3c.92) F_{y, r} = (1 - e^{-x/L_y}) F_{y, r \max} \langle \Theta_{YAW} \rangle$$

where L_y is the tire yawed rolling relaxation length. Differentiating this equation, there follows:

$$(3c.93) \frac{dF_{y, r}}{dx} = \frac{e^{-x/L_y}}{L_y} F_{y, r \max} \langle \Theta_{YAW} \rangle$$

Eliminating e^{-x/L_y} results in:

$$(3c.94) \quad F_{y,r} + L_y \frac{dF_{y,r}}{dx} = F_{y,r \max} \langle \Theta_{YAW} \rangle$$

Equation (3c.18) is obtained by using:

$$(3c.95) \quad \frac{dF_{y,r}}{dx} = \frac{dF_{y,r}}{dt} \bigg/ \frac{dx}{dt} \approx \frac{\dot{F}_{NCF}}{\dot{X}_{WN}}$$

where it is assumed for large airplane velocities that $\dot{X}_{WN} = dx/dt$. We see that the parameter S_{yRL} is the relaxation length. From Figure 39 of Reference 1, for most conditions, S_{yRL} is obtained from:

$$(3c.96) \quad S_{yRL} = .6 w (2.8 - .8 P/P_r) \\ = (.6)(6.6)(2.8 - .8) = 7.92 \text{ in}$$

Main Gear Characteristics

For many airplanes which have a conventional strut arrangement (similar to a B-58) most of the moment about the shock strut ϕ is taken out through the shock strut. In this case equations (3c.41) and (3c.42) would use $H_G = 0.0$. In the case of the F-111 gear the opposite result occurs so that $H_G = 1.0$ and $H_A = 0.0$. The following values apply to the F-111 gear:

$$(3c.97) \quad \left\{ \begin{array}{l} W_u = .723 \text{ lb sec}^2/\text{in} \\ W_{WM} \cdot W_{WV} = 1.667 \text{ lb sec}^2/\text{in} \\ S_{Gu} = 21.00 \text{ in} \\ S_{Gw} = 60.00 \text{ in} \\ S_{Gs} = 20.00 \text{ in} \\ H_G = 1.0 \\ H_A = 0.0 \end{array} \right.$$

If loads $F_R(t) = F_L(t) = F_0$ are applied as shown in figure 31, then because of symmetry, the result will be that $Q_R = Q_L$. But then equation (3c.47) says that $C_{u1} - C_{u2} = F_{UR}/S_{Gu} Q_R$ but $C_u = F_{UR}/S_{Gu} Q_R$ as shown in the 3 degree model. Thus

$$(3c.98) \quad C_{u1} - C_{u2} = C_u = 59,000 \text{ lb/in}$$

With the main gear at static, if a drag load of 18,000 lb. is applied to the left gear at the ground and -18,000 lb. is applied to the right gear at the ground the observed deflections with $Q = 0$ are $Q_L = .0236$ rad and $Q_R = -.0236$ rad. (Assuming a lateral beam torsional spring rate of 43.0×10^6 in lb/rad).

In the equations which describe the gear loading T_{SR} and T_{SL} can be chosen as 0 if Z_{GLL} and Z_{GLR} are the dimensions to the ground instead of the axle. Thus $Z_{GL} = Z_{GLL} = Z_{GLR} = 2.2 + 12.9 = 21.4$ in. Equations (3c.35), (3c.36), (3c.39), (3c.40), (3c.41) and (3c.42) can then be combined to give

$$\begin{aligned} (3c.99) \quad F_{UR} - F_{UL} &= \left(\frac{S_{GU} + Z_{GL}}{S_{GU}} \right) (F_{GR} - F_{GL}) \left(1 + H_G \left(\frac{S_{GW} - S_{GS}}{S_{GS}} \right) \right) \\ &= \left(\frac{21.0 + 21.4}{21.0} \right) (-36000) \left(1 + \left(\frac{60 - 20}{20} \right) \right) = -212,000 \text{ lb} \end{aligned}$$

Subtracting equation (3c.48) from (3.47) results in

$$(3c.100) \quad F_{UR} - F_{UL} = (C_{u1} + C_{u2}) S_{GU} Q_R - (C_{u1} + C_{u2}) S_{GU} Q_L$$

So that

$$(3c.101) \quad C_{u1} + C_{u2} = \frac{-212000}{(2)(21.0)(-.0236)} = 214,000 \text{ lb/in}$$

Adding and subtracting equations (3c.98) and (3c.101) results in

$$(3c.102) \quad C_{u1} = \frac{59000 + 214000}{2} = 136,500 \text{ lb/in}$$

$$(3c.103) \quad C_{u2} = \frac{214,000 - 59000}{2} = 77,500 \text{ lb/in}$$

At a fore and aft natural frequency of 137.5 rad/sec, the damping coefficients D_{u1} and D_{u2} are given as

$$(3c.104) \quad D_{u1} = \eta C_{u1} / \omega = \frac{(.054)(1.36 \times 10^5)}{(137.5)} = 53.4 \text{ lb sec/in}$$

$$(3c.105) \quad D_{u2} = \eta C_{u2} / \omega = \frac{(.054)(.775 \times 10^5)}{(137.5)} = 30.5 \text{ lb sec/in}$$

Aerodynamic Characteristics

The coefficients for equations (3c.62) thru (3c.69) have been derived in the 3 degree model. For the F-111A in the landing configuration and wings swept to 26 degrees as described in the 3 degree system, $C_{N\beta} = .0014$ and $C_{Y\beta} = -.021$. Then the coefficient C_{AY} is calculated from

$$(3c.106) \quad C_{AY} = -C_{Y\beta} = .021 \text{ deg}^{-1}$$

Let $\Delta X = FSA - FSCG$ as in the 3 degree system where $FSA = 526.8$ and $FSCG = 519.0$. Let b be the wing span. If $b = 756$ in., then

$$(3c.107) \quad C_{AN} = b C_{N\beta} - \Delta X C_{Y\beta}$$

$$(3c.108) \quad C_{AN} = (756)(.0014) - (7.80)(-.021) = 1.222 \text{ in/deg}$$

Airplane Characteristics

The parameters listed in Table 7 describing the airplane's dimensional and mass characteristics are those previously derived in the 3 degree model or simply a listing of the appropriate values applicable to the F-111 for which no derivation or computation is required.

Table 7 Airplane System (6 Degree) Parameters

SYMBOL	TYPE	VALUE	UNITS	DESCRIPTION
α_0	C	1.00	deg	Wing Angle of Incidence
α_{TH}	C	-.052	rad	Angle between Thrust & W.L.
α_w	V		deg	Wing Angle of Attack
A_{REF}	C	525.0	ft ²	Wing Reference Area
A_{VM}	V*		lb sec ² /in ²	M.G. Shock Strut Damping Coeff.
A_{VN}	V*		lb sec ² /in ²	N.G. Shock Strut Damping Coeff.
B_{AD}	C	0.00	deg ⁻¹	Aero Drag Parameter
B_{AL}	C	.128	deg ⁻¹	Aero Lift Parameter
B_{AM}	C	-.371	in/deg	Aero Moment Parameter
β	V		deg	Angle of Sideslip
C_{AD}	V		-	Aero Drag Coefficient
C_{AL}	V		-	Aero Lift Coefficient
C_{AM}	V		in	Aero Moment Coeff. (Pitch)
C_{AN}	C	1.222	in/deg	Aero Moment Coeff. (Yaw)
C_{AY}	C	.021	deg ⁻¹	Aero Side Force Coeff.
C_{LN}	C	2480	lb/in	Nose Gear Lateral Spring Rate
C_{MT}	C	9530	lb/in	M.G. Tire Vertical Spring Rate
C_{NT}	C	12,200	lb/in	N.G. Tire(s) Vertical Spring Rate
C_{PI}	C	37,060	lb/rad in	Parameters for P_{wc}
C_{P2}	C	12,353	lb/rad in ²	
C_{P3}	C	45,794	lb/rad	Drag Brace Characteristic Spring Rates
C_{P4}	C	10,500	lb/rad in	
C_{U1}	C	1.365×10^5	lb/in	Nose Gear Lateral Damping Coeff.
C_{U2}	C	.775 $\times 10^5$	lb/in	
D_{LN}	C	1.78	lb sec/in	M.G. Tire Vertical Damping Coeff.
D_{MT}	C	38.8	lb sec/in ²	N.G. Tire(s) Vertical Damping Coefficient
D_{NT}	C	50.6	lb sec/in ²	

Table 7 (Contd)

SYMBOL	TYPE	VALUE	UNITS	DESCRIPTION
D_{u1}	C	53.4	lb sec/in	Drag Brace Characteristic
D_{u2}	C	30.5	lb sec/in	Damping Coefficient
D_{vm}	C	0.0	lb sec/in	M. G. Shock Strut Linear Damping Coefficient
D_{vn}	C	0.0	lb sec/in	N. G. Shock Strut Linear Damping Coefficient
E_{AD}	C	-.0036	deg ⁻¹	Aero Drag Coefficient
E_{AL}	C	.022	deg ⁻¹	Aero Lift Coefficient
E_{AM}	C	-3.759	in/deg	Aero Moment Coefficient
F_{AD}	V		lb	Aero Drag
F_{AL}	V		lb	Aero Lift
F_{ASL}	V		lb	Side Force Due to Aero Lift
F_{ASY}	V		lb	Side Force Due to Yaw
F_{DN}	V		lb	N. G. Rolling Resistance
F_{DVL}	V		lb	Horizontal Load at M. G. Pivot
F_{DUR}	V		lb	
F_{GL}	V(I)		lb	Horizontal Load on M. G. Axle
F_{GR}	V(I)		lb	
F_{LN}	V		lb	Lateral Nose Gear Load
F_{NCF}	V		lb	Normal Cornering Force
F_{NCFO}	C	0.0	lb	Normal Cornering Force at Time ≈ 0
F_{NCF}	V		lb/sec	Time Derivative of Normal Cornering Force
F_{NCFS}	V		lb	Steady State Normal Cornering Force
F_{NML}	V(O)		lb	M. G. Tire Normal Load
F_{NMR}	V(O)		lb	

Table 7 (Contd)

SYMBOL	TYPE	VALUE	UNITS	DESCRIPTION
F_{NN}	V		lb	N.G. Tire Normal Load
F_{NTF}	V		lb	Nose Tire Friction Force
F_{SNS}	V		lb	Nose Tire Lateral Force
F_{STL}	V(I)		lb	M. G. Lateral Tire Force
F_{STR}	V(I)		lb	
F_{TL}	V		lb	
F_{TLO}	V		lb	M. G. Loads for Torque
F_{TR}	V		lb	Takeout Correction
F_{TRO}	V		lb	
F_{TH}	V		lb	Engine Thrust
F_{THV}	C	1000.	lb	Vertical Component of Engine Thrust
F_{THS}	V		lb	Side Component of Engine Thrust
F_{FUL}	V		lb	M. G. Loads in Fictitious Drag Brace
F_{UR}	V		lb	M. G. Shock Strut Load
F_{VML}	V		lb	
F_{VMR}	V		lb	M. G. Shock Strut Air Load Curve
F_{VMS}	V*		lb	N. G. Shock Strut Load
F_{VN}	V		lb	N. G. Shock Strut Air Load Curve
F_{VNS}	V*		lb	Gravitational Constant
G	C	386	in/sec ²	Aero Drag Parameter
G_{AD}	C	.240	-	Aero Lift Parameter
G_{AL}	C	-.016	-	Aero Moment (Pitch) Parameter
G_{AM}	C	2.286	in	Pilot's Steering Gain
G_{PIL}	C	3.0	sec ⁻¹	Torque Adjustment Parameter
H_A	C	0.0	-	$H_A + H_0 = 1$
H_{AP}	C	0.0	in	Height of Center of Pressure above C. G.

*Point Plot Input

Table 7 (Contd)

SYMBOL	TYPE	VALUE	UNITS	DESCRIPTION
H_G	C	1.0	-	Torque Adjustment Parameter
Θ_N	V		rad	Nose Wheel Turn Angle Relative to A_{PL} .
Θ_{N0}	C	0.0	rad	Θ_N at Time = 0
$\dot{\Theta}_N$	V		rad/sec	$d\Theta_N/dt$
Θ_{GR}	V		rad	M. G. Strut Rotation from Horizontal
Θ_{GL}	V		rad	Θ_G at Time = 0
Θ_{GL0}	C	.0329	rad	
Θ_{GR0}	C	.0329	rad	Angular Velocity of M. G. Strut
$\dot{\Theta}_{GL}$	V		rad/sec	
$\dot{\Theta}_{GR}$	V		rad/sec	$\dot{\Theta}_G$ at time = 0
$\dot{\Theta}_{GL0}$	C	0.0	rad/sec	
$\dot{\Theta}_{GR0}$	C	0.0	rad/sec	Angular Acceleration of M. G. Strut
$\ddot{\Theta}_{GL}$	V		rad/sec ²	
$\ddot{\Theta}_{GR}$	V		rad/sec ²	
Θ_{NMAX}	C	0.7	rad	Maximum Nose Wheel Turning Angle
Θ_{YAW}	C		rad	Nose Wheel Turning Yaw Angle
ψ	V		rad	Angle of Relative Wind
P	V		rad	Airplane Roll Angle
P_0	C	0.0	rad	P at Time = 0
\dot{P}	V		rad/sec	Airplane Roll Rate
\dot{P}_0	C	0.0	rad/sec	\dot{P} at Time = 0
\ddot{P}	V		rad/sec ²	Roll Acceleration
P_{wc}	V		lb/rad	Nose Tire Cornering Power
Q	V		rad	Airplane Pitch Angle
Q_0	C	.0329	rad	Q at Time = 0
\dot{Q}	V(o)		rad/sec	Pitch Rate

Table 7 (Contd)

SYMBOL	TYPE	VALUE	UNITS	DESCRIPTION
\dot{Q}_0	C	0.0	rad/sec	\dot{Q} at Time = 0
\ddot{Q}	V		rad/sec ²	Pitch Acceleration
Q_A	V		lb	Aero Press X Aref
Q_{AT}	V		lb	Aero Press X Aref (Includes Vwy)
Q_L	V		rad	Angular Position and Velocity
\dot{Q}_L	V		rad/sec	of M. G. Relative to the Airplane
\ddot{Q}_L	V		rad/sec	
\ddot{Q}_R	V		rad	Airplane Yaw Angle
R	C	0.0	rad	R at Time = 0
\dot{R}_0	V		rad/sec	Yaw Rate
\ddot{R}_0	C	0.0	rad/sec ²	\dot{R} at Time = 0
\ddot{R}	V		rad/sec ²	Yaw Acceleration
$R_{\theta M}$	C	23.32	in	M. G. Tire Undelected Radius
$R_{\theta N}$	C	10.80	in	N. G. Tire Undelected Radius
R_{HA}	C	.00238	slug/ft ³	Air Density
S_{GL}	C	26.50	in	#
S_{GS}	C	20.00	in	#
S_{GU}	C	21.00	in	#
S_{GW}	C	60.00	in	#
S_{HM}	C	36.20	in	#
S_{HN}	C	258.90	in	#
S_{HT}	V(I)		deg	Horizontal Tail Deflection
S_{MR}	V(O)		in	M. G. Tire Deflection
S_{ML}	V(O)		in	
\dot{S}_{MR}	V		in/sec	M. G. Tire Deflection Rate
\dot{S}_{ML}	V		in/sec	
S_N	V		in	N. G. Tire Deflection
\dot{S}_N	V		in/sec	N. G. Tire Deflection Rate

See Figure 25

Table 7 (Contd)

SYMBOL	TYPE	VALUE	UNITS	DESCRIPTION
SPI	C	1.925	in	Parameter of Cornering Power Pwc
STH	C	20.00	in	#
SVM	C	84.24	in	#
SVMU	C	36.74	in	#
SVN	C	85.86	in	#
SVRL	C	7.92	in	Nose Tire Relaxation Length (Yaw)
TAM	V		in lb	Aero Pitching Moment
TAY	V		in lb	Aero Yawing Moment
TSL	V(I)		in lb	Moment on M. G. Axle
TSR	V(I)		in lb	
TTH	C	20,000	in lb	Thrust Moment about C. G.
UNTF	C	.553	-	Nose Tire Friction Coefficient
UREN	C	.02	-	Nose Tire Rolling Resistance Coefficient
URF	V		-	Nose Tire Cornering Parameter
VWY	V*		in/sec	Crosswind
WA	C	147.6	lb sec ² /in	Airplane Mass
WIF	C	1.465×10^6	lb sec ² in	Roll Moment of Inertia
WIG	C	3.66×10^6	lb sec ² in	Pitch Moment of Inertia
WIR	C	4.93×10^6	lb sec ² in	Yaw Moment of Inertia
WWM	C	1.667	lb sec ² /in	M. G. Unsprung Mass
WUN	C	.453	lb sec ² /in	N. G. Unsprung Mass
WU	C	.723	lb sec ² /in	M. G. Upper Strut Mass
X	V		in	Horizontal Position of APL C.G.
X ₀	C	36.20	in	X at Time = 0
Ẋ	V		in/sec	Airplane Velocity in the x Direction
Ẍ ₀	C		in/sec	Velocity at Time = 0
Ẍ	V	2400	in/sec ²	Airplane Acceleration in the X Direction

*Point Plot Input

Table 7 (Contd)

SYMBOL	TYPE	VALUE	UNITS	DESCRIPTION
X_{AXL}	V(O)		in	M.G. Axle Undelected Location (x Direction)
\dot{X}_{AXL}	V(O)		in/sec	M.G. Axle Undelected Velocity (x Direction)
X_{WML}	V(I)		in	M.G. Tire Footprint Location and Velocity in the x direction
\dot{X}_{WML}	V(I)		in/sec	
X_{WMR}	V(I)		in	
\dot{X}_{WMR}	V(I)		in/sec	
X_{WN}	V		in	N.G. Tire Location (x direction) N.G. Tire Velocity (x direction) M.G. Undelected Axle Location (x Direction)
\dot{X}_{WN}	V		in/sec	
X_{AXZ}	V(O)		in	
\dot{X}_{AXZ}	V(O)		in/sec	
Y	V		in	M.G. Undelected Axle Velocity (x Direction) Horizontal C. G. Location (Y Direction)
Y_0	C	0.0	in	Y at Time = 0
\dot{Y}	V		in/sec	Airplane C.G. Velocity in Y Direction
\dot{Y}_0	C	0.0	in/sec	\dot{Y} at Time = 0
\ddot{Y}	V		in/sec ²	Airplane C.G. acceleration in Y Direction
Y_{AXL}	V(O)		in	M.G. Undelected Axle Location and Velocity in the Y Direction
\dot{Y}_{AXL}	V(O)		in/sec	
Y_{AXZ}	V(O)		in	
\dot{Y}_{AXZ}	V(O)		in/sec	
Y_{DLN}	V		in	N.G. Lateral Deflection N.G. Lateral Delta Velocity M.G. Tire Footprint Location In the Y Direction
\dot{Y}_{DLN}	V		in/sec	
Y_{ML}	V(I)		in	
Y_{MR}	V(I)		in	

Table 7 (Contd)

SYMBOL	TYPE	VALUE	UNITS	DESCRIPTION
Y_N	V		in	N.G. Lateral Location (γ Direction)
Y_{NO}	C	0.0	in	γ_N at Time = 0
\dot{Y}_N	V		in/sec	N.G. Lateral Velocity
\dot{Y}_{NO}	C	0.0	in/sec	$\dot{\gamma}_N$ at Time = 0
\ddot{Y}_N	V		in/sec ²	N.G. Lateral Acceleration
Z	V		in	Height of Apl C.G. above ground ref.
Z_0	C	82.36	in	Z at Time = 0
\dot{Z}	V		in/sec	Apl vertical velocity
\dot{Z}_0	C	0.0	in/sec	\dot{Z} at Time = 0
\ddot{Z}	V		in/sec ²	Apl Vertical acceleration
Z_{GO}	V(I)		in	Runway contour height
Z_{GDP}	V(I)		in/in	Runway contour slope (α Direction)
Z_{ELL}	V		in	Distance from Wu position to Axle
Z_{GLR}	V		in	M.G. Strut Velocity and Stroke
Z_{SML}	V		in	
\dot{Z}_{SML}	V		in/sec	
\ddot{Z}_{SML}	V		in	
\dot{Z}_{SMR}	V		in/sec	
\ddot{Z}_{SMR}	V		in	
Z_{SN}	V		in	N. G. Stroke
\dot{Z}_{SN}	V		in/sec	N.G. Stroke Velocity
Z_{WML}	V		in	M. G. Axle Height
Z_{WMR}	V		in	
Z_{WMLO}	C	20.91	in	M.G. Axle Height at Time = 0
Z_{WMRO}	C	20.91	in	
\dot{Z}_{WML}	V		in/sec	M.G. Axle Velocity
\dot{Z}_{WMR}	V		in/sec	

Table 7 (Contd)

SYMBOL	TYPE	VALUE	UNITS	DESCRIPTION
\dot{Z}_{WMLO}	C	0.0	in/sec	} M.G. Axle Velocity at Time = 0
\dot{Z}_{WMRO}	C	0.0	in/sec	
\dot{Z}_{WML}	V		in/sec ²	} M.G. Axle Vertical Acceleration
\dot{Z}_{WMR}	V		in/sec ²	
\dot{Z}_{WVN}	V		in	} N. G. Axle Vertical Location
\dot{Z}_{WNO}	C	10.02	in	
\dot{Z}_{WVN}	V		in/sec	} N.G. Axle Vertical Velocity
\dot{Z}_{WNO}	C	0.0	in/sec	
\dot{Z}_{WVN}	V		in/sec ²	} N. G. Axle Vertical Acceleration
F_{GVL}	V(I)		lb	
F_{GVR}	V(I)		lb	} M. G. Tire Unbalance

4a. WHEEL AND TIRE SYSTEM (FLYWHEEL)

Figure 33 shows the components of the wheel and tire system.

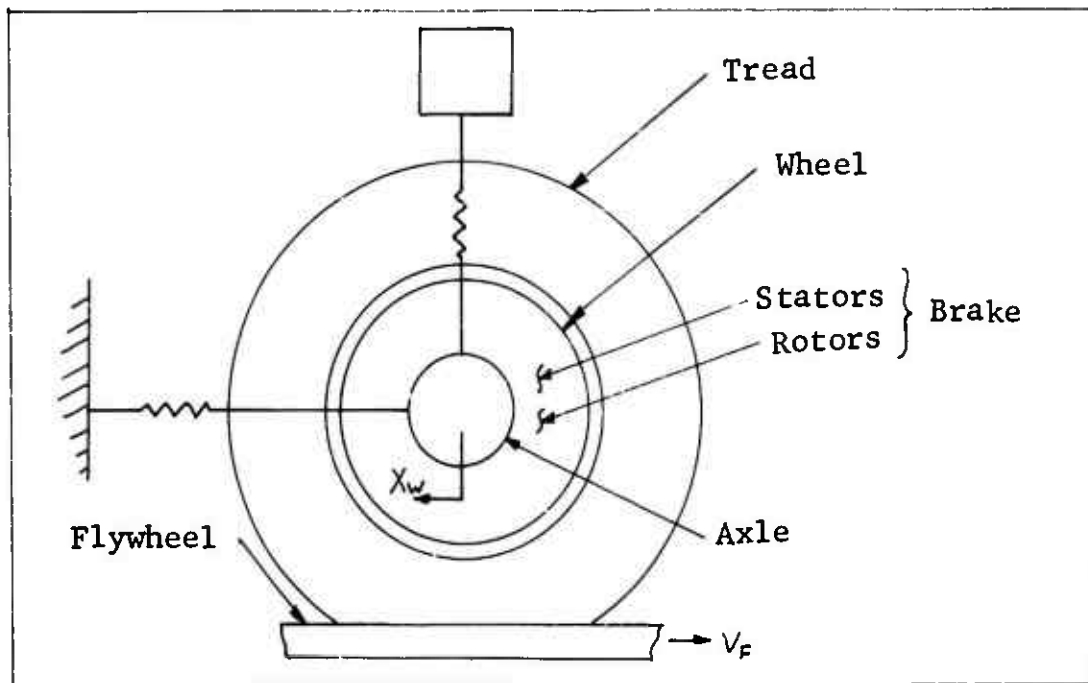


Figure 33 Components of the Wheel and Tire System

In the vertical, or Z direction, the axle, brake, wheel, tire, and lower shock strut are combined and operate as a single mass point. A description of this mode is found in the airplane system. The airplane system furnishes various inputs to the tire and wheel: V_F the airplane (flywheel surface) velocity; F_{NM} , the vertical load between the tire and pavement; S_M , the tire deflection. The brake torque T_{BT} is an input from the brake system.

The horizontal displacement of two mass points is considered. One mass point is made up of the axle, brake, wheel, and the inner part of the tire and its location is designated as x_w . The other mass point is the tire tread and its location is designated as x_{TT} .

In rotation, there are three mass points: the axle and stationary brake elements make up the first; the brake rotors, wheel, and inner tire make up the second; and the tire tread makes up the third. The angular positions of these three mass points are denoted respectively as θ_s , θ_w , and θ_T . Let F_G be the horizontal force acting on the

axle and let F_{TT} be the net horizontal force between the wheel and tire tread. Figure 34 shows the location of these forces. F_{BT} is the horizontal force between the tire and the flywheel surface.

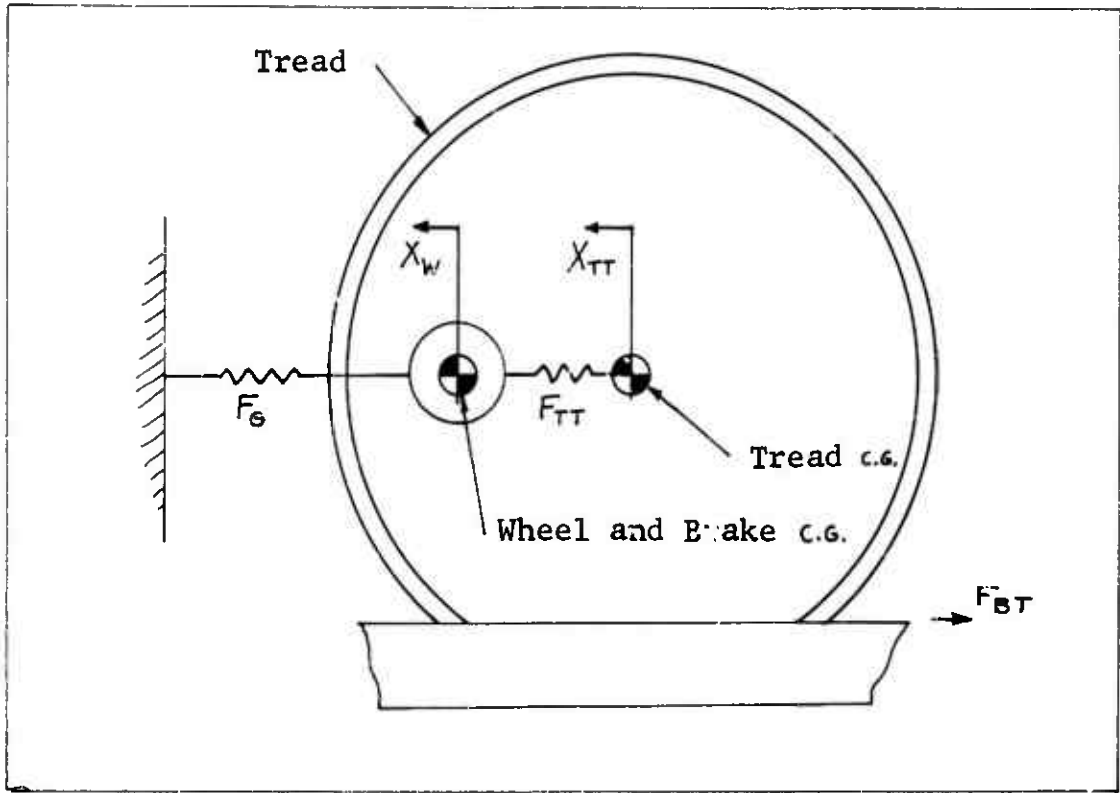


Figure 34 Tire Horizontal Model

A. Mathematical Description

Equations describing the tire and wheel behavior are developed by referring to Figure 34. Forces F_G and F_{TT} are defined by equations (4a.1), (4a.2), and (4a.3) as follows:

$$(4a.1) \quad F_G = -C_{GH} X_W - D_{GH} \dot{X}_W$$

$$(4a.2) \quad F_{TT} = C_{TT}(X_{TT} - X_W) + E_{TT}(X_{TT} - X_Y)$$

$$(4a.3) \quad D_{TT}(\dot{X}_Y - \dot{X}_W) = E_{TT}(X_{TT} - X_Y)$$

Equations (4a.2) and (4a.3) describe a type 2 spring-damper system as defined by Figure 38 and discussed in the parameter evaluation.

Let W_{GW} denote the mass of the axle, wheel, brake and inner part of the tire. Let W_{TE} denote the appropriate tire tread mass. Summing forces in the horizontal direction gives:

$$(4a.4) \quad W_{GW} \ddot{X}_W = F_G + F_{\cdot T}$$

$$(4a.5) \quad W_{TE} \ddot{X}_{TT} = -F_{TT} - F_{BT} + F_{\Theta RH}$$

Where $F_{\Theta RH}$ is a force produced by tire unbalance, the corresponding vertical part of this unbalance force is denoted by $F_{\Theta RV}$. These two forces are given in equations (4a.6) and (4a.7).

$$(4a.6) \quad F_{\Theta RH} = R_{K\Theta} W_T^2 \sin\langle\Theta_T\rangle$$

$$(4a.7) \quad F_{\Theta RV} = R_{K\Theta} W_T^2 \cos\langle\Theta_T\rangle$$

W_T and Θ_T are the rotational speed and position of the tire tread.

The rotational schematic of the wheel and tire system is shown in Figure 35 .

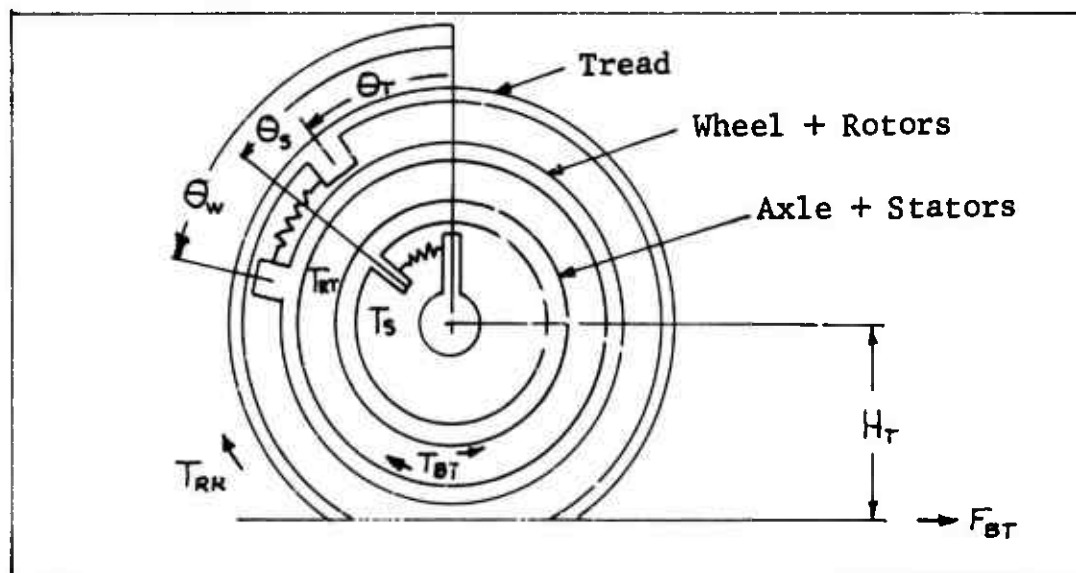


Figure 35 Tire Rotational Model

Let T_{RT} and T_s be defined by equations (4a.8), (4a.9), and (4a.10) as follows:

$$(4a.8) \quad T_{RT} = C_{RT}(\Theta_w - \Theta_T) + E_{RT}(\Theta_w - \Theta_Y)$$

$$(4a.9) \quad D_{RT}(\dot{\Theta}_Y - \dot{\Theta}_T) = E_{RT}(\Theta_w - \Theta_Y)$$

$$(4a.10) \quad T_S = C_{RS} \theta_S + D_{RS} \dot{\theta}_S$$

Let H_T be the height of the axle above the ground. Let T_{RR} be the torque on the tire that produces rolling resistance. These two quantities are given by:

$$(4a.11) \quad H_T = R_{\theta T} - S_M$$

$$(4a.12) \quad T_{RR} = \begin{cases} S_M (D_{SR} + D_{VR} W_T) & \text{if } W_T > 0 \\ 0 & \text{if } W_T = 0 \\ S_M (-D_{SR} + D_{VR} W_T) & \text{if } W_T < 0 \end{cases}$$

If T_{BT} is the brake torque, then torques can be summed to obtain the following three equations:

$$(4a.13) \quad W_{IS} \ddot{\theta}_S = T_{BT} - T_S$$

$$(4a.14) \quad W_{IW} \ddot{\theta}_W = -T_{RT} - T_{BT}$$

$$(4a.15) \quad W_{IT} \ddot{\theta}_T = H_T F_{BT} + T_{RT} - T_{RR}$$

The rolling radius of the tire is obtained using the methods of Reference 1. Denoting the rolling radius as R_T , it is defined as:

$$(4a.16) \quad R_T = R_{\theta T} - \frac{1}{3} S_M - U_{RR} (X_{TT} - X_W)$$

Let V_{RS} denote the velocity of the tire footprint. Relative to the flywheel surface with $W_T = 0$, let V_R be the relative velocity including W_T .

$$(4a.17) \quad V_{RS} = V_F + \dot{X}_{TT}$$

$$(4a.18) \quad V_R = V_{RS} - R_T W_T$$

Here V_F is the velocity of the flywheel surface. Adopting the convention, $W_T = \dot{\theta}_T$; $W_S = \dot{\theta}_S$; and $W_W = \dot{\theta}_W$, the relative angular velocity between the stators and rotors is denoted by W_B and is established by:

$$(4a.19) \quad W_B = W_W - W_S$$

When a tire is moving over a runway with any appreciable amount of standing water or slush, a hydrodynamic "wedge"

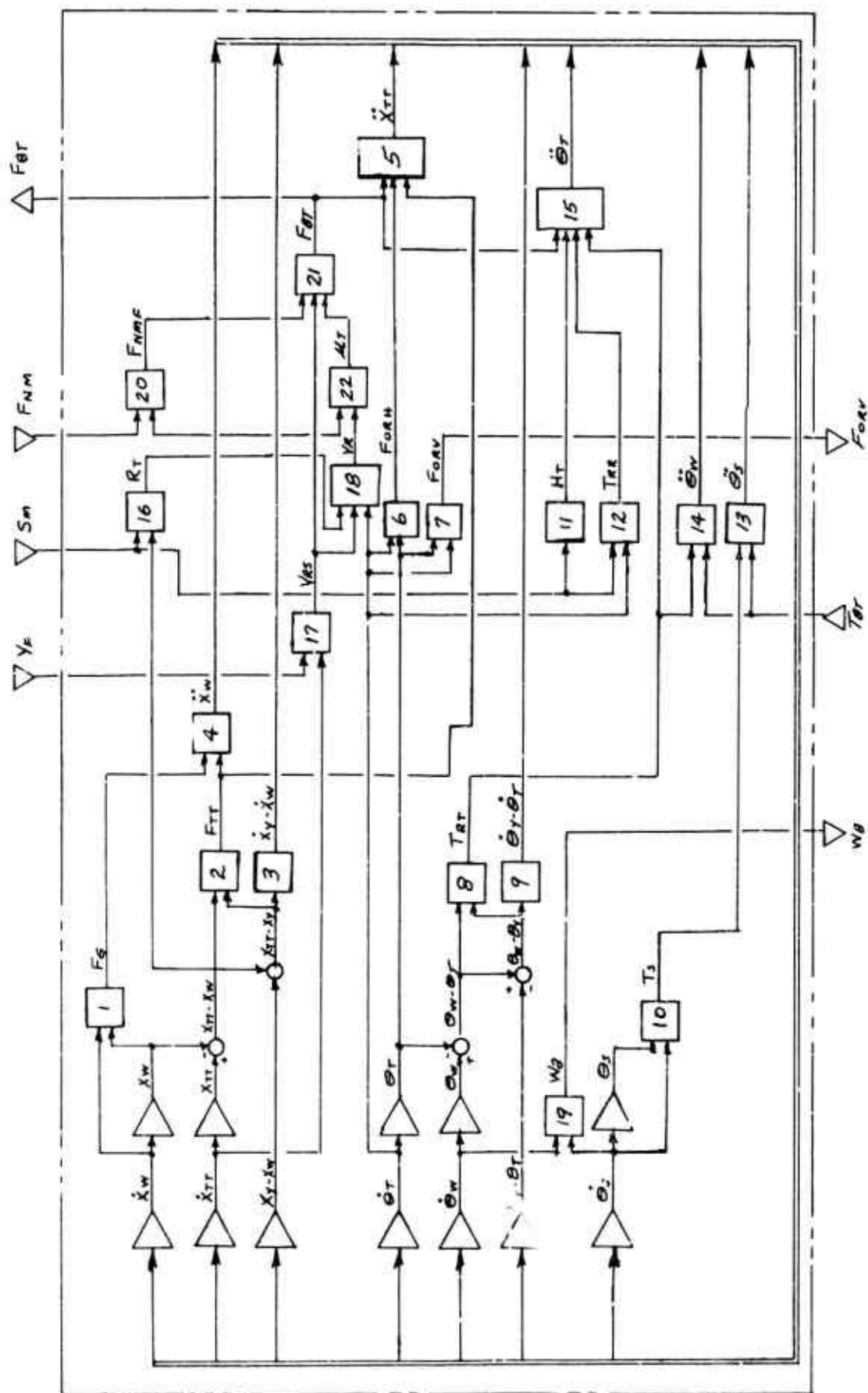


Figure 36 Wheel and Tire System (Flywheel) Equation Flow Diagram

of water starts separating the tread and runway surface. It is assumed that the length of this "wedge" is proportional to V_{RS}^2 and at hydroplaning speed, V_{HY} , the tread is completely separated from the runway. In equations (4a.20) and (4a.21) the coefficients C_{HY} and D_{HY} are used to define hydroplaning effects and water drag on the wheel. For dry runway conditions, C_{HY} and D_{HY} are zero. The horizontal force between the tire tread footprint and the runway surface is established by equations (4a.20), (4a.21), and (4a.22) as follows:

$$(4a.20) F_{NMF} = F_{NM} (1 - C_{HY} (V_{RS}/V_{HY})^2)$$

$$(4a.21) F_{BT} = F_{NMF} U_T + D_{HY} V_{RS}^2$$

$$(4a.22) U_T = \begin{cases} U_{T1} + (U_{T2} - E_T V_{RS}) e^{-\alpha V_R} & \text{if } V_R > 0 \\ 0 & \text{if } V_R = 0 \\ -U_{T1} - (U_{T2} - E_T V_{RS}) e^{\alpha V_R} & \text{if } V_R < 0 \end{cases}$$

Figure 36 is an equation flow diagram showing the relation between equations (4a.1) through (4a.22).

B. Parameter Evaluation

Gear Characteristics

The mass W_{GW} is made up of the mass of half the shock strut, half the lateral beam, the axle, the wheel, the brakes, and all but one-third of the tire tread. The sum of the masses of these components totals 616 LBM. Thus, $W_{GW} = 616/386 = 1.60 \text{ lb sec}^2/\text{in}$. The fore and aft natural frequency of the gear (as calculated from deflection data) is $21.84 \text{ cps} = 137.5 \text{ rad/sec}$. Using the gear mass, with all of the tire included (644 LBM), the spring rate C_{GH} can be calculated as:

$$(4a.23) C_{GH} = m \omega_n^2 = \left(\frac{644}{386}\right) (137.5)^2 = 31,500 \text{ lb/in}$$

A typical approach to estimate the damping coefficient is to use 3% critical. Thus,

$$(4a.24) D_{GH} = (.03) 2 \sqrt{m C_G} = (.06) \sqrt{\left(\frac{644}{386}\right) 31500} = 13.8 \frac{\text{lb sec}}{\text{in}}$$

Tire Tread Characteristics

The principle underlying the calculation of the tire friction coefficient is that compared to the rest of the tire, the tire "footprint" is totally inelastic. (The tire "footprint" is that portion of the tire tread which is in contact with the ground). Thus, if the velocity of the footprint and the friction vs. velocity curve for the rubber-surface interface are defined, the tire friction coefficient is established. In order to predict the motion of the footprint, the tire tread is assumed to behave like an inelastic ring which is supported on the wheel as shown in Figure 37.

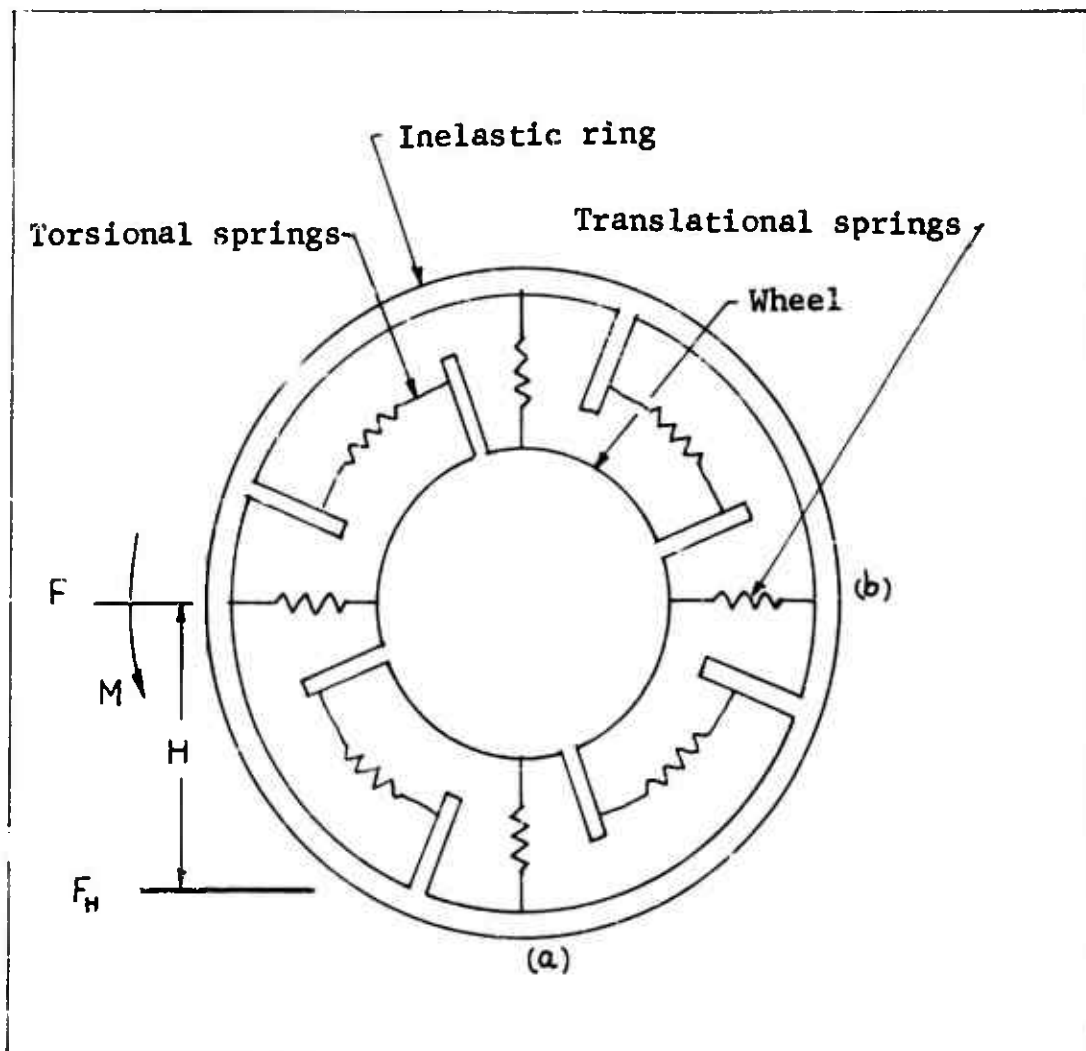


Figure 37 Tire Tread Model

The horizontal position of the footprint is assumed to be the same as the horizontal position of the ring center of gravity. A frictional force F_H applied at the ground can be resolved into a translational force $F = F_H$ acting at the ring C.G., plus a moment $M = F_H \cdot H$ acting about the ring C.G.

For an actual tire with distributed mass and elasticity approximately one-third of the tire would move with the footprint in response to force, F_H . Therefore, it is assumed for translation the mass of the ring, W_{TE} , is one-third of the tire tread mass, which is 84 LBM. Thus, $W_{TE} = (84)/(3 \times 386) = 0.0725 \text{ LBF SEC}^2/\text{IN}$.

For rotation the total tire tread mass is assumed to move in response to moment, M . Thus, the moment of inertia about its center of gravity is $W_{IT} = MR^2 = (84/386) (23^2) = 115 \text{ LBF SEC}^2/\text{IN}$.

References 1 (page 22) and 10 (Figure 8) are used to obtain values for the torsional and translational spring rates as shown in Figure 37. Under the application of the force F_H , the peripheral movement at point b is about 20% of the peripheral movement at point a (Figure 37 above). The expression for the footprint spring rate from Reference 1 is:

$$(4a.25) K_x = .6 d (P + 4P_r) \sqrt[3]{S_o/d}$$

Where for the F-111 with a vertical tire load of 25,000 lb,

$d = 46.65 \text{ in.} = \text{Tire diameter}$
 $P = 150 \text{ psi} = \text{Tire operating pressure}$
 $P_r = 150 \text{ psi} = \text{Tire rated pressure}$
 $S_o = 2.75 \text{ in.} = \text{Operating (static) deflection}$

Thus,

$$(4a.26) K_x = (.6)(46.65)(5)(150) \sqrt[3]{2.75/46.65} = 8150 \text{ lb/in}$$

The application of $F_H = 8150 \text{ lb.}$ causes the footprint to move one inch. At point b, the movement is .2 inches. Assuming that the movement at point b is all due to rotation, the apparent torsional spring rate is:

$$(4a.27) C_{RT} = \left(\frac{d}{2}\right) \frac{H F_H}{(.2)} = \frac{(23.32)(20.57)(8150)}{(.2)} = 19.5 \text{ MlbF/rad}$$

Since .8 inches of the 1.0 inch footprint motion is due to tread C.G. fore and aft translation, the apparent spring rate is:

$$(4a.28) C_{TT} = \frac{F_H}{.8} = \frac{8150}{.8} = 10,200 \text{ lb/in}$$

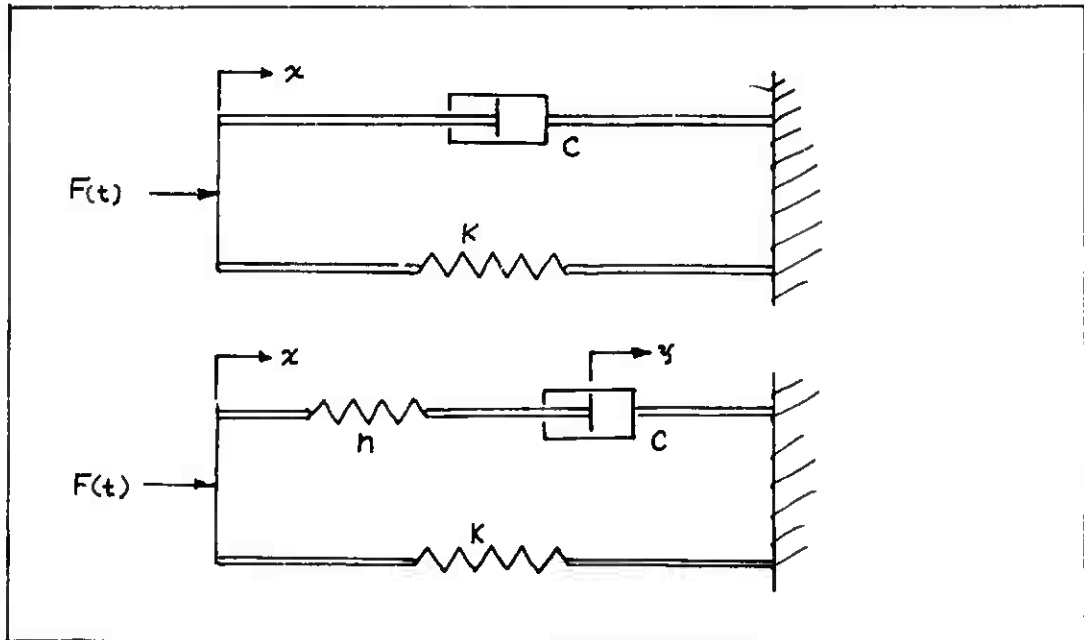


Figure 38 Tire Damping Models

It is well publicized and generally accepted that the elastic and damping characteristics of tires and other structural devices are not accurately described by the mathematically convenient linear spring-viscous damper representation over a wide frequency range. The behavior of rubber-like materials is particularly different than that described by the conventional model. To establish suitable mathematical descriptions of the various damping forces for tires and other elements of this study, several models were explored. Figure 38 depicts the two types of elastic systems which are used. The Type 1 model is a conventional system with viscous damping and Type 2 is a visco-elastic system, having elasticity and damping which varies with frequency. To compare the two, consider the effects of driving each with a variable force $F(t) = F_0 \cos \omega t$. In each case, the resultant deflection is $x = x_0 \cos(\omega t - \varphi)$

The loss coefficient, β , is defined by $\beta = \tan \varphi$. For a conventional system (Type 1 with c and k constant), the loss coefficient which is a measure of the damping is

given by:

$$(4a.29) \beta = c\omega/k$$

Reference 1 assumes that c is of the form $c = \eta k/\omega$ where η and k are constant. From this:

$$(4a.30) \beta = \eta$$

Reference 8 seems to indicate (p. 55) that the loss coefficient for tire tread rubber is somewhere between the above two values.

For the Type 2 system, shown in Figure 38, with c , n , and k constant, the loss coefficient is given by:

$$(4a.31) \beta = \left(\frac{c\omega}{k} \right) / \left(1 + \left(\frac{c\omega}{n} \right)^2 \left(1 + \frac{n}{k} \right) \right)$$

To represent a tire, the values $(c/k) = 1.56 \times 10^{-3}$ sec. and $(n/k) = 0.520$, were used to compute values of β for a range of frequencies. β versus ω is shown in Figure 39 for both Type 1 and Type 2 models, along with values of β taken from References 1 and 8. The value from Reference 1 is shown constant at all frequencies because the value is not identified with any frequency. The above values of (c/k) and (n/k) were chosen because they gave β values in best agreement with authoritative data.

Figure 39 shows both Type 1 and Type 2 models have relatively poor correlation with both data sources. Reference 8 indicates β is highly dependent upon temperature and tire rubber compound as might be expected. During damping model exploration, both Type 1 and Type 2 systems were examined dynamically on an analog computer. It was found that differences in their behavior were observable; however, since the damping forces are relatively small compared to the other forces, this difference was small. Either model is equally satisfactory for evaluating anti-skid operation. The Type 2 system is used for the tire because it is in closer agreement with recorded observations. The peak in the β versus frequency curve for the Type 2 system is in keeping with most of the contour plots for rubber-like materials as shown in Reference 7 and 8.

The tire elastic and damping coefficients are:

$$(4a.32) \quad \left\{ \begin{array}{l} D_{TT} = (1.56 \times 10^3) C_{TT} = 15.9 \text{ lb sec/in} \\ E_{TT} = (.52) C_{TT} = 5300 \text{ lb/in} \\ D_{RT} = (1.56 \times 10^3) C_{RT} = 30,400 \text{ in lb sec/rad} \\ E_{RT} = (.52) C_{RT} = 10.15 \times 10^6 \text{ in lb/rad} \end{array} \right.$$

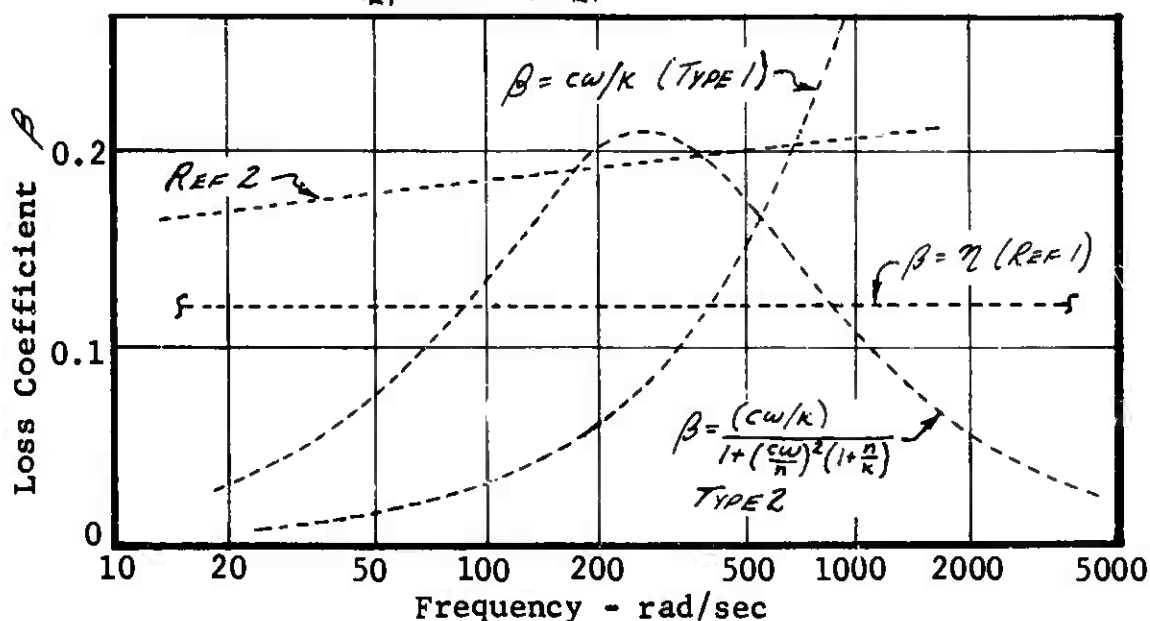


Figure 39 Model Loss Factors

The equation (4a.16) for the rolling radius R_T is a re-statement of equation (76 b) of Reference 1. To allow for circumferential decay length other than those equal to the outside free tire radius, a coefficient U_{RR} is provided. For this study U_{RR} is set equal to 1.0.

Axle Parameters

The observed torsional natural frequency of the axle (with brake stators) is 125 cps. The calculated value for its moment of inertia is 16.8 LBF SEC²/IN. Thus, the torsional spring rate, C_{RS} , is established as:

$$(4a.33) \quad C_{RS} = (2\pi 125)^2 (16.8) = 10.4 \times 10^6 \text{ in lb/rad}$$

For the steel axle, a value for η (in the Type 1 system in Figure 38) is probably something less than .01 (Reference 7). Thus, at resonance, if $c\omega/k = \eta$, then the damping coefficient is established as:

$$(4a.34) \quad D_{RS} = k\eta/\omega = (10.4 \times 10^6)(.01)/(2\pi 125) = 132 \text{ in lb sec/rad}$$

Tire Rolling Resistance

From Figure 17a of Reference 2, the rolling resistance coefficient, μ_r is given by $\mu_r = .012 + 1 \times 10^{-5}v$ where v is the axle speed in INCHES/SEC. Thus,

$$(4a.35) T_{RR} = \mu_r F_{RR} R_T = (.012 + 1 \times 10^{-5}V) F_{RR} R_T$$

$$\text{Or alternately, } = (.012 + 1 \times 10^{-5} \dot{\theta}_T R_T) (F_{RR}/\delta)(\delta) R_T$$

Since $F_{RR}/\delta = C_{MT}$, the rolling resistance coefficients are established as:

$$(4a.36) D_{SR} = .012 C_{MT} R_T = (.012)(9530)(20.57) = 2350 \text{ lb}$$

$$(4a.37) D_{VR} = 1 \times 10^{-5} C_{MT} R_T^2 = (9530 \times 10^{-5})(20.57)^2 = 40.3 \text{ lb sec}$$

Figure 40 shows the friction coefficient for a tire sliding (i.e. full skid) on a dry concrete runway as a function of velocity. This data is taken from Reference 3 and is applicable to a typical runway contaminated with rubber deposits from previous airplane operations. Table 8 below lists the appropriate coefficients for equation (4a.22) which apply for dry and wet runway surface conditions.

Table 8 Runway Friction Characteristics

SYMBOL	UNITS	WET CONCRETE	DRY CONCRETE
U_{T1}	-----	.050	.200
U_{T2}	-----	.180	.450
E_T	SEC/IN	$.065 \times 10^{-3}$	$.065 \times 10^{-3}$
α	SEC/IN	1.0×10^{-3}	2.5×10^{-3}

Initial Conditions

All initial conditions, except wheel and tire rotational speed, will be set to zero. From the airplane system at time = 0, $V_F = 2400$ and $S_M = 2.245$. Using equation (4a.16) results in:

$$(4a.38) R_T = R_{\theta T} - \frac{1}{3} S_M = 23.32 - \frac{1}{3} (2.245) = 22.67 \text{ in}$$

In order that V_R be zero, equations (4a.18) and (4a.19) show that:

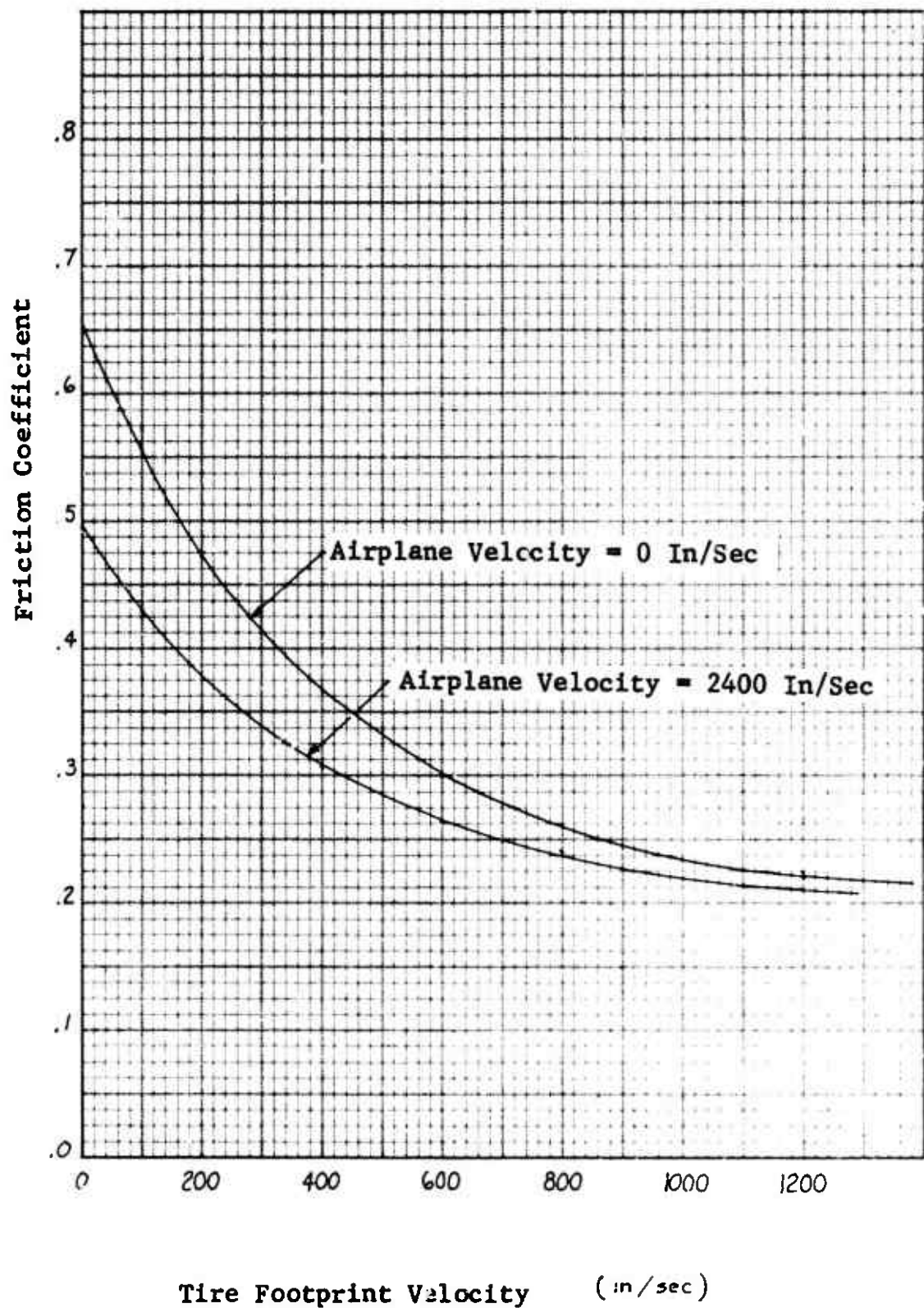


Figure 40 Tire Sliding Friction Coefficient

$$(4a.39) \quad \dot{\Theta}_{T0} = \dot{\Theta}_{W0} = V_F / R_T = 2400 / 22.67 = 105.9 \text{ rad/sec}$$

Table 9 Wheel and Tire System (Flywheel) Parameters

SYMBOL	TYPE	VALUE	UNITS	DESCRIPTION
α	C	2.5×10^{-3}	sec/in	Tire Friction Parameter
C_{GH}	C	3/500	lb/in	Fore and Aft Spring Rate at Axle
C_{RS}	C	10.4×10^6	in lb/rad	Axle Rotational Spring Rate
C_{RT}	C	19.5×10^6	in lb/rad	Tire to Wheel Rotational Spring Rate
C_{HY}	C	0.0	-	Controls Hydroplaning Influence
C_{TT}	C	10,200	lb/in	Tread to Wheel Spring Rate
D_{GH}	C	13.8	lb sec/in	Fore and Aft Damping Coefficient at Axle
D_{HY}	C	0.0	lb sec ² /in ²	Water Resistance Coefficient
D_{RS}	C	132.0	in lb sec/rad	Gear to Axle Rotational Damping Coefficient
D_{RT}	C	30,400	in lb sec/rad	Tire to Wheel Rotational Damping Coefficient
D_{SR}	C	2350	lb	Rolling Resistance Parameter
D_{TT}	C	15.9	lb sec/in	Tread to Wheel Damping Coefficient
D_{VR}	C	40.3	lb sec/rad	Rolling Resistance Parameter
E_{RT}	C	10.15×10^6	in lb/rad	Tire to Wheel Coupling Spring Rate
E_T	C	$.65 \times 10^{-4}$	sec/in	Tire Friction Correction Coeff.
E_{TT}	C	5300	lb/in	Tread to Wheel Coupling Spring Rate
$F_{\theta T}$	C		lb	Horizontal Force on Tire Footprint from Ground
F_G	V		lb	Horizontal Force at Axle
$F_{\theta RH}$	V		lb	Horizontal Wheel Unbalance Force
$F_{\theta RV}$	V(O)		lb	Vertical Wheel Unbalance Force
F_{NM}	V(I)		lb	Vertical Force between Tire and Ground
F_{NMF}	V		lb	Vertical Force not Supported by Water Film

Table 9 (Contd)

SYMBOL	TYPE	VALUE	UNITS	DESCRIPTION
F_{Tr}	V		lb	Net Force Between Tread & Wheel
H_r	V		in	Axle Height Above Ground ($H_r \leq R_{or}$)
θ_s	V		rad	Axle Rotation
$\dot{\theta}_{s0}$	C	0.0	rad	Axle Rotation at Time = 0
$\ddot{\theta}_s$	V		rad/sec	Axle Rotational Speed
$\dot{\theta}_{s0}$	C	0.0	rad/sec	Axle Rotational Speed at Time = 0
$\ddot{\theta}_s$	V		rad/sec ²	Axle Rotational Acceleration
θ_r	V		rad	Tire Tread Rotation
$\dot{\theta}_{r0}$	C	0.0	rad	Tire Tread Rotation at Time = 0
$\ddot{\theta}_r$	V		rad/sec	Tire Tread Rotational Speed
$\dot{\theta}_{r0}$	C	105.9	rad/sec	Tire Tread Rotational Speed at Time = 0
$\ddot{\theta}_r$	V		rad/sec ²	Tire Tread Rotational Acceleration
θ_w	V		rad	Wheel Rotation
$\dot{\theta}_{w0}$	C	0.0	rad	Wheel Rotation at Time = 0
$\ddot{\theta}_w$	V		rad/sec	Wheel Rotational Speed
$\dot{\theta}_{w0}$	C	105.9	rad/sec	Wheel Rotational Speed at Time = 0
$\ddot{\theta}_w$	V		rad/sec ²	Wheel Rotational Acceleration
θ_y	V		rad	Dummy Variables used to Simulate Visco-elastic Tire Characteristic
$\dot{\theta}_{y0}$	C	0.0	rad	Unbalance Coefficient
$\ddot{\theta}_y$	V		rad/sec	Undelected Tire Radius
R_{ko}	C	0.0	lb sec ² /rad ²	Tire Rolling Radius
R_{or}	C	23.32	in	Tire Deflection
R_r	V		in	Brake Torque
S_M	V(I)		in	
T_{BT}	V(I)		in lb	

Table 9 (Contd)

SYMBOL	TYPE	VALUE	UNITS	DESCRIPTION
T_{RR}	V		in lb	Torque Producing Rolling Resistance
T_{RT}	V		in lb	Torque between Tire (Tread) and Wheel
T_S	V		in lb	Axle Torque
U_{RR}	C	1.0	-	Rolling Radius Parameter
U_T	V		-	Tire Friction Coefficient
U_{T1}	C	.20	-	} Tire Friction Parameters
U_{T2}	C	.45	-	
V_F	V(I)		in/sec	Flywheel Surface Velocity
V_{HY}	C	2400	in/sec	Tire Hydroplaning Speed
V_R	V		in/sec	Velocity of Tire Footprint Relative to Flywheel
V_{es}	V		in/sec	Same as V_R except Rotational Effects Ignored
W_B	V(O)		rad/sec	Relative Rotational Speed Between Stators and Rotors
W_{GW}	C	1.60	lb sec ² /in	Effective Tire, Wheel, and Brake Mass
W_{IS}	C	16.8	in lb sec ² /rad	Axle Moment of Inertia (+ Stators)
W_{IT}	C	115.0	in lb sec ² /rad	Tread Moment of Inertia
W_{IW}	C	66.0	in lb sec ² /rad	Wheel & Rotors Moment of Inertia
W_S	V		rad/sec	$W_S = \dot{\theta}_S$
W_T	V		rad/sec	$W_T = \dot{\theta}_T$
W_{TE}	C	.0725	lb sec ² /in	Equivalent Tire Tread Mass
W_W	V		rad/sec	$W_W = \dot{\theta}_W$
X_{TT}	V		in	Location of Tire Tread C.G.
X_{TTO}	C	0.0	in	Location of Tire Tread C.G. at Time = 0

Table 9 (Contd)

SYMBOL	TYPE	VALUE	UNITS	DESCRIPTION
\dot{X}_{TT}	V	0.0	in/sec	Tread C.G. Velocity
\dot{X}_{TTO}	C	0.0	in/sec	Tread C.G. Velocity at Time = 0
\ddot{X}_{TT}	V		in/sec ²	Tread C.G. Acceleration
X_W	V		in	Horizontal Axle Location
X_{WO}	C	0.0	in	Horizontal Axle Location at Time = 0
\dot{X}_W	V		in/sec	Horizontal Axle Velocity
\dot{X}_{WO}	C	0.0	in/sec	Horizontal Axle Velocity at Time = 0
\ddot{X}_W	V		in/sec ²	Horizontal Axle Acceleration
X_Y	V		in	Dummy Variables Used to
X_{YO}	C	0.0	in	Simulate Visco-elastic Tire
\dot{X}_Y	V		in/sec	Characteristic

4b. WHEEL AND TIRE SYSTEM (3 DEGREE)

Figure 41 shows the components of the wheel and tire system. The wheel and tire system

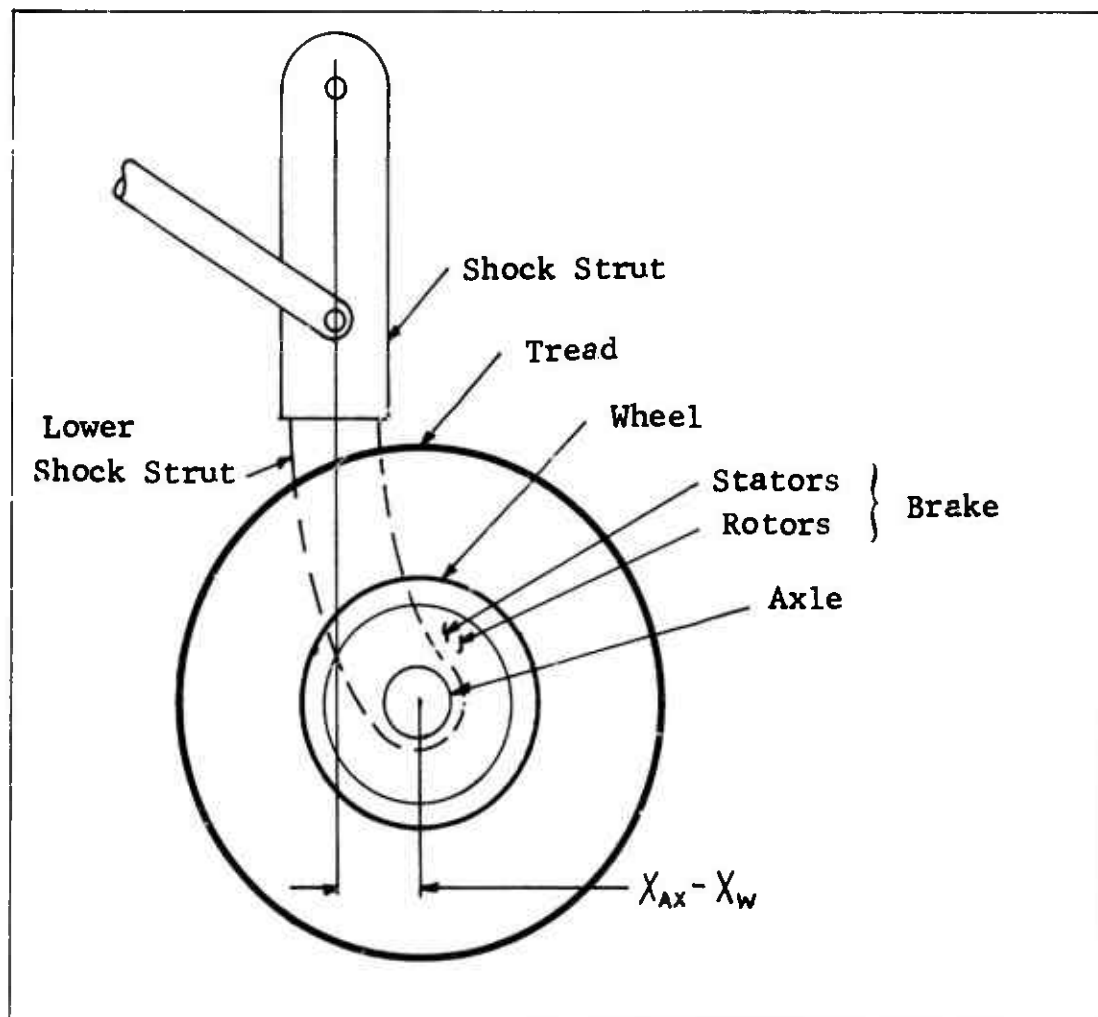


Figure 41 Components of the Wheel and Tire System

for the 3 degree airplane system is essentially the same as for the flywheel model. The Airplane System still furnishes the tire deflection S_M and the tire vertical load F_{NM} . The ground speed, however, is no longer furnished by the Airplane System, but is found by summing forces on the tire, wheel, brake, and axle mass. The horizontal force exerted on the axle by the airplane is calculated by obtaining the translational (X_{AX}) and rotational (θ_G) gear positions from the Airplane System.

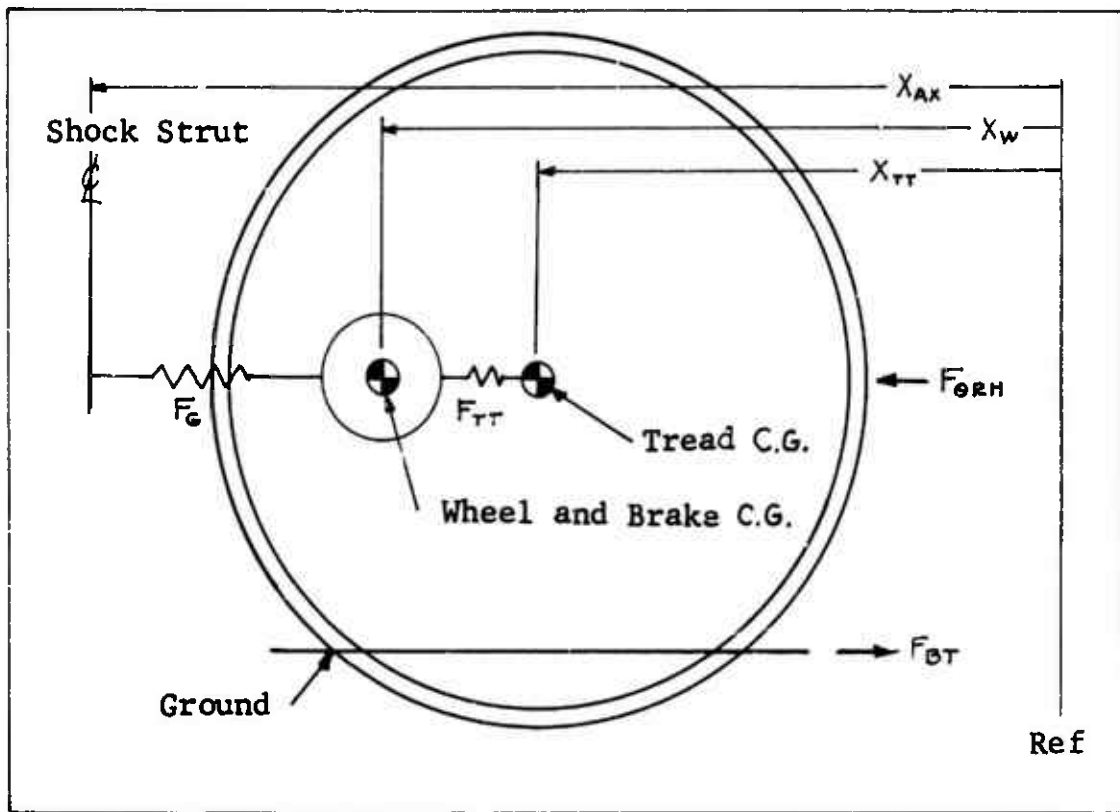


Figure 42 Tire Horizontal Model

Referring to Figure 42 equation (4a.1) in the flywheel system changes to

$$(4b.1) F_G = C_G (X_{AX} - X_W) + D_G (\dot{X}_{AX} - \dot{X}_W)$$

Equations (4b.2) through (4b.9) are listed for completeness, although they are the same as (4a.2) through (4a.9).

$$(4b.2) F_{TT} = C_{TT} (X_{TT} - X_W) + E_{TT} (X_{TT} - X_Y)$$

$$(4b.3) D_{TT} (\dot{X}_Y - \dot{X}_W) = E_{TT} (X_{TT} - X_Y)$$

$$(4b.4) W_{GW} \ddot{X}_W = F_G + F_{TT}$$

$$(4b.5) W_{TE} \ddot{X}_{TT} = -F_{TT} - F_{BT} + F_{\theta RH}$$

$$(4b.6) F_{\theta RH} = R_{KE} W_T^2 \sin \langle \theta_T \rangle$$

$$(4b.7) F_{\theta RV} = R_{KE} W_T^2 \cos \langle \theta_T \rangle$$

Figure 43 shows the rotational model of the wheel, tire, axle, and lower strut with the gear rotation θ_G added. Including the effect of θ_G there follows:

$$(4b.8) T_{RT} = C_{RT}(\theta_w - \theta_T) + E_{RT}(\dot{\theta}_w - \dot{\theta}_T)$$

$$(4b.9) D_{RT}(\dot{\theta}_T - \dot{\theta}_G) = E_{RT}(\theta_w - \theta_T)$$

$$(4b.10) T_S = C_{RS}(\theta_S - \theta_G) + D_{RS}(\dot{\theta}_S - \dot{\theta}_G)$$

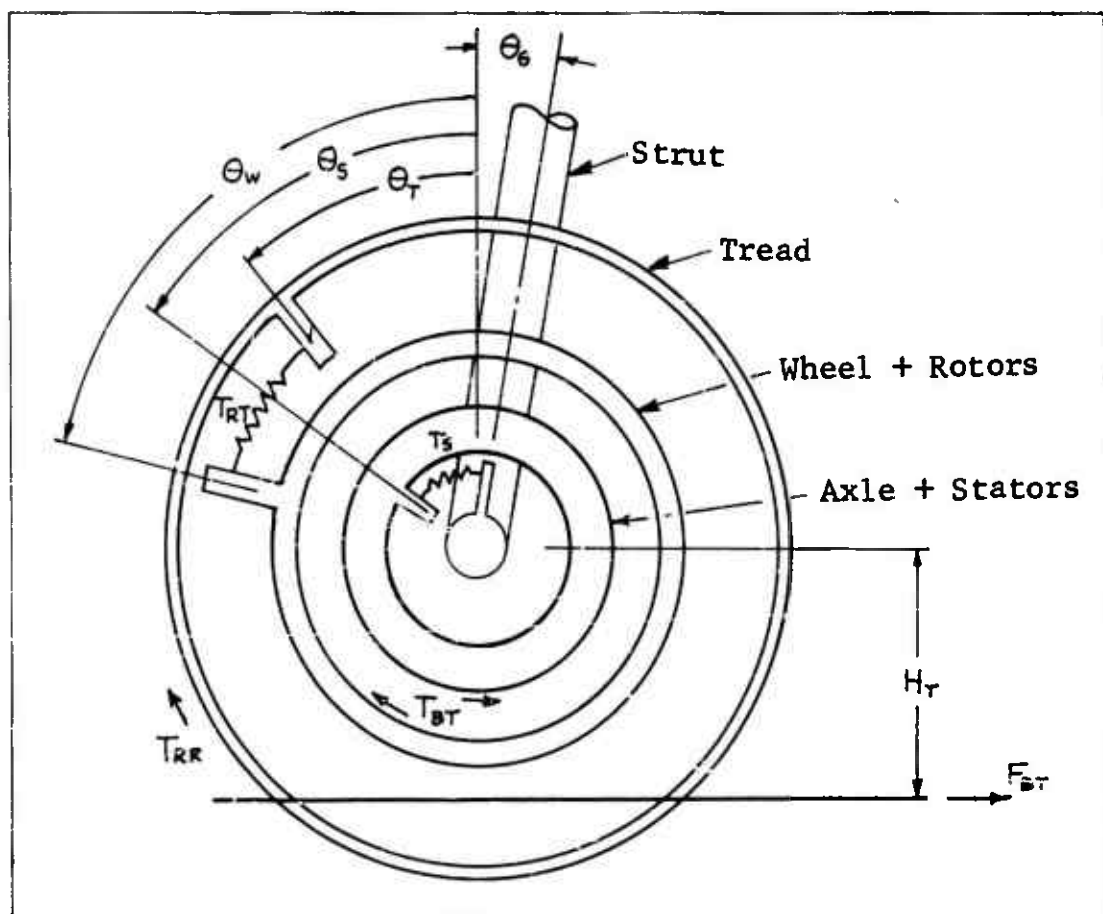


Figure 43 Tire Rotational Model

Equations (4b.11) through (4b.16) are the same as (4a.11) through (4a.16).

$$(4b.11) H_T = R_{ET} - S_M$$

$$(4b.12) T_{RR} = \begin{cases} S_M (D_{SR} + D_{VR} W_T) & \text{if } W_T > 0 \\ 0 & \text{if } W_T = 0 \\ S_M (-D_{SR} + D_{VR} W_T) & \text{if } W_T < 0 \end{cases}$$

$$(4b.13) W_{IS} \ddot{\theta}_S = T_{BT} - T_S$$

$$(4b.14) W_{IW} \ddot{\theta}_W = -T_{RT} - T_{BT}$$

$$(4b.15) W_{IT} \ddot{\theta}_T = H_T F_{BT} + T_{RT} - T_{RR}$$

$$(4b.16) R_T = R_{BT} - \frac{1}{3} S_M - U_{RR} (X_{TT} - X_W)$$

Because the ground is now stationary equation (4a.17) becomes

$$(4b.17) V_{RS} = \dot{X}_{TT}$$

The remaining equations are unchanged except for noting that the outputs X_{WM} and \dot{X}_{WM} required for the Airplane System are obtained by renaming X_{TT} . Thus $X_{WM} = X_{TT}$ and $\dot{X}_{WM} = \dot{X}_{TT}$. Continuing,

$$(4b.18) V_R = V_{RS} - R_T W_T$$

$$(4b.19) W_B = W_W - W_S$$

$$(4b.20) F_{NMF} = F_{NM} (1 - C_{HY} (V_{RS} / V_{HY})^2)$$

$$(4b.21) F_{BT} = F_{NMF} U_T + D_{HY} V_{RS}^2$$

$$(4b.22) U_T = \begin{cases} U_{T1} + (U_{T2} - E_T V_{RS}) e^{-\alpha V_R} & \text{if } V_R > 0 \\ 0 & \text{if } V_R = 0 \\ -U_{T1} - (U_{T2} - E_T V_{RS}) e^{\alpha V_R} & \text{if } V_R < 0 \end{cases}$$

B. Parameter Evaluation

The parameter values for this system are essentially the same as for the wheel and tire system that corresponds to the flywheel system. One difference is the values for C_G and D_G which are derived in the Airplane System (3 degree). These values are

$$(4b.23) \quad \begin{cases} C_G = 200,000 \text{ lb/in} \\ D_G = 78.6 \text{ lb sec/in} \end{cases}$$

Since this system moves with the airplane the initial conditions should match the Airplane model. Thus

$$(4b.24) \quad \begin{cases} X_{TTO} = 0.0 \text{ in} \\ \dot{X}_{TTO} = 2400 \text{ in/sec} \end{cases}$$

$$(4b.25) \quad \begin{cases} X_{WO} = 0.0 \text{ in} \\ \dot{X}_{WO} = 2400 \text{ in/sec} \end{cases}$$

From equation (4b.16)

$$(4b.26) \quad R_T = R_{ET} - \frac{1}{3} S_M = 23.32 - .80 = 22.52 \text{ IN}$$

Thus for a "spun up" tire, we have from equation (18)

$$(4b.27) \quad W_T = V_{RS} / R_T = 2400 / 22.52 = 106.7 \text{ rad/sec}$$

Then

$$(4b.28) \quad \dot{\Theta}_{TO} = \dot{\Theta}_{WO} = 106.7 \text{ rad/sec}$$

Also from equation (10), choose Θ_{SO}

$$(4b.29) \quad \Theta_{SO} = \Theta_{GO} = .0329 \text{ rad/sec}$$

Table 10 Wheel and Tire System (3 Degree) Parameters

SYMBOL	TYPE	VALUE	UNITS	DESCRIPTION
α	c	2.5×10^{-3}	sec/in	Tire Friction Parameter
C_G	c	2.0×10^5	lb/in	Fore and Aft Spring Rate at Axle
C_{RS}	c	10.4×10^6	in/lb/rad	Axle Rotational Spring Rate
C_{RT}	c	15.5×10^6	in/lb/rad	Tire to Wheel Rotational Spring Rate
C_{HY}	c	c.c	-	Controls Hydroplaning Influence
C_{TT}	c	10,200	lb/in	Tread to Wheel Spring Rate
D_G	c	78.6	lb sec/in	Fore and Aft Damping Coeff. at Axle
D_{HY}	c	c.c	lb sec ² /in ²	Water Resistance Coeff.
D_{RS}	c	132	in lb sec/rad	Gear To Axle Rotational Damping Coeff.
D_{RT}	c	30,400	in lb sec/rad	Tire to Wheel Rotational Damping Coeff.
D_{SR}	c	2350	lb	Rolling Resistance Parameter
D_{TT}	c	15.9	lb sec/in	Tread to Wheel Damping Coeff.
D_{VR}	c	40.3	lb sec/rad	Rolling Resistance Parameter
E_{RT}	c	10.15×10^6	in lb/rad	Tire to Wheel Coupling Spring Rate
E_T	c	$.65 \times 10^{-4}$	sec/in	Tire Friction Correction Coeff.
E_{TT}	c	5200	lb/in	Tread to Wheel Coupling Spring Rate
F_{BT}	v		lb	Horizontal Force on Tire Footprint from Ground
F_G	v(o)		lb	Horizontal Force at Axle
F_{GRH}	v		lb	Horizontal Wheel Unbalance Force
F_{GRV}	v(o)		lb	Vertical Wheel Unbalance Force
F_{GM}	v(i)		lb	Vertical Force Between Tire and Ground
F_{GMF}	v		lb	Vertical Force Not Supported by Water Film
F_{TR}	v		lb	Net Force Between Tread and Wheel

Table 10 (Contd)

SYMBOL	TYPE	VALUE	UNITS	DESCRIPTION
H_T	V		in	Axle Height Above Ground ($H_T \leq R_{ET}$)
θ_s	V		rad	Axle Rotation
$\dot{\theta}_{s0}$	C	.0329	rad	Axle Rotation at Time = 0
$\ddot{\theta}_s$	V		rad/sec	Axle Rotational Speed
$\dot{\theta}_{s0}$	C	0.0	rad/sec	Axle Rotational Speed at Time = 0
$\ddot{\theta}_s$	V		rad/sec ²	Axle Rotational Acceleration
θ_T	V		rad	Tire Tread Rotation
$\dot{\theta}_{T0}$	C	0.0	rad	Tire Tread Rotation at Time = 0
$\ddot{\theta}_T$	V		rad/sec	Tire Tread Rotational Speed
$\dot{\theta}_{T0}$	C	106.7	rad/sec	Tire Tread Rotational Speed at Time = 0
$\ddot{\theta}_T$	V		rad/sec ²	Tire Tread Rotational Acceleration
θ_W	V		rad	Wheel Rotation
$\dot{\theta}_{W0}$	C	0.0	rad	Wheel Rotation at Time = 0
$\ddot{\theta}_W$	V		rad/sec	Wheel Rotational Speed
$\dot{\theta}_{W0}$	C	106.7	rad/sec	Wheel Rotational Speed at Time = 0
$\ddot{\theta}_W$	V		rad/sec ²	Wheel Rotational Acceleration
θ_Y	V		rad	} Dummy Variables Used to Simulate Visco-Elastic Tire Characteristic.
$\dot{\theta}_{Y0}$	C	0.0	rad	
$\ddot{\theta}_Y$	V		rad/sec	
R_{k0}	C	0.0	lb sec ² /rad ²	Unbalance Coeff.
R_{ET}	C	23.32	in	Undelected Tire Radius
R_T	V		in	Tire Rolling Radius
S_M	V(i)		in	Tire Deflection

Table 10 (Contd)

SYMBOL	TYPE	VALUE	UNITS	DESCRIPTION
T_{Br}	v(i)		in lb	Brake Torque
T_{Re}	v		in lb	Torque Producing Rolling Resistance
T_{RT}	v		in lb	Torque Between Tire (Tread) and Wheel
T_s	v(o)		in lb	Axle Torque
U_{ER}	c	1.0	-	Rolling Radius Parameter
U_T	v		-	Tire Friction Coefficient
U_{T1}	c	.20	-	} Tire Friction Parameters
U_{T2}	c	.45	-	
V_{HY}	c	2400	-	Tire Hydroplaning Speed
V_R	v		in/sec	Velocity of Tire Footprint Relative to Flywheel
V_{RS}	v		in/sec	Sam ² as V_R except Rotational Effects Ignored
W_B	v(o)		rad/sec	Relating Rotational Speed Between Stators & Rotors
W_{GW}	c	1.6	lb sec ² /in	Effective Tire, Wheel, & Brake Mass
W_{IS}	c	16.8	in lb sec ² /rad	Axle Moment of Inertia (+ Stators)
W_{IT}	c	115.0	in lb sec ² /rad	Tread Moment of Inertia
W_{IW}	c	66.0	in lb sec ² /rad	Wheel and Rotors Moment of Inertia
W_s	v		rad/sec	$W_s = \dot{\theta}_s$
W_T	v		rad/sec	$W_T = \dot{\theta}_T$
W_{TE}	c	.0725	lb sec ² /in	Equivalent Tire Tread Mass
W_w	v		rad/sec	$W_w = \dot{\theta}_w$
X_{TT}	v		in	Location of Tire Tread C.G.
X_{TTO}	c	0.0	in	Location of Tire Tread C.G. at Time = 0

Table 10 (Contd)

SYMBOL	TYPE	VALUE	UNITS	DESCRIPTION
\dot{X}_{TR}	V		in/sec	Tread C.G. Velocity
\dot{X}_{TRO}	C	2400	in/sec	Tread C.G. Velocity at Time = 0
\ddot{X}_{TR}	V		in/sec ²	Tread C.G. Acceleration
X_W	V		in	Horizontal Axle Location
X_{WO}	C	0.0	in	Horizontal Axle Location at Time = 0
\dot{X}_W	V		in/sec	Horizontal Axle Velocity
\dot{X}_{WO}	C	2400	in/sec	Horizontal Axle Velocity at Time = 0
\ddot{X}_W	V		in/sec ²	Horizontal Axle Acceleration
X_Y	V		in	Dummy Variables Used to
X_{YO}	C	0.0	in	Simulate Visco-Elastic Tire
\dot{X}_Y	V		in/sec	Characteristic.
$\dot{\Theta}_G$	V(i)		rad	Gear Rotation
$\dot{\Theta}_G$	V(i)		rad/sec	Gear Rotational Velocity
X_{AX}	V(i)		in	Undelected Axle Position
\dot{X}_{AX}	V(i)		in/sec	Undelected Axle Velocity
X_{WM}	V(o)		in	Footprint Location (x Direction)
\dot{X}_{WM}	V(o)		in/sec	Footprint Velocity (x Direction)

4c. TIRE AND WHEEL SYSTEM (6 DEGREE)

The wheel and tire system for the six degree problem is the same as that described in the three degree system except for inclusion of the lateral mode. Equations (4c.1) through (4c.17) are the same as (4b.1) through (4b.17) in the three degree system.

A. Mathematical Description

$$(4c.1) \quad F_G = C_G (X_{AX} - X_W) + D_G (\dot{X}_{AX} - \dot{X}_W)$$

$$(4c.2) \quad F_{TT} = C_{TT}(X_{TT} - X_W) + E_{TT}(X_{TT} - X_Y)$$

$$(4c.3) \quad D_{TT}(\dot{X}_Y - \dot{X}_W) = E_{TT}(X_{TT} - X_Y)$$

$$(4c.4) \quad W_{GW} \ddot{X}_W = F_G + F_{TT}$$

$$(4c.5) \quad W_{TE} \ddot{X}_{TT} = -F_{TT} - F_{BT} + F_{ORH}$$

$$(4c.6) \quad F_{ORH} = R_{KH} W_T^2 \sin \langle \theta_T \rangle$$

$$(4c.7) \quad F_{ORV} = R_{KV} W_T^2 \cos \langle \theta_T \rangle$$

$$(4c.8) \quad T_{RT} = C_{RT}(\theta_W - \theta_T) + E_{RT}(\theta_W - \theta_Y)$$

$$(4c.9) \quad D_{RT}(\dot{\theta}_Y - \dot{\theta}_T) = E_{RT}(\theta_W - \theta_Y)$$

$$(4c.10) \quad T_S = C_{RS}(\theta_S - \theta_G) + D_{RS}(\dot{\theta}_S - \dot{\theta}_G)$$

$$(4c.11) \quad H_T = R_{\theta T} - S_M$$

$$(4c.12) \quad T_{RR} = \begin{cases} S_M (D_{SR} + D_{VR} W_T) & \text{if } W_T > 0 \\ 0 & \text{if } W_T = 0 \\ S_M (-D_{SR} + D_{VR} W_T) & \text{if } W_T < 0 \end{cases}$$

$$(4c.13) \quad W_{IS} \ddot{\theta}_S = T_{BT} - T_S$$

$$(4c.14) \quad W_{IW} \ddot{\theta}_W = -T_{RT} - T_{BT}$$

$$(4c.15) \quad W_{IT} \ddot{\theta}_T = H_T F_{BT} + T_{RT} - T_{RR}$$

$$(4c.16) \quad R_T = R_{\theta T} - \frac{1}{3} S_M - U_{RR} (X_{TT} - X_W)$$

$$(4c.17) \quad V_{RS} = \dot{X}_{TT} = \dot{X}_{WM} \quad \text{also } X_{WM} = X_{TT}$$

Equation (4b.18) which gives the relative velocity between the footprint and the ground is changed to account for the lateral footprint velocity \dot{Y}_M .

$$(4c.18) \quad V_R = \sqrt{V_{RX}^2 + \dot{Y}_M^2}$$

Equations (4b.19) and (4b.20) are unchanged.

$$(4c.19) \quad W_B = W_W - W_S$$

$$(4c.20) \quad F_{NMF} = F_{NM} (1 - C_{HY} (V_{RS} / V_{HY})^2)$$

Now V_{RX} is the relative velocity in the x direction so

$$(4c.21) \quad V_{RX} = V_{RS} - R_T W_T$$

Thus, the angle β_T which defines the friction force direction as shown in figure 45 is given by

$$(4c.22) \quad \beta_T = \tan^{-1} \langle \dot{Y}_M / V_{RX} \rangle$$

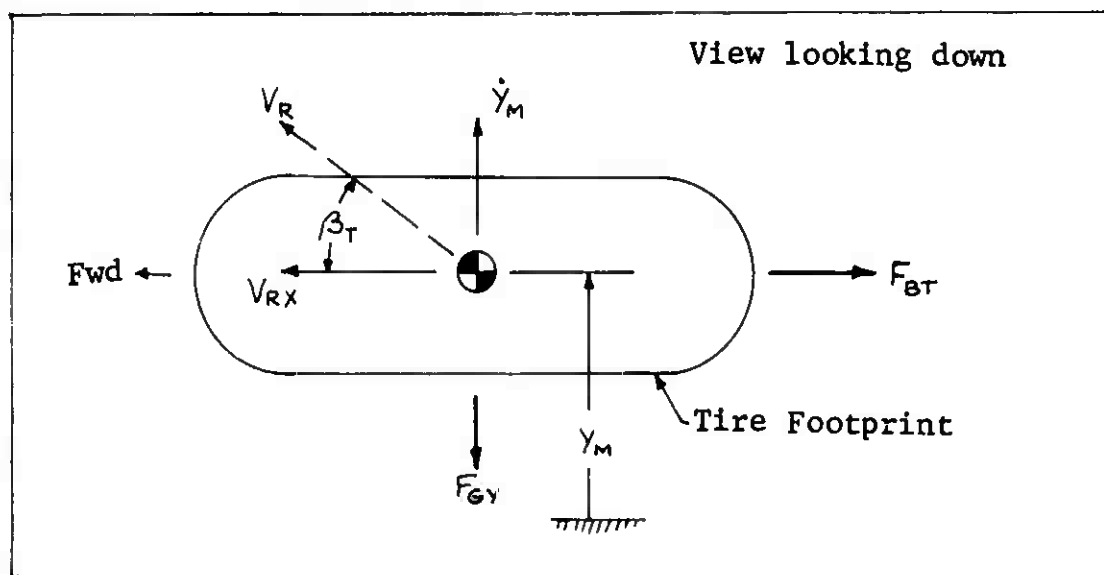


Figure 45 Footprint Friction Components



Thus, F_{BT} is now given by

$$(4c.23) F_{BT} = F_{NMF} U_T \cos \langle \beta_T \rangle + D_{HY} V_{RS}^2$$

and

$$(4c.24) U_T = \begin{cases} U_{T1} + (U_{T2} - E_T V_{RS}) e^{-\alpha V_R} & \text{if } V_R > 0 \\ 0 & \text{if } V_R \leq 0 \end{cases}$$

The lateral friction force F_{GY} is given by

$$(4c.25) F_{GY} = F_{NMF} U_T \sin \langle \beta_T \rangle$$

The airplane produces a lateral position Y_{AX} of the axle. If Y_M is the lateral location of the footprint, then a lateral force F_{ST} is produced and

$$(4c.26) F_{ST} = C_{ST} (Y_{AX} - Y_M) + D_{ST} (\dot{Y}_{AX} - \dot{Y}_M)$$

Finally, forces can be summed laterally on the footprint to obtain

$$(4c.27) W_{TE} \ddot{Y}_M = F_{ST} - F_{GY}$$

B. Parameter Evaluation

Wheel and Tire System Parameters

Most of the parameter values were derived in the wheel and tire system that was used with the flywheel. The only addition is the evaluation of C_{ST} and D_{ST} .

From reference 1 (p.15)

$$(4c.28) K_\lambda = \tau_\lambda \omega (P + .24 P_R) (1 - .7(\delta_0/\omega))$$

Assuming that $\delta_0 = 2.245$ in., then

$$(4c.29) C_{ST} = (2)(18)(1.24)(150)(1 - .7(2.245/18))$$

$$(4c.30) C_{ST} = 6460 \text{ lb/in}$$

$$\text{Using } \omega_n = \sqrt{K/m} = \sqrt{6460/.0725} = 298.4$$

Using $\eta = .1$ (from page 50 of Ref. 1) results in

$$(4c.31) D_{ST} = \eta C_{ST} / \omega_n = (.1)(6460)/298.4 = 2.165$$

Initial Conditions

The only difference between this and the three degree system is evaluating y_{M0} and \dot{y}_{M0} . It should be that $y_{M0} = y_{Ax(0)}$. Since this system is used for both right and left sides, then y_{M0} will differ. Assume that this system is used as the right wheel and tire. Then, $y_{M0} = y_{AxR}$ as in equation (4c.56). From this equation at Time = 0, (since $R = P = 0$), then

$$(4c.32) \quad y_{M0} = y_{AxR} = y_0 + S_{BW} = 0 + 60 = 60 \text{ in}$$

Similarly

$$(4c.33) \quad \dot{y}_{M0} = \dot{y}_{AxR} = \dot{y}_0 = 0.0 \text{ in/sec}$$

Table 11 Wheel and Tire System (6 Degree) Parameters

SYMBOL	TYPE	VALUE	UNITS	DESCRIPTION
α	C	2.5×10^{-3}	sec/in	Tire Friction Parameter
β_T	V		rad	Tire Footprint Friction Angle
C_G	C	2.0×10^5	lb/in	Fore and Aft Spring Rate at Axle
C_{RS}	C	10.4×10^4	in lb/rad	Axle Rotational Spring Rate
C_{RT}	C	19.5×10^6	in lb/rad	Tire to Wheel Rotational Spring Rate
C_{HY}	C	0.0	-	Controls Hydroplaning influence
C_{ST}	C	6460	lb/in	Tire Lateral Spring Rate
C_{TT}	C	10,200	lb/in	Tread to Wheel Spring Rate
D_G	C	78.6	lb sec/in	Fore and Aft Damping Coefficient at Axle
D_{HY}	C	0.0	lb sec ² /in ²	Water Resistance Coefficient
D_{RS}	C	132	in lb sec/rad	Gear to Axle Rotational Damping Coeff.
D_{RT}	C	30,400	in lb sec/rad	Tire to Wheel Rotational Damping Coeff.
D_{SR}	C	2350	lb	Rolling Resistance Parameter
D_{ST}	C	2.165	lb sec/in	Tire Lateral Damping Coefficient
D_{TT}	C	15.9	lb sec/in	Tread to Wheel Damping Coefficient
D_{VR}	C	40.3	lb sec/rad	Rolling Resistance Parameter
E_{RT}	C	10.15×10^6	in lb/rad	Tire to Wheel Coupling Spring Rate
E_T	C	$.65 \times 10^4$	sec/in	Tire Friction Correction Coefficient
E_{TT}	C	5300	lb/in	Tread to Wheel Coupling Spring Rate
F_{BT}	V		lb	Horizontal Force on Tire Footprint from Ground
F_G	V(o)		lb	Horizontal Force at Axle
F_{GY}	V		lb	Lateral Tire Load (On Ground)
F_{GH}	V		lb	Horizontal Wheel Unbalance Force
F_{GV}	V(o)		lb	Vertical Wheel Unbalance Force

Table 11 (Contd)

SYMBOL	TYPE	VALUE	UNITS	DESCRIPTION
F_{NM}	$v(I)$		lb	Vertical Force between Tire and Ground
F_{NMF}	v		lb	Vertical Force not supported by Water Film
F_{ST}	$v(o)$		lb	Lateral Tire Load (On Apl)
F_{TT}	v		lb	Net Force between Tread and Wheel
H_T	v		in	Axle Height Above Ground
θ_G	$v(I)$		rad	Gear Rotation
$\dot{\theta}_G$	$v(I)$		rad/sec	Gear Rotational Velocity
θ_S	v		rad	Axle Rotation
$\dot{\theta}_{SO}$	c	.0329	rad	Axle Rotation at Time = 0
$\dot{\theta}_S$	v		rad/sec	Axle Rotational Speed
$\dot{\theta}_{SO}$	c	0.0	rad/sec	Axle Rotational Speed at Time = 0
$\ddot{\theta}_S$	v		rad/sec ²	Axle Rotational Acceleration
θ_T	v		rad	Tire Tread Rotation
$\dot{\theta}_{TO}$	c	0.0	rad	Tire Tread Rotation at Time = 0
$\dot{\theta}_T$	v		rad/sec	Tire Tread Rotational Speed
$\dot{\theta}_{TO}$	c	106.7	rad/sec	Tire Tread Rotational Speed at Time = 0
$\ddot{\theta}_T$	v		rad/sec ²	Tire Tread Rotational Acceleration
θ_W	v		rad	Wheel Rotation
$\dot{\theta}_{WO}$	c	0.0	rad	Wheel Rotation at Time = 0
$\dot{\theta}_W$	v		rad/sec	Wheel Rotational Speed
$\dot{\theta}_{WO}$	c	106.7	rad/sec	Wheel Rotational Speed at Time = 0
$\ddot{\theta}_W$	v		rad/sec ²	Wheel Rotational Acceleration
θ_Y	v		rad	Dummy Variables used to
$\dot{\theta}_{YO}$	c	0.0	rad	Simulate Visco-Elastic Tire
$\ddot{\theta}_Y$	v		rad/sec	Characteristic

Table 11 (Contd)

SYMBOL	TYPE	VALUE	UNITS	DESCRIPTION
R_{ϕ}	C	0.0	lb sec ² /rad ²	Unbalance Coefficient
$R_{\phi T}$	C	23.32	in	Undelected Tire Radius
R_T	V		in	Tire Rolling Radius
S_M	V(I)		in	Tire Deflection
$T_{\phi T}$	V(I)		in lb	Brake Torque
T_{RR}	V		in lb	Torque Producing Rolling Resistance
T_{RT}	V		in lb	Torque Between Tire (Tread) and Wheel
T_S	V(O)		in lb	Axle Torque
U_{RR}	C	1.0	—	Rolling Radius Parameter
U_T	V		—	Tire Friction Coefficient
U_{T1}	C	.20	—	Tire Friction Parameters
U_{T2}	C	.45	—	
V_{HY}	C	2400	in/sec	Tire Hydroplaning Speed
V_R	V		in/sec	Velocity of Tire Footprint Relative to Flywheel
V_{RS}	V		in/sec	Same as V_{RX} except rotational effects ignored
V_{RX}	V		in/sec	Tire Footprint Relative Velocity in X Direction
W_B	V(O)		rad/sec	Relative Rotational Speed between Stators and Rotors
W_{EW}	C	1.6	lb sec ² /in	Effective Tire, Wheel, and Brake Mass
W_{IS}	C	16.8	in lb sec ² /rad	Axle Moment of Inertia (+ Stators)
W_{IT}	C	115	in lb sec ² /rad	Tread Moment of Inertia
W_{IW}	C	66.0	in lb sec ² /rad	Wheel and Rotors Moment of Inertia

Table 11 (Contd)

SYMBOL	TYPE	VALUE	UNITS	DESCRIPTION
W_s	V		rad/sec	$W_s = \dot{\theta}_s$
W_T	V		rad/sec	$W_T = \dot{\theta}_T$
W_{TE}	C	0.0725	lb sec ² /in	Equivalent Tire Tread Mass
W_w	V		rad/sec	$W_w = \dot{\theta}_w$
X_{TT}	V		in	Location of Tire Tread C. G.
X_{TTO}	C	0.0	in	Location of Tire Tread C. G. at Time = 0
\dot{X}_{TT}	V		in/sec	Tread C. G. Velocity
\dot{X}_{TTO}	C	2400	in/sec	Tread C. G. Velocity at Time = 0
\ddot{X}_{TT}	V		in/sec ²	Tread C. G. Acceleration
X_W	V		in	Horizontal Axle Location
X_{WO}	C	0.0	in	Horizontal Axle Location at Time = 0
\dot{X}_W	V		in/sec	Horizontal Axle Velocity
\dot{X}_{WO}	C	2400	in/sec	Horizontal Axle Velocity at Time = 0
\ddot{X}_W	V		in/sec ²	Horizontal Axle Acceleration
X_Y	V		in	Dummy Variables used to
X_{YO}	C	0.0	in	Simulate Visco-Elastic Tire
\dot{X}_Y	V		in/sec	Characteristic
Y_{AX}	V(I)		in	Undelected Axle Location (y Direction)
\dot{Y}_{AX}	V(I)		in/sec	Undelected Axle Velocity (y Direction)
X_{AX}	V(I)		in	Undelected Axle Location (x Direction)
\dot{X}_{AX}	V(I)		in/sec	Undelected Axle Velocity (x Direction)
Y_M	V(O)		in	Footprint Location (y Direction)
Y_{MO}	C	±60.0	in	Y_M at Time = 0 ($Y_{MO} = +60$, $Y_{MO} = -60$)
\dot{Y}_M	V		in/sec	Footprint Velocity
\dot{Y}_{MO}	C	0.0	in/sec	\dot{Y}_M at Time = 0

Table 11 (Contd)

SYMBOL	TYPE	VALUE	UNITS	DESCRIPTION
\ddot{y}_m	v		in/sec ²	Footprint Acceleration
x_{wm}	v(o)		in	Footprint Position (x Direction)
\dot{x}_{wm}	v(o)		in/sec	Footprint Velocity

5. WHEEL SPEED SENSOR

The primary input parameter to an electronic antiskid control circuit is an airplane wheel speed signal. For conventional control circuitry the input must be a direct current voltage. The wheel speed sensor may have any one of several forms such as a D.C. tachometer or an A.C. tachometer with variable voltage or frequency converted to a direct current voltage by suitable electronic circuitry. The control circuit input signal, E_G , is a function of the wheel's angular velocity relative to the axle (tachometer mount) and the characteristics of any associated electronic circuitry used for radio interference suppression and/or for conversion of A.C. frequency or voltage signals to D.C. voltage. To provide the means for mathematically describing the control circuit input signal for a variety of wheel speed sensors, two approaches are taken. The first, identified as Option 1, is applicable whenever there is a perceptible phase lag between actual wheel speed and the antiskid circuit input as is generally the case where A.C. voltage signals are converted to D.C. or where a D.C. tachometer is driven through an elastic coupling. A second simpler mathematical description, called Option 2, is provided to minimize computation difficulty and expense where no significant phase lag exists.

A. Mathematical Description

Option 1

Assume that a D.C. tachometer generator is mounted on the axle and is driven by the wheel. The output of the hypothetical generator is assumed to be applied to a linear force motor which acts upon a single degree of freedom damped spring mass system as shown on Figure 47. The control circuit input signal, E_G , is proportional to the mass displacement. By adjusting the relative characteristics of the linear force motor, hypothetical generator, spring, mass and damper a mathematical description of a wide variety of wheel speed sensors can be accommodated.

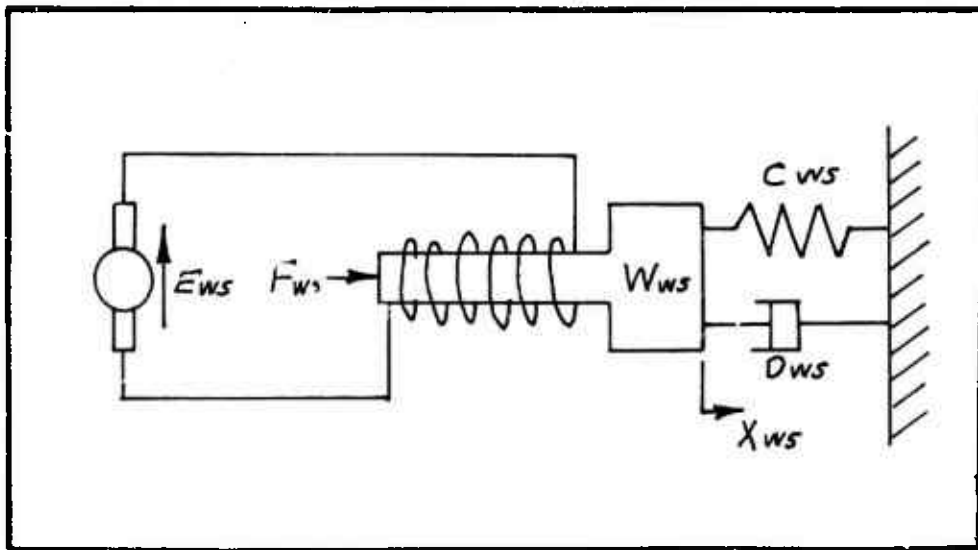


Figure 47 Wheel Speed Signal System

The output of the hypothetical generator, E_{ws} , is proportional to the wheel's angular velocity relative to the axle, W_B , as defined by equation (5.1). Angular velocity, W_B , is obtained as an output of the tire and wheel system.

$$(5.1) \quad E_{ws} = G_{ws} W_B$$

The force produced by the linear force motor, F_{ws} , is proportional to the generator output, E_{ws} , as defined by equation (5.2).

$$(5.2) \quad F_{ws} = C_{wg} E_{ws}$$

The hypothetical mass displacement, X_{ws} , is obtained from equation (5.3) which results from summing forces on the hypothetical mass, W_{ws} .

$$(5.3) \quad \ddot{X}_{ws} = \frac{F_{ws}}{W_{ws}} - \frac{C_{ws}}{W_{ws}} (\dot{X}_{ws}) - \frac{D_{ws}}{W_{ws}} (X_{ws})$$

The antiskid circuit wheel speed input voltage signal, E_G , is proportional to the hypothetical mass displacement, X_{ws} , as defined by equation (5.4).

$$(5.4) \quad E_G = C_{gv} X_{ws} + E_{sn}$$

In equation (5.4), E_{sn} is any extraneous "noise" which might be present due to the operation of other aircraft systems, etc.

The equation flow diagram is shown on Figure 48.

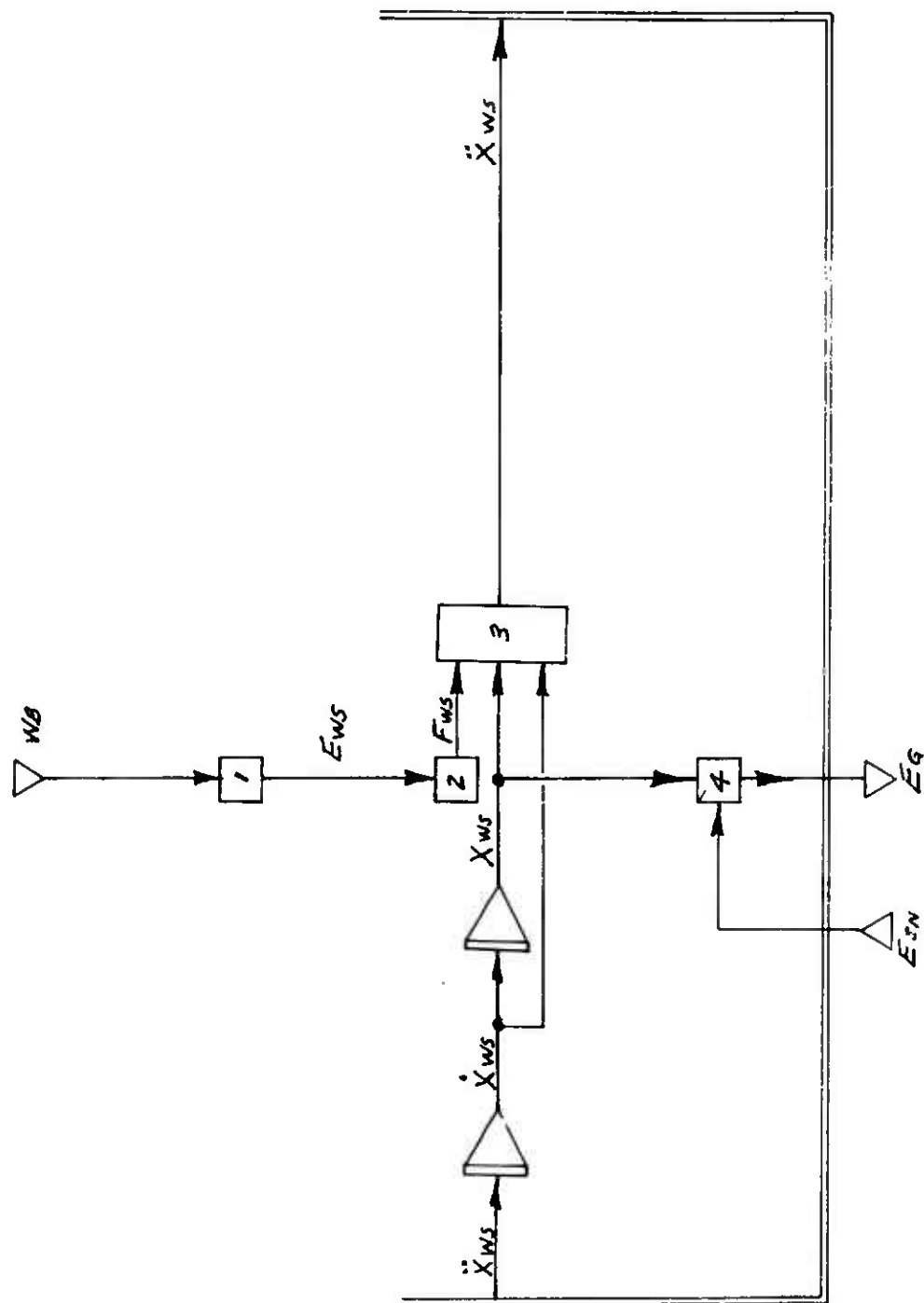


Figure 48 Wheel Speed Sensor Equation Flow Diagram (Option 1)

Option 2

For cases where the wheel speed transducer is a D.C. tachometer, or equivalent, driven through a rigid coupling (such as the F-104 and F-111) there is usually very small difference between the actual wheel speed and antiskid control circuit input (i.e., very low phase lag or attenuation) and the extra mathematical complication incurred by using a very high gain second order equation is not justified. For these cases the antiskid control circuit input voltage may be considered proportional to the wheel's angular velocity as defined by equation (5.5).

$$(5.5) \quad E_G = G_{WDC} W_B + E_{SN}$$

No equation flow diagram is shown for Option 2.

B. Parameter Evaluation

Option 1

The objective of using a single degree of freedom damped spring mass system to describe the antiskid control circuit input is to provide a mathematical "tool" whereby phase lag within the wheel speed sensor device can be accounted for. Consequently, the values for mass, spring rate and damping coefficient are chosen to produce the desired effect rather than to describe physical devices. The other coefficients are chosen to achieve compatibility with the control circuit. For the F-111 modulated antiskid circuit let the hypothetical tachometer coefficient be the same as for the actual F-111 tachometer, 12 volts per thousand RPM. Therefore:

$$(5.6) \quad G_{WS} = \frac{12 \times 60}{1000 \times 2\pi} = 0.1147 \text{ VOLT SEC/RAD}$$

Let the force motor coefficient, the elastic system spring rate and output voltage coefficient all be equal to unity so that for steady state conditions the control circuit input, E_G , is the tachometer output. Therefore:

$$(5.7) \quad \begin{aligned} C_{WG} &= 1.0 \text{ lbf/VOLT} \\ C_{WS} &= 1.0 \text{ lbf/INCH} \\ C_{CGV} &= 1.0 \text{ VOLT/INCH} \end{aligned}$$

Based on information furnished by the Goodyear Aerospace Corp. the component characteristics and arrangement which is usually utilized for converting A.C. frequency to D.C. voltage produces about 30 degrees (or greater) phase lag at 5 cps. The following equations from reference 12 describe the single degree of freedom system's behavior when an oscillatory force $X_0 K \sin \omega t$ is applied.

$$(5.8) \quad \frac{X}{X_0} = \frac{1}{\sqrt{[1 - (\omega/\omega_n)^2]^2 + (2\zeta\omega/\omega_n)^2}}$$

$$\tan \phi = \frac{2(\omega/\omega_n)\zeta}{1 - (\omega/\omega_n)^2}$$

In these equations ϕ is the phase angle, $\zeta = D_{ws}/2W_{ws}\omega_n$ is the damping factor, $\omega_n = \sqrt{C_{ws}/W_{ws}}$ is the undamped natural frequency, ω is the frequency of applied oscillatory loading, and X/X_0 is the magnification factor. If the degree of attenuation and phase angle are known at a particular frequency, the undamped natural frequency and damping factor are established. Assuming two percent attenuation and 30 degree phase lag at 5 cps, the equations above give an undamped natural frequency of 14.6 cps (91.8 RAD/SEC) and a damping factor of 0.746.

For an undamped natural frequency of 91.8 RAD/SEC and a spring rate, C_{ws} , of 1.0 lbf/in the mass, W_{ws} , is established as 0.1185×10^{-3} lbf sec²/in. The damping coefficient, D_{ws} , is established from the mass and damping factor as

$$(5.9) \quad D_{ws} = 0.1623 \times 10^{-2} \text{ lbf sec/in}$$

Option 2

For use with the F-111 modulated antiskid control circuit, use the actual F-111 tachometer output of 12 volts D.C. per 1000 RPM. Therefore:

$$(5.10) \quad G_{WDC} = \frac{12 \times 60}{1000 \times 2\pi} = 0.1147 \text{ VOLT SEC/RAD}$$

For use with the on-off antiskid circuit as installed on the F-104 (and B-58) the tachometer output is 20 volts per 1000 RPM. To make the on-off circuit compatible with the F-111 requires that the difference in tire size (46.5 inch dia. for F-111 versus 22 inch dia. for B-58) also be accounted for. Therefore, for the on-off antiskid circuit use:

$$(5.11) \quad G_{WOC} = (0.1147) \left(\frac{46.5}{22} \right) \left(\frac{20}{12} \right) = 0.4 \text{ VOLT SEC/RAD}$$

Table 12 Wheel Speed Sensor Parameters

SYMBOL	TYPE	VALUE	UNITS	DESCRIPTION
OPTION 1 FOR USE WITH F-111 MODULATED CIRCUIT				
C _{CGV}	C	1.0	VOLT/IN	Output Voltage Coefficient
C _{WG}	C	1.0	1bF/VOLT	Hypothetical Liner Force Motor Coefficient
C _{WS}	C	1.0	1bF/IN	Spring Rate (Hypothetical Spring)
D _{WS}	C	0.1623×10^{-2}	1bF SEC/IN	Damping Coefficient (Hypothetical Damper)
E _G	V(O)		VOLTS	Antiskid Control Circuit Input Signal
E _{WS}	V		VOLTS	Hypothetical Tachometer Voltage
F _{WS}	V		1bF	Hypothetical Linear Force Motor Output Force
G _{WS}	C	0.1147	VOLT SEC/RAD	Hypothetical Tachometer Voltage-Speed Coefficient
E _{SN}	V(I)	0.0	VOLTS	Input Signal "Noise"
W _{WS}	C	0.1185×10^{-3}	1bF SEC ² /IN	Mass (Hypothetical Mass)
W _B	V(I)		RAD/SEC	Wheel Angular Velocity Relative to Angle
X _{WS}	V		INCH	Hypothetical Mass Displacement
X _{WSO}	C	0.0	INCH	Hypothetical Mass Displacement at Time Zero
\dot{X}_{WS}	V		IN/SEC	Hypothetical Mass Velocity
\dot{X}_{WSO}	C	0.0	IN/SEC	Hypothetical Mass Velocity at Time Zero
\ddot{X}_{WS}	V		IN/SEC ²	Hypothetical Mass Acceleration
OPTION 2 FOR USE WITH F-111 MODULATED CIRCUIT				
G _{WDC}	C	0.1147	VOLT SEC/RAD	
E _{SN}	V(I)	0.0	VOLTS	

Table 1.2 (Contd)

SYMBOL	TYPE	VALUE	UNITS	DESCRIPTION
		OPTION 2 FOR USE WITH F104 ON-OFF CIRCUIT		
\bar{G}_{WOC} E_{SN}	C $V(I)$	0.4 0.0	VOLT SEC/RAD VOLTS	

6a. MODULATED ANTISKID CONTROL CIRCUIT

After introduction of on-off type antiskid systems, it became apparent from various analyses and studies of test results and operational performance that braking effectiveness could be increased if the number of antiskid cycles and their intensity could be minimized. To minimize antiskid cycling occurrences and intensity, it is necessary to control the amount of brake torque being applied such that the available friction torque is not exceeded for as much of the time as is possible. A number of devices utilizing various principles of operation have been used for this purpose. These devices predominately utilize the principle of regulating or "modulating" brake pressure to keep its value as near as possible to that which will produce a skid. One of the first of these type devices is a hydraulic pressure modulator comprised of an orifice and accumulator installed upstream from the pilot's metering valve and configured such that repetitive antiskid cycling causes a temporary reduction in pilot's metered pressure. The Convair Model 880 airplane's Hytrol MKI antiskid system with hydraulic modulation is a typical example of this type installation.

A subsequent development was the Bendix system which is used on Grumman A6A and Lockheed C141 aircraft. This system combines hydraulic modulation accomplished within the off-on type control valve with two levels of skid detection, (i.e., brake pressure reduction in two steps controlled by skid intensity). Further improvements have been achieved by utilizing a servo type pressure regulating valve with electronic control to achieve a wide range of control characteristics and better accommodate widely varying runway friction conditions encountered during aircraft operation. The Goodyear Adaptive system used on General Dynamics F-111 aircraft and the Hytrol MK II system used on McDonnell-Douglas F4C and LTV A7A aircraft are examples of the servo valve type systems. Within each of the types or classes of systems there are a number of variations in circuitry and component arrangement depending upon the aircraft type, landing gear arrangement and configuration, and the airplane's mission requirements. For this program a mathematical model of the F-111 airplane's Goodyear Adaptive Antiskid Control Circuit is developed. Models for other type circuits can be developed using similar procedures.

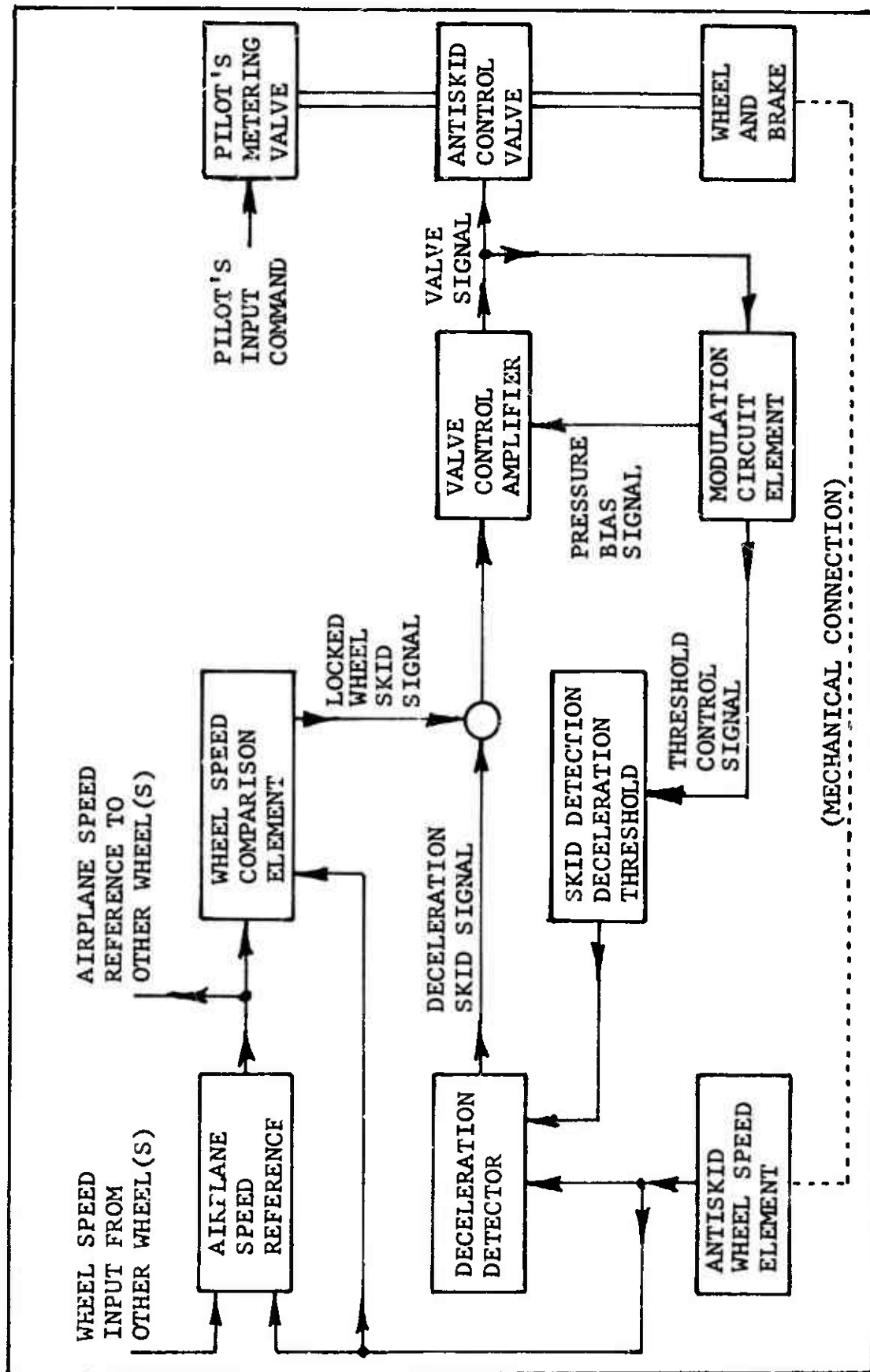


Figure 49 Modulated Antiskid Control Functional Block Diagram

Figure 49 is a block diagram showing the basic functional elements of the Goodyear adaptive antiskid control circuit as used on the F-111 airplane and showing the relationship of the control circuit to the other brake system components. During antiskid circuit operation, a wheel speed signal is provided as an input to a deceleration detector. Within the deceleration detector the wheel's deceleration rate is computed and compared to a threshold value provided by a skid detection threshold circuit element. The deceleration detector produces a skid signal proportional to the amount by which the wheel's deceleration rate exceeds the threshold value. The skid signal is applied to a valve control amplifier which in turn produces a valve control signal proportional to the input skid signal plus any pressure bias signal which might exist. The valve control signal is supplied to the antiskid control valve (a servo type pressure regulator) for brake pressure control and to a modulation circuit element. The modulation circuit element interprets the valve control signal and provides a pressure bias signal to the valve control amplifier and a threshold control signal to the skid detection threshold circuit element. The wheel speed signal is also supplied to the locked wheel prevention circuit elements consisting of an airplane speed reference and a wheel speed comparison element. When the airplane speed reference indicates that the airplane's speed exceeds "locked wheel arming speed" (usually 20 mph) and simultaneously the wheel speed is less than that which should exist for a slightly lower airplane speed (usually 10 mph), the wheel speed comparison circuit element produces a skid signal sufficient to fully release the brake. Locked wheel arming speed is chosen as some reasonably low speed below which a locked wheel is not particularly detrimental. The locked wheel feature is deactivated below locked wheel arming speed so that the airplane can be brought to a complete stop. The aircraft circuit also incorporates circuit elements for failure detection, automatic cutoff and prevention of brake application prior to touchdown. These logic type functions do not affect aircraft stopping performance and are not included in this analysis.

A. Modulated Antiskid Circuit Mathematical Description

A simplified schematic diagram of the Goodyear adaptive antiskid circuit for one wheel as used on F-111 type aircraft is shown on Figure 50. This circuit accom-

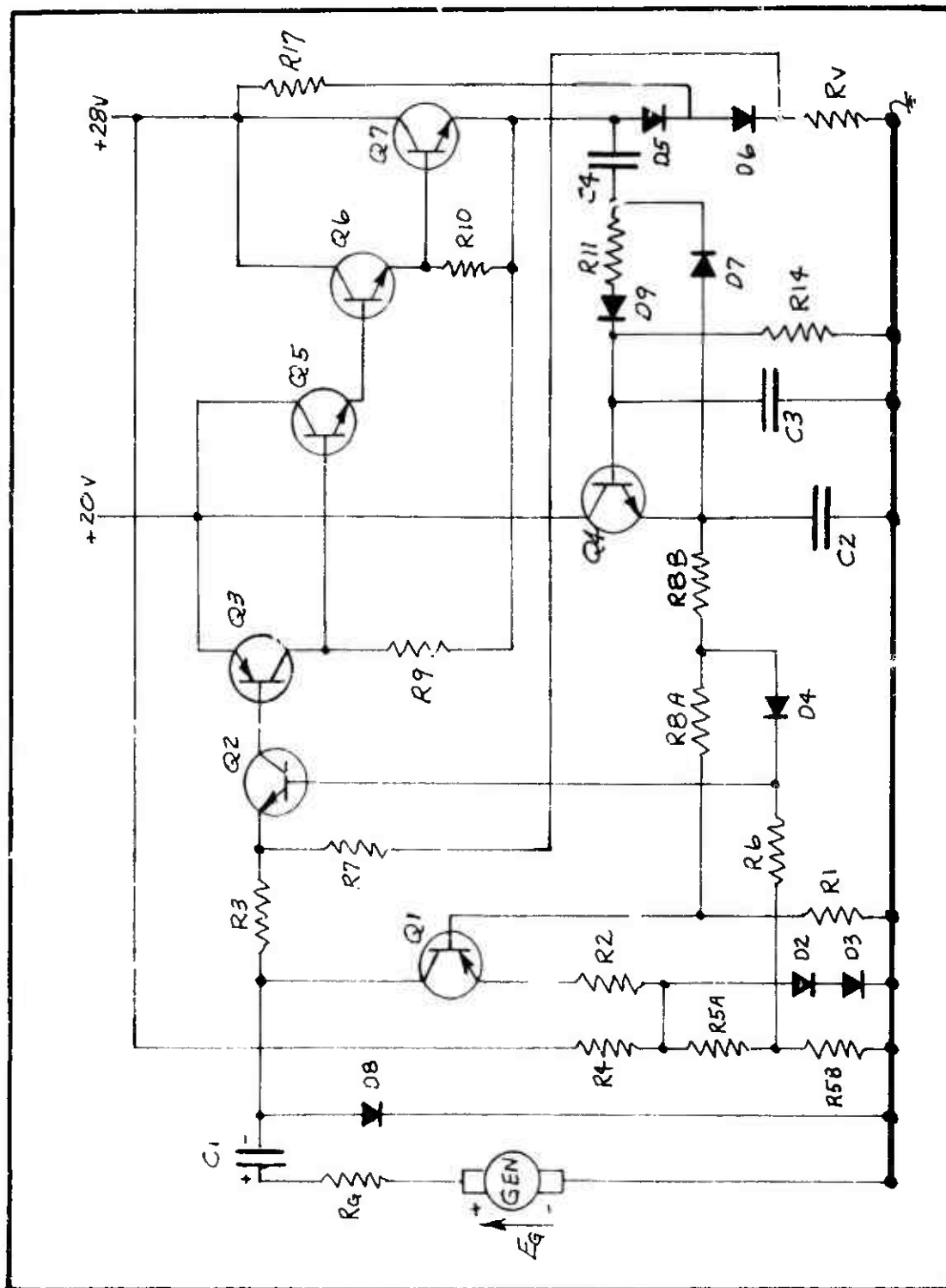


Figure 50 Modulated Antiskid Control Circuit Schematic

plishes deceleration skid control as previously described in the control circuit functional description as follows. An input voltage, E_G , is provided by a wheel driven D. C. tachometer generator (GEN). E_G charges the deceleration detector, capacitor, C_1 , through resistance R_6 and diode D_8 during wheel spin-up. For normal wheel deceleration rates, with no incipient skidding, the generator voltage will decrease relatively slowly and a small current will flow from the positive side of C_1 through R_6 , the generator, R_4 , R_2 , and transistor Q_1 to the negative side of C_1 . This current discharges capacitor C_1 and causes its voltage to closely follow E_G . Transistor Q_1 is the skid detection threshold circuit element. Q_1 is a current-limiting device that offers very low impedance to current below its threshold value and extremely high impedance to any current above that threshold. The threshold is controlled by R_2 . Diodes D_2 and D_3 provided bias voltage for the operation of Q_1 . When an incipient skid occurs, the generator voltage decreases rapidly and since Q_1 limits the discharge current into C_1 , the voltage at the negative side of C_1 decreases and causes current to flow through R_{5A} , R_6 , Q_2 , and R_3 . The current into the base of Q_2 is amplified by Q_2 , Q_3 , Q_5 , Q_6 and Q_7 , (the valve control amplifier) to produce a voltage across R_v , the antiskid valve coil. Voltage applied to the antiskid valve causes brake pressure to be reduced proportionally and thereby alleviate the incipient skid. Antiskid valve voltage is feedback to the amplifier input through R_7 to stabilize amplifier gain against changes due to temperature and component characteristic variations.

Antiskid valve voltage pulses are transmitted to the modulation circuit elements through capacitor C_4 . Within the modulation circuit element, consisting of C_4 , R_{11} , R_{14} , D_7 , C_3 , C_2 , D_9 and Q_4 , each increase in voltage to the valve produces an increase in the charge on C_3 . Voltage on C_3 causes Q_4 to charge C_2 . Since C_2 discharges through R_{8B} , R_{8A} , and R_1 , the voltage on C_2 provides a threshold control signal to Q_1 . The charge on C_3 , and in turn on C_2 , is a function of the amplitude and frequency of valve voltage pulses. Voltage on C_2 is also applied to Q_2 through R_{8B} and D_4 to provide a pressure bias signal to the valve control amplifier. The operation of the modulation circuit element results in an automatic threshold change to the skid sensing circuit and a bias to the valve control amplifier to match the braking conditions being encountered.

The equations listed in Tables 13, 14, 15, 16, and 17 describe the circuit's operation in accordance with the equation flow diagram shown on Figure 51. The assumptions and procedures used to develop these equations are described in Appendix I. The circuit has twelve possible modes of operation depending upon the instantaneous conditions which exist. The conditions which define the circuit's mode of operation at a particular instant are: (1) the current, A_{c4} , into capacitor C_4 is either positive, negative or zero, (2) the valve control amplifier is operating either in the cutoff mode or in the amplification mode, and (3) the modulating circuit element is either providing a pressure bias signal or it is not. Table 18 lists the twelve circuit modes resulting from combinations of the above circumstances. The valve amplifier condition is indicated by current A_{EQ2} being equal to or less than C607 in the cutoff mode and being greater than C607 in the amplification mode. The pressure bias signal is indicated as existing when voltage V_B is greater than zero and as not existing when V_B is equal to or less than zero.

The circuit condition which exists at a particular instant is established by assuming a condition and using the equations applicable to the assumed condition to test for the validity of the assumption. For instance, circuit condition number 1 assumes that current A_{c4} is positive; therefore, equation 6a-N8-1 from Table 16 must indicate a positive value of A_{c4} for the assumption to be correct. If so, then the equations for A_{EQ2} and V_B are similarly tested. If the assumed condition is correct, the applicable equations are used to compute the various currents and voltages. If the assumed condition is found to be incorrect, other conditions are successively assumed and tested until the correct condition is found.

B. Parameter Evaluation

Table 19 lists the parameters defining the modulated circuit's operation. The values for the constants are computed from various circuit element characteristics (resistance, capacitance, etc.) as described in reference 13 and in the semiconductor component manufacturers catalogs.

Table 13 Modulated Antiskid Circuit Equation Summary

Equation No.

Equation

$$(6a-1) \quad V_{C1} = \int \dot{V}_{C1} dt$$

$$(6a-A1) \quad \dot{V}_{C1} = A_{C1} C_{608}$$

$$(6a-2) \quad V_{C2} = \int \dot{V}_{C2} dt$$

$$(6a-A2) \quad \dot{V}_{C2} = A_{C2} C_{609}$$

$$(6a-3) \quad V_{C3} = \int \dot{V}_{C3} dt$$

$$(6a-A3) \quad \dot{V}_{C3} = A_{C3} C_{610}$$

$$(6a-4) \quad V_{C4} = \int \dot{V}_{C4} dt$$

$$(6a-4A) \quad \dot{V}_{C4} = A_{C4} C_{611}$$

$$(6a-5) \quad (E_G - V_{C1}) = E_G - V_{C1}$$

$$(6a-6) \quad A_{LWS} = \begin{cases} C_{617} & \text{FOR } V_F > C_{615} \text{ AND } E_G < C_{616} \\ 0 & \text{FOR } V_F \leq C_{615} \text{ OR } E_G \geq C_{616} \end{cases}$$

$$(6a-LW-1) \quad A_{VAI} = A_{EQ2} + A_{LWS}$$

$$(6a-N3) \quad A_{C3} = \begin{cases} A_{C4} - V_{C3} C_{619} - A_{BQ4} & \text{FOR } A_{C4} > 0 \\ -V_{C3} C_{619} - A_{BQ4} & \text{FOR } A_{C4} \leq 0 \end{cases}$$

$$(6a-N4) \quad E_V = A_{D5} C_{406} + C_{407}$$

$$(6a-N5-n) \quad \text{See Table 15}$$

$$(6a-N8-n) \quad \text{See Table 16}$$

$$(6a-N10) \quad A_{R3} = A_{EQ2} C_{612} + [E_V - (E_G - V_{C1})] C_{613}$$

$$(6a-N11) \quad A_{C1} = A_{D8} - A_{R3} - A_{CQ1}$$

$$(6a-N14) \quad A_{C2} = \begin{cases} A_{EQ4} + A_{C4} - V_{C2} C_{618} & \text{FOR } A_{C4} < 0 \\ A_{EQ4} - V_{C2} C_{618} & \text{FOR } A_{C4} \geq 0 \end{cases}$$

Table 13 Modulated Antiskid Circuit Equation Summary
(Contd)

Equation No.

Equation

$$(6a-Q-1C) \quad A_{Q1} = \begin{cases} C_{604} - C_{605} V_{c2} & \text{FOR } (E_G - V_{c1}) < 0 \\ = 0 & \text{FOR } (E_G - V_{c1}) \geq 0 \\ = 0 & \text{FOR } V_{c2} \geq C_{604}/C_{605} \end{cases}$$

$$(6a-Q4) \quad A_{EQ4} = C_{614} A_{BQ4}$$

$$(6a-R10) \quad A_{D8} = \begin{cases} (E_G - V_{c1}) C_{620} - C_{621} & \text{FOR } (E_G - V_{c1}) > C_{621}/C_{620} \\ = 0 & \text{FOR } (E_G - V_{c1}) \leq C_{621}/C_{620} \end{cases}$$

(6a-VB-n)

See Table 14

$$(6a-VQ4) \quad A_{BQ4} = \begin{cases} (V_{c3} - V_{c2}) C_{622} - C_{623} & \text{FOR } (V_{c3} - V_{c2}) > C_{623}/C_{622} \\ = 0 & \text{FOR } (V_{c3} - V_{c2}) \leq C_{623}/C_{622} \end{cases}$$

Table 14 Pressure Bias Signal Condition Test Equations

Circuit Condition, n	Pressure Bias Signal Test Equation (Equation 6a-VB-n)
1 & 2	$V_B = V_{C2} C_M - C_{464} (E_G - V_{C1}) - C_{465} (V_{C3} + V_{C4}) + C_{463}$
3 & 4	$V_B = V_{C2} C_M - C_{467} (E_G - V_{C1}) - C_{468} (V_{C3} + V_{C4}) + C_{466}$
5 & 6	$V_B = V_{C2} C_M - C_{558} (E_G - V_{C1}) + C_{559}$
7 & 8	$V_B = V_{C2} C_M - C_{560} (E_G - V_{C1}) + C_{561}$
9 & 10	$V_B = V_{C2} C_M - C_{582} (E_G - V_{C1}) - C_{583} (V_{C2} + V_{C4}) + C_{584}$
11 & 12	$V_B = V_{C2} C_M - C_{585} (E_G - V_{C1}) - C_{586} (V_{C2} + V_{C4}) + C_{587}$

Table 15 Summary of Equations for Computing Current A_{05}

Circuit Condition, n	Applicable Equation 6a-N5-n (See Note)
1 & 2	$A_{05} = A_{VAI} C_{606} - A_{C4}$
3 & 4	$A_{05} = A_{VAI} C_{606} C_{404} - C_{405} - A_{C4}$
5 & 6	$A_{05} = A_{VAI} C_{606}$
7 & 8	$A_{05} = A_{VAI} C_{606} C_{404} - C_{405}$
9 & 10	$A_{05} = A_{VAI} C_{606} - A_{C4}$
11 & 12	$A_{05} = A_{VAI} C_{606} C_{404} - C_{405} - A_{C4}$
Note: For all circuit conditions if $A_{05} < 0$, set $A_{05} = 0$	

Table 16 Capacitor C4 Current Mode Test Equations

Circuit Condition, n	Applicable Equation (6a-N8-n)
1	$A_{C4} = -(E_G - V_{C1})C_{476} - (V_{C3} + V_{C4})C_{477} - C_{478}$
2	$A_{C4} = V_{C2}C_{480} - (E_G - V_{C1})C_{479} - (V_{C3} + V_{C4})C_{481} - C_{482}$
3	$A_{C4} = -(E_G - V_{C1})C_{469} - (V_{C3} + V_{C4})C_{470} - C_{471}$
4	$A_{C4} = V_{C2}C_{473} - (E_G - V_{C1})C_{472} - (V_{C3} + V_{C4})C_{474} - C_{475}$
5-P	$+A_{C4} = -(E_G - V_{C1})C_{548} - (V_{C3} + V_{C4})C_{537} + C_{549} \text{ AND}$
5-N	$-A_{C4} = (E_G - V_{C1})C_{550} + (V_{C2} + V_{C4})C_{539} - C_{551}$
6-P	$+A_{C4} = V_{C2}C_{552} - (E_G - V_{C1})C_{553} - (V_{C3} + V_{C4})C_{537} - C_{554} \text{ AND}$
6-N	$-A_{C4} = -V_{C2}C_{555} + (E_G - V_{C1})C_{556} + (V_{C2} + V_{C4})C_{539} - C_{557}$
7-P	$+A_{C4} = -(E_G - V_{C1})C_{536} - (V_{C3} + V_{C4})C_{537} + C_{538} \text{ AND}$
7-N	$-A_{C4} = (E_G - V_{C1})C_{540} + (V_{C2} + V_{C4})C_{539} - C_{541}$
8-P	$+A_{C4} = V_{C2}C_{542} - (E_G - V_{C1})C_{543} - (V_{C3} + V_{C4})C_{537} - C_{544} \text{ AND}$
8-N	$-A_{C4} = -V_{C2}C_{545} + (E_G - V_{C1})C_{546} + (V_{C2} + V_{C4})C_{539} - C_{547}$
9	$A_{C4} = -(E_G - V_{C1})C_{589} - (V_{C2} + V_{C4})C_{588} + C_{590}$
10	$A_{C4} = V_{C2}C_{592} - (E_G - V_{C1})C_{593} - (V_{C2} + V_{C4})C_{591} + C_{594}$
11	$A_{C4} = -(E_G - V_{C1})C_{596} - (V_{C2} + V_{C4})C_{595} + C_{597}$
12	$A_{C4} = V_{C2}C_{599} - (E_G - V_{C1})C_{600} - (V_{C2} + V_{C4})C_{598} + C_{601}$

Table 17 Valve Amplifier Operating Mode Test Equations

Circuit Condition, n	Applicable Equation (6a-Q2-n) (See Note)
1	$AEQ2 = -(E_G - V_{C1}) C456 - (V_{C3} + V_{C4}) C457 + C458$
2	$AEQ2 = V_{C2} C461 - (E_G - V_{C1}) C459 - (V_{C3} + V_{C4}) C460 + C462$
3	$AEQ2 = -(E_G - V_{C1}) C446 - (V_{C3} + V_{C4}) C447 + C448$
4	$AEQ2 = V_{C2} C450 - (E_G - V_{C1}) C449 - (V_{C3} + V_{C4}) C451 + C452$
5	$AEQ2 = -(E_G - V_{C1}) C531 + C532$
6	$AEQ2 = V_{C2} C533 - (E_G - V_{C1}) C534 - C535$
7	$AEQ2 = -(E_G - V_{C1}) C526 + C527$
8	$AEQ2 = V_{C2} C528 - (E_G - V_{C1}) C529 - C530$
9	$AEQ2 = -(E_G - V_{C1}) C565 - (V_{C2} + V_{C4}) C566 + C567$
10	$AEQ2 = V_{C2} C568 - (E_G - V_{C1}) C569 - (V_{C2} + V_{C4}) C570 - C571$
11	$AEQ2 = -(E_G - V_{C1}) C575 - (V_{C2} + V_{C4}) C576 + C577$
12	$AEQ2 = V_{C2} C578 - (E_G - V_{C1}) C579 - (V_{C2} + V_{C4}) C580 - C581$
Note: For all Circuit Conditions if $AEQ2 < 0$, SET $AEQ2 = 0$	

Table 18 Modulated Antiskid Circuit Conditions

Circuit Condition	Capacitor C4 Current Mode (See Note 1)	Valve Amplifier Operating Mode (See Note 2)	Pressure Bias Signal Condition (See Note 3)
1	$Ac4 > 0$	$A_{EQ2} \leq C607$	$V_B \leq 0$
2	$Ac4 > 0$	$A_{EQ2} \leq C607$	$V_B > 0$
3	$Ac4 > 0$	$A_{EQ2} > C607$	$V_B \leq 0$
4	$Ac4 > 0$	$A_{EQ2} > C607$	$V_B > 0$
5	$Ac4 = 0$	$A_{EQ2} \leq C607$	$V_B \leq 0$
6	$Ac4 = 0$	$A_{EQ2} \leq C607$	$V_B > 0$
7	$Ac4 = 0$	$A_{EQ2} > C607$	$V_B \leq 0$
8	$Ac4 = 0$	$A_{EQ2} > C607$	$V_B > 0$
9	$Ac4 < 0$	$A_{EQ2} \leq C607$	$V_B \leq 0$
10	$Ac4 < 0$	$A_{EQ2} \leq C607$	$V_B > 0$
11	$Ac4 < 0$	$A_{EQ2} > C607$	$V_B \leq 0$
12	$Ac4 < 0$	$A_{EQ2} > C607$	$V_B > 0$

Notes:

1. Capacitor C4 is charging for $Ac4 > 0$, static for $Ac4 = 0$ and discharging for $Ac4 < 0$.
2. The valve amplifier is amplifying for $A_{EQ2} > C607$ and is cutoff for $A_{EQ2} \leq C607$.
3. A pressure bias signal exists for $V_B > 0$ and does not exist for $V_B \leq 0$.

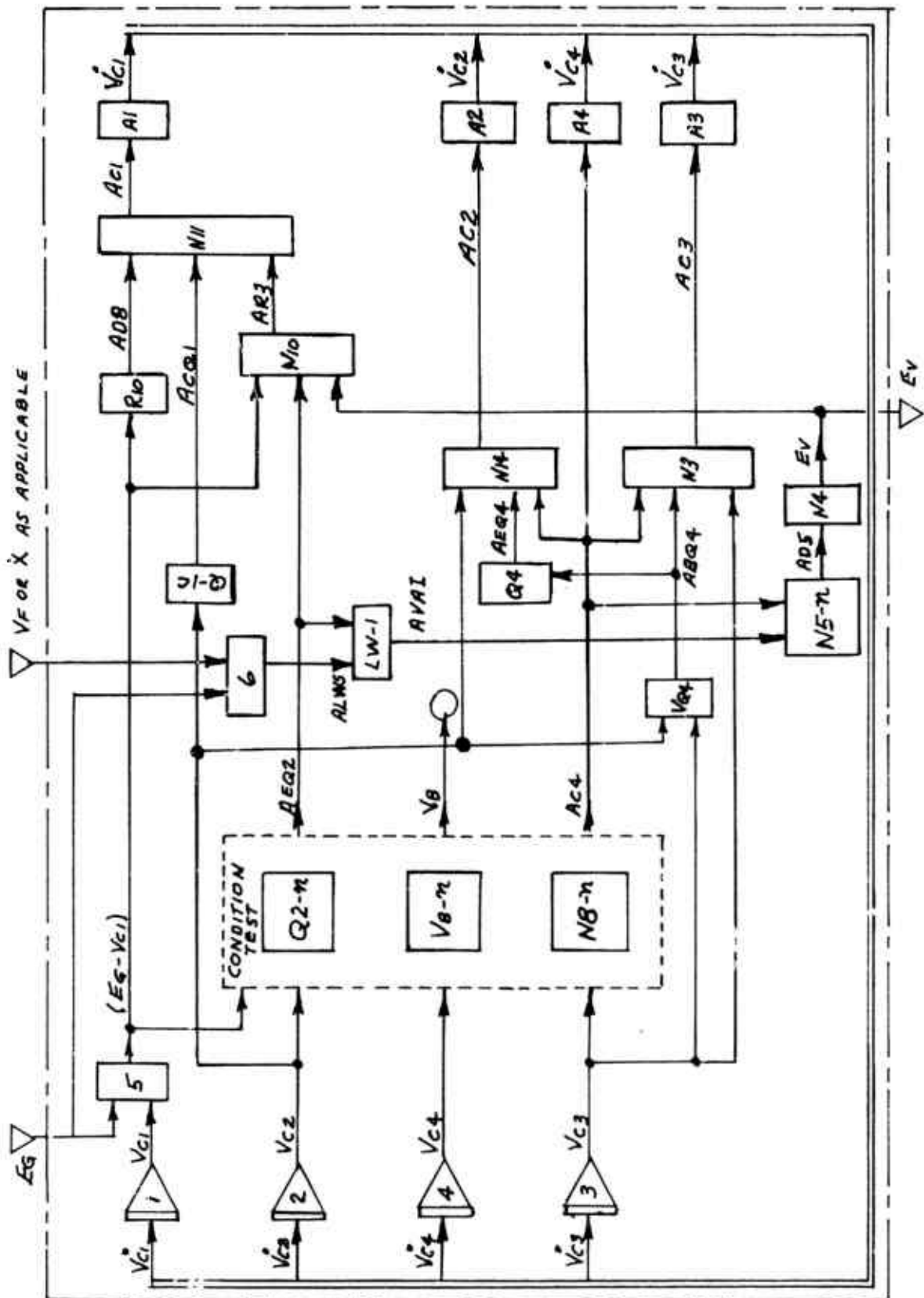


Figure 51 Modulated Antiskid Circuit Equation Flow Diagram

Table 19 Modulated Control System Parameters

Symbol	Type	Value	Units	Description (See Note)
A_{BQ4}	V		Amps	Transistor Q4 Base Current
A_{C1}	V		Amps	Current thru Capacitor C1
A_{C2}	V		Amps	Current thru Capacitor C2
A_{C3}	V		Amps	Current thru Capacitor C3
A_{C4}	V		Amps	Current thru Capacitor C4
A_{CQ1}	V		Amps	Transistor Q1 Collector Current
A_{D5}	V		Amps	Current thru Diode D5
A_{D8}	V		Amps	Current thru Diode D8
A_{EQ2}	V		Amps	Transistor Q2 Emitter Current
A_{EQ4}	V		Amps	Transistor Q4 Emitter Current
A_{R3}	V		Amps	Current thru Resistor R3
E_G	V(I)		Volts	Input Signal from Wheel Speed Sensor
V_B	V		Volts	Circuit Condition Determination Voltage
V_{C1}	V		Volts	Voltage Across Capacitor C1
V_{C10}	C	0.0	Volts	Voltage across Capacitor C1 at Time Zero
V_{C2}	V		Volts	Voltage across Capacitor C2
V_{C20}	C	0.0	Volts	Voltage across Capacitor C2 at Time Zero
V_{C3}	V		Volts	Voltage across Capacitor C3
V_{C30}	C	0.0	Volts	Voltage across Capacitor C3 at Time Zero
V_{C4}	V		Volts	Voltage across Capacitor C4
V_{C40}	C	0.0	Volts	Voltage across Capacitor C4 at Time Zero
E_V	V(O)		Volts	Antiskid Valve Voltage
A_{LWS}	V		Amps	Locked Wheel Skid Signal
V_F	V(I)		In/Sec	Flywheel Velocity
C_M	C	0.23	Dimless	VC2 Voltage Coefficient EQU VB-n

Note: All equation numbers in Description are preceded by 6a. For example, EQU VB-n means equations number 6a-VB-n.

Table 19 (Contd)

Symbol	Type	Value	Units	Description (See Note page 167)
C404	c	2476.0	Dimls	ACQ3 Coeff. EQU N7, N5-3-4, N5-7-8, N5-11-12
C405	c	0.106	Amps	Const EQU N7, N5-3-4, N5-78, N5-11-12
C406	c	66.0	Ohms	AD5 Coefficient EQU N4
C407	c	1.51	Volts	Const. EQU N4
C446	c	1.825×10^{-6}	Mhos	(EG-VC1) Coefficient EQU Q2-3
C447	c	0.144×10^{-8}	Mhos	(VC3 + VC4) Coefficient EQU Q2-3
C448	c	0.312×10^{-6}	Amps	Const EQU Q2-3
C449	c	1.86×10^{-6}	Mhos	(EG-VC1) Coefficient EQU Q2-4
C450	c	0.474×10^{-6}	Mhos	VC2 Coefficient EQU Q2-4
C451	c	0.1465×10^{-8}	Mhos	(VC3 + VC4) Coefficient EQU Q2-4
C452	c	-1.73×10^{-6}	Amps	Const EQU Q2-4
C456	c	34.0×10^{-6}	Mhos	(EG-VC1) Coefficient EQU Q2-1
C457	c	0.0269×10^{-6}	Mhos	(VC3 + VC4) Coefficient EQU Q2-1
C458	c	-17.1×10^{-6}	Amps	Const EQU QL-1
C459	c	52.0×10^{-6}	Mhos	(EG-VC1) Coefficient EQU Q2-2
C460	c	0.0411×10^{-6}	Mhos	(VC3 + VC4) Coefficient EQU Q2-2
C461	c	13.25×10^{-6}	Mhos	VC2 Coefficient EQU Q2-2
C462	c	-83.4×10^{-6}	Amps	Const EQU Q2-2
C463	c	-1.151	Volts	Const EQU VB1-2
C464	c	0.312	Dimls	(EG-VC1) Coefficient EQU VB1-2
C465	c	247.0×10^{-6}	Dimls	(VC3 + VC4) Coefficient EQU VB1-2
C466	c	-0.911	Volts	Const EQU VB3-4
C467	c	0.01675	Dimls	(EG-VC1) Coefficient EQU VB3-4
C468	c	13.2×10^{-6}	Dimls	(VC3 + VC4) Coefficient EQU VB 3-4
C469	c	975.0×10^{-6}	Mhos	(EG-VC1) Coefficient EQU N8-3
C470	c	110.0×10^{-6}	Mhos	(VC3 + VC4) Coefficient EQU N8-3

Table 19 (Contd)

Symbol	Type	Value	Units	Description (See Note page 167)
C471	C	388.0×10^{-6}	Amps	Const EQU N8-3
C472	C	995.0×10^{-6}	Mhos	(EG-VC1) Coefficient EQU N8-4
C473	C	254.0×10^{-6}	Mhos	VC2 Coefficient EQU N8-4
C474	C	110.0×10^{-6}	Mhos	(VC3 + VC4) Coefficient EQU N8-4
C475	C	1480.0×10^{-6}	Amps	Const EQU N8-4
C476	C	7.35×10^{-6}	Mhos	(EG-VC1) Coefficient EQU N8-1
C477	C	1090×10^{-6}	Mhos	(VC3 + VC4) Coefficient EQU N8-1
C478	C	-227.5×10^{-6}	Amps	Const EQU N8-1
C479	C	11.25	Mhos	(EG-VC1) Coefficient EQU N8-2
C480	C	2.87×10^{-6}	Mhos	VC2 Coefficient EQU N8-2
C481	C	109.0×10^{-6}	Mhos	(VC3 + VC4) Coefficient EQU N8-2
C482	C	-212.5×10^{-6}	Amps	Const EQU N8-2
C526	C	1.82×10^{-6}	Mhos	(EG-VC1) Coefficient EQU Q2-7
C527	C	0.471×10^{-6}	Amps	Const EQU Q2-7
C528	C	0.472×10^{-6}	Mhos	VC2 Coefficient EQU Q2-8
C529	C	1.85×10^{-6}	Mhos	(EG-VC1) Coefficient EQU Q2-8
C530	C	1.565×10^{-6}	Amps	Const. EQU Q2-8
C531	C	34.0×10^{-6}	Mhos	(EG-VC1) Coefficient EQU Q2-5
C532	C	-17.5×10^{-6}	Amps	Const. EQU Q2-5
C533	C	1325×10^{-6}	Mhos	VC2 Coefficient EQU Q2-6
C534	C	57.6×10^{-6}	Mhos	(EG-VC1) Coefficient EQU Q2-6
C535	C	83.5×10^{-6}	Amps	Const. EQU Q2-6
C536	C	981.0×10^{-6}	Mhos	(EG-VC1) Coefficient EQU N8-7P
C537	C	110.0×10^{-6}	Mhos	(VC3 + VC4) Coefficient EQU N8-5P, N8-6P, N8-7P, N8-8P
C538	C	-304.0×10^{-6}	Amps	Const EQU N8-7P

Table 19 (Contd)

Symbol	Type	Value	Units	Description (See Note page 167)
C 539	C	0.50	Mhos	(VC2 + VC4) Coefficient EQU N8-5N, N8-6N, N8-7N, N8-8N
C 540	C	4.46	Mhos	(EG-VC1) Coefficient EQU N8-7N
C 541	C	-0.78	Amps	Const. EQU N8-7N
C 542	C	255.0×10^{-6}	Mhos	VC2 Coefficient EQU N8-8P
C 543	C	0.0010	Mhos	(EG-VC1) Coefficient EQU N8-8P
C 544	C	0.0014	Amps	Const. EQU N8-8P
C 545	C	1.155	Mhos	VC2 Coefficient EQU N8-8N
C 546	C	4.53	Mhos	(EG-VC1) Coefficient EQU N8-8N
C 547	C	-5.78	Amps	Const. EQU N8-8N
C 548	C	7.42×10^{-6}	Mhos	(EG-VC1) Coefficient EQU N8-5P
C 549	C	228.0×10^{-6}	Amps	Const. EQU N8-5P
C 550	C	0.0337	Mhos	(EG-VC1) Coefficient EQU N8-5N
C 551	C	1.615	Amps	Const. EQU N8-5N
C 552	C	2.19×10^{-6}	Mhos	VC2 Coefficient EQU N8-6P
C 553	C	12.55×10^{-6}	Mhos	(EG-VC1) Coefficient EQU N8-6P
C 554	C	-274.0×10^{-6}	Amps	Const. EQU N8-6P
C 555	C	0.01315	Mhos	VC2 Coefficient EQU N8-6N
C 556	C	0.0572	Mhos	(EG-VC1) Coefficient EQU N8-6N
C 557	C	1.578	Amps	Const. EQU N8-6N
C 558	C	0.312	Dimls	(EG-VC1) Coefficient EQU VB5-6
C 559	C	-1.1545	Volts	Const EQU VB 5-6
C 560	C	0.0167	Dimls	(EG-VC1) Coefficient EQU VB7-8
C 561	C	-0.98968	Volts	Const EQU VB7-8
C 565	C	34.3×10^{-6}	Mhos	(EG-VC1) Coefficient EQU Q2-9
C 566	C	3.54×10^{-6}	Mhos	(VC2 + VC4) Coefficient EQU Q2-9

Table 19 (Contd)

Symbol	Type	Value	Units	Description (See Note page 167)
C567	C	-17.7×10^{-6}	Amps	Const. EQU Q2-9
C568	C	13.41×10^{-6}	Mhos	VC2 Coefficient EQU Q2-10
C569	C	52.6×10^{-6}	Mhos	(EG-VC1) Coefficient EQU Q2-10
C570	C	5.42×10^{-6}	Mhos	(VC2 + VC4) Coefficient EQU Q2-10
C571	C	66.5×10^{-6}	Amps	Const. EQU Q2-10
C575	C	22.7×10^{-6}	Mhos	(EG-VC1) Coefficient EQU Q2-11
C576	C	2.345×10^{-6}	Mhos	(VC2 + VC4) Coefficient EQU Q2-11
C577	C	-3.2×10^{-6}	Amps	Const. EQU Q2-11
C578	C	7.54×10^{-6}	Mhos	VC2 Coefficient EQU Q2-12
C579	C	29.55×10^{-6}	Mhos	(EG-VC1) Coefficient EQU Q2-12
C580	C	3.05×10^{-6}	Mhos	(VC2 + VC4) Coefficient EQU Q2-12
C581	C	36.8×10^{-6}	Amps	Const. EQU Q2-12
C582	C	0.314	Dimls	(EG-VC1) Coefficient EQU VB9-10
C583	C	0.0324	Dimls	(VC2 + VC4) Coefficient EQU VB9-10
C584	C	-1.156	Volts	Const EQU VB9-10
C585	C	0.208	Dimls	(EG-VC1) Coefficient EQU VB11-12
C586	C	0.0215	Dimls	(VC2 + VC4) Coefficient EQU VB11-12
C587	C	-1.0233	Volts	Const. EQU VB11-12
C588	C	0.0144	Mhos	(VC2 + VC4) Coefficient EQU N8-9
C589	C	0.001	Mhos	(EG-VC1) Coefficient EQU N8-9
C590	C	0.0468	Amps	Const. EQU N8-9
C591	C	0.0145	Mhos	(VC2 + VC4) Coefficient EQU N8-10
C592	C	380.0×10^{-6}	Mhos	VC2 Coefficient EQU N8-10
C593	C	0.00149	Mhos	(EG-VC1) Coefficient EQU N8-10
C594	C	0.0455	Amps	Const. EQU N8-10
C595	C	0.179	Mhos	(VC + VC4) Coefficient EQU N8-11

Table 19 (Contd)

Symbol	Type	Value	Units	Description (See Note page 167)
C596	C	1.59	Mhos	(EG-VC1) Coefficient EQU N8-11
C597	C	-0.28	Amps	Const. EQU N8-11
C598	C	0.228	Mhos	(VC2 + VC4) Coefficient EQU N8-12
C599	C	0.529	Mhos	VC2 Coefficient EQU N8-12
C600	C	2.07	Mhos	(EG-VC1) Coefficient EQU N8-12
C601	C	-2.64	Amps	Const. EQU N8-12
C604	C	16.1×10^{-6}	Amps	Const. EQU Q-1C
C605	C	7.25×10^{-6}	Mhos	VC2 Coefficient EQU Q-1C
C606	C	29.2	Dimensionless	Q3 Collector - Q2 Emitter Current Ratio
C607	C	1.46×10^{-6}	Amps	AEQ2 Comparison Constant
C608	C	0.027×10^{-6}	Volts/Amp Sec	Reciprocal of Capacitance C1
C609	C	3.03×10^{-6}	Volt/Amp Sec	Reciprocal of Capacitance C2
C610	C	0.631×10^{-6}	Volt/Amp Sec	Reciprocal of Capacitance C3
C611	C	0.222×10^{-6}	Volt/Amp Sec	Reciprocal of Capacitance C4
C612	C	0.901	Dimensionless	AEQ2 Coefficient EQU N10
C613	C	5.19×10^{-4}	Mhos	Emitter-Base Current Ratio - Q4
C614	C	20.0	Dimensionless	Locked Wheel Arming Speed
C615	C	352.0	In/Sec	Locked Wheel Signal Detection Speed
C616	C	0.92	Volts	Locked Wheel Signal Current
C617	C	2.76×10^{-4}	Amps	VC2 Coefficient EQU N14
C618	C	2.7×10^{-4}	Mhos	VC3 Coefficient EQU N3
C619	C	7.71×10^{-5}	Mhos	(EG-VC1) Coefficient EQU R10
C620	C	0.501	Mhos	Const. EQU R10
C621	C	600.0×10^{-6}	Amps	(VC3-VC2) Coefficient EQU VQ4
C622	C	846.0×10^{-6}	Mhos	Const. EQU VQ4
C623	C	593.0×10^{-6}	Amps	

6b. ON-OFF ANTISKID CONTROL CIRCUIT

Most aircraft on-off type antiskid systems operate according to the functional block diagram shown on Figure 52. The various functional elements may be electrical, mechanical or a combination of electrical and mechanical devices. If during braking the brake torque applied to the wheel exceeds the amount which can be reacted by friction at the tire-ground interface, the antiskid system operates to prevent tire skids as follows. A wheel speed signal is provided to a deceleration detection element where the wheel's deceleration rate is computed and compared to a threshold value which is provided by a skid detection threshold element. The deceleration detector produces a skid signal whenever the wheel's deceleration rate exceeds the threshold value. The wheel speed signal is also supplied to a wheel speed reference element and a wheel speed comparison element. The wheel speed reference element is a "memory" device which produces a "comparison index." The "comparison index" is the wheel's initial unbraked speed minus an adjustment to account for the aircraft's deceleration. The wheel speed comparison element compares wheel speed to the "comparison index" and produces a skid signal whenever the wheel speed is less than the "comparison index." The deceleration detection element initiates a skid signal and the wheel speed comparison element maintains the skid signal until the wheel has regained most of its initial speed. The skid signals from both the deceleration detection element and the wheel speed comparison element are transmitted to a valve control element which acts to control the antiskid valve such that the brake is released when a skid signal exists and the brake is applied when a skid signal does not exist.

An electrical system of the form shown on Figure 53 or a mechanical device as shown on Figure 55 are the most common means used for implementing the on-off antiskid system function.

Electrical On-Off Antiskid System

Figure 53 is a schematic diagram of the Goodyear electrical on-off antiskid control circuit as used on the Lockheed F104 and General Dynamics B-58 aircraft. This circuit accomplishes on-off antiskid control according to the preceding functional description as follows: The wheel speed

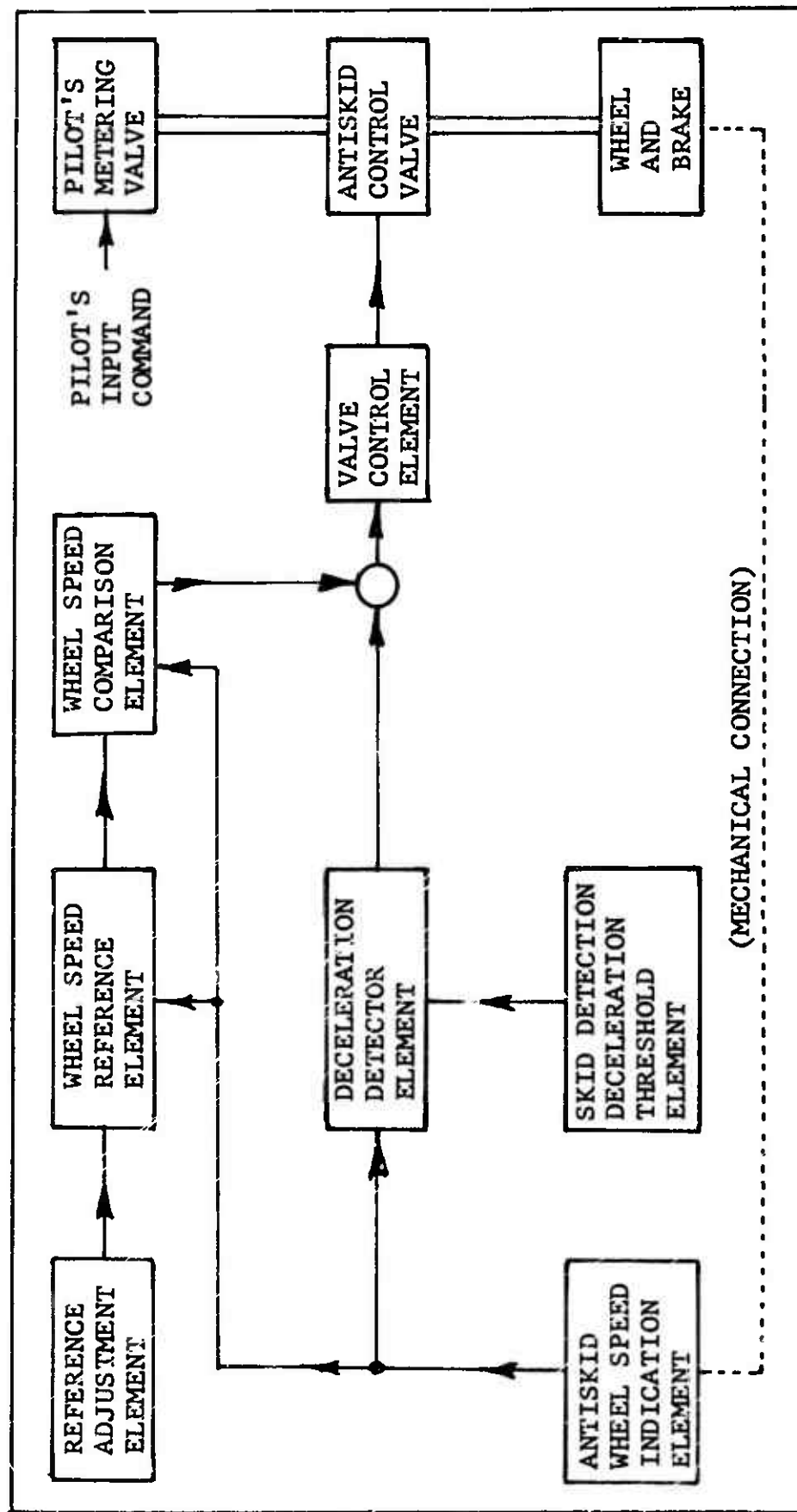
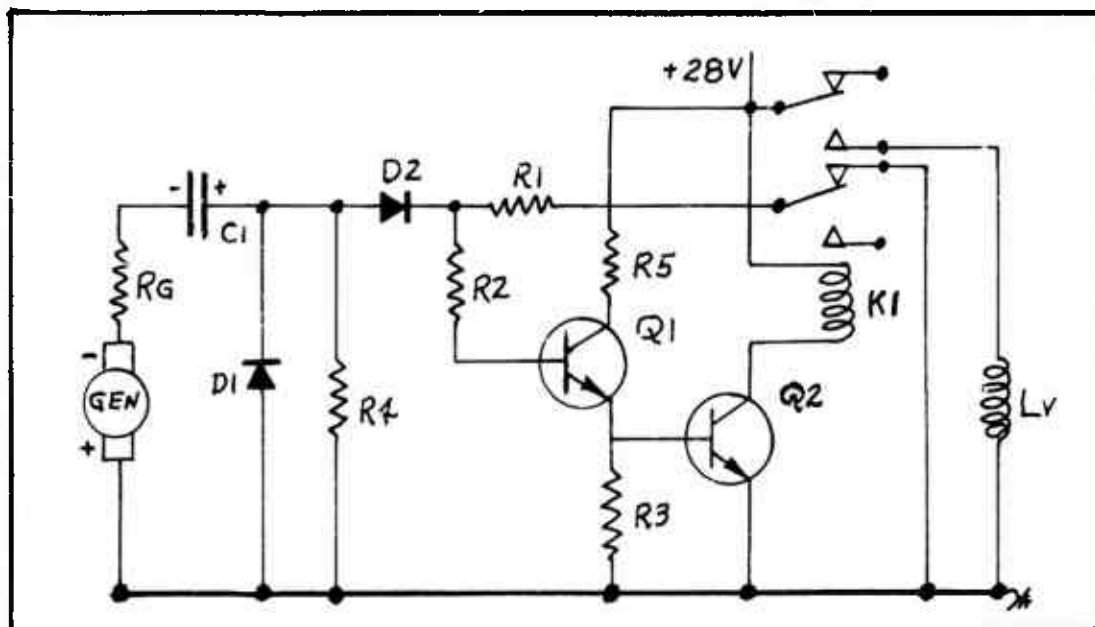
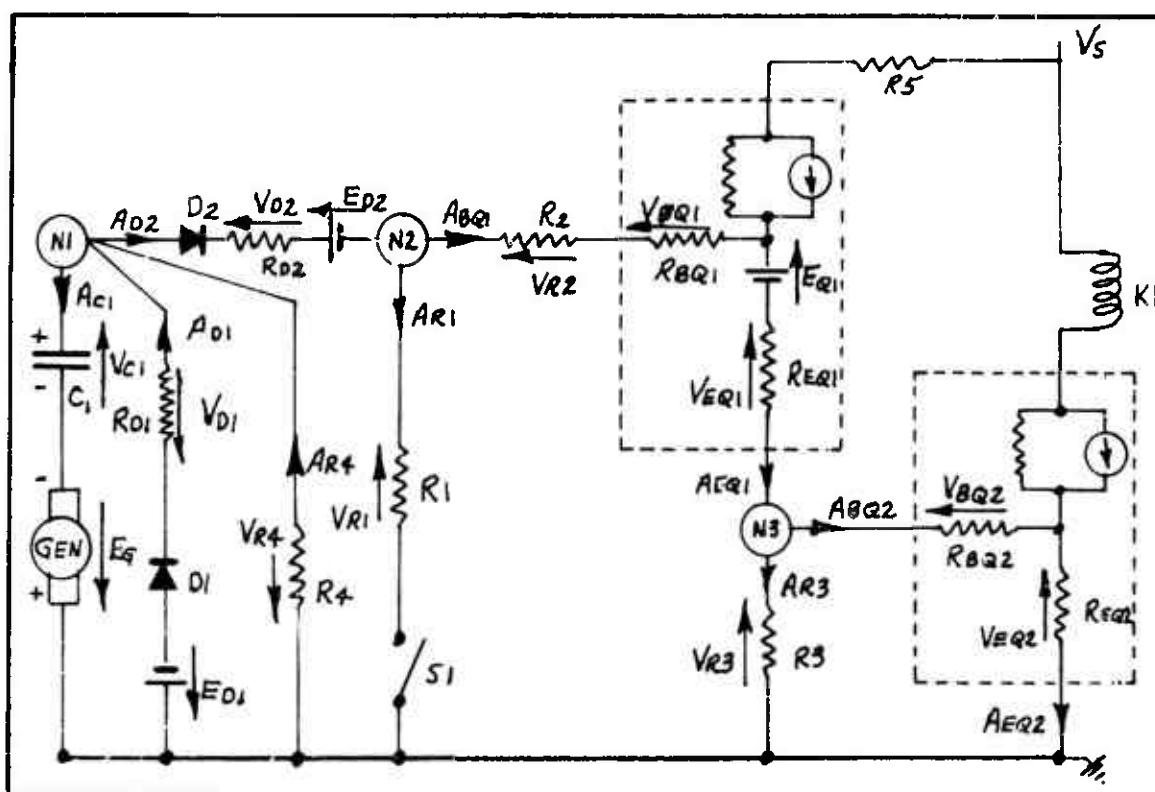


Figure 52 On-Off Antiskid Control Functional Block Diagram



(A) Schematic Diagram



(B) Mathematical Identification Showing Transistors and Diodes in Terms of their Equivalent Circuits

Figure 53 Electrical On-Off Antiskid Control Circuit

indication element, a wheel driven D. C. tachometer generator (GEN), supplies an input voltage EG which is proportional to wheel speed. EG charges capacitor C1 through R5, Diode D1 and Resistance RG during wheel spin-up. Capacitor C1 is both the deceleration detector and the wheel speed reference element. For normal wheel deceleration rates, with no incipient skidding, the generator voltage decreases relatively slowly and a small current will flow from the positive side of C1 through R5 and through D2 and R1, (GEN) and RG to the negative side of C1. This current discharges C1 and causes its voltage to closely follow EG. The amplifier comprised of R2, Q1, R3, R4 and Q2 acts as the skid detection deceleration threshold element, the wheel speed comparison element, and, in conjunction with relay K1, the valve control element. When an incipient skid occurs, the generator voltage decreases rapidly. R5 and R1 limit the discharge current flow into C1 so that the voltage at the positive side of C1 increases. The value of the voltage at the positive side of C1 is proportional to wheel deceleration rate. The amplifier characteristics are set so that when the voltage at the positive side of C1 is a value V_{SOR} or greater, enough current flows into the base of Q1 to cause Q2 to conduct sufficiently for relay K1 to actuate. When relay K1 actuates the supply voltage is applied to the antiskid valve coil LV. The voltage across the antiskid valve coil, EV, is equal to the supply voltage. Actuation of relay K1 also causes R1 to be disconnected from ground so that the resistance in the discharge path of C1 is increased to aid its action as a wheel speed reference. Voltage V_{SOR} is the skid detection threshold. More modern versions of this circuit utilize transistors to perform the function of relay K1; however, their operation is the same. Resistor R5 is the speed reference adjustment element.

A-1 Electrical On-Off Mathematical Description

The mathematical description of the electrical circuit's operation is developed from Figure 53(b) which is the schematic from Figure 53(a) with the transistors and diodes shown in terms of their equivalent circuits and the appropriate currents and voltages identified.

The voltage across capacitor C1 is defined by:

$$(6b-1-1) \quad V_{C1} = \int \dot{V}_{C1} dt$$

$$\text{where (6b-1-A1)} \quad \dot{V}_{C1} = A_{C1} C_{705} \quad (C_{705} = 1/C_1)$$

Current A_{C1} is established by summing currents at node (N1) as:

$$(6b-1-N1) \quad A_{C1} = A_{D1} + A_{R4} - A_{D2}$$

Using Ohm's law and summing voltages around the loop of which R_{D1} is a part, current A_{D1} is established as:

$$(6b-1-R1) \quad A_{D1} = (E_G - V_{C1} - E_{D1}) / R_{D1} \quad \text{FOR } (E_G - V_{C1} - E_{D1}) > 0$$

$$= 0 \quad \text{FOR } (E_G - V_{C1} - E_{D1}) \leq 0$$

To combine constants, write equation (6b-1-R1) as:

$$A_{D1} = (E_G - V_{C1}) C_{706} - C_{707} \quad \text{FOR } (E_G - V_{C1}) > \frac{C_{707}}{C_{706}}$$

$$= 0 \quad \text{FOR } (E_G - V_{C1}) \leq \frac{C_{707}}{C_{706}}$$

Noting that because of diode D1, A_{D1} is restricted to positive values only.

In a similar manner, using Ohm's law and summing voltages around the loop containing R_4 , current A_{R4} is established as:

$$(6b-1-V2) \quad A_{R4} = (E_G - V_{C1}) / R_4 \quad \text{OR} \quad A_{R4} = (E_G - V_{C1}) C_{708}$$

Summing currents at node (N2) gives:

$$(6b-1-N2) \quad A_{D2} = A_{BQ1} + A_{R1}$$

By Ohm's law the voltage across RD2 is

$$(6b-1-V3) \quad V_{D2} = A_{D2} R_{D2}$$

For the case where no skid signal exists and relay K1 is not actuated, R1 is connected to ground and a current AR1 may flow. Using Ohm's law and by summing voltages around the loop R1, D2, C1 and (GEN), AR1 is established as:

$$(6b-1-V4) \quad A_{R1} = (V_{C1} - E_G - E_{D2} - V_{D2}) / R_1$$

By substituting equation (N2) into equation (N1) current AC1 is established as:

$$(6b-1-N1)' \quad A_{C1} = A_{D1} + A_{R4} - A_{BQ1} - A_{R1}$$

Since the variables EG and VC1 are always used in the form of their difference, define the difference as:

$$(6b-1-3) \quad (E_G - V_{C1}) = E_G - V_{C1}$$

By substituting (6b-1-V3) and (6b-1-N2) into (6b-1-V4),

$$(6v-1-V4)' \quad A_{R1} = \frac{(V_{C1} - E_G - E_{D2})}{R_{D2} + R_1} - \frac{A_{BQ1} R_{D2}}{R_{D2} - R_1}$$

By summing currents at node (N3), current AEQ1 is

$$(6b-1-N3) \quad A_{EQ1} = A_{BQ2} + A_{R3}$$

By summing voltages around the loop containing R3 and the base and emitter of Q2,

$$(6b-1-V5) \quad 0 = V_{R3} - V_{BQ2} - V_{EQ2}$$

Note: For Q2 the base-emitted junction potential has been omitted to reduce mathematical complexity. This is justified because whether or not Q2 is conducting has negligible effect on current A_{C1} .

By substituting (6b-1-N3) along with the Ohm's law expressions $A_{BQ2} = V_{BQ2}/R_{BQ2}$ AND $A_{EQ2} = V_{EQ2}/R_{EQ2}$ and the transistor characteristic $A_{EQ2} = (h_{FE2} + 1) A_{BQ2}$ into (6b-1-V5) and solving for A_{BQ2} ,

$$(6b-1-V5)' \quad A_{BQ2} = \frac{A_{EQ1} R_3}{R_{BQ2} + R_3 + R_{EQ2} (h_{FE2} + 1)}$$

By substituting (6b-1-V5)' and (6b-1-N3) into the Ohm's law expression $V_{R3} = A_{R3} R_3$

$$(6b-1-2) \quad V_{R3} = R_3 A_{EQ1} \left[1 - \frac{R_3}{R_{BQ2} + R_3 + R_{EQ2} (h_{FE2} + 1)} \right]$$

By summing voltages around the loop $R_3, R_{EQ1}, E_{Q1}, R_{BQ1}, R_2, R_{D2}, C_1$ and (GEN)

$$(6b-1-V6) \quad 0 = V_{R3} + V_{EQ1} + E_{Q1} + V_{BQ1} + V_{R2} + E_{D2} + V_{D2} - V_{C1} + E_G$$

By substituting (6b-1-2) and (6b-1-V4) along with the Ohm's law expressions $V_{EQ1} = A_{EQ1} R_{EQ1}$, $V_{BQ1} = A_{BQ1} R_{BQ1}$ and $V_{R2} = A_{BQ1} R_2$ and the transistor characteristic $A_{EQ1} = (h_{FE1} + 1) A_{BQ1}$ into (6b-1-V6) and solving for A_{BQ1} :

$$(6b-1-V6)' \quad A_{BQ1} = (V_{C1} - E_G) \frac{C_{701} - C_{702}}{C_{701}} \text{ FOR } (V_{C1} - E_G) > \frac{C_{702}}{C_{701}}$$

$$= 0 \quad \text{FOR } (V_{C1} - E_G) \leq \frac{C_{702}}{C_{701}}$$

For the case where relay K1 is actuated and R1 is disconnected from ground the same substitution is made except that $V_{D2} = A_{BQ1} R_{D2}$ is used in place of equation (6b-1-V4). For the actual circuit components used on the aircraft, the resulting equation has coefficients that are negligibly different from (6b-1-V6)'; therefore, equation

(6b-1-V6)' will be used for both cases.

The value of ABQ_1 which causes relay K1 to be actuated is defined as, C700, the skid detection threshold current. From this definition and equation (6b-1-V4)'

$$\begin{aligned} (6b-1-V4-1) \quad ARI &= (V_G - E_S) C_{709} - C_{710} - ABQ_1 C_{711} \\ &\quad \text{FOR } ABQ_1 < C_{700} \\ &= 0 \quad \text{FOR } ABQ_1 \geq C_{700} \end{aligned}$$

When relay K1 is not actuated $EV = 0$, when relay K1 is actuated $EV = VS$; therefore,

$$\begin{aligned} (6b-1-EV) \quad EV &= 0 \quad \text{FOR } ABQ_1 < C_{700} \\ &= VS \quad \text{FOR } ABQ_1 \geq C_{700} \end{aligned}$$

The equation flow diagram for the electrical on-off control circuit is shown on Figure 54.

B-1 Electrical On-Off Parameter Evaluation

Table 20 lists the parameters and their values as applicable for the General Dynamics B-58 control circuit. (The same circuit is used on the Lockheed F-104.)

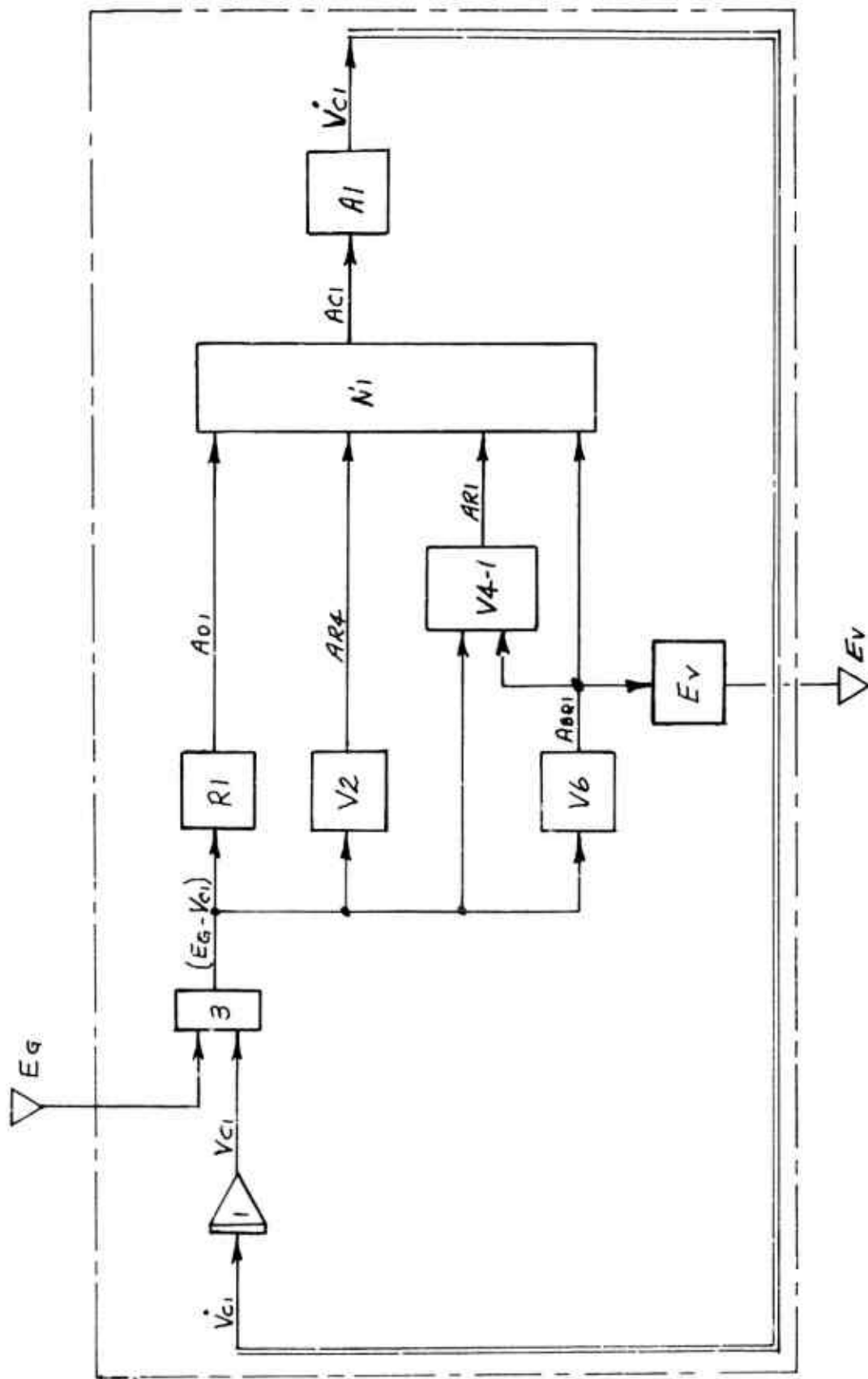


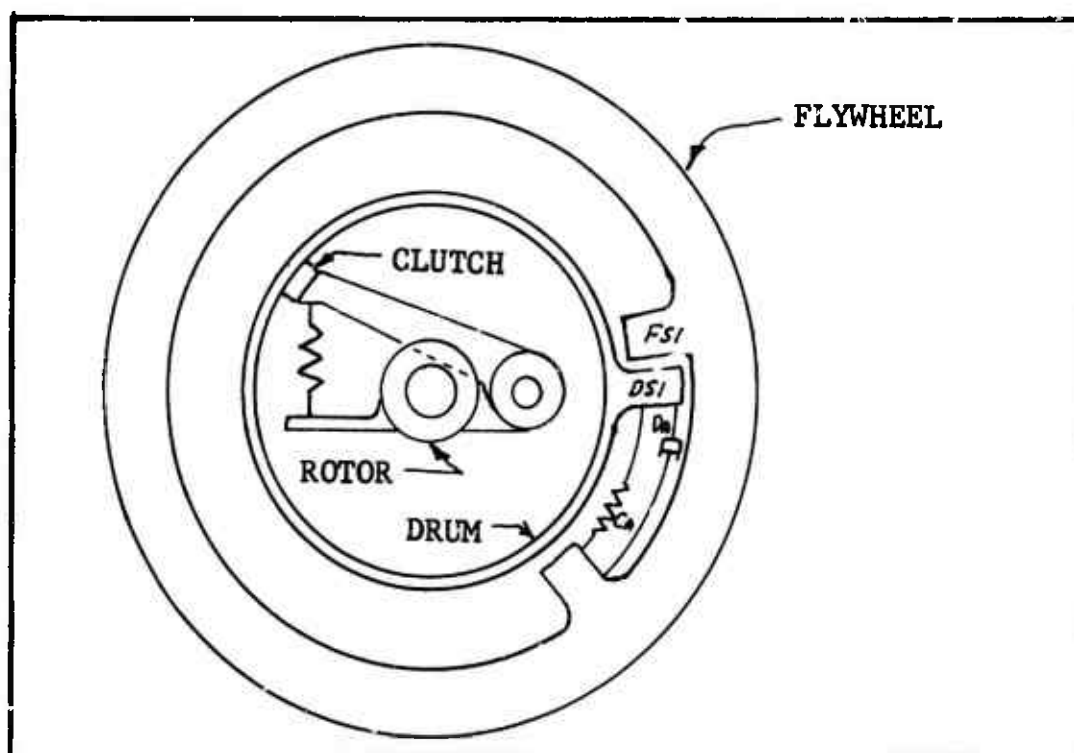
Figure 54 Electrical On-Off Circuit Equation Flow Diagram

Table 20 On-Off Control System Parameters

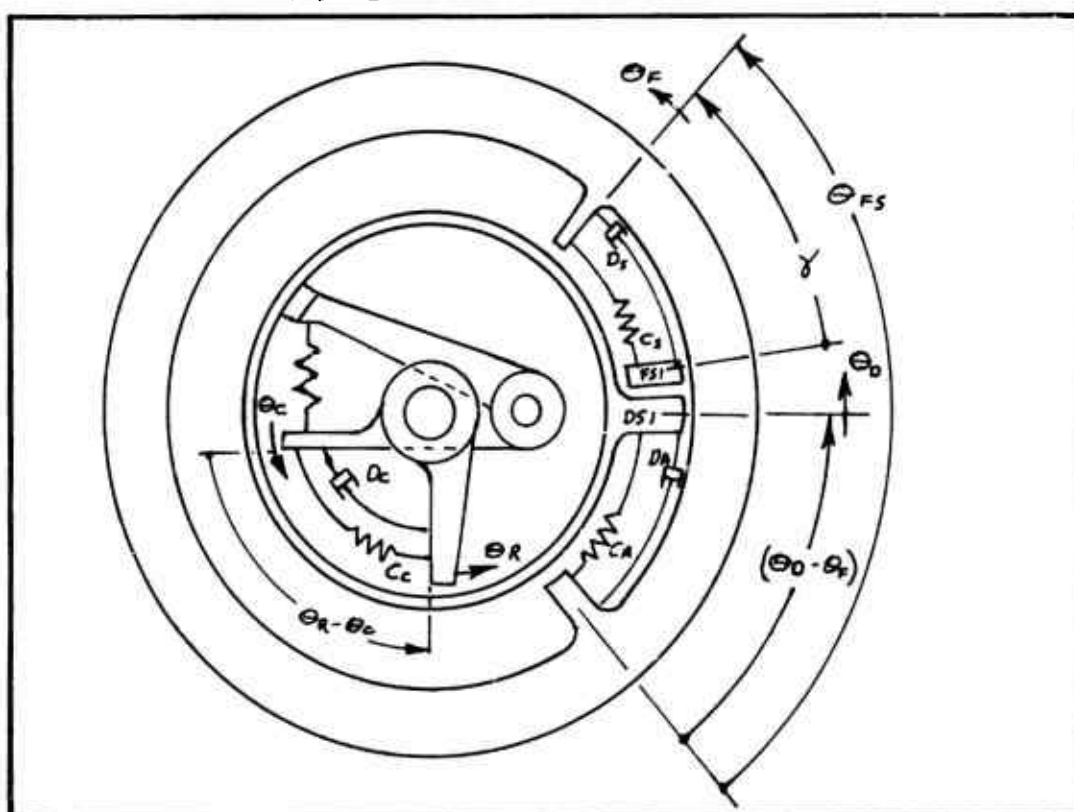
Symbol	Type	Value	Units	Description
ABQ1	V		Amps	Transistor Q1 Base Current
AC1	V		Amps	Current thru Capacitor C1
AD1	V		Amps	Current thru Diode D1
AR1	V		Amps	Current thru Resistor R1
AR4	V		Amps	Current thru Resistor R4
EG	V(I)		Volts	Input Signal from Wheel Speed Sensor
EV	V(O)		Volts	Antiskid Valve Voltage
VC1	V		Volts	Voltage across Capacitor C1
VC10	C	0.0	Volts	Voltage across Capacitor C1 at Time Zero
VC1	V		Volts/Sec	Capacitor C1 Voltage Change Rate
V5	C	28.0	Volts	Supply Voltage
C700	C	17.5×10^{-6}	Amps	Skid Detection Threshold Current
C701	C	6.6×10^{-6}	Mhos	(EG - VC1) Coefficient EQU V6
C702	C	0.86×10^{-6}	Amps	Constant EQU V6
C705	C	0.04×10^{-6}	Volt/Amp Sec	Reciprocal of Capacitance C1
C706	C	1667.0×10^{-6}	Mhos	(EG - VC1) Coefficient EQU K1
C707	C	1000.0×10^{-6}	Amps	Constant EQU R1
C708	C	19.35×10^{-6}	Mhos	(EG-VC1) Coefficient EQU V2
C709	C	161×10^{-6}	Mhos	(EG-VC1) Coefficient EQU V4-1
C710	C	96.8×10^{-6}	Amps	Constant EQU V4-1
C711	C	0.0768	Dimls	ABQ1 Coefficient EQU V4-1

Mechanical On-Off Antiskid Device

Figure 55 is a schematic drawing showing the operating principles of a commonly used mechanical on-off antiskid device of which the Hydroaire Hytrol Mk I and Dunlop Maxaret units are typical examples. The device operates as follows. The rotor (the wheel speed indication element) is connected to the aircraft wheel by some positive means such as a direct connection or gear train, etc., so that the rotor's angular velocity is a constant ratio of aircraft wheel speed. During spinup the motion of the rotor is transmitted through the clutch to the drum. The clutch is configured such that it is self-energizing for rotation in the direction of wheel rotation associated with forward airplane motion, shown here as counterclockwise. Stop (DSL) on the drum engages stop (FSL) on the flywheel, thereby transmitting torque to cause the velocity of the flywheel to be the same as the drum. The flywheel and the drum are connected by spring (CA) and damper (DA). As the aircraft wheel and rotor decelerate, a clockwise torque is transmitted through the clutch to the drum and from the drum through spring (CA) and damper (DA) to the flywheel. The amount of this torque is proportional to the product of the rotor's deceleration rate and the flywheel's inertia. The torque compresses spring (CA) so that the flywheel moves counterclockwise with respect to the drum. For steady airplane wheel deceleration the amount of relative motion between the flywheel and drum is proportional to the deceleration rate. A suitable mechanism (usually a set of electrical contact points or a cam device) connected between the flywheel and drum causes a valve to be actuated so that brake pressure is relieved whenever a pre-established amount of relative motion occurs. The clutch is also configured so that when the torque from the rotor to the drum is clockwise, the torque capacity is limited to some slightly greater amount than that required to initiate brake release. If the rotor experiences greater deceleration than that required to initiate brake release, the clutch slips and allows the drum and flywheel to overrun the rotor. The flywheel's inertia reacted by the drag of the clutch maintains a torque on spring (CA) so that the relative motion between the drum and flywheel (skid signal) is sustained until the flywheel's kinetic energy is dissipated or until the rotor has regained sufficient speed to eliminate clutch slippage. For this device the flywheel's inertia causing displacement of spring (CA) and damper (DA) is the



A. Functional Schematic



B. Mathematical Representation

Figure 55 Mechanical On-Off Antiskid Device

deceleration detector element, the clutch's overrunning drag torque on the drum is the reference adjustment element, the clutch is the wheel speed comparison element and the rotational kinetic energy of the flywheel is the wheel speed reference element.

A-2 Mechanical On-Off Mathematical Description

The mathematical description of the mechanical on-off anti-skid device is developed by referring to figure 55(b) which defines the applicable parameters and shows flywheel stop (FS1) represented by a spring-damper system. Also, a spring-damper system is added between the rotor and clutch carrier to represent the small motion which actually occurs during clutch operation.

At flywheel stop (FS1) there is a torque, T_S , which is exerted on the flywheel by the drum, if drum stop (DS1) is in contact with FS1. If the mass of FS1 is considered small in comparison to the stop spring (CS) and stop damper (DS) then, setting the sum of torques on FS1 at zero:

$$(6b-2-1) \quad T_S = C_S (\gamma_0 - \gamma) - D_S \dot{\gamma}$$

Where $C_S(\gamma_0 - \gamma)$ is the stop spring torque, $(-D_S \dot{\gamma})$ is the stop damper torque and γ_0 is the free length of spring CS.

Since T_S results from a contact force, it cannot be less than zero; therefore, if $\gamma + (\theta_D - \theta_F)$ is less than θ_{FS} then $T_S = 0$. Rewriting equation (1) solving for $\dot{\gamma}$ gives:

$$(6b-2-2) \quad \dot{\gamma} = (C_S (\gamma_0 - \gamma) - T_S) / D_S$$

γ is then established by:

$$(6b-2-3) \quad \gamma = \int \dot{\gamma} dt$$

γ as computed from (6b-2-2) and (6b-2-3) is compared to $\theta_{FS} - (\theta_D - \theta_F)$ to establish T_S . If T_S is other than zero, it is computed from (6b-2-1) using $\gamma = \theta_{FS} - (\theta_D - \theta_F)$ AND $\dot{\gamma} = -(\dot{\theta}_D - \dot{\theta}_F)$.

Substituting the above expressions for γ and $\dot{\gamma}$ into (6b-2-1) gives:

$$(6b-2-1-1) \quad T_S = C_S \left[\gamma_0 - \theta_{FS} + (\theta_D - \theta_F) \right] + D_S (\dot{\theta}_D - \dot{\theta}_F) \\ \text{FOR } [\gamma + (\theta_D - \theta_F) - \theta_{FS}] \geq 0 \\ = 0 \quad \text{FOR } [\gamma + (\theta_D - \theta_F) - \theta_{FS}] < 0$$

Summing torques on the flywheel gives:

$$(6b-2-4) \quad \ddot{\theta}_F = [T_S + C_A(\theta_D - \theta_F) + D_A(\dot{\theta}_D - \dot{\theta}_F)] / W_{FW}$$

Summing torques on the drum gives:

$$(6b-2-5) \quad \ddot{\theta}_D = [-T_S - C_A(\theta_D - \theta_F) - D_A(\dot{\theta}_D - \dot{\theta}_F) + T_C] / W_D$$

Where T_C is the clutch torque.

Subtracting (6b-2-4) from (6b-2-5) results in:

$$(6b-2-6) \quad (\ddot{\theta}_D - \ddot{\theta}_F) = \left(\frac{1}{W_D} + \frac{1}{W_{FW}} \right) [-T_S - C_A(\theta_D - \theta_F) - D_A(\dot{\theta}_D - \dot{\theta}_F)] + T_C / W_D$$

By integrating (6b-2-6) twice, $(\dot{\theta}_D - \dot{\theta}_F)$ and $(\theta_D - \theta_F)$ are established as

$$(6b-2-7) \quad (\dot{\theta}_D - \dot{\theta}_F) = \int (\ddot{\theta}_D - \ddot{\theta}_F) dt$$

$$(6b-2-8) \quad (\theta_D - \theta_F) = \int (\dot{\theta}_D - \dot{\theta}_F) dt$$

Substituting values for $(\theta_D - \theta_F)$ and $(\dot{\theta}_D - \dot{\theta}_F)$ computed from (6b-2-7) and (6b-2-8) into equation (6b-2-4) and integrating once establishes $\dot{\theta}_F$ as follows:

$$(6b-2-9) \quad \dot{\theta}_F = \int \ddot{\theta}_F dt$$

Combining the results from (6b-2-7) and (6b-2-9) establishes $\dot{\theta}_D$ as:

$$(6b-2-10) \quad \dot{\theta}_D = (\dot{\theta}_D - \dot{\theta}_F) + \dot{\theta}_F$$

The clutch will now be examined.

The torque exerted on the clutch carrier by the rotor, T_c , is defined by:

$$(6b-2-11) \quad T_c = C_c (\theta_R - \theta_c) + D_c (\dot{\theta}_R - \dot{\theta}_c)$$

If, as for the flywheel stop, it is assumed that the clutch carrier inertia is negligibly small, the torque between the clutch and the drum equals the torque between the rotor and the clutch carrier. In this case equation (6b-2-11) may be solved for $(\dot{\theta}_R - \dot{\theta}_c)$ and by integrating once $(\theta_R - \theta_c)$ is obtained:

$$(6b-2-12) \quad (\theta_R - \theta_c) = \int (\dot{\theta}_R - \dot{\theta}_c) dt$$

Where $(\dot{\theta}_R - \dot{\theta}_c)$ is obtained from the following version of (6b-2-11)

$$(6b-2-11-1) \quad (\dot{\theta}_R - \dot{\theta}_c) = [T_c - C_c (\theta_R - \theta_c)] / D_c$$

It follows that:

$$(6b-2-13) \quad \dot{\theta}_c = \dot{\theta}_R - (\dot{\theta}_R - \dot{\theta}_c)$$

If the clutch is configured so that there is no slipping for counterclockwise torque on the drum, $\dot{\theta}_c$ must equal $\dot{\theta}_o$ and any difference between $\dot{\theta}_R$ and $\dot{\theta}_o$ must be relative velocity between the clutch carrier and the rotor (i.e. $\dot{\theta}_R - \dot{\theta}_c$). If $\dot{\theta}_o$ is substituted for $\dot{\theta}_c$ in equation (6b-2-11) the resulting equation can be used to compute the torque required to force $\dot{\theta}_c$ to be equal to $\dot{\theta}_o$. Therefore, making this substitution,

$$(6b-2-11-2) \quad T_c = C_c (\theta_R - \theta_c) + D_c (\dot{\theta}_R - \dot{\theta}_o)$$

Equation (6b-2-11-2) adequately describes the component of clutch torque due to relative velocity; however, the component due to relative displacement is not satisfactorily described because the torque direction is independent of relative position. To compute the clutch torque for all conditions, equation (6b-2-11-2) will be modified and

a procedure for establishing the clutch condition will be defined. The clutch condition is established by the torque direction. The torque direction is determined by examining the direction the drum is attempting to move relative to the clutch. The direction of the drum's attempted movement relative to the clutch is established by comparing the drum velocity, $\dot{\Theta}_D$, to the velocity, $\dot{\Theta}_{CH}$, of a hypothetical or "index" clutch. The "index" clutch will be permitted to have slight slippage on the drum for counterclockwise torque so that there is a preceivable circumstance to indicate torque direction. To describe the "index" clutch motion relative to the rotor, equation (6b-2-11-1) is modified by substituting $\dot{\Theta}_{CH}$ and $\dot{\Theta}_{CH}$ for $\dot{\Theta}_C$ and $\dot{\Theta}_C$ as follows:

$$(6b-2-11-1M) \quad (\dot{\Theta}_R - \dot{\Theta}_{CH}) = [T_C - C_C(\Theta_R - \Theta_{CH})] / D_C$$

The clutch torque, T_C , is defined by equation (6b-2-11-3). $(\Theta_R - \Theta_{CH})$ is obtained from equation (6b-2-12) and $\dot{\Theta}_{CH}$ is then established from equation (6b-2-13), noting that in each case Θ_{CH} and $\dot{\Theta}_{CH}$ are used in place of Θ_C and $\dot{\Theta}_C$. The clutch condition is established by the difference between $\dot{\Theta}_{CH}$ and $\dot{\Theta}_D$ as follows:

- | | |
|--|---|
| For $(\dot{\Theta}_{CH} - \dot{\Theta}_D) > 0$ | Clutch torque is positive on the drum (clutch attempting to have positive velocity with respect to drum) |
| For $(\dot{\Theta}_{CH} - \dot{\Theta}_D) = 0$ | Clutch is not attempting to move relative to drum |
| For $(\dot{\Theta}_{CH} - \dot{\Theta}_D) < 0$ | Clutch torque is negative on the drum. (Drum is attempting to have positive velocity with respect to clutch). |

Now that the clutch condition is defined, equation (6b-2-11-2) is modified so that the torque direction is established by the direction of relative velocity between the drum and the clutch as follows:

$$\begin{aligned}
 (6b-2-11-3) \quad T_c &= G_c \langle \dot{\theta}_{CH} - \dot{\theta}_D \rangle \left| C_c (\theta_R - \theta_{CH}) \right| + D_c (\dot{\theta}_R - \dot{\theta}_D) \\
 &\quad \text{FOR } \left\{ G_c \langle \dot{\theta}_{CH} - \dot{\theta}_D \rangle \left| C_c (\theta_R - \theta_{CH}) \right| + D_c (\dot{\theta}_R - \dot{\theta}_D) \right\} > C750 \\
 &= C750 \\
 &\quad \text{FOR } \left\{ G_c \langle \dot{\theta}_{CH} - \dot{\theta}_D \rangle \left| C_c (\theta_R - \theta_{CH}) \right| + D_c (\dot{\theta}_R - \dot{\theta}_D) \right\} \leq C750
 \end{aligned}$$

The function $G_c \langle \dot{\theta}_{CH} - \dot{\theta}_D \rangle$ is defined as follows:

$$\begin{aligned}
 (6b-2-14) \quad G_c \langle \dot{\theta}_{CH} - \dot{\theta}_D \rangle &= +1.0 \quad \text{FOR } (\dot{\theta}_{CH} - \dot{\theta}_D) > 0 \\
 &= 0 \quad \text{FOR } (\dot{\theta}_{CH} - \dot{\theta}_D) = 0 \\
 &= -1.0 \quad \text{FOR } (\dot{\theta}_{CH} - \dot{\theta}_D) < 0
 \end{aligned}$$

The constant C750 is the value of clutch drag torque when the drum is overrunning the clutch.

The amount of relative motion between the flywheel and drum ($\theta_D - \theta_F$) is the skid signal. To be compatible with the electrical antiskid control circuits, assume the skid signal is produced by a set of electrical contact points; therefore,

$$\begin{aligned}
 (6b-2-15) \quad E_v &= V_s \quad \text{FOR } (\theta_D - \theta_F) \geq C751 \\
 &= 0 \quad \text{FOR } (\theta_D - \theta_F) < C751
 \end{aligned}$$

C751 is the skid detection threshold value of $(\theta_D - \theta_F)$. Also, for compatibility with the other parts of the analysis, let the input be derived from the wheel speed sensor output, EG, as follows:

$$(6b-2-16) \quad \dot{\theta}_R = C752 \ E_G$$

C752 is the conversion coefficient. The equation flow diagram for the mechanical on-off antiskid device is shown on Figure 56.

B-2 Mechanical On-Off Parameter Evaluation

No parameter evaluation has been accomplished for the mechanical on-off device because it is not applicable to the aircraft being considered.

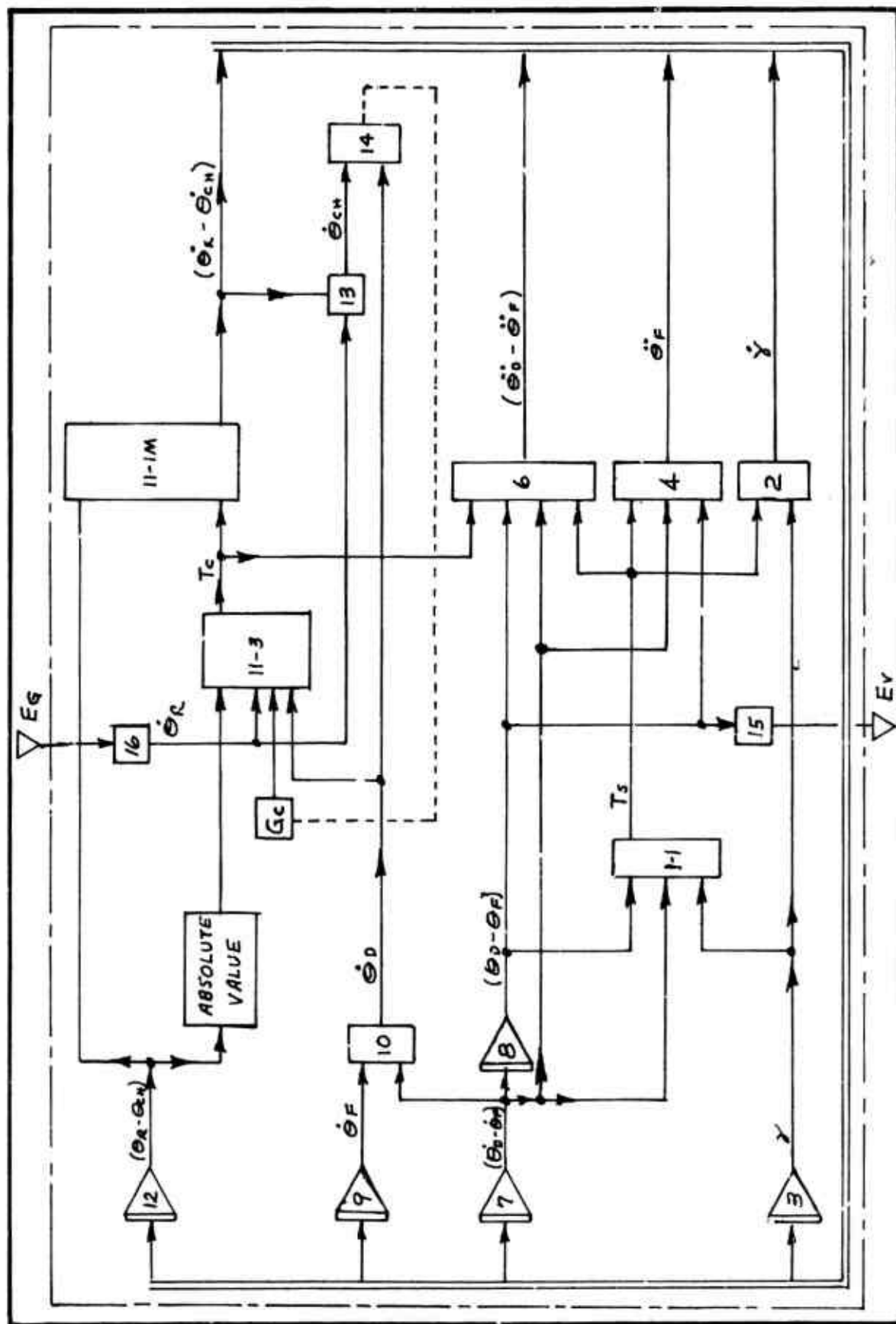


Figure 56 Mechanical On-Off Device Equation Flow Diagram

7. ANTISKID CONTROL VALVE

Aircraft antiskid control systems typically utilize a two-stage electrically operated pressure control valve. The first stage contains an electro-mechanical device such as a torque motor, solenoid or linear force motor which positions a hydraulic flow regulating element (flapper, nozzle or spool) such that a control pressure is produced. The control pressure is a function of the valve input pressure and the electrical input signal. The first stage control pressure is applied to the second stage hydraulic flow controlling power spool. The second stage spool is positioned by forces produced by the control pressure and valve output pressure in a manner such that output pressure is controlled in proportion to the first stage control pressure.

A. Mathematical Description

First Stage

The function of the first stage can be described mathematically by considering the control pressure producing element to be a single degree of freedom damped spring mass system as shown in Figure 57 acted upon by a force, F_{cv} , proportional to the electrical input signal.

$$(7.1) \quad F_{cv} = C_{scv} E_v$$

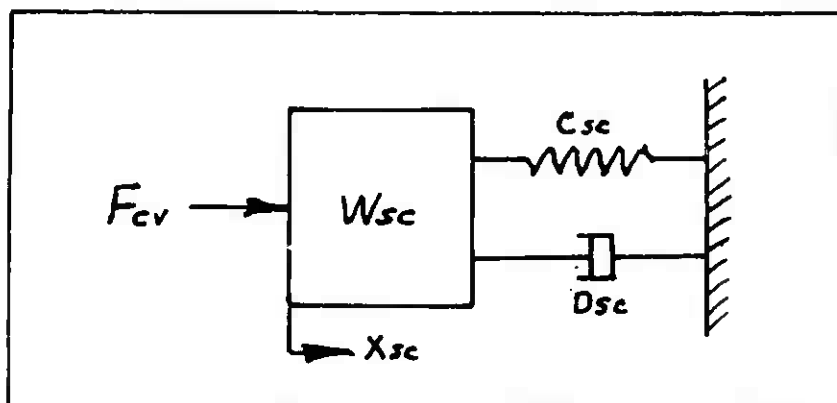


Figure 57 First Stage Spring Mass System

The first stage control pressure, P_{sc} , is defined as a function of the mass position, X_{sc} , according to Figure 58. X_{sc} is established by equation (7.2) which results from summing forces on the first stage mass, W_{sc} .

$$(7.2) \quad \ddot{X}_{sc} = \frac{F_{cv}}{W_{sc}} - \frac{C_{sc}}{W_{sc}} \dot{X}_{sc} - \frac{D_{sc}}{W_{sc}} X_{sc}$$

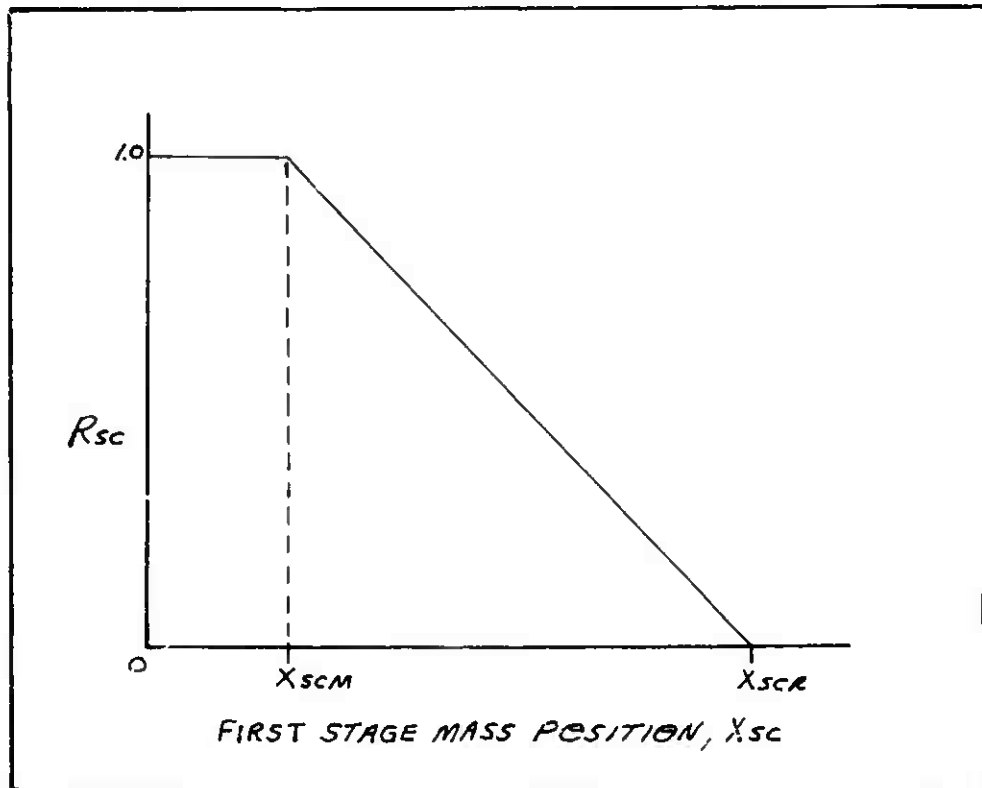


Figure 58 First Stage Control Pressure - Mass Position Relationship

$$(7.3) \quad P_{sc} = R_{sc} (P_{mv} - P_{cvr}) + P_{cvr}$$

$$(7.4) \quad R_{sc} = \begin{cases} 1.0 & \text{IF } X_{sc} \leq X_{scm} \\ \frac{X_{scr} - X_{sc}}{X_{scr} - X_{scm}} & \text{IF } X_{scm} < X_{sc} < X_{scr} \\ 0 & \text{IF } X_{sc} \geq X_{scr} \end{cases}$$

Second Stage

The physical arrangement of the F-111 antiskid valve second stage is shown schematically in Figure 59 . Most other antiskid valves have the same operating principles.

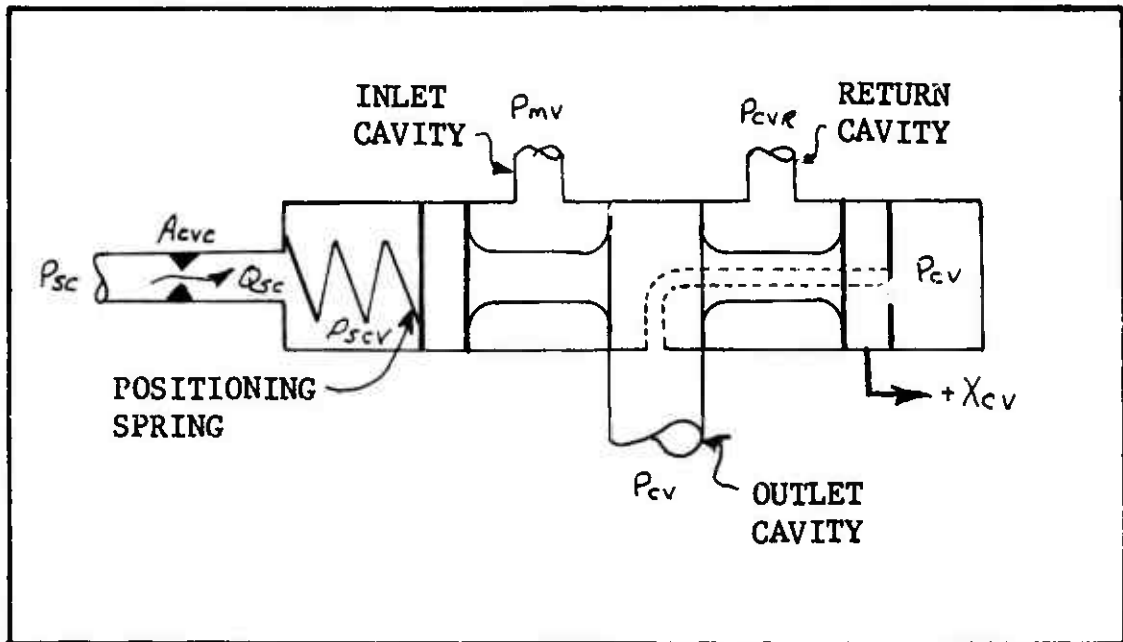


Figure 59 Antiskid Valve Second Stage

As described in the hydraulic system, the metering valve output pressure, P_{mv} , is supplied to the antiskid control valve second stage inlet. When the second stage spool is displaced in a positive direction a fluid passage opens permitting hydraulic flow from the metering valve to the antiskid valve outlet cavity. When the second stage spool is displaced in a negative direction a fluid passage opens permitting hydraulic flow from the outlet cavity to return. Therefore, the second stage spool position defines the hydraulic flow areas. The second stage spool position, X_{cv} , is established by equation (7.5) which results from summing forces on the spool mass, W_{cv} . Figure 60 shows a schematic of a single degree of freedom damped spring mass system representing the antiskid valve second stage spool. Springs, C_{cvs} , and dampers, D_{cvs} , are stops representing the spool's longitudinal restraint caused by its contact with the valve body. The forces acting on the spool are the positioning spring force, damping force, stop spring and damper forces and forces due to outlet cavity pressure, P_{cv} , and control chamber pressure, P_{scv} .

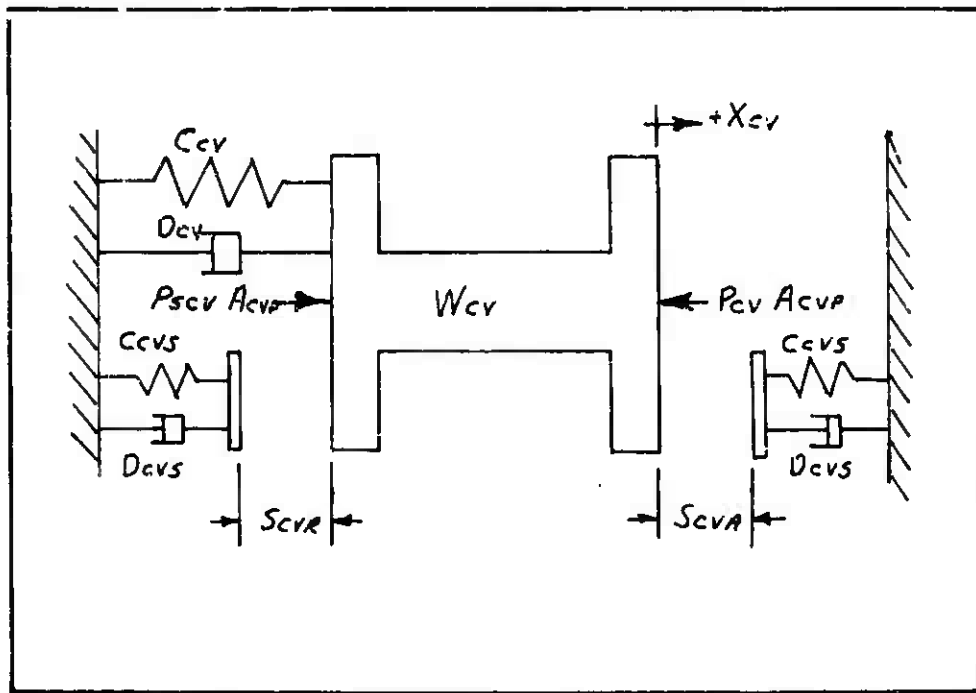


Figure 60 Second Stage Spool Forces

Summing forces on the second stage spool give:

$$(7.5) \quad \ddot{X}_{cv} = (P_{scv} - P_{cv}) \frac{A_{cvp}}{W_{cv}} + (X_{cvp} - X_{cv}) \frac{C_{cv}}{W_{cv}} - \frac{D_{cv}}{W_{cv}} (\dot{X}_{cv}) \\ + \frac{F_{cvSR}}{W_{cv}} + \frac{F_{cvSA}}{W_{cv}}$$

$$(7.6) \quad F_{cvSR} = \begin{cases} 0 & \text{IF } X_{cv} \geq -S_{cvR} \\ \frac{C_{cv}}{W_{cv}} (-X_{cv} - S_{cvR}) - \frac{D_{cvs}}{W_{cv}} (\dot{X}_{cv}) & \text{IF } X_{cv} < -S_{cvR} \end{cases}$$

$$(7.7) \quad F_{cvSA} = \begin{cases} 0 & \text{IF } X_{cv} \leq S_{cvA} \\ \frac{C_{cvs}}{W_{cv}} (-X_{cv} + S_{cvA}) - \frac{D_{cvs}}{W_{cv}} (\dot{X}_{cv}) & \text{IF } X_{cv} > S_{cvA} \end{cases}$$

The control chamber pressure, P_{scv} , is established by the first stage control pressure causing flow through the control orifice, A_{cvc} , and the control chamber volume, V_{scv} , as follows:

$$(7.8) \quad \dot{P}_{scv} = \frac{\beta_{cv}}{V_{scv}} (Q_{sc} - A_{cvp} \dot{X}_{cv})$$

$$(7.9) \quad V_{scv} = A_{cvp} (X_{cvc} + X_{cv})$$

$$(7.10) \quad Q_{sc} = A_{cvc} \phi(P_{sc}, P_{scv})$$

The function $\phi(x, y)$ is defined in the hydraulic system.

The hydraulic system contains provision for leakage flow associated with first stage pressure regulation and spool fit. Since these small flows have no effect on the valve's performance in the case under consideration, they have not been computed. Therefore, the following equations apply:

$$(7.11) \quad Q_{cv1} = 0$$

$$(7.12) \quad Q_{cv2} = 0$$

$$(7.13) \quad Q_{cv3} = 0$$

The Control Valve Equation Flow Diagram is shown on Figure 61

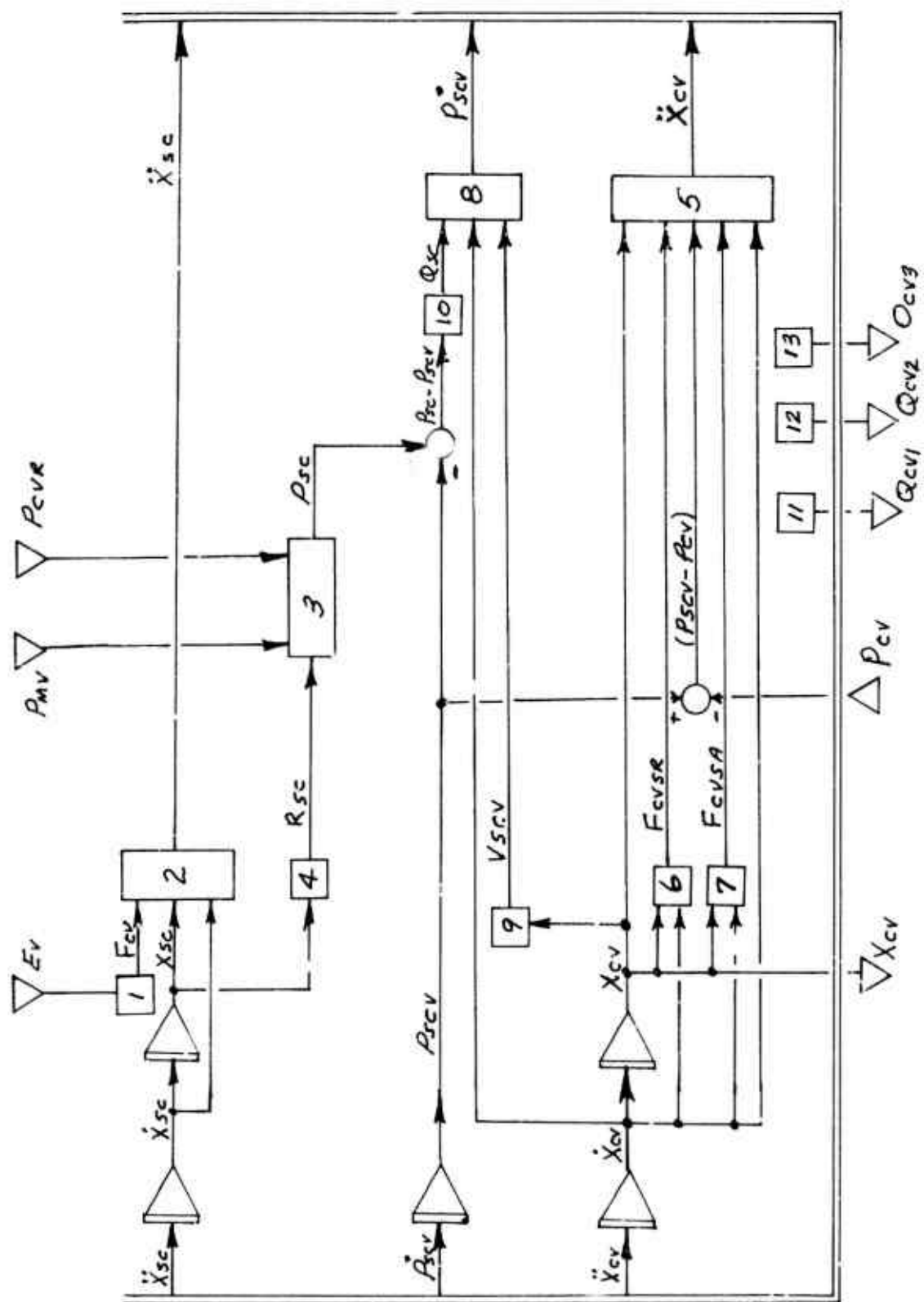


Figure 61 Antiskid Control Valve Equation Flow Diagram

B. Parameter Evaluation

The parameters used for describing the antiskid valve's first stage behavior are established from measured frequency response performance characteristics along with some features of its physical construction. Frequency response test results from the F-111 antiskid valve show 25 degrees phase lag at 5 cps. From various experiments it is known that the first stage accounts for most of the phase lag. The F-111 valve's approximate 700 cps undamped natural frequency is quite high compared to a more usual 100 cps value. Since antiskid operation is generally 10 cps or less and since the low frequency phase lag can be accurately described with a lower natural frequency system, an undamped natural frequency of 100 cps will be used to minimize computation difficulty.

Coefficients C_{scv} and C_{sc} are set arbitrarily so that static values of X_{sc} will be compatible with values of X_{scm} and X_{scr} (which are also arbitrarily chosen) and the proper valve voltage - output pressure relationship is achieved. In this example the following values are assigned:

$$\begin{aligned} C_{scv} &= 1.2 \text{ lbf/Volt} \\ C_{sc} &= 1.0 \text{ lbf/INCH} \\ (7.14) \quad X_{scm} &= 3.6 \text{ INCHES} \\ X_{scr} &= 14.4 \text{ INCHES} \end{aligned}$$

For 100 cps (628 RAD/SEC) undamped natural frequency and $C_{sc} = 1.0 \text{ lbf/IN}$, the mass W_{sc} is computed from $(W_n)^2 = C_{sc}/W_{sc}$

$$(7.15) \quad W_{sc} = 2.54 \times 10^{-6} \text{ lbf sec}^2/\text{IN}$$

Using the equations relating natural frequency and phase angle listed in the wheel speed sensor parameter evaluation and assuming the first stage has 20 degrees phase lag at 5 cps, the damping factor is established as 3.63. For the values of W_{sc} and C_{sc} above this damping factor results in:

$$(7.16) \quad D_{sc} = 11.6 \times 10^{-3} \text{ lbf sec/INCH}$$

The area, A_{cvp} , the stop clearances, S_{cva} and S_{cvr} , and the mass of the second stage spool, W_{cv} , are computed from the spool's physical dimensions as shown on the valve drawing.

$$\begin{aligned}
 A_{cvp} &= 0.05 \text{ IN}^2 \\
 W_{cv} &= 41.5 \times 10^{-6} \text{ lbf sec}^2/\text{IN} \\
 (7.17) \quad S_{cva} &= 0.03 \text{ INCH} \\
 S_{cvr} &= 0.03 \text{ INCH}
 \end{aligned}$$

The positioning spring rate, C_{cv} , and spool damping coefficient were established based on the valve's transient response characteristic where it was observed that a 50 cps about .5 critically damped transient pressure oscillation appeared. From this observation

$$\begin{aligned}
 C_{cv} &= 4.0 \text{ lbf/IN} \\
 (7.18) \quad D_{cv} &= 13.0 \times 10^{-3} \text{ lbf sec/IN}
 \end{aligned}$$

The stop spring, C_{cvs} , and damper, D_{cvs} , characteristics are arbitrarily chosen to be as high as possible within computation capability.

$$\begin{aligned}
 C_{cvs} &= 5000 \text{ lbf/IN} \\
 (7.19) \quad D_{cvs} &= 1.5 \text{ lbf sec/IN}
 \end{aligned}$$

The control orifice area, A_{cvc} , and control chamber length, X_{cvc} , are established by the valve's physical dimensions as shown on the valve drawing.

$$\begin{aligned}
 A_{cvc} &= 0.009 \text{ IN}^2 \\
 (7.20) \quad X_{cvc} &= 0.1 \text{ INCH}
 \end{aligned}$$

The control chamber fluid bulk modulus is that of MIL-H-5606 hydraulic fluid as used in the hydraulic system.

The undeflected positioning spring length was computed assuming it produced approximately the same force on the valve spool as 25 PSI pressure differential.

$$(7.21) \quad X_{cvp} = 0.2 \text{ INCH}$$

Table 21 lists the parameters and their values which are applicable to the F-111 and fluid control valve.

Table 21 Antiskid Control Valve Parameters

SYMBOL	TYPE	VALUE	UNITS	DESCRIPTION
A_{cvp}	c	0.05	INCHES^2	Second Stage Spool Area
A_{cvc}	c	0.009	INCHES^2	Control Pressure Chamber Orifice Area
β_{cv}	c	0.24×10^{-6}	lbF/IN^2	Control Chamber Fluid Bulk Modulus
C_{scv}	c	1.2	lbF/VOLT	First Stage Volts-Force Coefficient
C_{sc}	c	1.0	lbF/IN	First Stage Spring Rate
C_{cv}	c	4.0	lbF/IN	Second Stage Positioning Spring Rate
C_{cv5}	c	5000	lbF/IN	Second Stage Stop Spring Rate
D_{cv5}	c	1.5	$\text{lbF sec}/\text{IN}$	Second Stage Stop Damping Coefficient
D_{cv}	c	13.0×10^{-3}	$\text{lbF sec}/\text{IN}$	Second Stage Damping Coefficient
D_{sc}	c	11.6×10^{-3}	$\text{lbF sec}/\text{IN}$	First Stage Damping Coefficient
E_v	V(I)		VOLTS	Antiskid Valve Volts
F_{cv}	V		lbF	First Stage Driving Force
P_{mv}	V(I)		lbF/IN^2	Metering Valve Output Pressure
P_{cva}	V(I)		lbF/IN^2	Antiskid Valve Return Cavity Pressure
P_{sc}	V		lbF/IN^2	First Stage Output Control Pressure
P_{scv}	V		lbF/IN^2	Second Stage Control Chamber Pressure
P_{scv}	V		$\text{lbF}/\text{IN}^2 \text{sec}$	Rate of Change in Control Chamber Pressure
P_{scv0}	c	0.0	$\text{lbF}/\text{IN}^2 \text{sec}$	Control Chamber Pressure Change Rate at Time 0
Q_{cv1}	V(O)	0.0	IN^3/sec	Leakage Flow into Control Valve Inlet Cavity
Q_{cv2}	V(O)	0.0	IN^3/sec	Leakage Flow into Control Valve Inlet Cavity
Q_{cv3}	V(O)	0.0	IN^3/sec	Leakage Flow into Control Valve Return Cavity
Q_{sc}	V		IN^3/sec	Control Chamber Flow Rate
R_{sc}	V		IN^3/sec	First Stage Pressure Regulation Coefficient
S_{cva}	c	0.03	INCH	Second Stage Stop Clearance-Application

Table 21 (Contd)

SYMBOL	TYPE	VALUE	UNITS	DESCRIPTION
S_{cve}	c	0.03	INCH	Second Stage Stop Clearance-Release
P_{cv}	v(I)		lb ft / IN ²	Antiskid Valve Outlet Cavity Pressure
V_{scv}	v		IN ³	Second Stage Control Chamber Volume
W_{sc}	c	2.54×10^{-6}	lb ft sec ² / IN	First Stage Mass
W_{cv}	c	41.5×10^{-6}	lb ft sec ² / IN	Second Stage Spool Mass
X_{sc}	v		INCH	First Stage Mass Displacement
X_{sco}	c	0.0	INCH	First Stage Mass Displacement at Time = 0
\dot{X}_{sc}	v		IN / SEC	First Stage Mass Velocity
\dot{X}_{sco}	c	0.0	IN / SEC	First Stage Mass Velocity at Time = 0
\ddot{X}_{sc}	v		IN / SEC ²	First Stage Mass Acceleration
X_{cv}	v(o)		INCH	Second Stage Spool Displacement
X_{cvo}	c	0.03	INCH	Second Stage Spool Displacement at Time = 0
\dot{X}_{cv}	v		IN / SEC	Second Stage Spool Velocity
\dot{X}_{cvo}	c	0.0	IN / SEC	Second Stage Spool Velocity at Time = 0
\ddot{X}_{cv}	v		IN / SEC ²	Second Stage Spool Acceleration
X_{cvc}	c	0.1	INCH	Second Stage Clearance Length
X_{cvp}	c	0.2	INCH	Second Stage Position for Undelected Position Spring
X_{scm}	c	3.6	INCH	First Stage Mass Position for Zero Regulation
X_{scr}	c	14.4	INCH	First Stage Mass Position for Max Regulation
$\phi(x, y)$	f			Flow Function

8. HORIZONTAL TAIL CONTROL

In the 3 degree and 6 degree airplane models, the tail position can be controlled by two different means. The first is simply to require that the horizontal tail rotation be fixed at some value S_{HT} . The second is to fix the input commands S_{EST} and F_{PX} and then let the stability augmentation system adjust the tail setting S_{HT} .

A. Mathematical Description

Figure 62 shows a control system representation of the stability augmentation system.

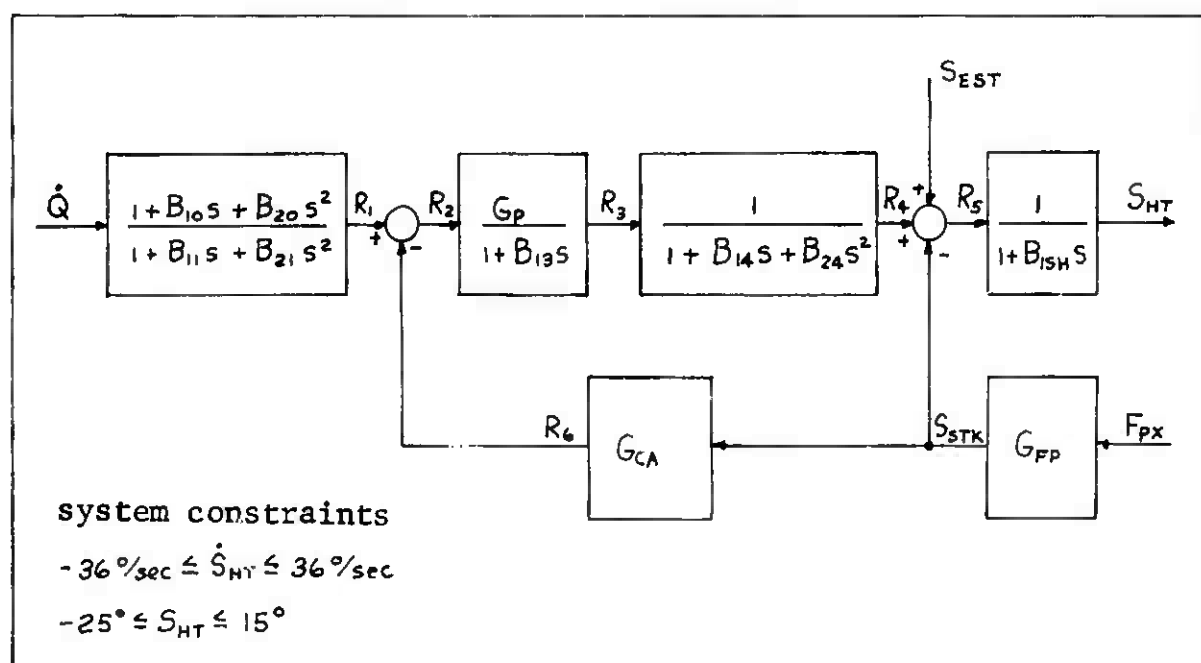


Figure 62 Stability Augmentation System

Using figure 62 as a guide, the following equations describe the stability augmentation system.

$$(8.1) \quad S_{STK} = G_{FP} F_{PX}$$

Where F_{PX} is the force exerted by the pilot on the stick.

$$(8.2) \quad R_6 = G_{CA} S_{STK}$$

Let U_Q and U_{QQ} be defined by

$$(8.3) \quad U_Q = \left(\frac{180}{\pi}\right) \int \dot{Q} dt$$

$$(8.4) \quad U_{QQ} = \int U_Q dt$$

Also, let U_{R1} and U_{RR1} be defined by

$$(8.5) \quad U_{R1} = \int R_1 dt$$

$$(8.6) \quad U_{RR1} = \int U_{R1} dt$$

Then

$$(8.7) \quad R_1 = (U_{QQ} + B_{10} U_Q + B_{20} \dot{Q} - U_{RR1} - B_{11} U_{R1}) / B_{21}$$

$$(8.8) \quad R_2 = R_1 - R_6$$

Let U_{R2} , U_{R3} , U_{RR3} , U_{R4} , and U_{RR4} be defined by

$$(8.9) \quad U_{R2} = \int R_2 dt$$

$$(8.10) \quad U_{R3} = \int R_3 dt$$

$$(8.11) \quad U_{RR3} = \int U_{R3} dt$$

$$(8.12) \quad U_{R4} = \int R_4 dt$$

$$(8.13) \quad U_{RR4} = \int U_{R4} dt$$

Then

$$(8.14) \quad R_3 = (G_P U_{R2} - U_{R3}) / B_{13}$$

$$(8.15) \quad R_4 = (U_{RR3} - U_{RR4} - B_{14} U_{R4}) / B_{24}$$

$$(8.16) \quad R_5 = R_4 + S_{EST} - S_{STK}$$

Because of rate and position limits, the equations that describe S_{HT} in terms of R_5 must be modified to reflect these limits. Let S_{HTP} be defined by

$$(8.17) \quad S_{HTP} = (R_5 - S_{HT}) / B_{15H}$$

Then

$$(8.18) S_{HT1} = \begin{cases} S_{HTDMX} & \text{if } S_{HTP} > S_{HTDMX} \\ S_{HTP} & \text{if } -S_{HTDMX} \leq S_{HTP} \leq S_{HTDMX} \\ -S_{HTDMX} & \text{if } S_{HTP} < -S_{HTDMX} \end{cases}$$

$$(8.19) \dot{S}_{HT} = \begin{cases} \min\{0.0, S_{HT1}\} & \text{if } S_{HT} \geq S_{HTMAX} \\ S_{HT1} & \text{if } S_{HTMIN} < S_{HT} < S_{HTMAX} \\ \max\{0.0, S_{HT1}\} & \text{if } S_{HT} \leq S_{HTMIN} \end{cases}$$

Finally the stick position F_{PX} may be positioned as a function of time by specifying two times and two loads.

$$(8.20) F_{PX} = \begin{cases} 0 & \text{if } T_{PX2} \leq T_{PX1} \\ F_{PX1} & \text{if } T \leq T_{PX1} < T_{PX2} \\ F_{PX2} & \text{if } T_{PX1} < T_{PX2} \leq T \\ F_{PX1} + (F_{PX2} - F_{PX1})(T - T_{PX1}) / (T_{PX2} - T_{PX1}) & \text{if } T_{PX1} < T < T_{PX2} \end{cases}$$

B. Parameter Evaluation

The values for the F-111A system parameters are listed in Table 22. In using this system for a braking problem the usual procedure is to first choose a steadystate value for S_{HT} (S_{HTSS}). Set $S_{HT0} = S_{HTSS} = S_{EST}$ and set $F_{PX} = 0$ ($T_{PX1} = T_{PX2} = 0$). Set all other initial conditions to zero.

Table 22 Horizontal Tail Control Parameters

SYMBOL	TYPE	VALUE	UNITS	DESCRIPTION
B ₁₀	C	0.4	sec	SAS Constants
B ₁₁	C	0.05	sec	
B ₁₃	C	0.50	sec	
B ₁₄	C	0.00249	sec	
B _{15H}	C	0.05	sec	
B ₂₀	C	3.58	sec ² deg / rad	Stick Force
B ₂₁	C	0.000555	sec ²	
B ₂₄	C	0.00037	sec ²	
F _{FX}	V		lb	Determine Stick Force
F _{FX1}	C	0.0	lb	
F _{FX2}	C	0.0	lb	
G _{CA}	C	3.6	sec ⁻¹	Command Augmentation Gain
G _{FP}	C	0.51	deg / lb	Stick Force Gain
G _P	C	0.375	sec ⁻¹	Augmentation Gain
Q	V(i)		rad/sec	Airplane Pitch Rate
R ₁	V		deg/sec	
R ₂	V		deg/sec	
R ₃	V		deg/sec	
R ₄	V		deg/sec	
R ₅	V		deg/sec	Intermediate SAS Variables
R ₆	V		deg/sec	
S _{EST}	C	-5.0	deg	
				Series Trim Input

Table 22 (Contd)

SYMBOL	TYPE	VALUE	UNITS	DESCRIPTION
SHT	V (o)		deg	Horizontal Tail Deflection
SHTO	C	-5.0	deg	when Time = 0
SHT	V		deg/sec	Horizontal Tail Deflection Rate
SHTI	V		deg/sec	Used to Calculate \dot{S}_{HT}
SHTP	V		deg/sec	
SHTDMX	C	36.0	deg/sec	Maximum Tail Deflection Rate
SHTMAX	C	15.0	deg	Maximum Tail Deflection
SHTMIN	C	-25.0	deg	Minimum Tail Deflection
SSTK	V		deg	Stick Position
T	V (i)		sec	Time
TPX1	C	0.0	sec	Used to Determine \bar{r}_{px}
TPX2	C	0.0	sec	
UQ	V		deg	
UQA	C	0.0	deg	
UQQ	V		deg/sec	
UQQC	C	0.0	deg/sec	
UR1	V		deg	
UR10	C	0.0	deg	
URR1	V		deg/sec	
URR10	C	0.0	deg/sec	
UR2	V		deg	
UR2C	C	0.0	deg	
				SAS Variables and Initial Conditions

Table 22 (Contd)

SYMBOL	TYPE	VALUE	UNITS	DESCRIPTION
U _{R3}	V		deg	} SAS Variables and Initial Conditions
U _{R3C}	C	0.0	deg sec	
U _{LR3}	V		deg sec	
U _{LR3C}	C	0.0	deg sec	
U _{R4}	V		deg sec	
U _{R4C}	C	0.0	deg sec ²	
U _{LR4}	V		deg sec ²	
U _{LR4C}	C	0.0	deg sec ²	

9a. RUNWAY SYSTEM (FLYWHEEL AND 3 DEGREE)

This runway system is essentially the same as the runway system for the 6 degree. In fact, the relation between the two is given by $Z_{6D}\langle x \rangle = \bar{Z}_{6D}\langle x, 0 \rangle$ and $\bar{Z}_{6DP}\langle x \rangle = \bar{Z}_{6PP}\langle x, 0 \rangle$. Even though this system is like the 6 degree system, the equations are listed below which take advantage of the fact that it takes less computer time to calculate $\bar{Z}_{6D}\langle x \rangle$ than $\bar{Z}_{6D}\langle x, 0 \rangle$. The data describing the runway is in tabular form and consists of runway elevation values as shown in table 24 as described in discussion of the 6 degree runway system. The data is from the center strip from station 4574 to station 6574.

A. Mathematical Description

Let $H_{RC}(i)$, $i = 1, 2, \dots, 1001$ denote the elevations at two foot intervals. As an example, $H_{RC}(5) = 9.686$. If x is a distance measured down the runway where x is in inches, then $z = \bar{Z}_{6D}\langle x \rangle$ and $\omega = \bar{Z}_{6DP}\langle x \rangle$ correspond to the elevation in inches and the slope in inches per inch. The values for z and ω are determined as outlined below. The function \bar{Z}_{6D} will have the property that $\bar{Z}_{6D}\langle 0 \rangle = 0$.

Let X_{LRO} be a constant such that $0 \leq X_{LRO} < 2000$. The input X_{LRF} in feet is derived from x such that $0 \leq X_{LRF} < 2000$ and for some integer k

$$(9a.1) \quad X_{LRF} = X_{LRO} + x/12 - 2000k$$

Let n be an integer such that $2(n-1) \leq X_{LRO} < 2n$ and define \bar{Z}_{6CO} by

$$(9a.2) \quad \bar{Z}_{6CO} = H_{RC}(n) + (H_{RC}(n+1) - H_{RC}(n))(X_{LRO} - 2n + 2)/2$$

If m is an integer such that $2(m-1) \leq X_{LRF} < 2m$ then z and ω are given by

$$(9a.3) \quad z = 12(H_{RC}(m) + (H_{RC}(m+1) - H_{RC}(m))(X_{LRF} - 2m + 2)/2 - \bar{Z}_{6CO})$$

$$(9a.4) \quad \omega = (H_{RC}(m+1) - H_{RC}(m))/2$$

Table 23 Runway System Parameters (Flywheel 1 and 3 Degree)

SYMBOL	TYPE	VALUE	UNITS	DESCRIPTION
$H_{RC}(i)$	C	*	Ft.	Center Runway Elevation Profile
ω	$v(o)$		In/In	Runway Slope at x ($\omega = Z_{GDP}(x)$)
x	$v(i)$		In.	Distance Down Runway
X_{LRO}	C	0.0	Ft.	Determines starting point (at time = 0) on Runway Profile
X_{LEF}	V		Ft.	Determines position on runway profile
z	$v(o)$		In.	Runway elevation at x
Z_{GCO}	$\#$ C		Ft.	Correction height

Determined from the constant X_{LRO}

* See Table 24 of the 6 degree runway system (use center, sta. 4574 to 6574)

9b. RUNWAY SYSTEM (6 DEGREE)

The runway system is not actually a "system" in the same sense as the brake system, for example. The runway system is simply a function called by the airplane system to supply values for ground slope and elevation. The data describing the runway is in tabular form and consists of runway elevation values as shown in Table 24. Except for a slight modification, the data in Table 24 is taken from station 4574 to station 6574 of runway 25 from reference 11. The left elevations and right elevations are 10 ft. to the left and 10 ft. to the right of center respectively. The elevations have been modified slightly so that the elevations at station 4574 match those at station 6574. This is done to provide an essentially "endless" runway by repeated use of a basic 2000 ft. strip.

A. Mathematical Description

Let $H_{RR}(i)$, $H_{RC}(i)$, $H_{RL}(i)$, $i = 1, 2, \dots, 1001$ denote the elevations at two foot increments of the right, center, and left runway strips respectively. As an example, $H_{RL}(11) = 9.550$ and $H_{RC}(5) = 9.686$. If x is a distance measured down the runway, and y is a distance measured out from the center of the runway where x and y are in inches, then $z = Z_{GD}(x, y)$ and $w = Z_{GP}(x, y)$ correspond to the elevation in inches and the slope in inches per inch. The values for z and w are determined as outlined below. The function Z_{GD} will be chosen in such a way that $Z_{GD}(0, y) = 0.0$ inches.

Let X_{LRF} and Y_{LRF} be the inputs in feet. Thus,

$$(9c.1) \quad Y_{LRF} = y/12$$

Let X_{LRO} be a constant such that $0 \leq X_{LRO} < 2000$. X_{LRF} is a number such that $0 \leq X_{LRF} < 2000$ and which also satisfies the following equation for some integer K .

$$(9c.2) \quad X_{LRF} = X_{LRO} + x/12 - 2000 K$$

Now let n be an integer such that $2(n-1) \leq X_{LRO} < 2n$.
 Define Z_{GRO} , Z_{GCO} , Z_{GLO} as follows:

$$(9c.3) \quad Z_{GRO} = H_{RR}(n) + \frac{1}{2}(H_{RR}(n+1) - H_{RR}(n))(X_{LRO} - 2n + 2)$$

$$(9c.4) \quad Z_{GCO} = H_{RC}(n) + \frac{1}{2}(H_{RC}(n+1) - H_{RC}(n))(X_{LRO} - 2n + 2)$$

$$(9c.5) \quad Z_{GLO} = H_{RL}(n) + \frac{1}{2}(H_{RL}(n+1) - H_{RL}(n))(X_{LRO} - 2n + 2)$$

Now let m be an integer such that $2(m-1) \leq X_{LRF} < 2m$.
 Define Z_{GRX} , Z_{GCX} , and Z_{GLX} as follows:

$$(9c.6) \quad Z_{GRX} = H_{RR}(m) + \frac{1}{2}(H_{RR}(m+1) - H_{RR}(m))(X_{LRF} - 2m + 2) - Z_{GRO}$$

$$(9c.7) \quad Z_{GCX} = H_{RC}(m) + \frac{1}{2}(H_{RC}(m+1) - H_{RC}(m))(X_{LRF} - 2m + 2) - Z_{GCO}$$

$$(9c.8) \quad Z_{GLX} = H_{RL}(m) + \frac{1}{2}(H_{RL}(m+1) - H_{RL}(m))(X_{LRF} - 2m + 2) - Z_{GLO}$$

If $Y_{LRF} \geq 0$, then

$$(9c.10) \quad Z = 12 (Z_{GCX} + (Z_{GRX} - Z_{GCX})(Y_{LRF}/10))$$

$$(9c.11) \quad \omega = (Y_{LRF}/20)(H_{RR}(m+1) - H_{RR}(m) - H_{RC}(m+1) + H_{RC}(m)) \\ + \frac{1}{2}(H_{RC}(m+1) - H_{RC}(m))$$

If $Y_{LRF} < 0$, then

$$(9c.12) \quad Z = 12 (Z_{GCX} + (Z_{GCX} - Z_{GLX})(Y_{LRF}/10))$$

$$(9c.13) \quad \omega = (Y_{LRF}/20)(H_{RC}(m+1) - H_{RC}(m) - H_{RL}(m+1) + H_{RL}(m)) \\ + \frac{1}{2}(H_{RC}(m+1) - H_{RC}(m))$$

Table 24 Three Track Elevation Profiles

(Stations and elevations are in feet)

STATION	ELEVATION		
	LEFT	CENTER	RIGHT
4574	9.597	9.703	9.593
4576	9.596	9.699	9.586
4578	9.593	9.696	9.581
4580	9.590	9.696	9.580
4582	9.590	9.686	9.580
4584	9.589	9.696	9.622
4586	9.580	9.688	9.629
4588	9.574	9.685	9.625
4590	9.570	9.686	9.616
4592	9.563	9.693	9.622
4594	9.564	9.704	9.634
4596	9.563	9.692	9.616
4598	9.556	9.676	9.611
4600	9.558	9.676	9.613
4602	9.592	9.694	9.612
4604	9.594	9.699	9.627
4606	9.595	9.711	9.641
4608	9.600	9.704	9.601
4610	9.604	9.703	9.605
4612	9.594	9.696	9.602
4614	9.585	9.697	9.606
4616	9.572	9.699	9.608
4618	9.569	9.702	9.607

Table 24 (Contd)

Station	Elevation			Station	Elevation			Station	Elevation		
	Left	Center	Right		Left	Center	Right		Left	Center	Right
4620	9.565	9.697	9.531	4760	9.557	9.667	9.567	4900	9.590	9.716	9.603
4622	9.572	9.658	9.631	4762	9.560	9.668	9.564	4902	9.593	9.714	9.582
4624	9.578	9.677	9.534	4764	9.567	9.668	9.561	4904	9.593	9.717	9.585
4626	9.583	9.687	9.589	4766	9.565	9.676	9.568	4906	9.598	9.714	9.587
4628	9.583	9.693	9.533	4768	9.567	9.676	9.567	4908	9.591	9.711	9.584
4630	9.583	9.681	9.593	4770	9.563	9.664	9.564	4910	9.589	9.716	9.578
4632	9.584	9.694	9.537	4772	9.561	9.660	9.557	4912	9.589	9.713	9.585
4634	9.591	9.699	9.534	4774	9.563	9.673	9.561	4914	9.592	9.712	9.581
4636	9.593	9.698	9.601	4776	9.565	9.675	9.561	4916	9.588	9.711	9.585
4638	9.594	9.693	9.537	4778	9.564	9.677	9.567	4918	9.587	9.710	9.592
4640	9.593	9.691	9.530	4780	9.560	9.678	9.574	4920	9.589	9.705	9.585
4642	9.588	9.691	9.538	4782	9.557	9.678	9.575	4922	9.586	9.696	9.578
4644	9.586	9.687	9.589	4784	9.552	9.683	9.574	4924	9.588	9.685	9.576
4646	9.584	9.667	9.531	4786	9.554	9.686	9.580	4926	9.589	9.695	9.572
4648	9.583	9.668	9.569	4788	9.571	9.682	9.536	4928	9.585	9.701	9.571
4650	9.568	9.673	9.557	4790	9.572	9.703	9.587	4930	9.586	9.702	9.573
4652	9.573	9.659	9.569	4792	9.573	9.702	9.531	4932	9.590	9.711	9.571
4654	9.574	9.674	9.553	4794	9.583	9.704	9.594	4934	9.594	9.707	9.568
4656	9.572	9.681	9.554	4796	9.582	9.703	9.587	4936	9.590	9.699	9.569
4658	9.565	9.665	9.567	4798	9.576	9.702	9.588	4938	9.590	9.692	9.567
4660	9.570	9.654	9.564	4800	9.557	9.697	9.590	4940	9.588	9.684	9.566
4662	9.573	9.659	9.561	4802	9.580	9.696	9.586	4942	9.583	9.687	9.573
4664	9.579	9.674	9.554	4804	9.583	9.699	9.593	4944	9.581	9.688	9.566
4666	9.574	9.669	9.569	4806	9.530	9.701	9.588	4946	9.582	9.682	9.562
4668	9.572	9.677	9.565	4808	9.593	9.698	9.585	4948	9.580	9.692	9.567
4670	9.577	9.677	9.554	4810	9.588	9.694	9.579	4950	9.576	9.679	9.569
4672	9.570	9.694	9.574	4812	9.585	9.697	9.581	4952	9.576	9.678	9.578
4674	9.568	9.681	9.581	4814	9.581	9.698	9.593	4954	9.571	9.687	9.578
4676	9.571	9.685	9.587	4816	9.578	9.700	9.583	4956	9.575	9.682	9.579
4678	9.577	9.690	9.591	4818	9.579	9.693	9.579	4958	9.581	9.689	9.585
4680	9.576	9.680	9.595	4820	9.572	9.686	9.578	4960	9.581	9.686	9.581
4682	9.554	9.631	9.589	4822	9.534	9.679	9.574	4962	9.582	9.678	9.585
4684	9.564	9.690	9.587	4824	9.589	9.676	9.574	4964	9.583	9.695	9.589
4686	9.535	9.632	9.535	4826	9.589	9.680	9.568	4966	9.580	9.699	9.588
4688	9.569	9.687	9.590	4828	9.590	9.686	9.571	4968	9.576	9.709	9.587
4690	9.571	9.696	9.534	4830	9.593	9.689	9.574	4970	9.574	9.696	9.585
4692	9.578	9.635	9.537	4832	9.535	9.684	9.581	4972	9.576	9.685	9.585
4694	9.578	9.632	9.597	4834	9.596	9.693	9.585	4974	9.571	9.682	9.584
4696	9.577	9.693	9.532	4836	9.535	9.695	9.594	4976	9.576	9.690	9.579
4698	9.555	9.733	9.636	4838	9.590	9.698	9.599	4978	9.576	9.685	9.583
4700	9.573	9.694	9.531	4840	9.530	9.701	9.603	4980	9.573	9.679	9.583
4702	9.567	9.696	9.630	4842	9.598	9.710	9.598	4982	9.580	9.678	9.588
4704	9.557	9.715	9.533	4844	9.586	9.704	9.596	4984	9.579	9.691	9.592
4706	9.571	9.702	9.596	4846	9.590	9.691	9.537	4986	9.585	9.698	9.591
4708	9.570	9.714	9.533	4848	9.591	9.689	9.596	4988	9.593	9.695	9.595
4710	9.568	9.696	9.598	4850	9.586	9.695	9.595	4990	9.590	9.699	9.589
4712	9.555	9.694	9.535	4852	9.579	9.694	9.598	4992	9.589	9.689	9.591
4714	9.562	9.695	9.593	4854	9.577	9.683	9.535	4994	9.593	9.695	9.592
4716	9.558	9.631	9.596	4856	9.585	9.693	9.595	4996	9.597	9.704	9.597
4718	9.560	9.638	9.531	4858	9.586	9.696	9.593	4998	9.598	9.709	9.590
4720	9.562	9.691	9.593	4860	9.588	9.694	9.587	5000	9.633	9.732	9.594
4722	9.554	9.689	9.533	4862	9.591	9.690	9.585	5002	9.602	9.715	9.602
4724	9.565	9.689	9.592	4864	9.535	9.686	9.595	5004	9.608	9.703	9.610
4726	9.555	9.687	9.532	4866	9.535	9.683	9.602	5006	9.607	9.724	9.609
4728	9.576	9.690	9.596	4868	9.594	9.680	9.631	5008	9.635	9.728	9.619
4730	9.590	9.693	9.532	4870	9.589	9.692	9.603	5010	9.608	9.730	9.613
4732	9.582	9.630	9.604	4872	9.590	9.685	9.600	5012	9.609	9.721	9.614
4734	9.579	9.699	9.533	4874	9.587	9.685	9.598	5014	9.607	9.710	9.611
4736	9.579	9.653	9.539	4876	9.531	9.678	9.596	5016	9.597	9.703	9.604
4738	9.578	9.691	9.594	4878	9.584	9.677	9.595	5018	9.587	9.711	9.599
4740	9.578	9.695	9.587	4880	9.593	9.673	9.594	5020	9.586	9.701	9.592
4742	9.575	9.674	9.587	4882	9.595	9.685	9.594	5022	9.587	9.691	9.583
4744	9.570	9.676	9.575	4884	9.599	9.688	9.595	5024	9.588	9.682	9.580
4746	9.577	9.695	9.572	4886	9.610	9.693	9.594	5026	9.581	9.666	9.577
4748	9.593	9.695	9.573	4888	9.632	9.699	9.596	5028	9.582	9.671	9.575
4750	9.587	9.670	9.571	4890	9.632	9.704	9.599	5030	9.581	9.672	9.576
4752	9.582	9.664	9.573	4892	9.535	9.703	9.598	5032	9.582	9.679	9.578
4754	9.581	9.680	9.572	4894	9.530	9.713	9.537	5034	9.590	9.694	9.583
4756	9.583	9.673	9.574	4896	9.535	9.715	9.596	5036	9.589	9.692	9.585
4758	9.572	9.674	9.571	4898	9.596	9.715	9.593	5038	9.582	9.691	9.587

Table 24 (Contd)

Station	Elevation			Station	Elevation			Station	Elevation		
	Left	Center	Right		Left	Center	Right		Left	Center	Right
5041	9.581	9.689	9.587	5180	9.586	9.735	9.630	5320	9.657	9.805	9.695
5042	9.583	9.686	9.582	5182	9.577	9.743	9.633	5322	9.658	9.810	9.692
5044	9.578	9.682	9.578	5184	9.597	9.745	9.638	5324	9.667	9.803	9.693
5046	9.585	9.683	9.573	5186	9.632	9.755	9.643	5326	9.668	9.799	9.692
5048	9.572	9.680	9.571	5188	9.599	9.756	9.640	5328	9.576	9.797	9.689
5050	9.571	9.683	9.563	5190	9.591	9.750	9.637	5330	9.675	9.803	9.690
5052	9.575	9.684	9.568	5192	9.595	9.757	9.641	5332	9.677	9.806	9.695
5054	9.579	9.686	9.575	5194	9.621	9.756	9.650	5334	9.680	9.812	9.697
5056	9.580	9.685	9.588	5196	9.597	9.753	9.652	5336	9.686	9.811	9.702
5058	9.569	9.679	9.571	5198	9.595	9.745	9.639	5338	9.689	9.823	9.702
5060	9.568	9.702	9.593	5200	9.595	9.741	9.533	5340	9.683	9.812	9.704
5062	9.582	9.696	9.591	5202	9.591	9.747	9.635	5342	9.680	9.811	9.703
5064	9.577	9.686	9.553	5204	9.631	9.758	9.648	5344	9.675	9.807	9.705
5066	9.558	9.679	9.579	5206	9.610	9.759	9.655	5346	9.572	9.813	9.599
5068	9.569	9.663	9.555	5208	9.623	9.767	9.559	5348	9.680	9.816	9.701
5070	9.575	9.662	9.557	5210	9.630	9.779	9.662	5350	9.694	9.818	9.704
5072	9.574	9.665	9.553	5212	9.623	9.772	9.661	5352	9.699	9.810	9.704
5074	9.568	9.666	9.562	5214	9.626	9.755	9.559	5354	9.705	9.813	9.706
5076	9.571	9.670	9.557	5216	9.623	9.768	9.660	5356	9.710	9.811	9.708
5078	9.569	9.675	9.555	5218	9.619	9.773	9.557	5358	9.714	9.817	9.707
5080	9.558	9.679	9.566	5220	9.620	9.772	9.650	5360	9.707	9.809	9.599
5082	9.565	9.690	9.553	5222	9.622	9.765	9.659	5362	9.699	9.813	9.700
5084	9.559	9.697	9.570	5224	9.627	9.761	9.648	5364	9.697	9.804	9.703
5086	9.566	9.695	9.565	5226	9.528	9.766	9.652	5366	9.697	9.808	9.701
5088	9.555	9.664	9.557	5228	9.624	9.757	9.658	5368	9.702	9.802	9.709
5090	9.553	9.664	9.556	5230	9.630	9.756	9.657	5370	9.708	9.797	9.706
5092	9.565	9.663	9.557	5232	9.634	9.772	9.661	5372	9.713	9.799	9.706
5094	9.565	9.674	9.557	5234	9.647	9.777	9.661	5374	9.719	9.811	9.705
5096	9.564	9.672	9.566	5236	9.637	9.765	9.652	5376	9.731	9.822	9.711
5098	9.562	9.678	9.559	5238	9.625	9.777	9.659	5378	9.737	9.835	9.715
5100	9.565	9.694	9.574	5240	9.627	9.778	9.550	5380	9.744	9.832	9.721
5102	9.555	9.702	9.576	5242	9.622	9.775	9.668	5382	9.746	9.833	9.722
5104	9.565	9.736	9.577	5244	9.638	9.779	9.675	5384	9.751	9.835	9.732
5106	9.573	9.704	9.581	5246	9.643	9.780	9.684	5386	9.761	9.837	9.730
5108	9.569	9.702	9.575	5248	9.641	9.779	9.689	5388	9.764	9.852	9.729
5110	9.564	9.699	9.582	5250	9.645	9.780	9.695	5390	9.768	9.850	9.733
5112	9.571	9.697	9.577	5252	9.653	9.771	9.697	5392	9.769	9.854	9.735
5114	9.568	9.694	9.583	5254	9.655	9.783	9.702	5394	9.770	9.865	9.736
5116	9.554	9.658	9.577	5256	9.656	9.783	9.703	5396	9.780	9.862	9.731
5118	9.561	9.689	9.575	5258	9.657	9.793	9.725	5398	9.781	9.865	9.738
5120	9.552	9.676	9.553	5260	9.662	9.793	9.714	5400	9.777	9.871	9.737
5122	9.542	9.675	9.555	5262	9.663	9.787	9.729	5402	9.777	9.860	9.737
5124	9.544	9.676	9.570	5264	9.653	9.782	9.708	5404	9.777	9.870	9.743
5126	9.534	9.677	9.571	5266	9.664	9.784	9.705	5406	9.783	9.862	9.742
5128	9.537	9.672	9.567	5268	9.664	9.786	9.692	5408	9.781	9.858	9.745
5130	9.536	9.657	9.565	5270	9.650	9.787	9.675	5410	9.782	9.868	9.757
5132	9.547	9.667	9.567	5272	9.657	9.785	9.683	5412	9.785	9.865	9.760
5134	9.549	9.657	9.558	5274	9.655	9.782	9.681	5414	9.786	9.864	9.763
5136	9.539	9.661	9.561	5276	9.652	9.789	9.575	5416	9.783	9.871	9.763
5138	9.535	9.652	9.553	5278	9.641	9.780	9.667	5418	9.777	9.873	9.762
5140	9.542	9.653	9.549	5280	9.633	9.778	9.562	5420	9.775	9.877	9.760
5142	9.545	9.651	9.557	5282	9.629	9.766	9.662	5422	9.780	9.883	9.766
5144	9.548	9.664	9.565	5284	9.626	9.757	9.557	5424	9.787	9.880	9.770
5146	9.552	9.678	9.573	5286	9.621	9.775	9.665	5426	9.783	9.872	9.775
5148	9.555	9.672	9.574	5288	9.635	9.775	9.557	5428	9.785	9.869	9.777
5150	9.552	9.675	9.573	5290	9.639	9.773	9.667	5430	9.787	9.862	9.784
5152	9.565	9.664	9.570	5292	9.643	9.775	9.666	5432	9.790	9.857	9.786
5154	9.565	9.674	9.573	5294	9.655	9.780	9.666	5434	9.797	9.875	9.793
5156	9.578	9.698	9.535	5296	9.664	9.793	9.659	5436	9.796	9.887	9.793
5158	9.590	9.705	9.590	5298	9.652	9.801	9.557	5438	9.795	9.883	9.792
5160	9.599	9.715	9.591	5300	9.657	9.801	9.674	5440	9.787	9.882	9.787
5162	9.589	9.718	9.694	5302	9.653	9.805	9.587	5442	9.786	9.887	9.785
5164	9.589	9.723	9.697	5304	9.651	9.808	9.689	5444	9.781	9.877	9.783
5166	9.598	9.719	9.693	5306	9.657	9.806	9.685	5446	9.777	9.870	9.774
5168	9.632	9.723	9.617	5308	9.657	9.803	9.691	5448	9.785	9.866	9.773
5170	9.671	9.735	9.515	5310	9.659	9.801	9.664	5450	9.791	9.865	9.767
5172	9.599	9.730	9.623	5312	9.662	9.809	9.699	5452	9.784	9.857	9.764
5174	9.592	9.738	9.527	5314	9.653	9.808	9.701	5454	9.770	9.855	9.763
5176	9.592	9.732	9.633	5316	9.655	9.807	9.700	5456	9.771	9.856	9.767
5178	9.597	9.734	9.534	5318	9.660	9.805	9.702	5458	9.772	9.850	9.767

Table 24 (Contd)

Station	Elevation			Station	Elevation			Station	Elevation		
	Left	Center	Right		Left	Center	Right		Left	Center	Right
5463	9.777	9.869	9.753	5621	9.838	9.917	9.862	5740	9.964	10.058	9.944
5462	9.763	9.861	9.789	5622	9.837	9.926	9.851	5742	9.967	10.052	9.943
5464	9.768	9.859	9.787	5604	9.831	9.921	9.862	5744	9.964	10.056	9.946
5466	9.767	9.858	9.791	5606	9.831	9.931	9.866	5746	9.962	10.049	9.946
5468	9.769	9.852	9.788	5608	9.836	9.937	9.876	5748	9.970	10.056	9.959
5470	9.785	9.886	9.792	5511	9.828	9.936	9.875	5750	9.972	10.064	9.966
5472	9.797	9.893	9.795	5612	9.827	9.926	9.874	5752	9.972	10.089	9.974
5474	9.801	9.897	9.811	5514	9.824	9.939	9.876	5754	9.967	10.088	9.977
5476	9.803	9.900	9.797	5616	9.828	9.946	9.879	5756	9.966	10.092	9.981
5478	9.814	9.896	9.795	5618	9.829	9.953	9.876	5758	9.974	10.091	9.983
5480	9.810	9.915	9.799	5620	9.837	9.957	9.897	5760	9.982	10.098	9.985
5482	9.811	9.920	9.803	5622	9.841	9.956	9.884	5762	9.980	10.101	9.982
5484	9.812	9.927	9.806	5624	9.846	9.953	9.931	5764	9.976	10.097	9.985
5486	9.819	9.929	9.813	5626	9.846	9.961	9.879	5766	9.975	10.098	9.983
5488	9.818	9.922	9.817	5628	9.846	9.973	9.884	5768	9.979	10.100	9.976
5491	9.815	9.927	9.817	5630	9.843	9.972	9.887	5770	9.978	10.087	9.975
5492	9.807	9.931	9.801	5532	9.849	9.978	9.893	5772	9.967	10.094	9.976
5494	9.807	9.920	9.793	5634	9.850	9.977	9.896	5774	9.970	10.087	9.975
5496	9.793	9.919	9.783	5535	9.859	9.979	9.906	5776	9.970	10.092	9.974
5498	9.792	9.918	9.776	5638	9.860	9.986	9.909	5778	9.967	10.097	9.975
5500	9.795	9.925	9.774	5640	9.864	9.993	9.916	5780	9.963	10.095	9.976
5502	9.797	9.903	9.771	5642	9.867	9.999	9.925	5782	9.963	10.089	9.979
5504	9.800	9.935	9.775	5644	9.862	10.006	9.927	5784	9.957	10.084	9.976
5506	9.797	9.904	9.779	5646	9.857	10.008	9.929	5786	9.943	10.077	9.977
5508	9.799	9.905	9.784	5648	9.862	10.011	9.936	5788	9.934	10.067	9.979
5510	9.799	9.906	9.788	5650	9.873	10.017	9.945	5790	9.930	10.067	9.983
5512	9.802	9.902	9.785	5652	9.883	10.021	9.951	5792	9.927	10.064	9.982
5514	9.801	9.904	9.784	5654	9.897	10.023	9.952	5794	9.914	10.062	9.980
5516	9.831	9.903	9.795	5655	9.897	10.041	9.955	5796	9.915	10.066	9.978
5518	9.803	9.932	9.790	5658	9.903	10.043	9.956	5798	9.912	10.074	9.975
5520	9.803	9.934	9.795	5660	9.907	10.039	9.956	5800	9.910	10.071	9.975
5522	9.802	9.892	9.800	5662	9.910	10.039	9.954	5802	9.913	10.073	9.984
5524	9.801	9.900	9.803	5664	9.916	10.046	9.949	5804	9.925	10.091	9.987
5526	9.806	9.904	9.814	5665	9.914	10.039	9.945	5806	9.927	10.088	9.994
5528	9.800	9.889	9.807	5668	9.911	10.033	9.942	5808	9.933	10.105	10.001
5530	9.797	9.887	9.815	5670	9.913	10.030	9.939	5810	9.942	10.131	10.002
5532	9.797	9.904	9.824	5672	9.916	10.020	9.932	5812	9.947	10.125	9.994
5534	9.799	9.913	9.827	5674	9.914	10.028	9.926	5814	9.963	10.123	9.991
5536	9.814	9.909	9.826	5676	9.926	10.037	9.929	5816	9.965	10.108	9.984
5538	9.818	9.929	9.827	5678	9.929	10.044	9.937	5818	9.973	10.113	9.987
5540	9.817	9.933	9.827	5680	9.926	10.049	9.944	5820	9.970	10.104	9.985
5542	9.825	9.937	9.829	5692	9.923	10.057	9.950	5822	9.975	10.101	9.985
5544	9.822	9.922	9.835	5694	9.925	10.042	9.949	5824	9.970	10.095	9.986
5546	9.823	9.927	9.835	5695	9.933	10.052	9.949	5826	9.967	10.091	9.987
5548	9.828	9.938	9.839	5698	9.930	10.052	9.951	5828	9.963	10.095	9.998
5550	9.826	9.927	9.833	5699	9.929	10.054	9.954	5830	9.961	10.105	10.004
5552	9.820	9.930	9.843	5692	9.936	10.055	9.952	5832	9.963	10.107	10.011
5554	9.822	9.933	9.847	5694	9.947	10.053	9.949	5834	9.960	10.118	10.015
5556	9.821	9.922	9.850	5696	9.944	10.043	9.942	5836	9.959	10.121	10.014
5558	9.822	9.930	9.854	5698	9.939	10.028	9.937	5838	9.963	10.115	10.013
5560	9.829	9.950	9.860	5700	9.939	10.032	9.929	5840	9.960	10.111	10.017
5562	9.833	9.947	9.855	5702	9.914	10.029	9.929	5842	9.967	10.105	10.016
5564	9.847	9.956	9.858	5704	9.917	10.024	9.925	5844	9.963	10.103	10.009
5565	9.853	9.947	9.862	5706	9.913	10.030	9.932	5846	9.957	10.115	10.004
5568	9.849	9.947	9.861	5708	9.921	10.036	9.936	5848	9.964	10.112	10.003
5573	9.845	9.961	9.860	5710	9.929	10.040	9.943	5850	9.977	10.103	9.996
5572	9.836	9.948	9.855	5712	9.931	10.044	9.947	5852	9.985	10.115	9.995
5574	9.841	9.963	9.871	5714	9.929	10.044	9.949	5854	9.990	10.111	9.993
5576	9.841	9.962	9.878	5715	9.935	10.052	9.952	5856	9.991	10.105	9.993
5578	9.843	9.963	9.877	5718	9.933	10.055	9.954	5858	9.988	10.105	9.994
5580	9.845	9.963	9.879	5720	9.934	10.056	9.953	5860	9.987	10.100	10.003
5582	9.840	9.970	9.875	5722	9.939	10.048	9.942	5862	9.989	10.095	10.003
5584	9.839	9.953	9.874	5724	9.938	10.050	9.949	5864	9.983	10.091	9.999
5586	9.841	9.954	9.852	5726	9.940	10.054	9.957	5866	9.971	10.088	9.992
5588	9.843	9.954	9.861	5728	9.945	10.049	9.956	5868	9.962	10.092	9.988
5590	9.835	9.943	9.861	5730	9.949	10.054	9.955	5870	9.957	10.081	9.985
5592	9.836	9.934	9.862	5732	9.950	10.053	9.956	5872	9.952	10.088	9.979
5594	9.834	9.930	9.862	5734	9.953	10.043	9.949	5874	9.950	10.073	9.976
5595	9.830	9.911	9.865	5736	9.958	10.041	9.949	5876	9.943	10.064	9.973
5598	9.830	9.916	9.853	5738	9.956	10.040	9.939	5878	9.947	10.061	9.965

Table 24 (Contd)

Station	Elevation			Station	Elevation			Station	Elevation		
	Left	Center	Right		Left	Center	Right		Left	Center	Right
5880	9.945	10.055	9.957	6020	9.962	10.082	9.979	6160	9.937	10.079	10.011
5882	9.943	10.041	9.954	6022	9.954	10.083	9.975	6152	9.937	10.086	10.012
5884	9.947	10.025	9.947	6024	9.953	10.086	9.972	6164	9.938	10.078	10.015
5886	9.943	10.026	9.946	6026	9.953	10.087	9.975	6166	9.940	10.096	10.016
5888	9.945	10.028	9.952	6028	9.957	10.076	9.971	6168	9.940	10.093	10.014
5890	9.952	10.021	9.957	6030	9.960	10.085	9.973	6170	9.938	10.096	10.009
5892	9.957	10.038	9.957	6032	9.953	10.096	9.972	6172	9.943	10.076	9.997
5894	9.961	10.053	9.980	6034	9.959	10.092	9.959	6174	9.945	10.085	10.006
5896	9.953	10.065	9.994	6036	9.973	10.096	9.964	6176	9.942	10.080	10.005
5898	9.971	10.071	10.009	6038	9.973	10.093	9.960	6178	9.939	10.079	10.002
5900	9.978	10.075	10.006	6040	9.973	10.089	9.959	6180	9.942	10.070	10.002
5902	9.993	10.072	10.008	6042	9.978	10.089	9.958	6182	9.938	10.062	9.997
5904	10.002	10.091	10.009	6044	9.976	10.087	9.955	6184	9.942	10.059	9.995
5906	10.009	10.089	10.007	6046	9.973	10.088	9.955	6186	9.955	10.063	9.995
5908	10.017	10.102	10.003	6048	9.973	10.084	9.951	6188	9.946	10.057	9.986
5910	10.032	10.112	9.997	6050	9.972	10.094	9.946	6190	9.943	10.065	9.985
5912	10.027	10.114	10.002	6052	9.993	10.073	9.946	6192	9.934	10.062	9.973
5914	10.039	10.117	10.004	6054	9.991	10.082	9.946	6194	9.936	10.049	9.962
5916	10.038	10.116	10.008	6056	9.992	10.089	9.951	6196	9.930	10.049	9.955
5918	10.040	10.119	10.010	6058	9.998	10.093	9.949	6198	9.929	10.059	9.954
5920	10.041	10.119	10.005	6060	9.993	10.092	9.954	6200	9.927	10.049	9.954
5922	10.038	10.109	10.001	6062	9.996	10.093	9.952	6202	9.929	10.081	9.955
5924	10.038	10.123	10.002	6064	9.979	10.091	9.942	6204	9.922	10.075	9.949
5926	10.013	10.113	9.998	6066	9.970	10.093	9.943	6206	9.914	10.071	9.946
5928	9.994	10.105	10.000	6068	9.970	10.082	9.942	6208	9.912	10.061	9.945
5930	9.983	10.111	10.004	6070	9.973	10.076	9.955	6210	9.908	10.071	9.949
5932	9.990	10.110	10.004	6072	9.976	10.083	9.963	6212	9.897	10.060	9.953
5934	9.997	10.098	10.000	6074	9.977	10.086	9.968	6214	9.894	10.058	9.949
5936	9.987	10.104	9.997	6076	9.993	10.088	9.973	6216	9.887	10.062	9.949
5938	9.993	10.098	9.990	6078	9.993	10.088	9.981	6218	9.889	10.061	9.944
5940	9.982	10.093	9.991	6080	9.990	10.103	9.993	6220	9.887	10.063	9.941
5942	9.983	10.091	9.996	6082	9.993	10.108	9.986	6222	9.886	10.068	9.935
5944	9.980	10.099	9.990	6084	9.997	10.105	9.995	6224	9.880	10.061	9.929
5946	9.976	10.098	9.975	6086	9.990	10.089	9.996	6226	9.877	10.055	9.925
5948	9.982	10.092	9.980	6088	9.993	10.092	9.998	6228	9.873	10.063	9.916
5950	9.993	10.091	9.984	6090	9.993	10.083	9.996	6230	9.867	10.061	9.914
5952	10.003	10.095	9.987	6092	9.977	10.096	9.996	6232	9.860	10.055	9.912
5954	10.008	10.101	9.992	6094	9.976	10.089	9.991	6234	9.853	10.043	9.915
5956	10.009	10.125	9.997	6096	9.954	10.092	9.982	6236	9.850	10.044	9.922
5958	10.010	10.123	10.000	6098	9.965	10.083	9.983	6238	9.846	10.041	9.921
5960	10.003	10.135	10.000	6100	9.953	10.085	9.986	6240	9.841	10.031	9.919
5962	10.000	10.138	10.002	6102	9.956	10.076	9.988	6242	9.844	10.021	9.916
5964	9.995	10.128	9.997	6104	9.941	10.081	9.998	6244	9.854	10.015	9.909
5966	9.994	10.115	9.988	6106	9.957	10.079	9.996	6246	9.848	10.008	9.903
5968	9.993	10.103	9.994	6108	9.955	10.076	9.987	6248	9.843	9.997	9.897
5970	9.987	10.100	9.977	6110	9.952	10.074	9.998	6250	9.844	10.009	9.898
5972	9.987	10.094	9.974	6112	9.946	10.072	9.985	6252	9.840	10.018	9.895
5974	9.984	10.097	9.958	6114	9.944	10.077	9.992	6254	9.836	10.013	9.899
5976	9.997	10.099	9.959	6116	9.943	10.075	9.975	6256	9.833	10.022	9.903
5978	9.991	10.095	9.954	6118	9.941	10.071	9.977	6258	9.827	10.013	9.899
5980	9.993	10.098	9.950	6120	9.941	10.079	9.975	6260	9.820	10.001	9.891
5982	9.992	10.095	9.950	6122	9.938	10.063	9.963	6262	9.821	10.004	9.886
5984	9.997	10.090	9.947	6124	9.938	10.070	9.969	6264	9.821	9.993	9.883
5986	9.995	10.092	9.955	6126	9.935	10.074	9.968	6266	9.826	9.996	9.879
5988	9.987	10.094	9.957	6128	9.940	10.073	9.972	6268	9.828	9.958	9.881
5990	9.984	10.093	9.963	6130	9.936	10.072	9.977	6270	9.830	9.963	9.882
5992	9.983	10.083	9.957	6132	9.933	10.076	9.974	6272	9.830	9.964	9.881
5994	9.976	10.038	9.966	6134	9.937	10.059	9.970	6274	9.831	9.972	9.879
5996	9.976	10.098	9.954	6136	9.943	10.077	9.969	6276	9.832	9.978	9.884
5998	9.975	10.086	9.965	6138	9.940	10.070	9.967	6278	9.833	9.984	9.885
6000	9.977	10.075	9.954	6140	9.934	10.061	9.970	6280	9.827	9.984	9.885
6002	9.960	10.071	9.959	6142	9.935	10.073	9.971	6282	9.823	9.974	9.890
6004	9.953	10.072	9.953	6144	9.937	10.066	9.972	6284	9.824	9.973	9.891
6006	9.945	10.073	9.965	6146	9.933	10.057	9.977	6286	9.824	9.967	9.890
6008	9.951	10.071	9.958	6148	9.936	10.066	9.981	6288	9.823	9.958	9.882
6010	9.956	10.068	9.977	6150	9.932	10.074	9.987	6290	9.820	9.949	9.879
6012	9.955	10.077	9.991	6152	9.930	10.069	9.996	6292	9.815	9.957	9.871
6014	9.953	10.079	9.994	6154	9.933	10.066	10.004	6294	9.806	9.952	9.863
6016	9.967	10.083	9.997	6156	9.932	10.082	10.005	6296	9.807	9.953	9.855
6018	9.965	10.070	9.995	6158	9.936	10.071	10.006	6298	9.819	9.941	9.851

Table 24 (Contd)

Station	Elevation			Station	Elevation			Station	Elevation		
	Left	Center	Right		Left	Center	Right		Left	Center	Right
6301	9.818	9.937	9.852	6392	9.754	9.864	9.779	6484	9.651	9.752	9.657
6302	9.817	9.935	9.853	6394	9.743	9.856	9.775	6486	9.651	9.755	9.657
6304	9.822	9.937	9.849	6396	9.727	9.853	9.772	6488	9.648	9.751	9.649
6306	9.815	9.934	9.855	6398	9.723	9.846	9.755	6490	9.643	9.737	9.645
6308	9.811	9.928	9.852	6400	9.719	9.854	9.781	6492	9.641	9.734	9.639
6310	9.809	9.931	9.851	6402	9.716	9.849	9.780	6494	9.636	9.730	9.637
6312	9.807	9.936	9.847	6404	9.721	9.855	9.779	6496	9.636	9.732	9.640
6314	9.806	9.937	9.845	6406	9.727	9.854	9.780	6498	9.635	9.730	9.643
6316	9.803	9.939	9.843	6408	9.734	9.846	9.784	6500	9.637	9.734	9.637
6318	9.796	9.943	9.841	6410	9.744	9.849	9.787	6502	9.641	9.736	9.635
6320	9.794	9.944	9.835	6412	9.753	9.853	9.785	6504	9.642	9.738	9.641
6322	9.789	9.949	9.822	6414	9.753	9.855	9.776	6506	9.640	9.736	9.642
6324	9.784	9.947	9.829	6416	9.757	9.856	9.774	6508	9.641	9.739	9.641
6326	9.781	9.948	9.830	6418	9.759	9.858	9.773	6510	9.640	9.737	9.639
6328	9.783	9.949	9.832	6420	9.758	9.862	9.770	6512	9.638	9.739	9.637
6330	9.782	9.941	9.833	6422	9.755	9.859	9.773	6514	9.639	9.735	9.639
6332	9.783	9.944	9.832	6424	9.752	9.861	9.765	6516	9.637	9.735	9.637
6334	9.786	9.938	9.834	6426	9.754	9.862	9.753	6518	9.634	9.733	9.635
6336	9.787	9.956	9.842	6428	9.751	9.856	9.760	6520	9.633	9.736	9.638
6338	9.794	9.956	9.841	6430	9.744	9.859	9.755	6522	9.627	9.740	9.637
6340	9.796	9.950	9.839	6432	9.739	9.852	9.751	6524	9.626	9.733	9.634
6342	9.793	9.954	9.835	6434	9.732	9.847	9.743	6526	9.623	9.731	9.630
6344	9.792	9.934	9.834	6436	9.729	9.834	9.733	6528	9.620	9.727	9.625
6346	9.794	9.938	9.823	6438	9.724	9.833	9.724	6530	9.612	9.721	9.620
6348	9.793	9.923	9.826	6440	9.721	9.831	9.720	6532	9.608	9.713	9.616
6350	9.784	9.931	9.825	6442	9.717	9.827	9.720	6534	9.610	9.704	9.609
6352	9.783	9.921	9.825	6444	9.716	9.826	9.714	6536	9.607	9.702	9.604
6354	9.783	9.929	9.820	6446	9.716	9.822	9.713	6538	9.602	9.713	9.597
6356	9.779	9.924	9.812	6448	9.717	9.822	9.707	6540	9.597	9.695	9.594
6358	9.782	9.914	9.814	6450	9.720	9.821	9.711	6542	9.599	9.701	9.595
6360	9.786	9.927	9.804	6452	9.721	9.827	9.713	6544	9.597	9.698	9.592
6362	9.790	9.910	9.798	6454	9.718	9.834	9.714	6546	9.594	9.696	9.591
6364	9.794	9.908	9.789	6456	9.721	9.831	9.719	6548	9.602	9.699	9.593
6366	9.797	9.914	9.786	6458	9.721	9.830	9.720	6550	9.593	9.702	9.590
6368	9.795	9.912	9.786	6460	9.720	9.824	9.720	6552	9.598	9.706	9.604
6370	9.794	9.914	9.785	6462	9.724	9.829	9.711	6554	9.598	9.692	9.595
6372	9.794	9.916	9.754	6464	9.718	9.827	9.711	6556	9.590	9.704	9.605
6374	9.792	9.915	9.786	6466	9.707	9.817	9.710	6558	9.591	9.707	9.603
6376	9.787	9.904	9.788	6468	9.698	9.812	9.704	6560	9.588	9.708	9.601
6378	9.782	9.898	9.791	6470	9.693	9.808	9.596	6562	9.589	9.704	9.594
6380	9.791	9.903	9.788	6472	9.693	9.811	9.683	6564	9.591	9.693	9.587
6382	9.778	9.903	9.784	6474	9.682	9.799	9.582	6566	9.590	9.695	9.585
6384	9.776	9.901	9.785	6476	9.680	9.786	9.681	6568	9.590	9.696	9.589
6386	9.774	9.888	9.784	6478	9.677	9.777	9.680	6570	9.591	9.702	9.594
6388	9.773	9.884	9.779	6480	9.660	9.766	9.673	6572	9.597	9.701	9.593
6390	9.762	9.879	9.776	6482	9.653	9.758	9.663	6574	9.597	9.703	9.593

Table 25 Runway System Parameters (6 Degree)

SYMBOL	TYPE	VALUE	UNITS	DESCRIPTION
$H_{RC}(i)$	C	*	Ft	Center runway elevation profile
$H_{RL}(i)$	C	*	Ft	Left runway elevation profile
$H_{RR}(i)$	C	*	Ft	Right runway elevation profile
w	V (o)		In/In	Runway slope at coordinate (X,Y)
x	V (I)		In	Distance down the runway
X_{LIZO} ★	C	0.0	Ft	Determines starting point (at time = 0) on runway profile
X_{LEF}	V		Ft	Determines position on runway profile
y	V (I)		In	Distance from runway C., Inches
Y_{LEF}	V		Ft	Distance from runway C., Feet
z	V (o)		In	Runway elevation at coordinate (X,Y)
Z_{ECO}	C	±	Ft	Center profile height at time = 0
Z_{GCX}	V		Ft	Center profile height
Z_{OLO}	C	±	Ft	Left profile height at time = 0
Z_{OLX}	V		Ft	Left profile height
Z_{ERO}	C	±	Ft	Right profile height at time = 0
Z_{ERX}	V		Ft	Right profile height

* See Table 24 for values of H_{RC} , H_{RL} and H_{RE} . Use station 4574 to 6574.

± Determined from the constant X_{LRO}

★ This input allows starting the airplane on a different part of the runway profile even though its distance down the runway is the same.

SECTION IV

TOTAL SYSTEM ANALYSIS

Three different total system mathematical models have been formulated to perform antiskid analysis. The first model which is referred to as the flywheel system represents an antiskid system installed on a wheel and brake which are mounted on a dynamometer. The second system, referred to as the three degree system, represents an antiskid system installed on a wheel and brake mounted on a rigid airplane which is allowed three degrees of freedom (longitudinal translation down the runway, translation vertically, and pitch rotation). The third system, referred to as the six degree system, represents a rigid airplane having all six degrees of freedom and equipped with a conventional single wheeled main landing gear incorporating independent antiskid control of each brake. All of these systems are created utilizing the models described in Section III. The basic reason for utilizing three models is economics. The six degree system takes at least twice as long to run as the flywheel system and not all antiskid system parameters require the sophistication of the six degree system. However, it might be necessary to check certain effects under the most comprehensive circumstances.

The "Basic Control System" is made of the following models as described in Section III:

1. Brake System
2. Hydraulic System
3. Wheel Speed Sensor
4. Control System
5. Antiskid Control Valve

To form the flywheel system, the "Basic Control System" is combined with the 3a. Airplane System (Flywheel), 4a. Wheel and Tire System (Flywheel), and the 9a. Runway System. To form the three degree system, the "Basic Control System" is combined with the 3b. Airplane System (3 Degree), 4b. Wheel and Tire System (3 Degree), 8. Horizontal Tail Control System, and 9a. Runway System. The six degree system incorporates two separate "Basic Control Systems" and two separate 4c. Wheel and Tire Systems. These are combined with a 3c. Airplane System (6 Degree) which utilizes the

8. Horizontal Tail Control and 9c. Runway System (6 Degree). The model flow diagrams are shown in Figures 64 , 65 , and 66 . When utilizing the "Basic Control Systems" with the six degree system, the variables communicating with the airplane model are reidentified to correspond to the right or left side of the airplane. Thus, X_{AXR} is X_{AX} in the right side and X_{AXL} is X_{AX} in the left side.

The high degree of modularity used in this analysis is desirable for three reasons. The first reason is that it is easy to combine the component models together to form different types of overall systems. This is true not only from modeling considerations but especially from programming aspects. As an example, the only basic change required to accommodate a twin or tandem gear would be to remodel the strut in the airplane system. The second reason for modularity is the difficulty in being completely general. Should a component arise which is not described by the existing models, it is easy to create a new program for the new model without having to modify the operation of other systems. Thus, from the programming point of view, to incorporate a new wheel speed sensor for example, the new model program can fall back on the existing read, write, and logic statements of the existing wheel speed model. The input and output variables of the new component model are automatically incorporated properly into the overall computational procedure, unless some new variables are defined. The third reason for using a modular approach is to take advantage of the different response characteristics of the different component models. In the digital procedures utilized for computation, essentially a "fixed step" integration technique is employed. The step size used in a "slow" responding model does not have to be as small as one used in a "fast" model. Thus, different component models utilize different size integration steps which minimizes the overall time of computation.

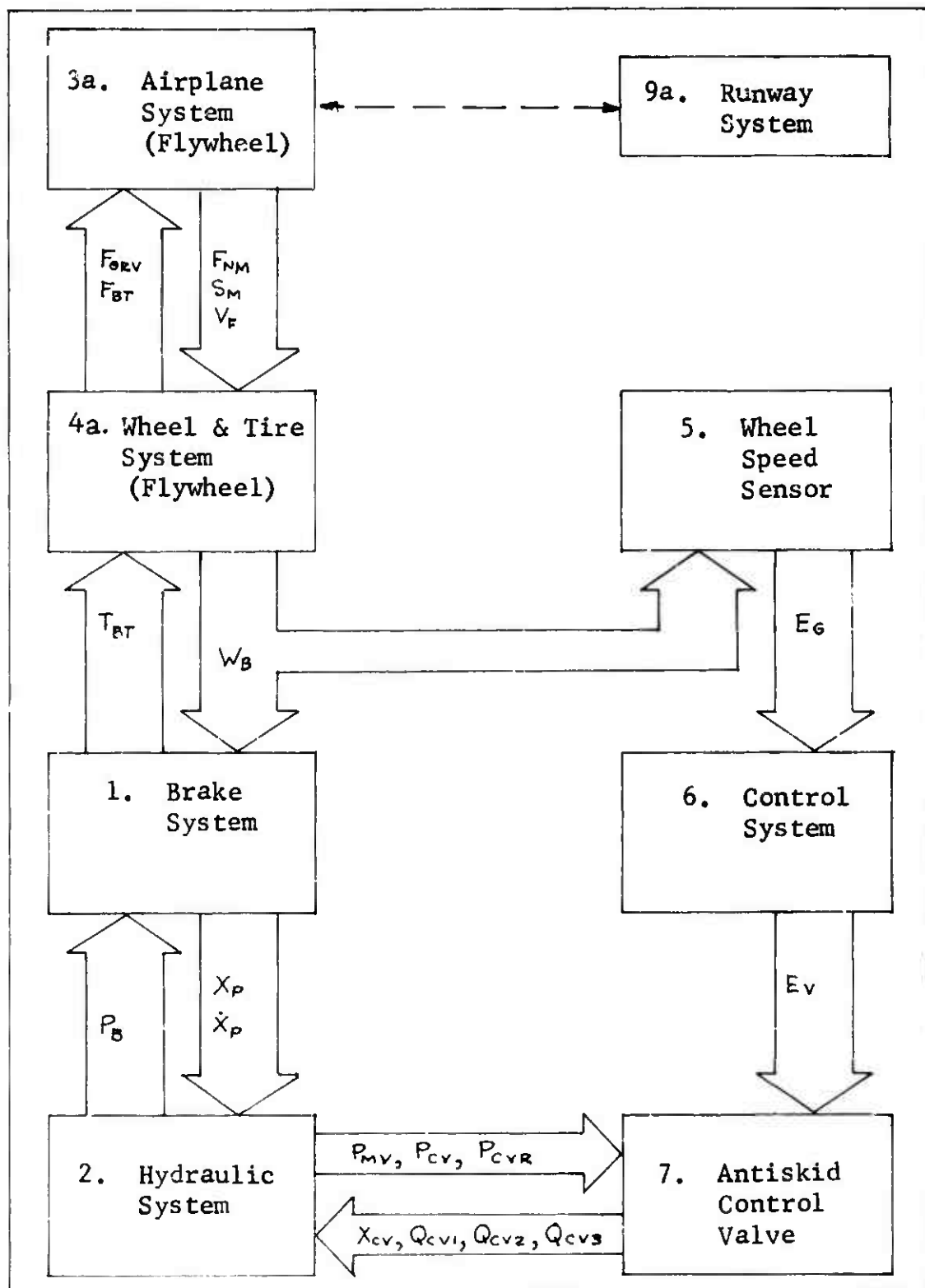


Figure 64 Flywheel System

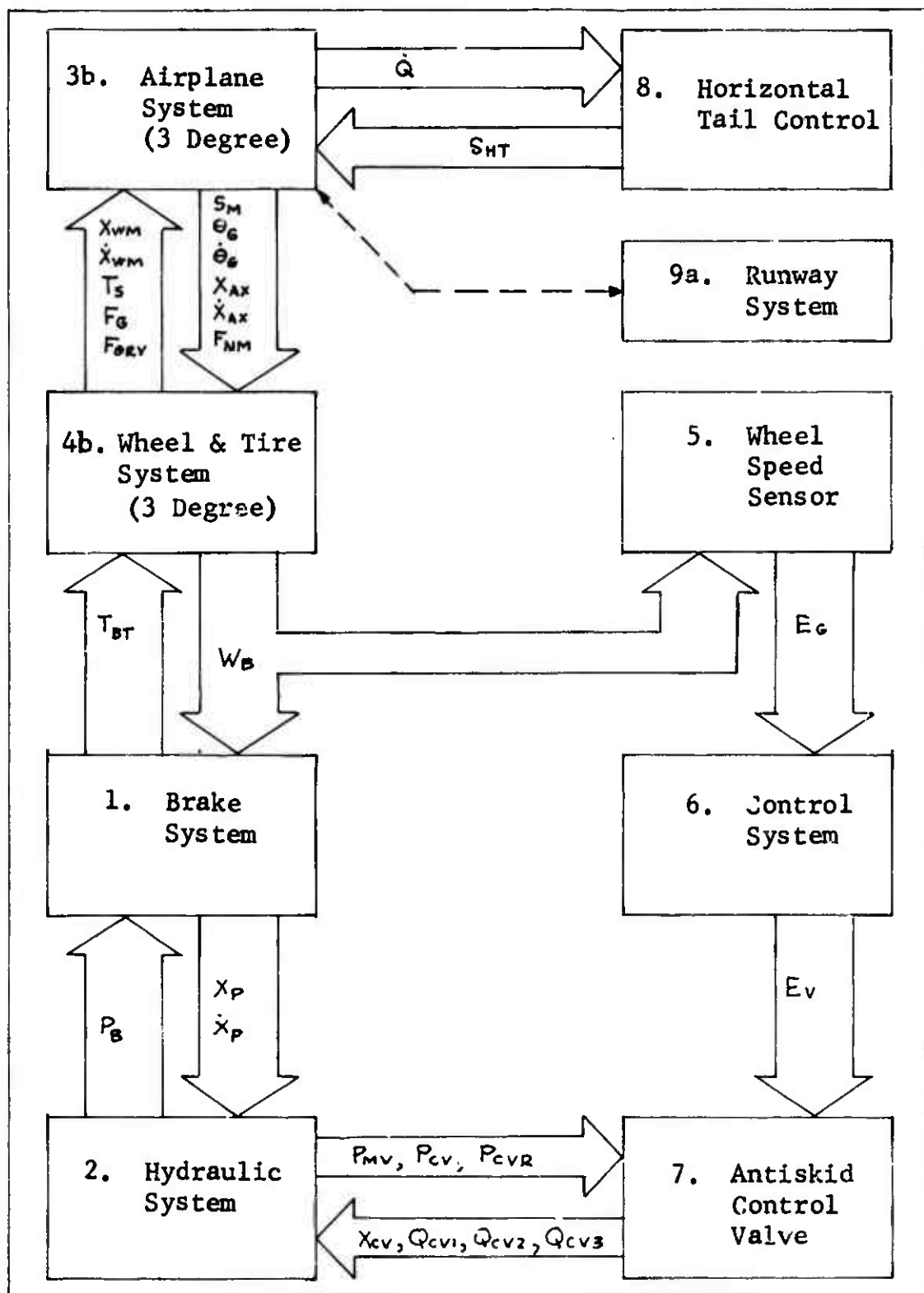


Figure 65 Three Degree System

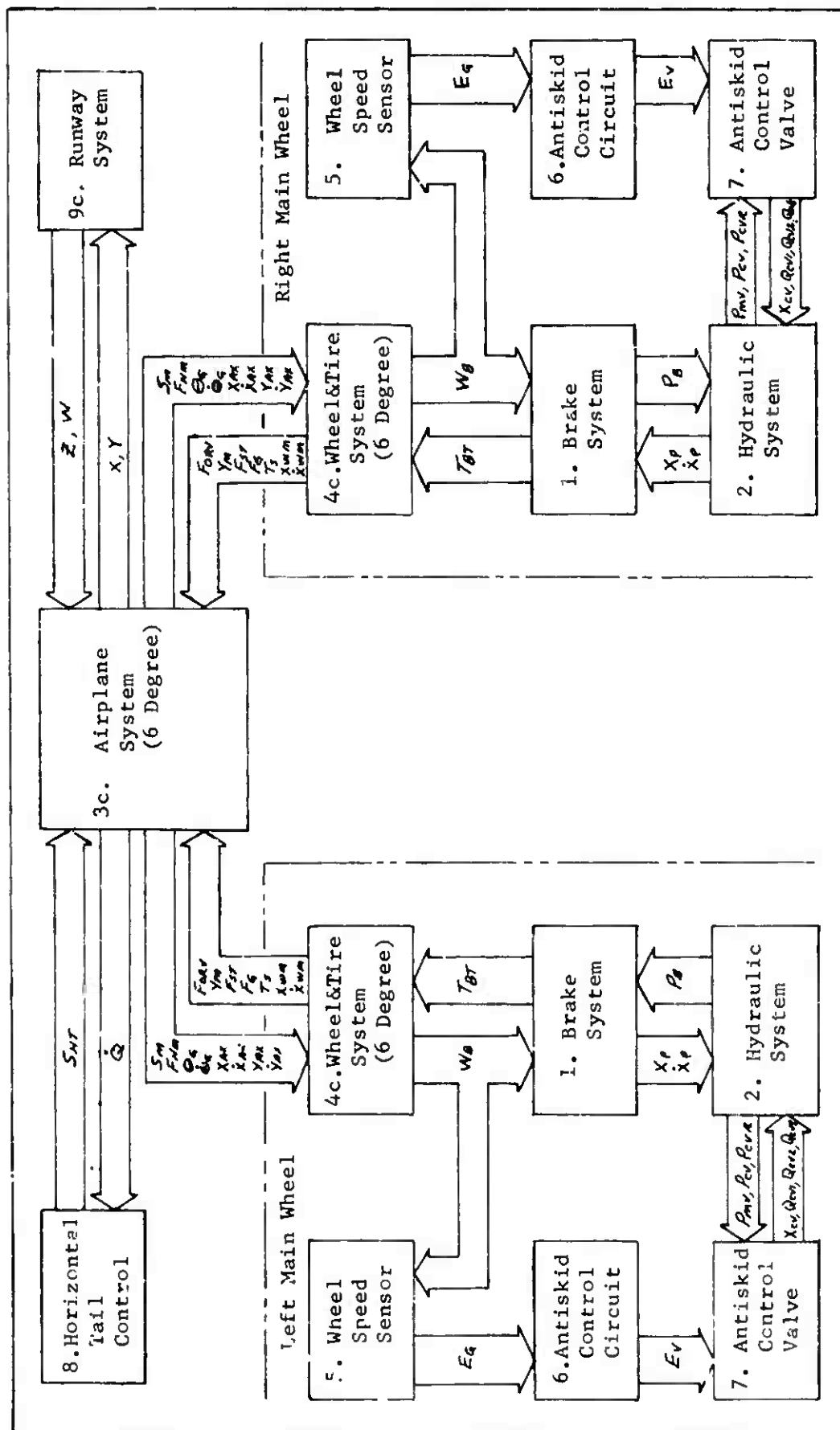


Figure 66 Six Degree System

SECTION V

SAMPLE CASE ANALYSIS

A digital computer solution of the composite total system mathematical models for the flywheel and three degree systems have been programed and checked out. In addition, during the development of the individual component mathematical models an analog computer program was used to conduct various explorations and prove the equations. Figure 67 presents an example of on-off antiskid operation as recorded from the analog computer program of the flywheel system. The analog computer results are shown because they are more easily related to aircraft operational data. The digital computer program is a solution of the same equations.

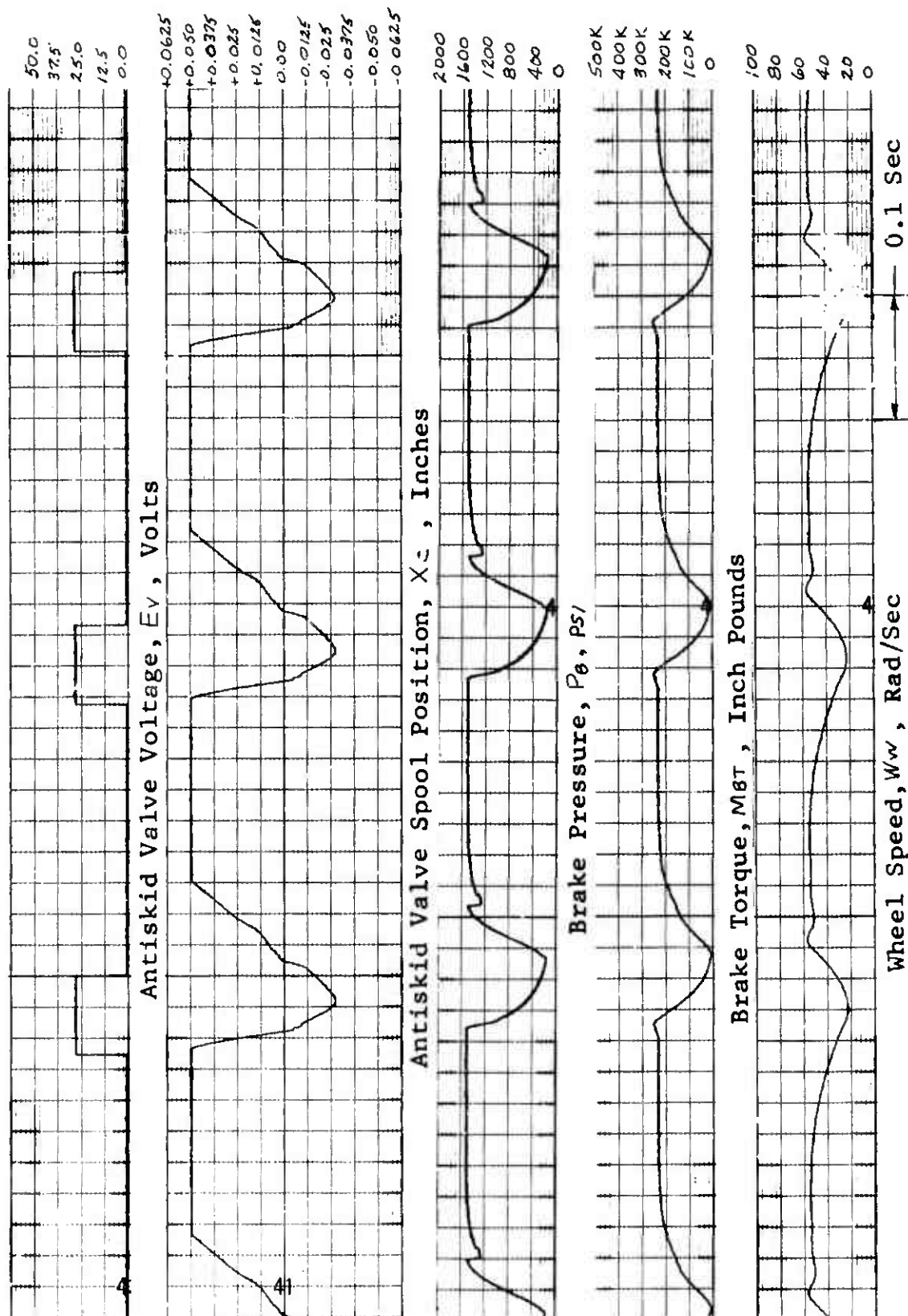


Figure 67 Analog Computer On-Off Antiskid Operation

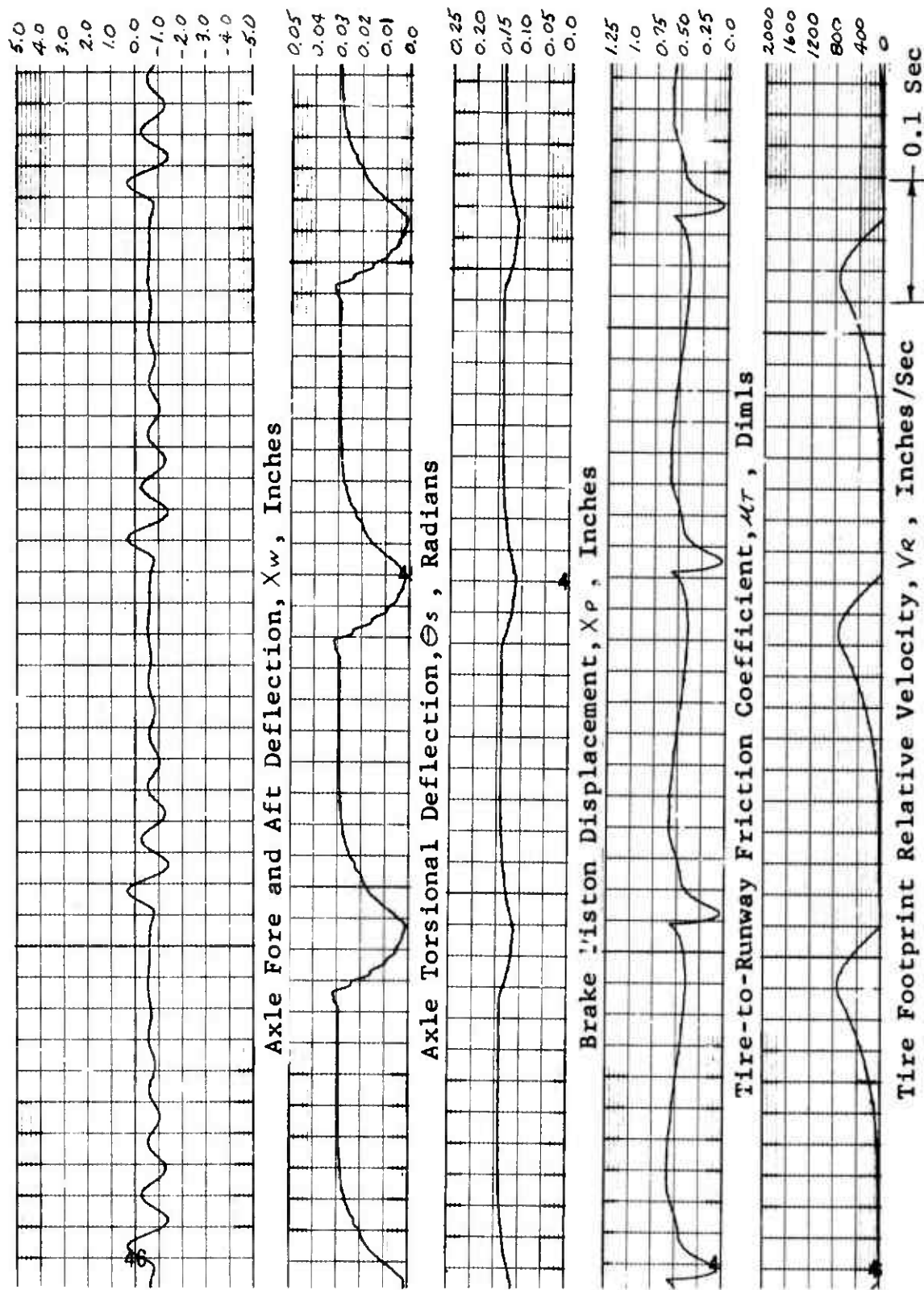


Figure 67 (Contd)

REFERENCES

1. Smiley, Robert F. and Horne, Walter B. Mechanical Properties of Pneumatic Tires with Special Reference to Modern Aircraft Tires. NASA TR R-64.
2. Leland, T. J. W. and Taylor, G. R. Effects of Tread Wear on the Wet Runway Braking Effectiveness of Aircraft Tires. J. Aircraft Vol. 2 No. 2, March - April 1965.
3. Horne, W. B. and Leland, T. J. W. Influence of Tire Tread Pattern and Runway Surface Condition of Braking Friction and Rolling Resistance of a Modern Aircraft Tire. NASA TN D-1376.
4. Parker O-Ring Handbook, Parker Seal Company, Culver City, California, Cleveland, Ohio. Catalog 5700, June 1957
5. Daugherty, R. L. and Ingersoll, A. C. Fluid Mechanics McGraw-Hill 1954.
6. Blackburn, J. F., Reethof, G., and Shearer, J. L. Fluid Power Control. The M. I. T. Press 1960.
7. Lee, L. T. A Graphical Compilation of Damping Properties of Both Metallic and New Metallic Materials. AFML-TR-66-169. May 1966.
8. Ungar, E. E. and Hatch, D. K. High Damping Materials Prod. Eng. Vol. 32, No. 16, pp. 44-56, April 17, 1961.
9. Campbell, James E. Investigation of the Fundamental Characteristics of High Performance Hydraulic Systems, USAF Technical Report No. 5997, June 1950 ATI No. 91966.
10. Tanner, J. A. and Batterson, S. A. An Experimental Study of the Elastic Properties of Several Aircraft Tires During the Application of Braking Loads. Langley Working Paper 592. May 6, 1968.
11. Morris, J. G. Three Track Elevation Profiles Measured at Two United States Government Installations. NASA TN D-5545.

REFERENCES

(Continued)

12. Thomson, W. T. Mechanical Vibrations. Prentice-Hall, Inc. 1953.
13. Technical Manual No. T. O. 4BA8-22-3, Overhaul Instructions with Illustrated Parts Breakdown, Skid Control Box Part No. 9543941 (Goodyear)
14. Transistor Circuit Design, Engineering Staff of Texas Instruments, Inc., Edited by Joseph A. Walston and John R. Miller, McGraw-Hill Book Co. 1963
15. Riddle, Robert L. and Ristenbatt, Marlin P. Transistor Physics and Circuits. Prentice Hall 1958.
16. Nanavati, Rajendra P. An Introduction to Semiconductor Electronics, McGraw-Hill Book Company 1963.

APPENDIX I

DERIVATION OF EQUATIONS DESCRIBING THE OPERATION OF THE GOODYEAR ADAPTIVE ELECTRONIC ANTISKID CONTROL CIRCUIT

The mathematical description of the operation of the Goodyear adaptive electronic antiskid control circuit as shown on Figure 50 is developed with conventional circuit analysis techniques using Kirchhoff's Laws. Figure 68 is the schematic diagram from Figure 50 with the transistors and diodes shown in terms of their equivalent circuits and the various currents and voltages identified. The transistor and diode equivalent circuits are adaptations of equivalent circuits developed and described in references 13, 14 and 15. Some of the diode forward resistances are combined with other resistance in series with the diodes and are not shown separately. Also, since the current through R_6 (the output resistance of the wheel speed signal source) has three non-mutually influencing components, R_6 is included in R_3 , R_{08} and R_{15} to simplify equations. Other simplifications will be described and discussed during the development of equations.

Referring to Figure 68, the circuit equations are developed as follows:

The voltage across capacitor C_1 is defined as:

$$(1) \quad V_{C1} = \int V_{C1} \, dt$$

$$(A1) \quad \dot{V}_{C1} = A_{C1}/C_1 \quad \text{OR} \quad \dot{V}_{C1} = A_{C1} C_{608}$$

A_{C1} is the current through C_1 and C_1 is the capacitance. A_{C1} is established by summing currents at node (N11) as:

$$(N11) \quad A_{C1} = A_{08} - A_{12}$$

Using Ohm's law and summing voltages around the loop of which R_{08} is a part, A_{08} is established as:

$$(R10) \quad A_{08} = (E_G - V_{C1} - E_{08})/R_{08} \quad \text{FOR } (E_G - V_{C1} - E_{08}) > 0$$

$$= 0 \quad \text{FOR } (E_G - V_{C1} - E_{08}) \leq 0$$

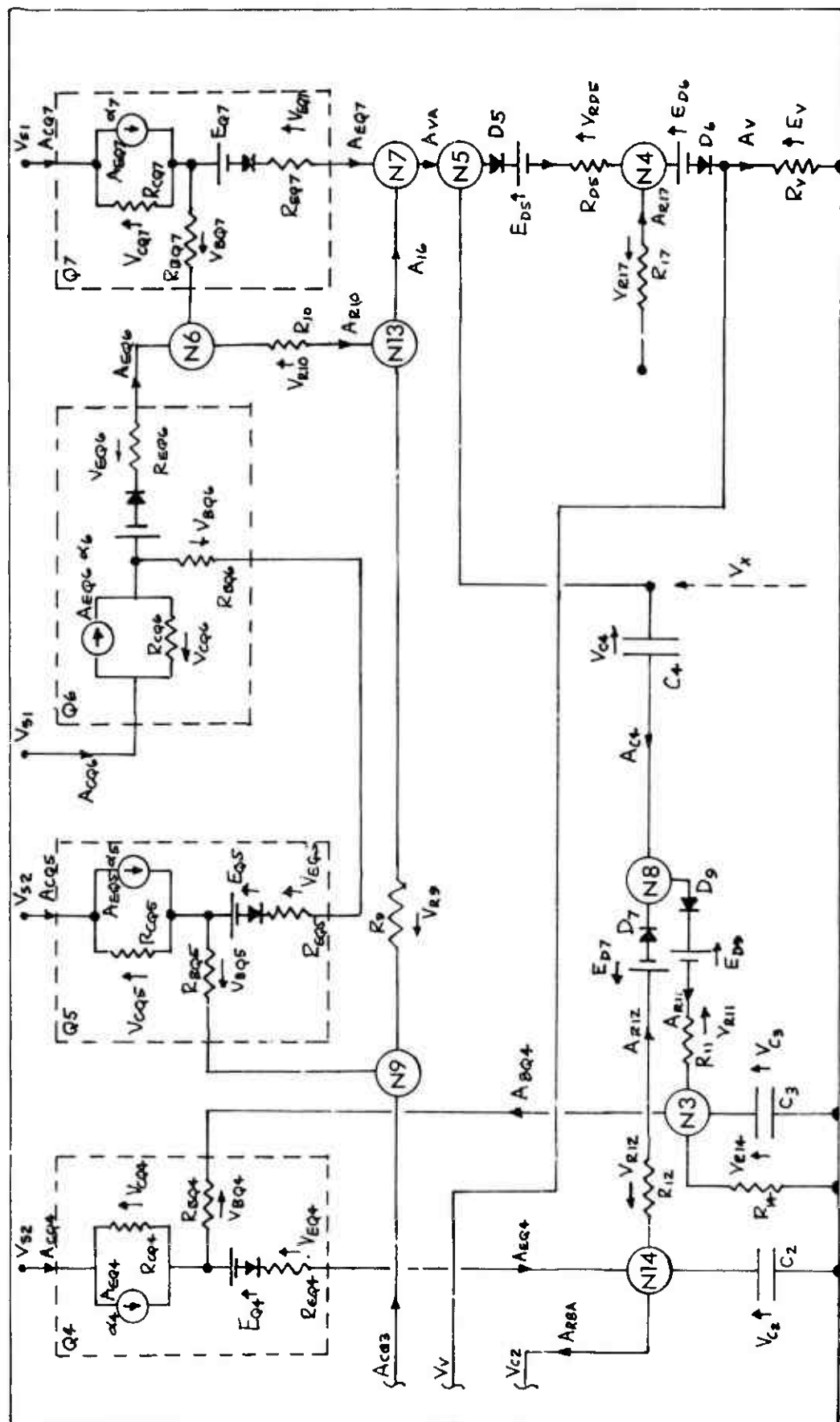


Figure 68 (Contd)

Noting that because of diode D_8 , A_{D8} is restricted to positive values only.

To combine constants, write equation (R10) as:

$$(R10) \quad A_{D8} = (E_G - V_{C1}) C_{620} - C_{621} \quad \text{FOR } (E_G - V_{C1}) > C_{620}/C_{621} \\ = 0 \quad \text{FOR } (E_G - V_{C1}) \leq C_{620}/C_{621}$$

By summing currents at Node (N12), current A_{12} is established as:

$$(N12) \quad A_{12} = A_{R3} + A_{CQ1}$$

Substituting equation (N12) into equation (N11) gives:

$$(N11)' \quad A_{C1} = A_{D8} - A_{R3} - A_{CQ1}$$

To compute A_{CQ1} it is desirable to first obtain equations for the voltages at the base and emitter of Q_1 in terms of the base and emitter currents and the appropriate voltage sources. The voltage at the base of Q_1 is V_{R1} . Summing currents at Node (N1) establishes current A_{R1} as:

$$(N1) \quad A_{R1} = A_{BQ1} + A_{R8A}$$

Summing voltages around the loop R_1, R_{8A}, R_{8B} to V_{C2} gives: $V_{R8A} + V_{R8B} = V_{C2} - V_{R1}$. If the current through diode D_4 is assumed negligible, then $A_{R8A} = A_{R8B}$. (Because of the relative resistances, the current through D_4 is a very small fraction of the current through R_{8B}). By Ohm's law, $V_{R8A} + V_{R8B} = A_{R8A} (R_{8A} + R_{8B})$ and $V_{R1} = A_{R1} R_1$. Substitution into equation (N1) and solving for V_{R1} gives:

$$(N1)' \quad V_{R1} = R_1 \left(A_{BQ1} + \frac{V_{C2}}{R_{8A} + R_{8B}} \right) / \left(1 + \frac{R_1}{R_{8A} + R_{8B}} \right)$$

The voltage at Node (N2) is $E_{D2} + V_{R02}$. (Here two diodes $D2$ and $D3$ as shown on Figure 50 are combined in an equivalent single diode). Summing currents at Node (N2) establishes current A_{D2} as:

$$(N2): A_{D2} = A_{R4} - A_{R5} - A_{EQ1}$$

By Ohm's law, $V_{R02} = A_{D2} R_{D2}$, $V_{R4} = A_{R4} R_4$, and $(V_{R5A} + V_{R5B}) = A_{R5} (R_{5A} + R_{5B})$ (Note: Because of the relative resistances, A_{R6} is a very small component of the current in R_{5A} and is assumed to be zero when computing V_{R02} .) Summing voltages around the appropriate loops establishes that $V_{R4} = V_{S1} - V_{R02} - E_{D2}$ and $V_{R5A} + V_{R5B} = V_{R02} + E_{D2}$. By substitution into equation (N2) and solving for V_{R02} gives:

$$(N2)': V_{R02} = \frac{\left[\frac{V_{S1}}{R_4} - E_{D2} \left(\frac{1}{R_4} + \frac{1}{R_{5A} + R_{5B}} \right) - A_{EQ1} \right]}{\left(\frac{1}{R_{D2}} + \frac{1}{R_4} + \frac{1}{R_{5A} + R_{5B}} \right)}$$

Summing voltages around the loop through which A_{BQ1} (the base of current $Q1$) flows results in:

$$(Q-1) E_{D2} + V_{R02} - V_{R2} - V_{EQ1} - E_{Q1} - V_{BQ1} - V_{R1} = 0$$

By substituting $V_{R2} = A_{EQ1} R_2$, $V_{EQ1} = A_{EQ1} R_{EQ1}$ and $V_{BQ1} = A_{BQ1} R_{BQ1}$ (From Ohm's Law) along with equations (N1)', (N2)', and the basic transistor relationship $A_{EQ1} = (h_{FE1} + 1) A_{BQ1}$ into equation (Q-1) and solving for A_{EQ1}

$$(Q-1)': A_{EQ1} = C_{602} - C_{603} V_{C2}, \text{ WHERE}$$

$$C_{602} = \frac{\left\{ E_{D2} \left[1 - \left(\frac{1}{R_4} + \frac{1}{R_5} \right) / \left(\frac{1}{R_{D2}} + \frac{1}{R_4} + \frac{1}{R_5} \right) \right] + V_{S1} \left(\frac{1}{R_4} \right) / \left(\frac{1}{R_{D2}} + \frac{1}{R_4} + \frac{1}{R_5} \right) - E_{Q1} \right\}}{\left\{ R_2 + R_{EQ1} + \frac{R_{BQ1}}{(h_{FE1} + 1)} + \frac{R_1}{(h_{FE1} + 1)} / \left(1 + \frac{R_1}{R_B} \right) + 1 / \left(\frac{1}{R_{D2}} + \frac{1}{R_4} + \frac{1}{R_5} \right) \right\}}$$

$$C_{603} = \frac{\frac{R_1}{R_1 + R_B}}{\left\{ R_2 + R_{EQ1} + \frac{R_{BQ1}}{(h_{FE1} + 1)} + \frac{R_1}{(h_{FE1} + 1)} / \left(1 + \frac{R_1}{R_B} \right) + 1 / \left(\frac{1}{R_{D2}} + \frac{1}{R_4} + \frac{1}{R_5} \right) \right\}}$$

And where in the above $R_5 = R_{5A} + R_{5B}$ and $R_8 = R_{8A} + R_{8B}$.

For Q_1 to operate as a transistor, V_{CQ1} must be positive. Using equation (Q-1)', the basic transistor characteristic (Q2) $A_{CQ1} = h_{FE1} A_{EQ1} / (h_{FE1} + 1)$ and by writing the voltage loop equation through D_2, Q_1, R_{15}, C_1 and (GEN) it can be shown that V_{CQ1} is positive for $(E_G - V_{C1})$ negative; therefore, equation (Q-1)' is applicable only for $(E_G - V_{C1}) < 0$. Substituting (Q-1) into (Q-2) gives the following equation:

$$\begin{aligned} (Q-1C) \quad A_{CQ1} &= C_{604} - C_{605} V_{C2} \quad \text{FOR } (E_G - V_{C1}) < 0 \\ &= 0 \quad \text{FOR } (E_G - V_{C1}) \geq 0 \\ &= 0 \quad \text{FOR } V_{C2} \geq C_{604} / C_{605} \end{aligned}$$

$$C_{604} = C_{602} \left(\frac{h_{FE1}}{h_{FE1} + 1} \right)$$

$$C_{605} = C_{603} \left(\frac{h_{FE1}}{h_{FE1} + 1} \right)$$

By summing currents at node (N10), current A_{R3} is established as:

$$(N10) \quad A_{R3} = A_{EQ2} + A_{R7}$$

To compute the components of A_{R3} (i.e., A_{EQ2} and A_{R7}) it is desirable to have equation (N10) in a form where A_{R7} is expressed in terms of the appropriate voltages and resistances. By summing voltages around the loop R_V, R_7, R_3, C_1 and GEN , V_{R7} is established as:

$$(V7) \quad V_{R7} = E_V - V_{R3} - (E_G - V_{C1})$$

Substituting equation (V7) along with $V_{R3} = A_{R3} R_3$ and $V_{R7} = A_{R7} R_7$ into (N10) gives:

$$(N10)' \quad A_{R3} = \frac{A_{EQ2}}{1 + R_3/R_7} + \frac{E_V}{(R_7 + R_3)} - \frac{(E_G - V_{C1})}{(R_7 + R_3)}$$

To combine constants write as:

$$(N10)' \quad A_{R3} = A_{EQ2} C_{612} + [E_V - (E_G - V_{C1})] C_{613}$$

To compute current A_{EQ2} , sum voltages around the loop through which A_{BQ2} flows:

$$(Q-2) \quad V_Y - V_{BQ2} - E_{Q2} - V_{EQ2} - V_{R3} - (E_6 - V_{C1}) = 0$$

Here voltage V_Y is the base voltage on Q2 and is either $(V_{R5B} - V_{R6})$ or $(V_{C2} - V_{R8B} - E_{D4})$ whichever is the largest; therefore, there will be a version of equation (Q-2) for each of these conditions. To establish which condition exists, it is necessary to compute $(V_{R5B} - V_{R6})$ and $(V_{C2} - V_{R8B} - E_{D4})$

During derivation of Equation (N2)' it was observed that $V_{R5A} + V_{R5B} = V_{R02} + E_{D2}$ and it was assumed that A_{R6} was small when compared to A_{R5} . Using the same assumption V_{R5B} is established as follows by Ohm's Law:

$$(R-5) \quad V_{R5B} = A_{R5} R_{5B}$$

By substituting $A_{R5} (R_{5A} + R_{5B}) = V_{R5A} + V_{R5B}$ into equation (R-5) above gives:

$$(R-5)' \quad V_{R5B} = R_{5B} (V_{R02} + E_{D2}) / (R_{5A} + R_{5B})$$

By substituting equation (N2)' for V_{R02} and investigating the influence of A_{EQ1} within its allowable range, it can be seen that for practical purposes V_{R5B} is a constant.

To compute V_{R6} , it can be seen that A_{R6} equals A_{BQ2} when V_Y is $V_{R5B} - V_{R6}$; therefore, $V_{R6} = A_{BQ2} R_6$ by Ohm's law.

By Ohm's Law $V_{R8B} = A_{R8B} R_{8B}$. Since the current through D4 is very small and may be assumed zero, and since A_{BQ1} is such a small component of the current through R1 that it can be assumed zero, by Ohm's Law:

$$(V8) \quad A_{R8B} = A_{R8A} = V_{C2} / (R_1 + R_{8A} + R_{8B})$$

Therefore:

$$(V_{C2} - V_{R5B} - E_{D4}) = \left[V_{C2} \left(\frac{R_1 + R_{\theta A}}{R_1 + R_{\theta A} + R_{\theta B}} \right) - E_{D4} \right]$$

To establish whether $V_Y = (V_{R5B} - V_{R6})$ OR

$$V_Y = \left[V_{C2} \left(\frac{R_1 + R_{\theta A}}{R_1 + R_{\theta A} + R_{\theta B}} \right) - E_{D4} \right]$$

A voltage V_B will be defined as follows:

$$(VB) \quad V_B = \left[V_{C2} \left(\frac{R_1 + R_{\theta A}}{R_1 + R_{\theta A} + R_{\theta B}} \right) - E_{D4} \right] - (V_{R5B} - R_6 A_{BQ2})$$

$$\text{if } V_B > 0, (VY-1) \quad V_Y = [V_{C2} C_m - E_{D4}]$$

$$\text{if } V_B \leq 0, (VY-2) \quad V_Y = [V_{R5B} - R_6 A_{BQ2}]$$

where C_m above is defined as:

$$C_m = \left(\frac{R_1 + R_{\theta A}}{R_1 + R_{\theta A} + R_{\theta B}} \right)$$

Before proceeding with the computation of A_{R3} , the valve control amplifier and modulation circuit elements will be examined to develop equations for E_V and V_{C2} .

By summing currents at Node (N5) current A_{D5} is established as:

$$(N5) \quad A_{D5} = A_{VA} - A_{C4}$$

The voltage at Node (N5) is defined as V_X . Summing voltages around the loop R_V , D_6 , D_5 and V_X gives:

$$(VX) \quad V_X = E_V + E_{D6} + V_{R_{D5}} + E_{D5}$$

$$(EV) \quad E_V = A_{D5} C_{406} + C_{407}$$

By summing currents at Node (N4), current A_{R17} is established as:

$$(N4) \quad A_{R17} = A_V - A_{D5}$$

By substituting equations (N4), (N5), and (EV) into equation (VX) and by using Ohm's Law to establish that $E_V = A_V R_V$, $V_{R17} = A_{R17} R_{17}$ and $V_{R05} = A_{D5} R_{D5}$, VX is established as:

$$(VX) \quad V_X = A_{D5} C_{406} + C_{401}$$

By substituting equation (EV) into (N4) and using the relationships $E_V = A_V R_V$ and $V_{R17} = A_{R17} R_{17}$ EV is established as:

$$(N4) \quad E_V = A_{D5} C_{406} + C_{407}$$

The operation of transistors Q2, Q3, Q5, Q6, and Q7 will now be considered to develop an equation for current A_{VA} (Valve Control Amplifier Output Current).

By summing currents at Node (N7) current A_{VA} is established as:

$$(N7) \quad A_{VA} = A_{EQ7} + A_{I6}$$

By summing currents at Node (N13), current A_{I6} is established as:

$$(N13) \quad A_{I6} = A_{R10} + A_{R9}$$

By summing currents at Node (N6), current A_{R10} is established as:

$$(N6) \quad A_{R10} = A_{EQ6} - A_{BQ7}$$

By summing currents at Node (N9), current A_{R9} is established as:

$$(N9) \quad A_{R9} = A_{CQ3} - A_{BQ5}$$

Summing voltages around the loop, R_{EQ7} , R_{BQ7} and R_{10} gives:

$$(V10) \quad V_{R10} = V_{EQ7} + E_{Q7} + V_{BQ7}$$

By using the relationships $V_{R10} = A_{R10} R_{10}$, $V_{EQ7} = A_{EQ7} R_{EQ7}$ and $V_{BQ7} = A_{BQ7} R_{BQ7}$ as established by Ohm's law along with the transistor characteristic $A_{EQ7} = (h_{FE7} + 1) A_{BQ7}$ and substitution equation (N6) into (V10) and solving for A_{BQ7} :

$$(V10)' \quad A_{BQ7} = \frac{A_{EQ6} R_{10} - E_{Q7}}{[(h_{FE7} + 1) R_{EQ7} + R_{BQ7} + R_{10}]}$$

By substituting (V10)' and (N6) into the relationship $V_{R10} = A_{R10} R_{10}$

$$(A10) \quad V_{R10} = A_{EQ6} C_{402} + C_{403} E_{Q7}$$

Summing voltages around the loop R_{10} , R_{EQ6} , R_{BQ6} , R_{EQ5} , R_{BQ5} and R_9 gives:

$$(V9) \quad 0 = V_{R10} + V_{EQ6} + E_{Q6} + V_{BQ6} + V_{EQ5} + E_{Q5} + V_{BQ5} - V_{R9}$$

By substituting equations (A10) and (N9) into (V9) along with transistor characteristics $A_{EQ6} = (h_{FE6} + 1) A_{BQ6}$ and $A_{EQ5} = (h_{FE5} + 1) A_{BQ5}$ and the Ohm's Law relationships $V_{R9} = A_{R9} R_9$, $V_{EQ6} = A_{EQ6} R_{EQ6}$, $V_{BQ6} = A_{BQ6} R_{BQ6}$, $V_{EQ5} = A_{EQ5} R_{EQ5}$ and $V_{BQ5} = A_{BQ5} R_{BQ5}$ and solving for A_{EQ6} :

$$(V9)' \quad A_{EQ6} = \frac{A_{CQ3} R_9 - (E_{Q6} + E_{Q5} + C_{403} E_{Q7})}{\left[C_{402} + R_{EQ6} + \frac{R_{BQ6} + R_{EQ5}}{(h_{FE6} + 1)} + \frac{R_{BQ5} + R_9}{(h_{FE5} + 1)(h_{FE6} + 1)} \right]}$$

Substituting equations (N13), (N6), (N9), and (V9)' into equation (N7) along with transistor characteristics $A_{EQ5} = (h_{FE5} + 1) A_{BQ5}$ and $A_{EQ6} = (h_{FE6} + 1) A_{BQ6}$ and solving for A_{VA} gives:

$$(N7)' \quad A_{VA} = A_{CQ3} C_{404} - C_{405}$$

It should be noted that these operations involving Q5, Q6, and Q7 assume that A_{CQ3} is large enough such that A_{VA} is not negative and that the applicable supply voltages, V_{S1} and V_{S2} , are large enough to keep V_{CQ1} , V_{CQ6} and V_{CQ5} positive at all times. The latter assumption can be proven to be true for the range of currents experienced during circuit operation. If A_{CQ3} is not greater than C_{405}/C_{404} , insufficient voltage is developed across R_9 to cause Q5, Q6 and Q7 to operate. For A_{CQ3} less than C_{405}/C_{404} all of A_{CQ3} goes through R_9 and $A_{VA} = A_{CQ3}$; therefore, equation (N7)' has two forms depending on the value of A_{CQ3} . Write these two forms as follows:

$$(N7)'' \quad A_{VA} = A_{CQ3} C_{404} - C_{405} \quad \text{FOR } A_{CQ3} > C_{405}/C_{404}$$

$$= A_{CQ3} \quad \text{FOR } A_{CQ3} \leq C_{405}/C_{404}$$

Supply voltage V_{S2} is large enough so that voltages V_{CQ3} and V_{EQ3} are always positive and a small leakage current A_{CQ30} flows. All the equations developed here are for the increment of A_{CQ3} above the leakage value.

By using the transistor characteristics $A_{CQ3} = h_{FE3} A_{BQ3}$
 $A_{CQ2} = A_{EQ2} h_{FE2} / (h_{FE2} + 1)$

And if at Node N15 $A_{LWS} = 0$, $A_{BQ3} = A_{CQ2}$ then:

$$(Q3) \quad A_{CQ3} = A_{EQ2} C_{606}$$

$$\text{WHERE} \quad C_{606} = \frac{(h_{FE2})(h_{FE2})}{(h_{FE2} + 1)}$$

The operation of the modulating circuit element will now be examined. To compute valve voltage E_V from equation (N4)' the value of current A_{D5} which is established by Equation (N5) is required. Equation (N5) shows that a

component of A_{D5} is A_{C4} . Before developing equations for computing A_{C4} some observations relative to the operation of C4 and Q4 are helpful.

By summing currents at Node (N8) current A_{C4} is established as:

$$(N8) \quad A_{C4} = A_{R11} - A_{R12}$$

However, because of diodes D7 and D9 currents A_{R11} and A_{R12} have limitations depending upon the direction of voltage across the diodes. Summing voltages around the loop C3, R11, D9, C4 to V_X gives:

$$(V11) \quad V_{C3} + V_{R11} + E_{D9} + V_{C4} - V_X = 0$$

Substituting equation (V11) into the expression $V_{R11} = A_{R11} R_{11}$ as established by Ohm's law gives:

$$(V11)' \quad A_{R11} = \frac{V_X - V_{C4} - E_{D9} - V_{C3}}{R_{11}} \quad \text{FOR } (V_X - V_{C4} - E_{D9} - V_{C3}) > 0$$

Because of D9, $A_{R11} = 0$ FOR $(V_X - V_{C4} - E_{D9} - V_{C3}) \leq 0$

Summing voltages around the loop C3, R12, D7, C4, to V_X gives:

$$(V12) \quad V_{C2} - V_{R12} - E_{D7} + V_{C4} - V_X = 0$$

Substituting equation (V12) into the expression $V_{R12} = A_{R12} R_{12}$ as established by Ohm's law gives:

$$(V12)' \quad A_{R12} = \frac{V_{C2} - E_{D7} + V_{C4} - V_X}{R_{12}} \quad \text{FOR } (V_{C2} - E_{D7} + V_{C4} - V_X) > 0$$

Because of D7 $A_{R12} = 0$ FOR $(V_{C2} - E_{D7} + V_{C4} - V_X) \leq 0$

Summing voltages around the loop C3 through Q4 to C2 gives:

$$(V-Q4) \quad V_{C3} - V_{BQ4} - E_{Q4} - V_{EQ4} - V_{C2} = 0$$

Since the currents A_{BQ4} and A_{EQ4} in transistor Q4 are restricted to positive values only, voltages V_{BQ4} and V_{EQ4} are always positive; therefore, equation (V-Q4) shows that V_{C2} is always less than V_{C3} by an amount at least equal to E_{Q4} . Also, because of diodes D7 and D9, no current can flow from C3 through R11, D9, D7 and R12 to C2. For these circumstances, it is observed (1) that for A_{C4} positive, all of A_{C4} passes through R11 and all of A_{R11} is A_{C4} and (2) that for A_{C4} negative, all of A_{C4} passes through R12 and all of A_{R12} is $-A_{C4}$.

Since there cannot be positive A_{R11} and positive A_{R12} simultaneously, equation (N8) evolves to:

$$\begin{aligned} (N8)' \quad A_{C4} &= A_{R11} & \text{FOR } A_{R11} > 0 \\ A_{C4} &= 0 & \text{FOR } A_{R11} = 0 \text{ AND } A_{R12} = 0 \\ A_{C4} &= -A_{R12} & \text{FOR } A_{R12} > 0 \end{aligned}$$

By substituting equations (N5), (VX)' and (N7)'' into equations (V11)' and (V12)', equations for A_{C4} are developed for each case.

The remaining equations for the modulation circuit element will now be developed. Substituting the expressions $V_{BQ4} = A_{BQ4} R_{BQ4}$ and $V_{EQ4} = A_{EQ4} R_{EQ4}$ as established by Ohm's law along with the transistor characteristic $A_{EQ4} = (h_{FE4} + 1) A_{BQ4}$ into equation (V-Q4) and solving for A_{BQ4} gives:

$$\begin{aligned} (V-Q4)' \quad A_{BQ4} &= \frac{V_{C3} - E_{Q4} - V_{C2}}{[R_{BQ4} + (h_{FE4} + 1) R_{EQ4}]} \\ & \text{FOR } (V_{C3} - E_{Q4} - V_{C2}) > 0 \\ &= 0 & \text{FOR } (V_{C3} - E_{Q4} - V_{C2}) \leq 0 \end{aligned}$$

To combine constants, write equation (V-Q4) as:

$$\begin{aligned}
 (V-Q4) \quad ABQ4 &= (V_{C3} - V_{C2}) C_{622} - C_{623} \\
 &\quad \text{FOR } (V_{C3} - V_{C2}) > C_{623} / C_{622} \\
 &= 0 \quad \text{FOR } (V_{C3} - V_{C2}) \leq C_{623} / C_{622}
 \end{aligned}$$

Also, since current AEQ4 is needed, define the transistor characteristic as equation Q4:

$$\begin{aligned}
 (Q-4) \quad AEQ4 &= ABQ4 C_{614} \\
 \text{where } C_{614} &= (h_{FE4} + 1)
 \end{aligned}$$

By summing currents at Node (N14) current $AC2$ is established as:

$$(N14) \quad AC2 = AEQ4 - AR12 - AR8A$$

Using the same assumption relative to $AR8A$ as was made for equations (N1)' and (V8) and by Ohm's Law $AR8A$ is established by equation (V8) as:

$$(V8) \quad AR8A = \frac{V_{C2}}{R_1 + R_{8A} + R_{8B}} \quad (\text{Repeated})$$

By summing currents at Node (N3) current $AC3$ is established as:

$$(N3) \quad AC3 = AR11 - AR14 - ABQ4$$

Current $AR14$ is computed from $V_{C3} = AR14 R_{14}$ established by Ohm's law and $ABQ4$ is computed from equation (V-Q4)' and Equation (Q-4).

Equation (N8)' establishes that:

$$\begin{aligned} AR_{12} &= -AC_4 && \text{FOR } AC_4 < 0 \\ &= 0 && \text{FOR } AC_4 \geq 0 \end{aligned}$$

$$\begin{aligned} AR_{11} &= AC_4 && \text{FOR } AC_4 > 0 \\ &= 0 && \text{FOR } AC_4 \leq 0 \end{aligned}$$

Substituting the above and equation (V8) into equation (N14) gives:

$$\begin{aligned} (N14)' \quad AC_2 &= AEQ_4 + AC_4 - VC_2 C_{618} && \text{FOR } AC_4 < 0 \\ &= AEQ_4 - VC_2 C_{618} && \text{FOR } AC_4 \geq 0 \end{aligned}$$

Similarly, by substituting the above AR_{11} to AC_4 relationship and $VC_3 = AR_{14} R_{14}$ into equation (N3) AC_3 is established as:

$$\begin{aligned} (N3)' \quad AC_3 &= AC_4 - VC_3 C_{619} - ABQ_4 && \text{FOR } AC_4 > 0 \\ &= -VC_3 C_{619} - ABQ_4 && \text{FOR } AC_4 \leq 0 \end{aligned}$$

The voltages across capacitors C2, C3 and C4 are established by:

$$(2) \quad VC_2 = \int VC_2 \dot{t} dt$$

$$(A2) \quad VC_2 = C_{609} AC_2$$

$$(3) \quad VC_3 = \int VC_3 \dot{t} dt$$

$$(A3) \quad VC_3 = C_{610} AC_3$$

$$(4) \quad VC_4 = \int VC_4 \dot{t} dt$$

$$(A4) \quad \dot{V}_{c4} = C_{611} A_{c4}$$

All of the equations describing the antiskid circuit's operation have now been developed; however, to obtain a computer solution of these equations, they have to be converted to a suitable form so that there are no "closed loops." Also, since the equations for A_{eq2} , A_{VA} and A_{c4} have different forms depending upon which circumstances exist, a procedure must be established to define which form of equations (Q2), (N7)" and (N8)' applies for each instance. There are twelve (12) possible combinations of circumstances as shown on Table 18. The procedure for defining which condition exists will be to assume a condition and develop a set of equations based on the assumption. Using these equations, the assumption will be tested. If the test is affirmative, the assumed condition exists. If the test is negative, the assumption is incorrect and other assumed conditions are tested until an affirmative test result is obtained. To illustrate this procedure, the equations for circuit condition 4 will be developed:

For circuit condition 4 A_{c4} is positive, A_{eq3} greater than C_{405}/C_{404} and V_B greater than zero. Substitute equation (N5) and the applicable version of equation (N7)" into equation (VX)'.

$$(VX)'\text{-4} \quad V_X = (A_{eq3} C_{404} - C_{405} - A_{c4}) C_{400} + C_{401}$$

From equations (N8)' and (V11)' A_{c4} is established as:

$$(N8)'\text{-P} \quad A_{c4} = \frac{V_X - V_{c4} - E_{04} - V_{c3}}{R_{11}}$$

Substitute (VX)'\text{-4} into (N8)'\text{-P} and solve for A_{c4}

$$(N8)'\text{-P4}$$

$$A_{c4} = \frac{A_{eq3} C_{404} C_{400}}{R_{11} + C_{400}} - \frac{(V_{c4} + V_{c3})}{R_{11} + C_{400}} - \frac{(E_{04} + C_{405} C_{400} - C_{401})}{R_{11} + C_{400}}$$

Now substitute equations (N5), (N7)" and (N8)'-P4 into equation (N4)' and solve for EV

(N4)'-4

$$EV = \frac{R_V}{R_{11} + C_{400}} \left[A_{CQ3} C_{404} R_{11} C_{406} + (V_{C4} + V_{C2}) C_{406} - (C_{405} R_{11} - E_{D4} + C_{401}) C_{406} + C_{407} (R_{11} + C_{400}) \right]$$

Substituting equations (N4)'-4, (N10)', (Vy-1), and (Q3) into equation (Q-2) and solving for A_{EQ2} gives:

$$(Q-2)-4 \quad A_{EQ2} = -(E_G - V_{C1}) C_{449} + V_{C2} C_{450} - (V_{C3} + V_{C4}) C_{451} + C_{452}$$

Substituting equations (Q-2)-4 and (Q3) into equation (N8)'-P4 gives:

$$(N8)'-P4 \quad A_{C4} = -(E_G - V_{C1}) C_{472} + V_{C2} C_{473} - (V_{C3} + V_{C4}) C_{474} - C_{475}$$

Substituting equations (Q-2), (N10)', (N4)'-4, and (Vy-2) into equation (VB) results in:

$$(VB-3,4) \quad V_B = V_{C2} C_m - C_{467} (E_G - V_{C1}) - C_{468} (V_{C3} + V_{C4}) + C_{466}$$

Now using equations (VB)-4, (Q-2)-4, (Q3) and (N8)'-P4 the assumption that $A_{C4} > 0$, $A_{CQ3} > C_{405}/C_{404}$ and $V_B > 0$ can be tested. If the test is affirmative, then values for A_{C4} , A_{R3} and EV can be computed. If the test is negative another condition must be tested for.

Tables 14, 16 and 17 are a summary of test equations developed in the same manner as above. Since equation (Q3) establishes a linear relationship between A_{EQ2} and A_{CQ3} and since A_{EQ2} needs to be computed as a step in the computation of A_{R3} , the test equations for A_{CQ3} will be performed implicitly by computing A_{EQ2} and comparing its computed value to C607 where C607 is defined as:

$$C607 = \frac{C_{405}}{(C_{404})(C_{606})}$$

Currents A_{C4} and A_{EQ2} are computed using the applicable test condition equations.

As shown on Figure 49 the locked wheel prevention circuit elements also have an input to the valve control amplifier. In the equations thus far it has been assumed that the locked wheel skid signal, $ALWS$ at node (N15), is zero. When computing the valve voltage, it is necessary that the non-zero value of $ALWS$ be accounted for. If $ALWS$ is not zero then equation (Q3) is:

$$(Q3-1) \quad ACQ3 = C606 A_{EQ2} + hFE3 ALWS$$

Since $ALWS$ is a two valued variable (i.e. either zero or the value required to drive the amplifier as necessary to achieve full brake release) insofar as valve voltage computation is concerned, it can be considered as a current which can be added to A_{EQ2} in Equation (Q3). If we define a current $AVAI$, valve amplifier input current, as:

$$(LW-1) \quad AVAI = A_{EQ2} + ALWS$$

and treat this current like A_{EQ2} in equation (Q3) and if we substitute equations (Q3) and (N7)" into equation (N5) an equation for computing A_{DS} is formulated for each circuit condition. Current A_{DS} is then used in equation (N4) to compute EV. Table 15 lists the version of equation (N5) which is to be used for computing current A_{DS} for each circuit condition.

Since the variables EG and VC1 are always used in the form of their difference, we will define the difference as equation (5)

$$(5) \quad EG - VC_1 = (EG - VC_1)$$

For the cases where the antiskid control circuit mathematical model is used with the flywheel system or three dimensional airplane system, the flywheel velocity, VF, or the airplane velocity, X, as applicable, will be used as the airplane speed reference circuit element. The wheel speed comparison element will be described as follows:

$$(6) \quad \begin{aligned} ALWS &= C617 \quad \text{FOR } VF > C615 \text{ AND } EG < C616 \\ &= 0 \quad \text{FOR } VF \leq C615 \text{ OR } EG \geq C616 \end{aligned}$$

1. ORIGINATING ACTIVITY (Corporate author) General Dynamics Fort Worth Division Fort Worth, Texas 76101		2a. REPORT SECURITY CLASSIFICATION Unclassified	
		2b. GROUP	
3. REPORT TITLE Aircraft Antiskid Performance and System Compatibility Analysis			
4. DESCRIPTIVE NOTES (Type of report and inclusive dates) Final Report (August 1969 to September 1970)			
5. AUTHOR(S) (First name, middle initial, last name) Byron H. Anderson Wayne C. Kreger			
6. REPORT DATE February, 1971	7a. TOTAL NO. OF PAGES 246	7b. NO. OF REFS 16	
8a. CONTRACT OR GRANT NO. F33615-70-C-1004	9a. ORIGINATOR'S REPORT NUMBER(S) AFFDL-TR-70-128		
b. PROJECT NO. 1369	9b. OTHER REPORT NO(S) (Any other numbers that may be assigned this report) General Dynamics No. FZM-5560		
c. Task Area No. 10			
d. Work Unit No. 001			
10. DISTRIBUTION STATEMENT This document is subject to special export controls and each transmittal to foreign governments or foreign nationals may be made only with prior approval of the Air Force Flight Dynamics Laboratory (F&M), Wright-Patterson Air Force Base, Ohio 45433.			
11. SUPPLEMENTARY NOTES		12. SPONSORING MILITARY ACTIVITY Air Force Flight Dynamics Laboratory Wright-Patterson Air Force Base, Ohio 45433	
13. ABSTRACT The operation of an aircraft antiskid wheel brake control system has the potential for producing adverse aircraft dynamic behavior and structural damage. Anti-skid operation is also a major influence upon stopping performance. Unless the characteristics and effects of antiskid operation can be defined, an aircraft's capability for safe, reliable and economical accomplishment of its intended usage cannot be assured. This report presents an analysis procedure for predicting antiskid operational characteristics and the inter-related effects upon the aircraft and its performance. The analytical procedure is the development of mathematical equations for a comprehensive description of antiskid system components, the significantly influencing aircraft systems and the characteristics of the surface upon which the aircraft is operating. The mathematical description includes such considerations as landing gear dynamics, tire elasticity, brake torque response characteristics, antiskid electronic circuitry, brake hydraulic control system dynamics, runway surface profile and tire-to-runway friction characteristics. Both on-off and "modulated" antiskid systems are analyzed. Procedures for quantitative evaluation of the influencing parameters and examples of their usage are also presented. The implementation of the analytical prediction procedure by simultaneous solution of all the mathematical equations on an electronic computer is described.			

14.	KEY WORDS	LINK A		LINK B		LINK C	
		ROLE	WT	ROLE	WT	ROLE	WT
	Antiskid Analysis Brake System Performance Aircraft Stopping Performance						

Unclassified

Security Classification